SUNIL POUDEL

Effect of Antioxidant and Pro-oxidant on Bone mineralization and Remodelling

UAlg FMCB
UNIVERSIDADE DO ALGARVE
FACULDADE DE MEDICINA E CIÊNCIAS BIOMÉDICAS

2022

SUNIL POUDEL

Effect of Antioxidant and Pro-oxidant on Bone mineralization and Remodelling

Programa de Doutoramento em
Ciências Biomédicas

BioMedAqu H2020-MSCA-ITN 2017 n. 766347

Trabalho efetuado sob a orientação de:
Prof. Leonor Cancela,
Prof. Paulo Gavaia

UAlg FMCB
UNIVERSIDADE DO ALGARVE
FACULDADE DE MEDICINA E CIÊNCIAS BIOMÉDICAS

2022

Effect of Antioxidant and Pro-oxidant on Bone mineralization and remodelling

Declaração de autoria do trabalho

Declaro ser o autor deste trabalho, que é inédito e original. Autores e trabalhos consultados encontram-se devidamente citados no texto e constam da listagem de referências incluída.

_____

FUNDING:

This work was made possible with the financial support of the European Union's Horizon 2020 research and innovation programme under the Marie Skłodowska-Curie grant agreement No 766347- BioMedAqu, and by the Portuguese Foundation for Science and Technology (FCT) through the projects UIDB/04326/2020, UIDP/04326/2020 and LA/P/0101/2020.

ACKNOWLEDGEMENTS

This dissertation is dedicated to all of the people who have provided me with the essential knowledge, counsel, and support throughout the course of my PhD.

Prof. Dr. Leonor Cancela, my supervisor, is to be commended for opportunity to work on this project, which has effectively broadened my academic horizons in ways I never imagined possible. I'd also like to express my gratitude to Prof. for demonstrating what a true leader looks and acts like.

I'd want to express my gratitude to my co-supervisor, Dr. Paulo Gavaia, for all of his assistance and for accepting me into the BIOSKEL laboratory. I'd also like to express my gratitude to my supervisors for their commitment to support me whenever I needed it.

All members of the BIOSKEL lab (Dr. Vincent Laizé, Dr. Joana Rosa, Dr. Vania Roberto, Dr. João Santos, Dr. Marcio Simao, Dr. Natércia Conceicao, Dr. Nadia Silva, Gil Martins, Tatiana Varela, Helena Caiado, Marco Tarasco, Alessio Carletti, Debora Varela, Daniela Castro, Katia Pes, Matthew Castaldi and Michele Loiodice) are to be thanked for their assistance and the environment. I'd also like to thank all of my former and current coworkers for putting up with me in both good and terrible times, and for providing me with a fun and challenging work environment.

A particular thanks to the BIOMEDAQ project members and all the Early-stage researchers (Leticia Amoraga, Caroline Caetano, Javier Cantillo, Silvia Cotti, Zachary Dellacqua, Claudia Biagio, Lucia Drabikova, Ali Kiai, Navdeep Kumar, Ratish Raman, Jerry Maria, Yiyen Tseng and Sivagurunathan) for their assistance, humour, engorgements, and all of the stimulating comments and lectures. I'd like to express my gratitude to everyone in the University of Las Palmas team, especially Prof Marisol Izquierdo, Yiyen Tseng, and Sivagurunathan Ulaganathan, for their assistance in the microdiets preparation and seabream trial.

I would like to thank my parents, my father and mother for supporting me unconditionally. I am exceptionally indebted to my wife Sadikshya Gautam, for making me a better person and for supporting me unconditionally and my sister for all the support. Thank you all for believing in me for all this time.

ABSTRACT

Osteoporosis is characterized by abnormal bone with low bone mass and degradation of skeleton microarchitecture, thus leading to bone fragility and risk of fracture. Oxidative stress induces an imbalance in osteoblast and osteoclast activity that leads to bone degradation, consequently resulting in osteoporotic phenotype. In addition, oxidative stress is a primary cause of secondary osteoporosis caused by specific medications.

Understanding the role of oxidative stress in the development of primary and secondary osteoporosis could lead to further research towards preventive and therapeutic measures to combat this significant cause of mortality and morbidity worldwide. Antioxidant supplementation has improved bone mineral density and lowered the risk of fragility fractures. While it is not experimentally evident if the antioxidant activity is the cause of this alteration. Hence, this work aimed to counteract/rescue specific medication-induced secondary osteoporosis by supplementing antioxidants on *in vitro* and *in vivo* models. In addition, to provide insights into the molecular mechanisms on medication-induced bone impairment, the transcriptome of murine osteoblasts treated with antioxidants (Resveratrol and MitoTEMPO) and pro-oxidants (Doxorubicin) alone or in combination was analyzed. RNA-Seq data revealed that osteocrin and p53 are the responsible players on doxorubicin-induced bone impairment and its reversal by resveratrol. We further studied the effect of antioxidants and pro-oxidant on osteoclast differentiation, where we found out that doxorubicin also increased osteoclast differentiation. Based on our *in vitro* results, we confirm the effect of Resveratrol, MitoTEMPO on Doxorubicin-induced bone impairment with the zebrafish (osteocytic bone) and seabream (non-osteocytic bone) models. Our data indicate that regular supplementation of antioxidants effectively improves overall growth, mineralization and counteracts pro-oxidant induced bone pathologies on both models.

In conclusion, this work proposes that the negative effect of the specific medication (i.e., Doxorubicin) can be reversed by regular supplementation of antioxidants (i.e., Resveratrol and MitoTEMPO). Furthermore, this work also proposes osteocrin as a key

responsible factor for doxorubicin-induced bone impairment, and its reversal. Osteocrin can be further exploited as a communicator molecule for crosstalk between bone and other tissues.

Keywords: Antioxidants, Pro-oxidants, Oxidative stress, Resveratrol, MitoTEMPO, Doxorubicin, Osteoblasts, Osteoclasts, zebrafish, seabream, Osteocrin, p53, Secondary Osteoporosis

RESUMO

A osteoporose é uma doença caracterizada por um osso anormal com baixa massa óssea e pela degradação da microarquitetura do esqueleto, conduzindo assim à fragilidade óssea e a um elevado risco de fraturas. Existem várias causas descritas para a origem desta condição, sendo a mais comum a osteoporose primária ou senil, provocada pelo envelhecimento e que afeta principalmente as mulheres pós-menopausa, mas também os homens idosos. Representa cerca de 95% dos casos em mulheres e 80% em homens. A principal causa da osteoporose primaria é a diminuição dos níveis de estrogénio, particularmente a rápida redução que ocorre nas mulheres durante a menopausa, embora esta diminuição também ocorra nos homens com mais de 50 anos. A deficiência de estrogênio leva à rápida perda óssea.

A osteoporose secundária representa menos de 5% dos casos em mulheres e cerca de 20% em homens e é causada por diversos fatores, como doenças, distúrbios hormonais, medicação, como corticosteroides ou fármacos quimioterápicos, ou pelo consumo de álcool e drogas. Entre os mecanismos que levam ao aparecimento da osteoporose secundária, associada a tratamentos terapêuticos com medicamentos específicos, está o stress oxidativo, que induz um desequilíbrio na atividade osteoblástica e osteoclástica que leva à degradação óssea, resultando consequentemente no fenótipo osteoporótico. Compreender o papel do stress oxidativo no desenvolvimento da osteoporose primária e secundária poderia levar a uma investigação mais aprofundada no sentido de medidas preventivas e terapêuticas para combater esta causa significativa de mortalidade e morbilidade em todo o mundo.

Alguns estudos mostraram que a suplementação com antioxidantes levou a melhorias na densidade mineral óssea e diminuiu o risco de fraturas de fragilidade. Embora não existam evidências experimentais para provar que a atividade antioxidante foi a causa desta alteração. Por isso, o objetivo deste trabalho visou contrariar ou recuperar a osteoporose secundária induzida por medicação específica, através da suplementação com antioxidantes, utilizando para tal a modelos *in vitro* e *in vivo*. Adicionalmente, para procurar identificar quais os mecanismos moleculares sobre a deficiência óssea

induzida pela medicação, foi realizada uma análise ao transcritoma de células osteoblásticas de ratinho (MC3T3-E1) tratadas com antioxidantes (Resveratrol; RES e MitoTEMPO; MT) ou com pró-oxidantes (Doxorrubicina; DOX) sozinhos ou em combinações entre estes. Os dados da sequenciação do ARN revelaram que a osteocrina e o p53 são as moléculas intervenientes responsáveis pela deficiência óssea induzida pela DOX e estão também envolvidas na sua reversão destes efeitos pelo co-tratamento com RES.

Estudamos ainda a diferenciação de células de ratinho RAW 264.7 na linhagem osteoclástica, de forma a determinar os efeitos e investigar os mecanismos da diferenciação osteoclástica induzida pelo pró-oxidante DOX. Foi utilizado o ativador de Sirt 1 resveratrol (RES) para neutralizar os efeitos induzidos pela DOX. As células RAW 264.7 foram diferenciadas em osteoclastos sob co-tratamento com DOX e RES. Foi observado que a DOX aumentou a diferenciação de osteoclastos *in vitro,* ao passo que o tratamento com RES inibiu a diferenciação osteoclástica induzida pelo DOX, mas tal não se verificou com MT. O tratamento com RES reduziu a expressão do marcador de fusão osteoclástica *Oc-stamp* e dos marcadores de diferenciação *Ran*k, *Trap*, *Ctsk* e *Nfatc1*. Inversamente, o tratamento com RES induziu a sobre expressão dos genes antioxidantes *Sod 1* e *Nrf 2*, enquanto DOX reduziu significativamente a expressão *FoxM1*, resultando em stress oxidativo*.* A utilização da linha transgénica de peixe zebra repórter para catepsina K (*Tg[ctsk:DsRed*]) permitiu verificar o aumento da expressão *in vivo* de *ctsk* significativamente o sinal de ctsk, enquanto o co-tratamento RES resultou numa redução significativa do número de células positivas. Adicionalmente foi observado que a exposição a RES conseguiu reverter efeitos negativos da DOX no desenvolvimento do trato intestinal, com redução da mucosite, e nos efeitos sobre o comportamento locomotor e padrão de locomoção que foram significativamente afetados no tratamento com DOX.

Com base nos resultados *in vitro*, foi estudado o efeito do RES e MT na prevenção de malformações ósseas induzida pela DOX, utilizando os modelos de peixe-zebra (osso osteocítico) e dourada (osso anosteocítico). Estes dois modelos foram submetidos a tratamentos nutricionais com dietas suplementadas em DOX, RES e MT durante o

crescimento larvar. Os nossos dados indicam que a suplementação regular com antioxidantes melhorou efetivamente o crescimento global, a mineralização das estruturas esqueléticas e contrariou a incidência e a gravidade das malformações ósseas induzidas por pro-oxidantes em ambos os modelos. Observou-se ainda uma redução da expressão de genes por ação da DOX, como os marcadores de osteoblastos (*osteocalcina* e *osterix/sp7*) e de genes antioxidantes, incluindo catalase, glutatião peroxidase 1, superóxido dismutase 1, e hsp90, sugerindo que a formação de espécies reativas de oxigénio (ROS) é central para a perda óssea induzida por DOX. A expressão dos genes antioxidantes foi significativamente aumentada pelo RES sozinho ou em tratamento combinado. Uma vez mais foi observada uma melhoria do desenvolvimento intestinal, com aumento do tamanho dos villi intestinais e redução da inflamação, tanto em peixe zebra como em dourada.

Em conclusão, este trabalho propõe que o efeito negativo da medicação específica (DOX) possa ser revertido por suplementação regular com antioxidantes (RES e MT). Além disso, este trabalho propõe também a osteocrina como fator responsável pela deficiência óssea induzida pelo DOX, e a sua inversão. A osteocrina pode ser ainda mais explorada como molécula comunicadora para a conversa cruzada entre o osso e outros tecidos.

TABLE OF CONTENTS

PREAMBLE

This dissertation is divided into five main chapters, each organized according to the scientific article format. Chapter 1 is divided into two parts; the first part consists of a general introduction of bone biology and the second part consists of an overall review on antioxidant and pro-oxidant on bone biology. Chapter 2 (Molecular Mechanism) is divided into two parts; the first part (Transcriptomic analysis of signalling pathways associated with reversal of doxorubicin-induced osteoblastic differentiation of MC3T3-E1 cells) focuses on the molecular mechanism behind doxorubicin-induced bone impairment and the reversal effect of resveratrol on osteoblast cells. In the second part (Resveratrol-mediated reversal of Doxorubicin-induced osteoclast differentiation alleviating oxidative stress via *FoxM1* expression) focuses on the effect on resveratrol, MitoTEMPO and doxorubicin on osteoclast differentiation. Chapter 3 (*in vivo* osteocytic model) focuses on translating the results obtained from *in vitro* experiment to the osteocytic bone model. Chapter 4 (*in vivo* non-osteocytic model) focuses on translating the results obtained from *in vitro* experiment to the non-osteocytic bone model. Finally, chapter 5 contains general conclusions and future perspectives of this dissertation in an integrative way. To contextualize each chapter, the concept of the task and objectives will be described briefly as a preamble at the beginning. All the documents in this dissertation were written by the author, who planned, designed, and performed all of the experiments and analytical processes. In collaborative contexts, a few experiments were carried out.

Ethical statement

People involved in animal handling and experimentation received proper training (category B courses accredited by FELASA, the Federation of Laboratory Animal Science Associations) and all fish facilities were accredited by the Portuguese National Authority for Animal Health (DGAV, authorization no. 0421/2021). All experimental procedures involving animals followed the European Directive 2010/63/EU and the related guidelines (European Commission, 2014) and Portuguese legislation (Decreto-Lei 113/2013) for animal experimentation and welfare.

CHAPTER 1

GENERAL INTRODUCTION

PREAMBLE

Chapter 1 is divided into two parts; the first part is a general introduction, and the second part is an overall review of antioxidants and pro-oxidants on bone biology. Chapter 1 serves as a guide through the state of the art of project. The first part explains concepts of bone homeostasis, osteoblastogenesis and osteoclastogenesis and their signalling pathways. The information is presented to understand the concept of signalling pathways on osteoblast and osteoclast differentiation. The second part discusses the background on metabolic bone disorders, the concept of bone remodelling and their mechanism, the role of oxidative stress on the bone remodelling process, the role of antioxidant and pro-oxidant on bone remodelling and fish as a model of oxidative stress in bone. Chapter 1 ends with the scientific questions and objectives of the project.

1.1. General Introduction

1.1.1 Homeostasis of bone

Bone is a dynamic organ that supports soft tissue, provides mechanical protection for vital organs, and constantly remodels. The old and defective bone is replaced and fixed to replenish the skeleton and preserve skeletal health (1). Homeostasis of bone mass in a healthy adult requires an exquisite balance between bone resorption by osteoclasts and bone formation by osteoblasts; disturbance of such balance is the root cause for various bone disorders including osteoporosis which is characterized as the predominant activity of osteoclasts over osteoblasts (2,3). Existing evidence from previous studies suggests the involvement of multiple factors in the maintenance of the bone homeostasis (4). During the resorption, growth factors such as insulin-like growth factors (IGFs) or transforming growth factor β (TGF-βs) are released to promote the initialization of bone formation (5,6). After resorption by osteoclasts, the factors deposited on the surface of bone initialize the upcoming process of bone formation (4).

The unbalance in the homeostasis of bone causes various diseases, including metabolic bone diseases which are considered the third most common endocrine disorders after diabetes and thyroid diseases. The common metabolic bone diseases (MBD) include osteoporosis, rickets/ osteomalacia, fluorosis, primary hyperparathyroidism (PHPT) and Paget's disease of bone, while the rare MBD include tumor induced osteomalacia, fibrous dysplasia, osteogenesis imperfecta and others (7).

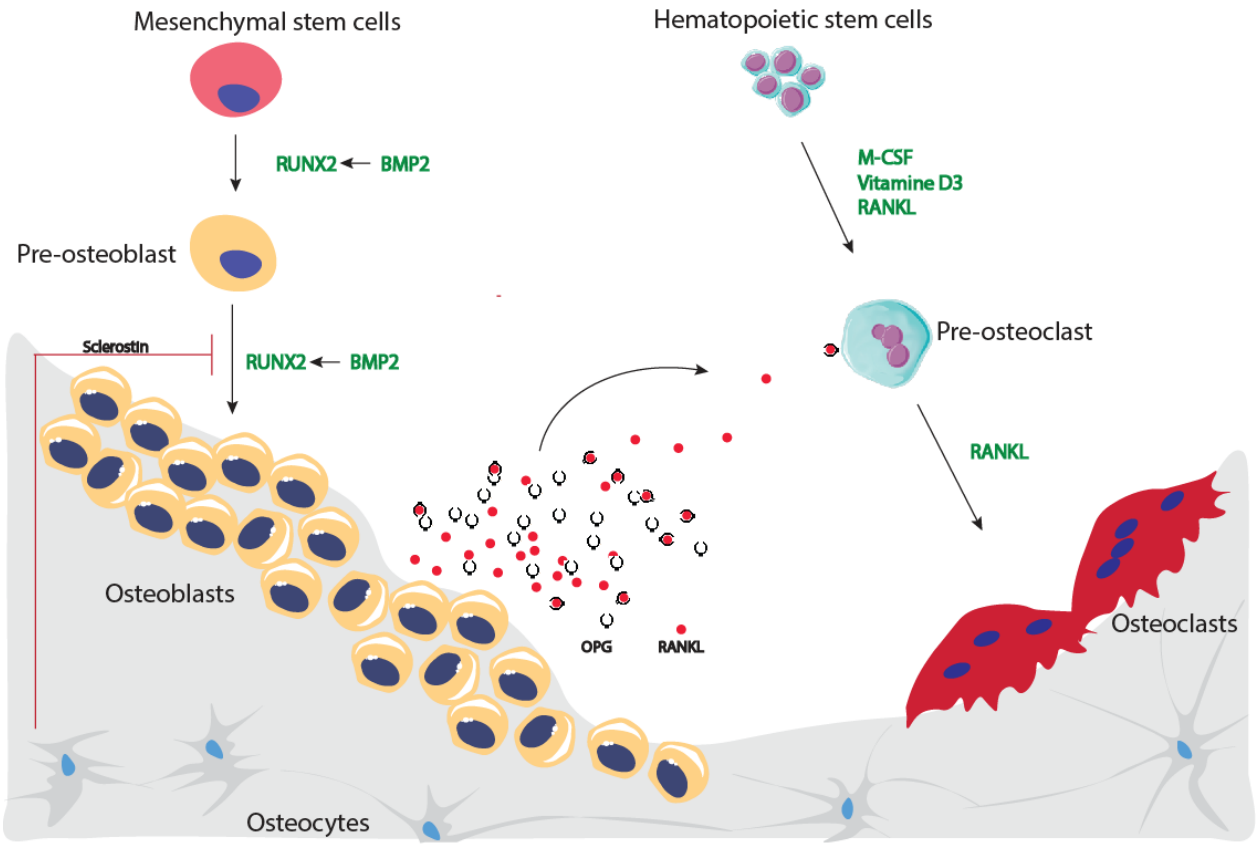

Figure 1.1.1: Homeostasis of bone. Homeostasis of bone is maintained by the signalling molecules secreted by osteoblasts, osteocytes, and osteoclasts to check and balance influence each activity. Osteoblasts are differentiated under the signal of BMP2 and RUNX2 and produce OPG and RANKL to activate or inhibit osteoclast differentiation, osteoclast differentiation is activated after the activation of M-CSF, RANKL on haemopoietic stem cells. Osteoclasts also secrete coupling factors such as BMP6, sclerostin to inhibit osteoblast differentiation. Figure adapted from Han, Yujiao, *et al.*(8). Acronyms: Bone morphogenetic protein (BMP), Runt-related transcription factor 2 (RUNX2), Macrophage colony-stimulating factor (M-CSF), Receptor activator of nuclear factor-κB ligand (RANKL) and Osteoprotegerin (OPG).

Bone is a dynamic tissue that supports soft tissues and provides mechanical protection for vital organs. On the other hand, it controls phosphate and calcium homeostasis contains bone marrow responsible for hematopoiesis and provides a point of attachment for the muscles (1,9). Homeostasis of bone is a complex process in which a new one replaces old bone in a cycle comprised of phases such as initiation of bone resorption by osteoclast, the transition from resorption to new bone formation and bone

formation by osteoblast (10,11). Osteoblasts, osteoclasts, osteocytes are the cellular units of these coordinated actions (12).

Osteoblasts

Osteoblasts are the bone-forming cells located on the bone surface, comprising 4-6% of the total resident bone cells (13). These cuboidal cells are mesenchymal stem cell (MSC) derived. The commitment of these stem cells towards osteoprogenitor differentiation requires the induction of specific gene expression in a programmed manner, such as expression of the bone morphogenetic protein (BMPs), wingless family members (Wnt) pathways, along with the differentiation-specific markers (Runx2, ALP, OC, SP7, etc.) (14). Furthermore, during the transition from pre-osteoblast to mature osteoblast, bone matrix proteins such as osteocalcin (OC or bone Gla protein - BGP), osteopontin (OPN) and bone sialoprotein (BSP) are produced. Therefore, these are considered as markers of mature bone since only mature osteoblasts produce them. In addition, these proteins regulate bone mineralization and bone resorption (15).

Osteoclasts

Mononuclear cells from the hematopoietic stem cell lineage fuse together and differentiate into multinucleated osteoclasts, that possess resorptive activity on bone. The activation of the resorptive cells occurs on the triggering of several factors, such as Macrophage colony-stimulating factor (M-CSF) and RANK ligand (RANKL) secreted by the osteoprogenitor lineage (13).

Osteocytes

Osteocytes are the most abundant and long-living cells in bone. They comprise 90-95 % of the total bone cells with a lifespan of up to 25 years (16). Osteocytes are mesenchymal stem cell (MSC) derived osteoblasts that undergo morphological and structural changes to become embedded in the bone matrix. This subpopulation of osteoblasts are incorporated into the bone matrix at the end of the bone formation cycle forming a network (17). Similar to osteoblasts, osteocytes produce bone matrix proteins such as osteopontin, osteocalcin and dentin matrix protein 1 (DMP1), which positively regulate bone formation. In addition, when bone mineral density is high, osteocytes

produce sclerostin, which inhibits osteoblastogenesis and activates osteoclastogenesis (17).

1.1.2 Osteoblast differentiation

Factors mediating osteoblastic differentiation:

Runt-related transcription factor 2 *(Runx2).* Predominantly Runx2 is a factor known to be a master regulator of osteoblastic differentiation. In adults, Runx2 levels are low. Similarly, Runx2 expressed outside the skeleton manifests ectopic calcification (18). Osteopontin, bone sialoprotein, osteocalcin, osteoprotegerin, RANKL and many others are regulated genes downstream from Runx2 signaling (19).

Wnt/Notch signalling in Runx2 regulation is the most studied. The imbalance between the Wnt and Notch pathways leads to ectopic mineralization (20). Wnt ligand is a paracrine glycoprotein that signals via several pathways, among which the so-called "Canonical pathway is one of the most relevant for osteoblast differentiation (21).

Osterix (Osx or SP7), a gene downstream of Wnt, is also a zinc-finger transcription factor, plus serve as a negative feedback loop by inhibiting Wnt (22). In addition, Osx knockout mice showed the commitment of mesenchymal stem cells (MSCs) to the osteoblastic lineage and its further differentiation with the expression of osteocalcin and Col1α1. These mice had short non-mineralized limbs at birth (23), proving that Osx is a master regulator of osteoblast differentiation and function.

Paracrine and endocrine factors influencing osteoblastic differentiation:

Bone morphogenetic proteins (BMPs) are cytokines essential for postnatal ossification (24) and imperative components for skeletal development (25,26). BMPs are members of the TGF-β superfamily, and their signaling is typical: the ligand binds to a receptor on the cell surface, which activates receptor SMADs (SMAD 1/5/8). In addition, they trigger the effector SMADs (SMAD 4) that translocate to the nucleus and bind to cofactors regulating transcription of target genes. Osteogenic BMPs are BMP2 and BMP4 (27).

Besides BMPs, other growth factors that influence osteoblast differentiation are mainly TGF-βs and IGFs, which activates fibroblast growth factors (FGFs) and Osx (28,29).

FGFs, although being primarily a fibroblast-stimulatory factor, also promotes osteoblast differentiation. FGF signaling is supposed to act via Mitogen-activated protein kinase (MAPK), protein kinase C (PKC) and phosphatidylinositol 3-kinase (PI3K), but the exact mechanisms are still unknown (24).

Vitamin D is essential in regulating the Runx2 target genes. Vitamin D receptor makes a complex with Runx2 and several other cofactors on the target gene promoter (e.g. osteocalcin) and stimulates expression of bone-specific genes (24,30).

Parathyroid hormone (PTH) is an upstream regulator of Runx2 (22). The PTH effect is time-dependent over bone metabolism. PTH has both anabolic and catabolic effects on bone. When the level of PTH is elevated continuously, bone resorption occurs, whereas if the elevation is intermittent, osteoblastic differentiation is stimulated. This is probably because the intermittent exposure results in the release of TGF-β from resorbing bone (24), leading to higher osteoblastic activity.

Mammalian/ mechanistic target of rapamycin (mTOR), is a serine-threonine kinase member of PI3K family with homologs in all eukaryotes (31). mTOR stimulates osteoblast differentiation through BMP signaling (32), IGF (33,34) and activates aerobic glycolysis via Wnt signaling (32).

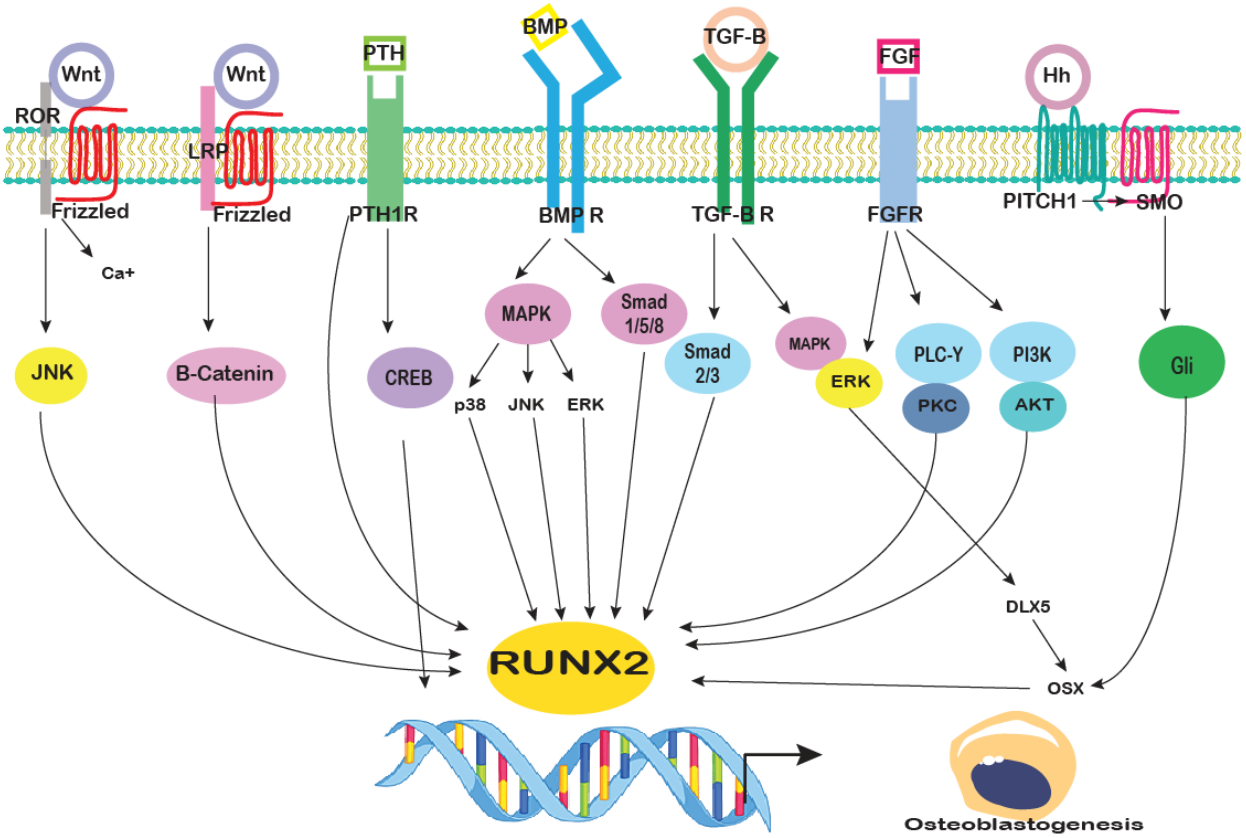

Figure 1.1.2: Illustration of different Osteoblast differentiating pathways. Regulatory pathways in RUNX2 mediated osteoblast differentiation. Wnt pathway activates RUNX2 by β-catenin stabilization; Wnt also activates RUNX2 through JNK via ROR receptor. Parathyroid hormone activates osteoblast differentiation through activation of CREB. BMP can activate osteoblastogenesis through MAPK and SMAD1/5/8 activation. TGF-β activates SMAD 2/3 and MAPK. Fibroblastic growth factor activates P3K/AKT and Sonic hedgehog acts through OSX. Figure adapted from Chen *et al.*(35). Acronyms: Receptor tyrosine kinase-like orphan receptors (ROR), Parathyroid Hormone (PTH), Parathyroid Hormone 1 receptor (PTH 1R), Bone morphogenetic protein (BMP), Bone morphogenetic protein receptor (BMP R), Transforming growth factor β (TGF-B), Transforming growth factor β receptor (TGF-B R), Fibroblast growth factors (FGF), Fibroblast growth factor receptor (FGF R), Hedgehog (Hh), c-Jun N-terminal kinase (JNK), Beta-catenin (B-catenin), cAMP Response Element-Binding Protein (CREB), Mitogen-activated protein kinase (MAPK), Extracellular signal-regulated kinases (ERK), Phospholipase C-gamma (PLC-Y), Protein kinase C (PKC), Phosphatidylinositol 3-kinase (PI3K), Distal-Less Homeobox 5 (DLX5), Osterix (Osx) and Runt-related transcription factor 2 (RUNX2). Macrophage colony-stimulating factor (M-CSF), Receptor activator of nuclear factor-κB ligand (RANKL) and Osteoprotegerin (OPG).

1.1.3. Osteoclast differentiation

Factors mediating osteoclast differentiation:

Osteoclasts differentiate from the bone marrow-derived monocyte/macrophage lineage cells under the control of two essential cytokines. The binding of the M-CSF to its receptor colony-stimulating factor-1 (c-FMS) provides signals required for the proliferation and survival of osteoclast precursor cells. In contrast, the binding of RANKL to RANK stimulates signals required for osteoclast differentiation and the resorptive function as well as the survival of mature osteoclasts (36).

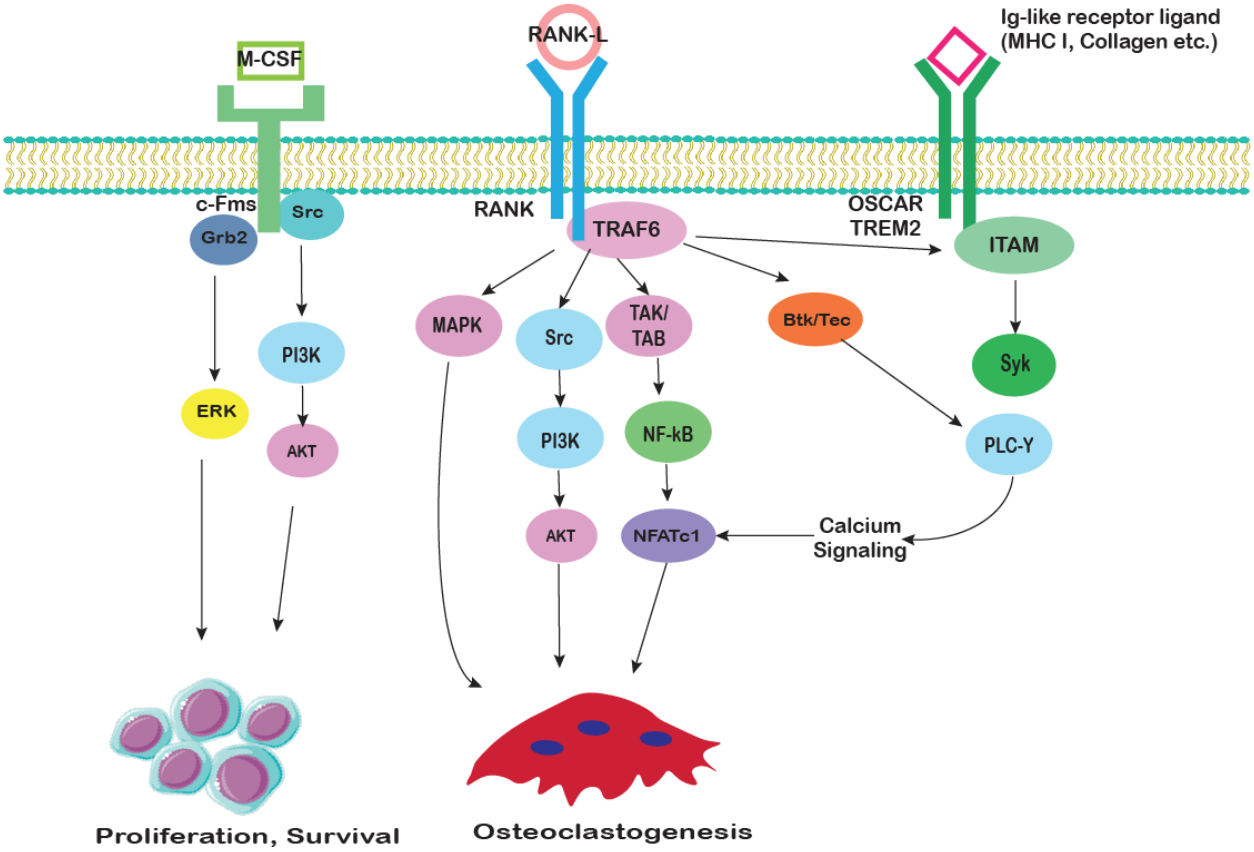

Figure 1.1.3: Illustration of Osteoclast differentiating pathways. M-CSF and RANKL activate osteoclast differentiation. M-CSF signaling on osteoclast induces proliferation and survival through ERK and AKT activation. Whereas Osteoclastogenesis is activated upon RANKL recruiting TRAF6 and activating MAPKs, AKT and NFATc1. In addition, osteoclast regulatory receptor (OSCAR) activates calcium signaling, which robust NFATc1 induction. Figure adapted from Feng X, Teitelbaum SL and Kim JH, *et al.* (36,37). Acronyms: Macrophage colony-stimulating factor (M-CSF), Colony-stimulating factor-1 receptor (c-Fms), Receptor activator of nuclear factor-κB ligand (RANKL), Receptor activator of nuclear factor-κB (RANK), Osteoclast-associated receptor (OSCAR), Extracellular signal-regulated kinases (ERK), Phosphatidylinositol 3-kinase (PI3K), Tumor necrosis factor receptor associated factor 6 (TRAF6), Mitogen-activated protein kinase (MAPK), Nuclear factor-κB (NF-kB), TGF-β-activated kinase (TAK), TAK-1-binding protein (TAB), Bruton's tyrosine kinase (Btk), Immunoreceptor tyrosine-based activation motif (ITAM) and Phospholipase C-gamma (PLC-Y). Receptor tyrosine kinase-like orphan receptors (ROR), Parathyroid Hormone (PTH), Parathyroid Hormone 1 receptor (PTH 1R), Bone morphogenetic protein (BMP), Bone morphogenetic protein receptor (BMP R), Transforming growth factor β (TGF-B), Transforming growth factor β receptor (TGF-B R), Fibroblast growth factors (FGF), Fibroblast growth factor receptor (FGF R), Hedgehog (Hh), c-Jun N-terminal kinase (JNK), Beta-catenin (B-catenin), cAMP Response Element-Binding Protein (CREB), , Protein kinase C (PKC), Distal-Less Homeobox 5 (DLX5), Osterix (Osx) and Runt-related transcription factor 2 (RUNX2). , Receptor activator of nuclear factor-κB ligand (RANKL) and Osteoprotegerin (OPG).

M-CSF - c-FMS SIGNALING

M-CSF plays an essential role in supporting the proliferation and survival of osteoclast precursor cells. The binding of M-CSF to its corresponding receptor c-FMS results in auto-and trans-phosphorylation of specific tyrosine residues in the cytoplasmic tail of c-FMS (38). Activation of c-FMS further interacts with c-Src, which recruits the PI3K that activates the Akt pathway. Therefore, M-CSF-induced activation of c-FMS results in enhanced osteoclast precursor proliferation and survival through the ERK and PI3K/Akt pathways (38,39).

RANK-RANKL- OPG SIGNALING

RANKL secreted by osteoblast binds to the RANK in osteoclast precursor cells. Binding of RANKL to RANK leads to recruitment of TNF receptor-associated factor (TRAF) adaptor proteins to the cytoplasmic domain of RANK. TRAF 6 transmits the RANKL/RANK signal to downstream targets such as nuclear factor kappa B (NF-κB), c-Jun N-terminal kinase (JNK), extracellular signal-regulated kinase (ERK), p38, Akt, and NFATc1 (40). Once ERK, JNK, and p38 are activated through MEK1/2, MKK7 and MKK6 further activate their downstream targets such as c-Fos, AP-1 transcription factors, and MITF in osteoclast precursors (36). Similarly, to RANKL, Osteoprotegerin (OPG) is also secreted by osteoblasts and protects the skeleton from resorption of bone by binding to RANKL and preventing it from binding with RANK. The RANKL/OPG ratio in bone is essential for bone mass in normal conditions and often affected in disease states (41).

CHAPTER 1.2

Oxidative stress in bone: Balancing Antioxidants and Pro-oxidants

Sunil Poudel

M. Leonor Cancela

Paulo J. Gavaia

Chapter to be submitted to Bone

Oxidative stress in bone: Balancing Antioxidants and Pro-oxidants

ABSTRACT

Oxidative stress alters the bone remodeling process, causing an unbalance between osteoclast and osteoblast activity, leading to metabolic bone diseases and contributing to the pathogenesis of skeletal system disorders, including primary and secondary osteoporosis, characterized by low bone mineral density and a decrease in bone mass. Several clinical studies suggested the involvement of antioxidant and/or pro-oxidant systems in the pathology of bone. To improve the antioxidant defense capability of the cell, different types of antioxidants can be used as supplements. However, the mechanism of action of pro-oxidants and antioxidants on bone is not fully understood. The present review briefly discussed the role of antioxidants and pro-oxidants on bone remodeling and balancing antioxidants with pro-oxidants on bone metabolism and their signaling pathways.

1.2.1 Introduction

Oxidative stress is the state where the production of reactive oxygen species (ROS) overwhelms the intrinsic antioxidant defense. The imbalance between antioxidant and pro-oxidant mechanisms affects cellular molecules such as protein, lipids and DNA. (42,43).

Oxidative stress alters the bone remodeling process, causing an imbalance between osteoclast and osteoblast activity. This can lead to metabolic bone diseases and contribute to the pathogenesis of skeletal system disorders including osteoporosis, which is characterized by low bone mineral density and a decrease in bone mass (42). Several clinical studies suggested the involvement of antioxidant and/or pro-oxidant systems in the development of bone pathologies, including osteoporosis (44–47)

Previous studies have shown that antioxidants acting directly and/or counteracting the effect of pro-oxidants, contribute to the activation of osteoblast differentiation, mineralization processes and reduction of osteoclast activity. These antioxidants act as direct scavengers of ROS (48). Oxidative stress activates the differentiation of pre-osteoclasts in osteoclasts and strengthens bone resorption. A significant increase in the number and activity of osteoclasts as well as in the tartrate-resistant acid phosphatase (TRAP) levels was observed when hydrogen peroxide (H_2O_2) was added to cultures of human marrow mononuclear cells (49). ROS induce the apoptosis of osteoblasts and osteocytes, cells localized in the bone matrix and derived from mature osteoblasts, thus favoring osteoclastogenesis (42,50).

ROS elicit a spectrum of responses ranging from proliferation, growth, differentiation arrest to cell death by activating numerous signaling pathways. Indeed, mitogen-activated protein kinases (MAPKs) such as extracellular signal-regulated kinases (ERK1/2), c-Jun-N terminal kinase (JNK) and p38 MAPK are involved in osteoblast or osteocyte apoptosis (51–53). High levels of ROS block and reduce the osteoblast activity and differentiation, therefore the mineralization and osteogenesis (48,54,55). These events increase bone remodeling turnover with consequent alteration and decrease in bone mass. Antioxidants have opposing effects, and they contribute to the differentiation of osteoblasts and bone formation (56), maintaining vital osteocytes,

which contribute to osteoblast activity and osteogenesis while reducing the osteoclast differentiation and their activity (42).

On the other hand, the loss of antioxidants leads to accelerated bone loss through the activation of a tumor necrosis factor-alpha (TNFα)-dependent signaling pathway, and the administration of antioxidants such as vitamin C, E, N-acetyl-cysteine (NAC) and LA, has beneficial effects in individuals with osteoporosis (57). It has also been demonstrated that the administration of vitamin E can maintain bone mineral density in elderly men, and it promotes healing of osteoporotic fractures in ovariectomized rats, inducing bone regeneration (58). Many *in vitro* and *in vivo* experiments demonstrate that these events are regulated by redox-sensitive signaling pathways involving MAPKs, β-catenin and NF-kB activity. In this way, antioxidants have an important role in maintaining a normal bone remodeling and protecting bone health by preventing and/or reducing inflammatory state and bone loss through inhibition of osteocyte apoptosis, while mitigating osteoclast activity. Consequently, antioxidants increase osteoblast activity and induce osteogenesis (42).

1.2.2. Molecular Mechanism of ROS in Bone

ROS are reactive molecules and free radicals [(H_2O_2), superoxide anion (O_2^-), and hydroxyl radical ($HO^\bullet$)], which are produced during aerobic respiration at the site of the electron transport chain (59). ROS are molecules with highly unstable oxygen free radicals which converts into more stable and freely diffusible non-radicals such as hydrogen peroxide and hypochlorous acid (60,61). ROS play an important role as regulatory mediators in signaling processes and homeostasis. These reactive species regulate cell survival, proliferation and differentiation, cellular metabolism and apoptosis. (59,62). ROS serves as an intracellular secondary messenger for cellular function, such as apoptosis, gene expression, and the activation of cell signaling cascades (42,59,61).

Hydrogen peroxide (H_2O_2) and superoxide anion(O_2^-) are the most fundamental molecules studied on ROS, and H_2O_2 is the best described ROS signaling molecule (63).

ROS are produced from endogenous and exogenous sources in the cells, with the organelles responsible for cellular respiration, such as mitochondria, endoplasmic

reticulum and peroxisomes, as the endogenous sources of ROS. In contrast, exogenous sources are the external factors such as pollution, smoke, tobacco, alcohol, transitional metals, pesticides, chemotherapy and radiation (64). Mitochondria and NADPH oxidase are two significant contributors of endogenous ROS and there is a crosstalk between mitochondria and NADPH oxidase through ROS in animal models (65).

In cancer, elevated levels of ROS and O_2^- are the result of reduction of the antioxidant defense system, increased glucose metabolism through PDKs (Warburg effect), increased production of oxidant production from mitochondria, NADPH oxidases (NOX), lipoxygenases, cyclooxygenases (COX), cytochrome P450 enzymes and xanthine oxidases (66–69).

Wnt/β-catenin

In canonical Wnt signaling, β-catenin functions as an intracellular signaling molecule. Wnt binds with Frizzled (Fz) cognate receptors and LRP5/6 co-receptors, respectively. While Wnt signaling is in an off-state, β-catenin phosphorylates complex composed of Axin, GSK-3β, CK1α and APC which undergoes ubiquitination and proteasome degradation. During the on-state, Wnt binds with the Fz receptor and LRP5/6 co-receptor. Disheveled recruits complex (Axin, GSK-3β, CK1a and APC) towards the receptor complex on the cell membrane, resulting on β-catenin stabilization. This allows the accumulation of β-catenin in the cytoplasm, which translocate into the nucleus. β-catenin displaces transcriptional co-repressor Groucho from TCF transcriptional factor and activates gene transcription (70). Nuclear β-catenin stimulates osteoblastic markers, promotes osteoblast differentiation, and is essential for the activation of ROS-induced FoxO signalling (71,72). In osteoblastic cell differentiation models, occurs oxidative stress-induced association of β-catenin with FoxOs, where H_2O_2 promotes FoxO mediated transcription, reducing wnt/TCF mediated transcription and osteoblast differentiation (73). Peroxisome proliferator-activated receptor -gamma1 and -gamma2 (PPARγ) inhibit osteoblast differentiation while increasing adipocyte differentiation. FoxOs signalling suppresses the expression and Transcriptional activity of PPARγ (73,74).

Mitogen-activated protein Kinases (MAPK)

The MAPK pathways have an important role in cell differentiation, proliferation and apoptosis (75). ERK, p38 kinases and JNK are the three groups of MAP kinase studied the most (76). MAP kinases regulate osteoblastogenesis via its downstream signaling pathways, making it a central signal transducer in the regulation of bone mass (77–79). ERK pathways downstream are Ras, RAF, ERK1/2, MAP kinase kinases, MEK1/2, and the terminal MAP kinases. Components of p38 pathways are p38 α, β, γ and δ and MAP kinase kinase 3/ 6 (MKK3/6). Components of the JNK pathway are JNK1/2 and MAP kinase kinase 4/ 7 (76). ERK signaling pathway plays an important role in osteoblast differentiation and bone formation *in vitro* and *in vivo* (80). ERK activation in osteoprogenitors is required for bone formation during skeletal development and bone homeostasis by controlling osteoblast master regulators RUNX2, ATF4 and β-catenin (81). CHIP assay of ERK signaling shows that active ERK binds to osteocalcin and bone sialoprotein promoters in osteoblast (82). Similarly, p38 MAPK pathways promote osteoblast differentiation by promoting the phosphorylation of RUNX2 on different locations such as S28, S31, S244, S301, S319, and S472 (77). JNK signaling positively regulates osteoblast differentiation while JNK inhibitors inhibited late-stage osteoblast differentiation, mineralization, and expression of Bsp, Ocn, Atf4, and Fra1. Therefore, overexpression of JNK1/2 promotes osteoblast differentiation (83,84). ROS was found to mediate RANKL induced osteoclast differentiation and subsequent activation of JNK, p38 and ERK1/2 (59,85). In contrast, H_2O_2 activates ERK-dependent NF-kB activation, which inhibits osteoblast differentiation (55,86).

Nuclear factor-kappa B (NF-κB)

Activation of NF-kB is observed upon the stimulation of various kinds of cytokines. The most prominent activators are receptor activators of NF-κB ligand (RANKL), TNFα, ROS, lymphotoxin, bacterial endotoxins, CD40L, Toll-like receptor (TLR) ligands, and interleukin-1 (IL-1). When ligands (TNFα or RANKL) bind with the receptor, signaling clusters are formed at the distal end of the receptor. These signaling clusters consist of proteins such as TNF receptor-associated factors (TRAFs), cellular inhibitors of

apoptosis (c-IAP), the tyrosine kinase c-Src TNF receptor-interacting protein (RIP) and p62. The complex recruits MAPK by utilizing lysine 63-linked polyubiquitination chains (K63-pUB), which activate the canonical pathways by MAP kinases TGF-β-activated kinase (TAK1) and alternative IKK by NF-κB-inducing kinase (NIK). Activated IKKα and IKKβ phosphorylate p100/NF-κB and IκB respectively. After the degradation, p52-RelB and p50/p65 dimers are translocated to the nucleus, bind specific DNA sequences and activate transcription (87–89). In addition, NF-kB p50 and p52, RANKL and TNF induce osteoclast differentiation by activating c-Fos and NFATc1 (90).

H_2O_2, a source for endogenous ROS, induces osteoclast differentiation (59). When the antioxidants N-acetyl-l-cysteine (NAC) and glutathione were used in pretreatment to osteoclasts, RANKL-induced Akt, NF-kB, and ERK activation were reduced. In addition, the reduction of NF-kB activity by the antioxidant was associated with reduced IKK activity and IkB alpha phosphorylation. Furthermore, NAC also inhibit RANKL induced Actin ring formation and bone-resorbing activity of osteoclast (91). Therefore, these data show strong evidence on the role of ROS in osteoclast differentiation.

In osteoblasts, inhibition of IKK/NF-kB increases the expression of Fra-1, which is an essential factor for bone matrix formation. Therefore, therapeutics targeting IKK/NF-kB may help to improve bone formation and treatment of osteoporosis (92). Similarly, NF-κB RelB inhibits osteoblast differentiation and bone formation. In addition, RelB targets the Runx2 promoter and inhibits Runx2 activation (93).

1.2.3. Oxidative stress in Remodeling and Bone disease

Homeostasis of bone mass in a healthy adult requires an exquisite balance between bone resorption by osteoclasts and bone formation by osteoblasts. Disturbances of such balance are the main cause for different bone disorders, including osteoporosis which is characterized by the predominant activity of osteoclasts over osteoblasts (2,3). The role of oxidative stress in bone disease and remodeling is mainly investigated by assessing the effect of H_2O_2, ROS and O_2^- on osteoblast and osteoclast function and in bone remodeling.

Bone resorption

At the beginning of 1990s, the first relationship between ROS, specifically O_2^- and the formation and activation of osteoclasts, was described (94,95). ROS is required for RANKL-induced osteoclast differentiation on bone marrow (BM) precursor cells (85,91,96). Similarly, H_2O_2 plays a crucial role in osteoclast formation (97). The antioxidant enzyme glutathione peroxidase 1 (Gpx1) is expressed in osteoclastic cells responsible for hydrogen peroxide's intracellular degradation. Overexpression of Gpx1 in the osteoclastic cell line RAW 264.7 prevents RANKL-induced osteoclastogenesis (49). Simvastatin, a lipid-lowering drug, decreased tartrate-resistant acid phosphatase (TRAP) expression and inhibited intracellular ROS in murine RAW 264.7 cells, suggesting that simvastatin suppress these H_2O_2-induced signaling pathways in osteoclastogenesis (98).

Recently it was found that oxidative stress with high ROS and high resorption of bone was observed upon administration of iron. Iron stimulated osteoclast differentiation *in vivo* via JNK, ERK and NF-kB pathways (99). Rosmarinic acid and arbutin suppressed osteoclast differentiation by inhibiting ROS in RAW 264.7 cells (100). Ormeloxifene, a selective estrogen receptor modulator (SERM), inhibited osteoclast formation induced by RANKL. Ormeloxifene also suppress RANKL-induced ROS production and inhibits activation of ERK1/2 (MAPK3/MAPK1), JNK (MAPK8) transcription factors (NF-κB and AP-1)(101). When osteoclast precursors are incubated with high glucose concentrations (D-glucose), these inhibit RANKL-induced osteoclast formation and ROS production (102). Thus, these studies indicate that ROS affects bone resorption by directly promoting osteoclast formation and activity.

Bone formation

Osteoblasts are the primary bone-forming cells located on the bone surface, comprising 4-6% of the total resident bone cells (13). Bone loss can result from either decreased bone formation, i.e. osteoblast differentiation or increased bone resorption, i.e. osteoclast activation. H_2O_2 shows strong evidence on the inhibition of osteoblast differentiation (54). H_2O_2 induced oxidative stress and suppressed bone formation in primary mouse BMSCs, characterized by decreased alkaline phosphatase activity (103)

and mineralization (54). Metallothionein, an inhibitor of ROS, showed to protect BMSCs against H_2O_2 induced inhibition of osteoblast differentiation, providing strong evidences on the crucial role of oxidative stress in the inhibition of osteoblastogenesis (103). H_2O_2 increased apoptotic markers (caspase -3 and caspase -9) and reduced sirtuin 1 levels. In contrast, monotropein suppressed ROS induced apoptosis by activating mitochondrial apoptotic signaling and NF-kB signaling pathways (104). Hydrogen peroxide induces G2 cell cycle arrest and inhibits cell proliferation, both concentration and time-dependently in the mouse osteoblast cell line MC3T3-E1, and in the human osteoblast-like cell line MG63 (105). In primary rabbit BMSCs, H_2O_2 treated osteoblast showed reduced expression of alkaline phosphatase (ALP), osteoprogenitors (CFU-O), collagen 1a and Runx2 (55). Nrf2, which regulates antioxidant enzymes, was increased while treating MC3T3-E1 cells with H_2O_2; while ALP, Runx2 and BGP gene expression was downregulated, together with a mineralization reduction (106). Simvastatin has been found to affect bone metabolism. It increases bone formation by promoting osteoblast differentiation and mineralization (98).

These data show the dual property of ROS in bone metabolism and signaling. ROS not only promotes osteoclast formation and activation but also inhibits osteoblast differentiation.

Bone formation/resorption coupling

The key communicators between osteoblast and osteoclast are osteoprotegerin (OPG), the RANK and the RANKL. These cytokines play an important role in bone remodeling (2,3).

The interconnection between RANK, RANKL and OPG are crucial in bone remodeling and function as a critical molecular link between osteoblast and osteoclast (107,108).

RANKL increased endogenous ROS through TNF receptor-associated factors, Rac1 and NADPH oxidase in bone marrow monocyte-macrophage lineage cells. Conversely, N-acetylcysteine inhibited bone marrow monocyte-macrophage cell response to RANKL, increased ROS and activation of JNK, p38, MAPK and ERK, resulting in osteoclast differentiation (85). Increased level endogenous ROS by H_2O_2 and O_2^- induced stimulation of RANKL mRNA and protein expression in human osteoblast like

cells (MG63 cell line, primary bone marrow derived osteoblast and calvaria-derived osteoblast) which activates osteoclast differentiation (86).

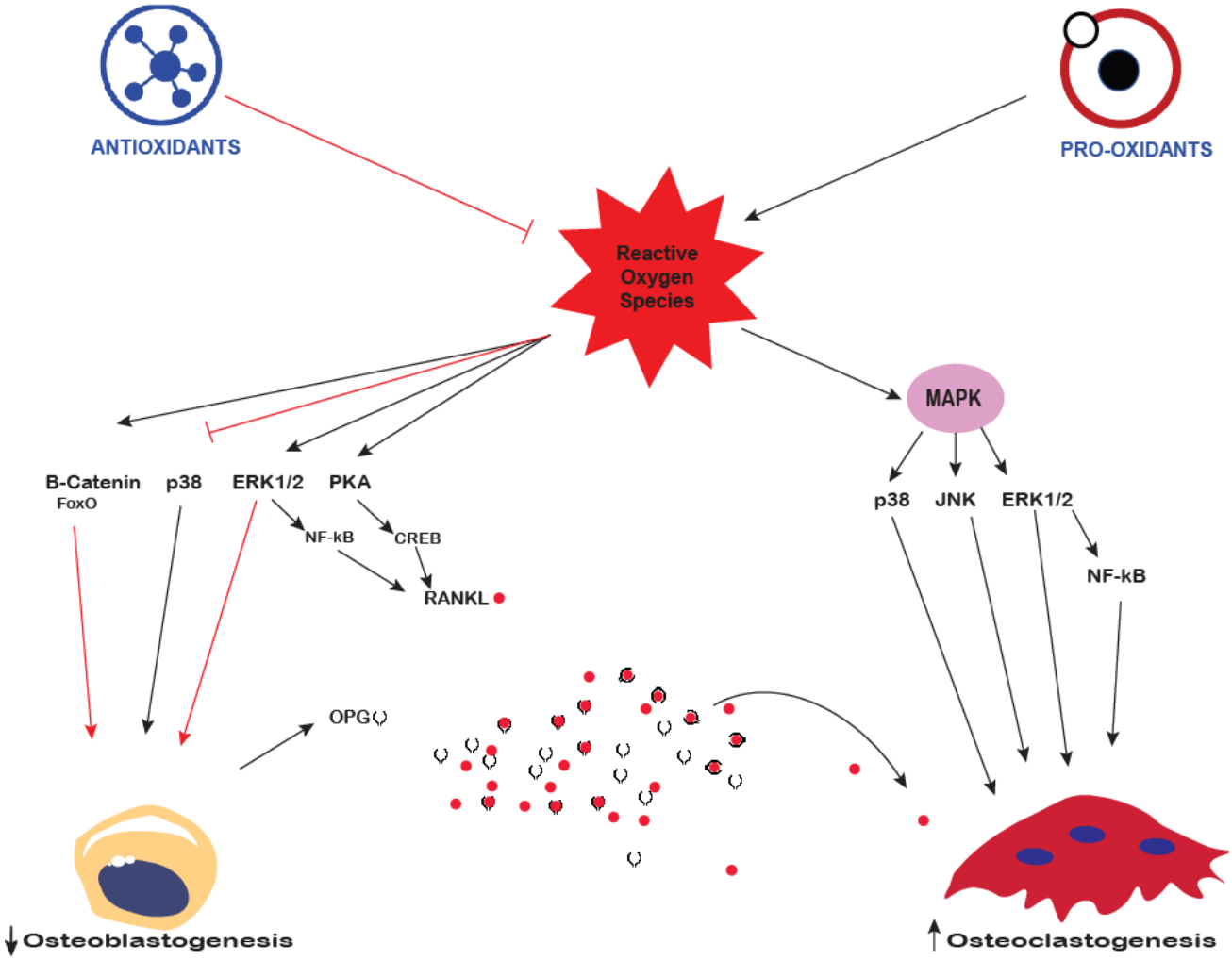

Figure 1.2.1: Molecular mechanism of ROS signaling on bone. ROS inhibits osteoblast differentiation whereas promotes osteoclast differentiation. ROS increases bone resorption directly through the activation of MAPK kinases pathways and indirectly through the OPG/RANKL ratio. Antioxidants inhibit the ROS signaling pathways, whereas pro-oxidants promote ROS signaling. Acronyms: Beta-catenin (B-catenin), Extracellular signal-regulated kinases (ERK), Nuclear factor-κB (NF-kB), Protein kinase A (PKA), cAMP Response Element-Binding Protein (CREB), Receptor activator of nuclear factor-κB ligand (RANKL), Osteoprotegerin (OPG) and c-Jun N-terminal kinase (JNK).

1.2.4. Oxidative Stress-induced Bone disease

Oxidative stress alters osteoclast and osteoblast activity, affecting bone remodeling, which results in various skeleton pathologies characterized by low bone density and

bone mass (42,49). Several clinical studies suggested the involvement of antioxidant and/or pro-oxidant systems in the pathology of bone (44–47). ROS is involved mainly by promoting bone resorption and inhibiting bone formation during bone homeostasis (91,95,102). Recent studies suggest that oxidative stress is involved in metabolic bone diseases including osteoporosis, metabolic dysfunctions such as diabetes associated bone disease, inflammatory diseases such as rheumatoid arthritis and bone tumors.

Metabolic bone disease (Osteoporosis)

Metabolic bone diseases are disorders of bone strength usually caused by abnormalities of bone mass or bone structure, lack of vitamin D and/or minerals, such as osteoporosis which is the most common, osteogenesis imperfecta, rickets/ osteomalacia, fluorosis primary hyperparathyroidism (PHPT) and Paget's disease (109,110). Osteogenesis imperfecta is a condition characterized by the presence of an abnormal matrix on osteoblastic cells due to a collagen defect (COL1A1 and COL1A2), leading to an imbalance between osteoblast and osteoclast activities and resulting in high bone turnover (110).

Osteoporosis is a disease characterized by low bone mass and density as well as deterioration of bone structure which causes bone fragility and increased risk of fracture (42,109). Osteoporosis can be classified into various types, and the common forms are "primary osteoporosis (idiopathic osteoporosis, age-related osteoporosis)"- caused by a specific factor such as age, nutrition, and physical activity. Bone loss resulting from a specific disease, medication or other external factor is known as "secondary osteoporosis" (109).

The primary trigger for osteoporosis in women is estrogen deficiency following menopause (111). Oxidative stress plays a central role in the onset of postmenopausal osteoporosis(112). The biochemical analysis of serum from women with postmenopausal osteoporosis showed a significantly decreased level of SOD, total antioxidant capacity, glutathione peroxidase and folate whereas, increased homocysteine and nitric oxide suggesting that oxidative stress may serve as a potential biomarker in the etiopathophysiology and clinical course of postmenopausal osteoporosis (112). Loss of estrogens or androgens (as in menopause or after

ovariectomy) compromise the defense mechanism against oxidative stress in bone, resulting in increased bone resorption. The hallmark of acute loss of sex steroids is an increased rate of bone remodeling. Estrogen deficiency increases the lifespan of osteoclasts and decreases that of osteoblasts (113).

Oxidative stress in postmenopausal osteoporosis is associated with activation of NADPH oxidase and/or decreased antioxidant enzymes and GSH levels (114,115). H_2O_2 is essential for oxidative stress-induced estrogen deficiency loss and osteoclast formation and activation (49). With age-related osteoporosis, there is a decrease in the OPG/RANKL ratio. Similarly, osteocyte apoptosis also plays a significant role on osteoclast activation (116).

Table 1.2.1: Diseases and medication that cause or contribute to secondary osteoporosis (109,117).

Diseases that contribute to Osteoporosis		Medications that contribute to Osteoporosis	
Endocrine Disorders	Glucocorticoid-induced osteoporosis	Hormones and Drugs with Actions on	Glucocorticoids
	Hyperthyroidism	the Endocrine System	Thyroid Hormone
	Hypogonadism		Hypogonadism-inducing agents
	Hyperparathyroidism		Aromatase Inhibitors
	Diabetes mellitus		Medroxyprogesterone Acetate
	Growth hormone deficiency and acromegaly		GnRH Agonists
Gastrointestinal, Hepatic	Celiac disease		Thiazolidinediones
and Nutritional Disorders	Inflammatory bowel disease		
	Gastric bypass surgery	Cancer Chemotherapeutic Drugs	
	Anorexia nervosa	Drugs with Actions on the Central	Antidepressants
	Hemochromatosis and chronic liver diseases	Nervous System	Anticonvulsants
Hematological disorders	Monoclonal gammopathy of uncertain significance		
	Multiple myeloma	Drugs with Actions on the Immune	Calcineurin Inhibitors
	Systemic mastocytosis	System	Antiretroviral Therapy
	Beta thalassemia major		
Renal Disorders	Idiopathic hypercalciuria		
	Renal tubular acidosis	Anticoagulants	heparin
	Chronic kidney disease	Diuretics	Loop diuretics
Autoimmune Disorders	Rheumatoid arthritis		
	Systemic lupus erythematosus	Drugs with Actions on the	Proton Pump Inhibitors
	Ankylosing spondylitis	Gastrointestinal Tract	
	Multiple sclerosis		
Genetic Disorders	Cystic Fibrosis	Others	Lithium
	Ehlers-Danlos		Methotrexate
	Glycogen Storage Diseases		Parenteral Nutrition
	Gaucher's Disease		Thyroxine
	Hemochromatosis		
	Osteogenesis Imperfecta		
	Porphyria		
	Riley-Day Syndrome		

Diabetes associated bone disease

Diabetes is associated with increased levels of oxidative stress, decreased bone quality, and increased fracture risk (118). The pathophysiology of bone disease in diabetic patients involves increased oxidative stress, altered osteoblast and osteoclast activities with increased sclerostin, decreased osteocalcin, decreased IGF1, microvasculature change, and advanced glycation end-products accumulation leading to decreased bone turnover and altered bone quality (118,119).

The Streptozotocin-induced type 1 diabetic mice model and primary bone marrow cell culture showed increased osteoclast activation initiated by hypoxia and metabolic acidosis. In addition, the activation of osteoclast resulted from the reduction of the RANKL/OPG ratio (120). Similarly, streptozotocin-induced diabetic mice showed osteopenia and an increased level of oxidative stress (121).

In vitro studies have shown that advanced glycation end products AGEs suppress mineralization of mouse stromal ST2 cells and human mesenchymal stem cells by inducing TGF-β activity, inhibition of differentiation and mineralization of osteoblastic cells (122).

Metformin, an well-known anti-diabetic medication, decreases ROS, increases osteogenic properties of adipose-derived multipotent mesenchymal stem cells and increases bone density and mineralization in healthy mice (123). Furthermore, on hyperglycemic state treated with metformin, intracellular ROS and advanced glycation end-products (AGEs) in collagen and serum levels of IGF-1 were decreased, which are beneficial for bone formation (124). Therefore, further studies are needed to provide further insight on the role of oxidative stress and its relationship to diabetic induced bone disorder.

Inflammatory diseases (Rheumatoid/Osteo Arthritis)

Rheumatoid arthritis is an autoimmune disease with a characteristic pattern of joint destruction resulting from loss of cartilage and increased bone resorption that mainly occurs in the knee and hip joints (125). Patients with rheumatoid arthritis showed increased ROS formation, protein oxidation, lipid peroxidation, DNA damage and

decreased antioxidant defense system leading to oxidative stress and disease chronicity (126).

The degenerative joint disease osteoarthritis is the most common musculoskeletal disease with increased provenance due to ageing. The factor responsible for osteoarthritis includes oxidative stress and ROS overproduction, which regulates intracellular signaling processes, extracellular matrix synthesis and degradation, chondrocyte senescence and apoptosis, synovial inflammation, and dysfunction of the subchondral bone (127). In patients with osteoarthritis, elevated ROS production and oxidative stress were found, whereas antioxidant enzymes, such as SOD, CAT, GPX and Paraoxonase 1, were decreased in these patients (128,129).

In a clinical study of synovial fluid from osteoarthritis patients, increased ROS levels stimulated vascular endothelial growth factor receptor 1 and 2 (VEGFR-1 and -2) and vascular endothelial growth factor (VEGF) expression, resulting in cartilage degradation (130). Similarly, the *in vivo* mouse model showed that NADPH oxidase expressed by chondrocytes is the main contributor to ROS formation in synovial fluid, which is responsible for increased oxidative stress inside the joint and for mediating cartilage degradation by regulating metalloproteinase (131).

Increased oxidative stress upregulates redox-sensitive transcription factors such as NF-kB, which increase proinflammatory cytokines such as cyclooxygenase-2, IL-8 and iNOS in osteoarthritis tissue. In addition, in osteoarthritis, an increased level of ROS inhibits PI3K/AKT pathways and activate MEK/ERK pathways (132).

ROS also serves as a signaling intermediate in the activation of JNK by IL-1 and TNF-α. TNF-α and bFGF induce ROS production through NADPH oxidase, which upregulated c-fos expression. Similarly, ROS regulate IL-1β induction of c-fos and MMP-1 expression (133).

1.2.5. Oxidative stress in bone remodeling: role of antioxidants and Pro-oxidants

The antioxidant system within the body is responsible for neutralizing the effect of ROS and consists of enzymatic antioxidants such as superoxide dismutase, catalase, glutathione peroxidases, thioredoxin and non-enzymatic antioxidants such as vitamins (Vitamin A, C and E), minerals (Copper, Zinc, and Selenium), flavonoids (flavonols,

anthocyanins, isoflavonoids, flavanones and flavones), polyphenols (hydroxycinnamic and hydroxybenzoic acids) and carotenoids, which directly or indirectly reduce the oxidative stress of the cells (134,135).

Vitamin A, Vitamin C and Vitamin E

Vitamin C

Vitamin C is a well-known inducer of osteoblast differentiation. Vitamin C regulates extracellular matrix composition/collagen homeostasis and plays an essential role in the differentiation of mesenchymal stem cells towards osteoblasts, chondrocytes, and tendons (136).

Vitamin C is a naturally obtained reducing substance. Endogenously, Vitamin C serves to balance and maintain intracellular redox reactions. The ROS [superoxide anion (O_2^-), singlet oxygen (O_2^-), hydroxyl radical (OH^-) and hypochlorous acid (HClO)] produced during mitochondrial oxidative phosphorylation are reduced by vitamin C (137).

Several studies have revealed osteogenic properties of ascorbic acid in *in vitro* cell differentiation on human and murine pre-osteoblast via inducing deposition of the extracellular collagen matrix, expression of osteoblast differentiation-specific genes such as alkaline phosphatase, osteocalcin, osteopontin, osteonectin and runt-related transcription factor 2 (Runx2) (138–141). In addition, ascorbic acid promotes the differentiation of the stromal ST2 cell line into osteoblast by increasing collagen type I matrix formation via activation of BMPs (142). Ascorbic acid combined with dexamethasone and β-glycerophosphate positively promotes differentiation of mouse embryonic stem cells into osteoblast (143).

In the case of *in vitro* osteoclast differentiation, ascorbic acid showed both stimulatory and inhibitory effects. Ascorbic acid significantly inhibited the cell proliferation, mRNA and protein expression of carbonic anhydrase, number of tartrate-resistant acid phosphatase positive multinucleated cells (TRAP) and resorption lacunae area induced by RANKL in RAW 264.7 cells (144). However, when treating embryonic stem cells with ascorbic acid the number of TRAP-positive cells were significantly increased (145). Similarly, when treating the stromal cell with ascorbic acid and 1α, 25-dihydroxy-vitamin,

RANKL expression was increased by fivefold, and TRAP-positive cells were decreased (146).

Previous *in vivo* experiments showed that vitamin C prevented bone turnover in ovariectomized mice. This improvement in bone turnover was seen in bone mineral density, and micro-CT parameters are the result of stimulation of bone formation as showed by the histomorphometry result, bone markers measurement and qPCR (147).

Vitamin E

Vitamin E is a lipid-soluble vitamin with two subgroups; tocopherol and tocotrienol, and eight isoforms: α, β, γ, and δ isomers of tocopherols and tocotrienols (148). It has an excellent antioxidant capacity, which differs among the isomers. *In vivo* experiments on nicotine-treated rats showed that vitamin E increased the trabecular bone and protects bone calcium loss (149) on the study of the effect of vitamin E (α -tocopherol and δ -tocopherol) on the primary osteoblast cells from rat calvariae. Tocopherol initially decreased alkaline phosphatase activity and expression of osteocalcin, while in the final stage of osteoblast differentiation, ALP activity and osteocalcin were returned to normal levels compared with control groups (150). In addition, human mesenchymal stem cells proliferation was enhanced after α -tocopherol treatment. The expression of alkaline phosphatase, Runx2, bone morphogenetic protein, matrix metalloproteinase 2, and transforming growth factor-beta 1 were significantly increased in the α -tocopherol treated cells (151).Co-cultures of mouse bone marrow cells and calvarial osteoblasts showed that α-tocopheryl succinate decreased RANKL expression in osteoblasts and further inhibited osteoclastogenesis induced by IL-1(152).

Vitamin A

Vitamin A (retinol) is a fat-soluble vitamin mainly associated with vision supplied by food intake of retinyl esters and carotenoids. Retinol is converted to all-trans retinoic acid (ATRA), an active form of vitamin A (153,154). Vitamin A has both catabolic and anabolic effects on bone. Retinol may act as an effective antioxidant by donating H ion as well as acting as pro-oxidant by yielding reactive hydroxyl radical (155).

Many *in vitro* studies report that ATRA inhibits osteoblastic differentiation and functions, alkaline phosphatase activity, osteocalcin expression, mineralization on fetal rat calvaria cells (156) and human osteoblastic cells (157,158). ATRA also inhibited bone nodule mineralization in primary human osteoblasts and MC3T3-E1 cell culture and decreased mRNA expression of osteoblast differentiation markers Runx2, Sp7, Alp l, osteocalcin, and Col1a1(159,160).

An *in vivo* experiment in mice with oral vitamin A showed decreased periosteal circumference and bone mineral content concluding that clinically relevant doses of vitamin A have a negative impact on the amount of cortical bone in mice (153).

Minerals (Copper, Zinc, and Selenium)

Zinc is an essential micro-element with the antioxidant capacity required for bone formation. Supplement of zinc reduced oxidative stress biomarkers in the elderly (161,162). Zinc serves as a cofactor in many metalloenzymes and is extremely important in skeleton health. Zinc stimulates bone formation and mineralization *in vivo* (163) and *in vitro* (164). Zinc deficiency has been linked with impaired osteoblast functions with decreased collagen synthesis and alkaline phosphatase (165); similarly, during calvaria tissue cultures and osteoblast cell cultures, increased osteoblast differentiation and mineralization, alkaline phosphatase, and decreased bone resorption were seen (163,166). On murine preosteoblastic cell line MC3T3-E1 similar results with increased osteoblast proliferation, alkaline phosphatase activity, mineralization and collagen formation were seen while treated with zinc (167).

In the bone, zinc deficiency induced oxidative stress due to iron accumulation and downregulation of antioxidants such as Mt1a, Mt2A and Cu/Zn-SOD. In addition, deficient zinc also increased cytokines-induced osteoclast differentiation (TNFα- and IL-1β-induced RANKL expression) and activation, expression of osteoclast differentiation genes whereas decreased osteoblast differentiation gene expression (ALP, Oc, Col1a1, Runx2 and Osterix/Sp7) (168).

Copper also plays an important role in bone health maintenance and other biological processes, including antioxidant defense, enzymatic reactions, iron metabolism, nucleic acid synthesis and immune function. *In vivo* studies showed that copper-deficient diet

reduced bone mineral content and bone strength (161,165). High/low copper level in serum both indicate deformities on the bone. Lower serum copper significantly decreased bone mineral density of femur and femoral neck, whereas higher serum levels are significantly associated with increased total fracture. Therefore moderate serum copper is essential for vital bone health (169).

Selenium is an essential trace mineral that plays an important role in cellular redox status and is beneficial for bone health (170). Selenium is also a constituent of selenoproteins whose major function is antioxidative scavengers, and deficiency of selenium has been reported to influence bone metabolism (171). Deficient selenium in mice showed impaired bone metabolism, osteopenia with increased bone resorption, altered bone microarchitecture, reduced bone mineral density and bone volume through the decreased antioxidative potential (170,172). Similarly, a cohort study of humans found that higher selenium levels showed higher hip bone mineral density and lower bone formation and resorption markers. Higher selenoprotein was initially associated with higher hip and lumbar spine bone mineral density and higher hip BMD after the six years follow-up and with lower osteocalcin and type 1 collagen (173).

Natural Flavonoids antioxidants

Resveratrol (RES) is a polyphenolic (3,4′,5-trihydroxystilbene) compound that is naturally found in a variety of plant foods such as grapes, cranberries, and nuts (174). RES has anti-inflammatory, estrogenic, antioxidant and proliferative properties, which can influence bone metabolism (175). RES increases bone mineral density by promoting osteoblastogenesis and inhibiting osteoclastogenesis; pharmacological therapies currently available work either by promoting osteoblast activity or by inhibiting osteoclast activity. Therefore, RES may have advantages over the therapeutics in use (176). Similarly, RES also stimulates osteoblastogenesis by acting as an estrogen agonist (177). Therefore, RES may act as an effective therapeutic agent for age-related degenerative diseases such as osteoporosis (178,179).

Human bone marrow-derived mesenchymal stem cells (MSC) exposed to RES presented an increased gene expression of the critical osteogenic transcription factors Runx2 and Osterix. Furthermore, RES activated the estrogen-mediated extracellular

signal-regulated kinase (ERK) 1/2 signaling pathway regulating osteoblast differentiation and proliferation (180). In addition, RES activated AMP-activated protein kinase (AMPK), which regulates osteoblast differentiation and inhibits bone resorption by acting as a negative regulator of RANKL (181). RES also augmented Wnt signaling, which stimulated osteoblastogenesis and bone formation (182).

Activation of Sirt1 was found to upregulate Runx2 gene expression resulting in differentiation of human MSC towards the osteoblastic lineage upon treatment with RES (183). RES also suppressed osteoclastogenesis by acting through Sirt1. During the interaction between RANK - RANKL, Sirt1 binds to RANK, thus inhibiting RANKL signaling pathways (184,185).

Marine extracts

Antioxidants from marine sources are getting significant attention at present. Marine antioxidants research has been mainly focused on the antioxidant capacity of the crude extract (186). In addition, marine micro/macro-algae are an essential source of antioxidants such as polyphenols, tocopherols and carotenoids (187). These marine antioxidants are mainly composed of chlorophylls, carotenoids, tocopherol derivatives (188) and polyphenols (189).

Fucoidans are the antioxidants (fucose-containing, sulfated polysaccharides) mostly found in brown seaweeds and algae (190). When used to treat human osteoblast cells, fucoidan increased cell proliferation and differentiation markers (191). Similarly, fucoidan increased mRNA expression of BMP-2, COL I, ALP, BSP, osteocalcin and osteonectin in 7F2 cells and increased bone density and bone ash weight in mice (192). Furthermore, in human alveolar bone marrow-derived mesenchymal stem cells treated with fucoidan cell proliferation was induced, with increased ALP activity and calcium deposition, while mRNA expression of osteoblast differentiation markers such as Runx-2, ALP, Col Iα and osteocalcin was found to be increased. Moreover, BMP-2-Smad1/5/8 expression was increased, and activation of JNK, ERK and p38 MAPK was seen (193).

A phycobiliprotein, C-phycocyanin extracted from blue-green algae, reduces osteoclast formation and activation, acting through NF-kB signaling pathways. In addition, C-

phycocyanin blocks the degradation of cytosolic IκB-α therefore activates downstream markers c-Fos and NFATc1 (194).

Skeletonema costatum

Polyphenolic compounds isolated from marine algae exhibit a broad spectrum of beneficial biological properties, including antioxidant, anticancer, antimicrobial, anti-inflammatory, and anti-diabetic activities, along with several other bioactivities centered on their antioxidant properties (195). Marine organisms are an auspicious source of antioxidants and osteogenic compounds. Algal sources have shown excellent osteogenic properties and drug discovery potential (196). Skeletonema costatum is a species of microalgae that contains high antioxidant properties, therefore they have a high potential for having an anabolic effect of bone.

Mitochondrial targeted antioxidants

Mito-TEMPO (MT) is a mitochondrion targeted antioxidant (197). Triphenylphosphonium chloride (MitoTEMPO) is a superoxide scavenger and a physiochemical compound mimicking superoxide dismutase from mitochondria. It can easily pass through the lipid bilayers and accumulate in the mitochondria (198). Mitochondria are the primary source of ROS and the main sites of ROS-induced damage. Mitochondrial dysfunction essentially influences osteoblasts through the regulation of mitophagy, apoptosis, and mitochondrial DNA damage. Therefore, improving mitochondrial functions through the application of antioxidants can prevent cytotoxicity and dysfunction in osteoblasts (199).

Mitochondrial ROS are essential for the hypoxic enhancement of osteoclast differentiation (200). Effect of mitochondrial reactive oxygen species (mtROS) on osteoclast differentiation and resorption in the hypoxic environment was reversed by the mitochondria-specific antioxidant MitoQ (201), which prevented the hypoxic induction of NF-κB and calcineurin-NFAT pathway. In contrast, NAC (N-acetyl-cysteine), ascorbate and 1, 2-bis (2 aminophenoxy) ethane N, N, N′, N′-tetra acetic acid (BAPTA) inhibited osteoclast formation at high concentrations (201). Mitochondrial antioxidants increase osteoblast differentiation while decreasing osteoclast differentiation.

Alpha-lipoic acid

Alpha-Lipoic acid (ALA) is also known as thioctic acid (1,2-dithiolane-3-pentanoic acid). It is a cofactor of mitochondrial respiratory enzymes (pyruvate dehydrogenase and α-ketoglutarate dehydrogenase) (202). *ALA* serves as a powerful antioxidant working through different mechanisms such as scavenging free radicals, chelation of metal ions and regeneration of endogenous and exogenous antioxidants such as vitamin C and E, ubiquinone and glutathione (202–204). Numerous experiments showed the antioxidant capacity of ALA that effectively inhibits ROS induced implication on various pathologies such as ischemia-reperfusion injury, diabetes-induced oral implant failure and radiation injury (205,206). ALA was orally administrated for 30 days in an experiment with rats, and bone was examined. TGF-β expression was significantly higher in ALA treated groups, and similarly, it was confirmed by histopathological, radiographical, CT, and biomechanical analyses. The serum levels of cytokines (TNF-α and IL-6) and bone markers (osteopontin and osteocalcin) were significantly increased, indicating that ALA accelerates bone fracture healing (206). ALA inhibited COX-2 activity and PGE2 production and increased RANKL expression, thereby inhibiting osteoclast formation and bone loss (207). Similarly, in *in vitro* cell differentiation, ALA scavenged ROS suppressed bone marrow-derived osteoclast differentiation by RANKL and TNF-α expression and inhibited NF-kB activation (208).

Prooxidants

Prooxidants have a negative impact on skeletal health. In addition, some endogenous pro-oxidants such as hydrogen peroxide (discussed previously in the mechanism of ROS) directly affect bone remodeling through various cell signaling pathways. Some therapeutic drugs working on oxidative mechanisms give rise to secondary osteoporosis.

Hydrogen peroxide (H_2O_2)

H_2O_2 is a well-known inducer of oxidative stress in various cell lines. Hydrogen peroxide, in turn, may be partially reduced to hydroxyl radical (•OH) or fully reduced to water with the production of free radicals (209).

$H_2O_2 + e^- \rightarrow HO^- + {}^{\bullet}OH_2$

$H^+ + 2\ e^- + H_2O_2 \rightarrow 2\ H_2O$

H_2O_2 occurs in normal metabolism in mammalian cells and is a crucial metabolite in oxidative stress. H_2O_2 modulates the activity of transcription factors AP-1, NRF2, CREB, HSF1, HIF-1, TP53, NF-κB, NOTCH, SP1 and SCREB-1 (210). On BMSCs and calvarial osteoblasts, exposure to a low dose of H_2O_2 (0.1 mM) showed decreased expression of osteoblastic differentiation markers, while a higher dose of H_2O_2 (1 mM) induced cell death (211).

Prooxidant Drug - doxorubicin

Doxorubicin (DOX) has been known as the primary form of anticancer drug which causes toxicity, characterized by massive accumulation of ROS and reactive nitrogen species (RNS) as central working mechanisms (212). Breast cancer patients who are already at increased risk of developing bone metastases and osteolytic bone damage, are often treated with doxorubicin. Unfortunately, DOX has been reported to induce damage to the bone. Moreover, DOX treatment increases circulating levels of TGFβ in murine pre-clinical models. TGFβ has been implicated in promoting osteolytic bone damage due to increased osteoclast-mediated resorption and suppression of osteoblastic differentiation. Therefore, in a pre-clinical breast cancer bone metastasis model, administration of doxorubicin would accelerate bone loss in a TGFβ-mediated manner (213). Multiple lines of evidence demonstrate several adverse effects of doxorubicin on the bone. Childhood recipients of DOX suffer long term bone damage in the form of reduced adult height and increased fracture risk (214). A recent study indicated that premenopausal breast cancer patients treated with a DOX/cyclophosphamide combination exhibited low bone mineral density and significant bone loss (215), suggesting a cause and effect relationship between DOX treatment and systemic bone loss. DOX exposure caused a 60% reduction in bone formation in normal rats, suggesting a potential for reduced osteoblast differentiation (216) (217). DOX has also been shown to negatively regulate trabecular bone volume and cortical bone thickness in rabbits (218). At a cellular level, doxorubicin has been reported to inhibit cell proliferation and parameters of cell differentiation in MC3T3 mouse

osteoblasts (219). DOX-induced ROS overproduction occurs inside mitochondria and is mediated by the mitochondrial NADPH oxidase (mitoNOX) activity (220). These adverse effects increase the concern for breast cancer patients who have received DOX as a part of their treatment regimen because these patients are already at high risk for bone loss and pathological fracture (213).

1.2.6. Balancing Pro-oxidants with Antioxidants

As discussed previously, oxidative stress results in bone turnover altering the bone remodeling process, causing an imbalance between osteoclast and osteoblast activity. ROS are primarily involved in increasing oxidative stress by promoting bone resorption and inhibiting bone formation during bone homeostasis. Several clinical studies suggest the importance of the antioxidant system to reduce the effect of bone pathologies (42–47,49,91,95,102).

The multifunctional polyphenolic compound RES has been shown to increase bone formation in numerous *in vivo* and *in vitro* experiments that increase bone formation by osteoblastogenesis or decreased resorption by inhibition of osteoclastogenesis via balancing oxidative stress within the bone cell (176–185,221,222). In addition, many studies showed that RES reduces the endogenous ROS and activates various signaling pathways (223,224). In the case of secondary osteoporosis, RES was shown to prevent the effect of specific therapeutic drugs over bone. Furthermore, RES showed a protective effect over glucocorticoid-induced bone damage by reducing oxidative stress. Therefore, RES may be a good candidate drug for use against osteoporosis (225).

Similarly, in osteoporosis induced by excessive iron, resveratrol significantly prevents bone loss. RES rescued the inhibitory effect of excess iron on Runx2, OCN and type I collagen. FOXO1 upregulation as well as an equilibrium between antioxidant/pro-oxidant were observed (226). On a controlled clinical trial with type 2 diabetes patients, 500 mg supplementation with RES prevented the loss of bone density (227).

Antioxidant from blue-green algae, C-phycocyanin, attenuates osteoclast differentiation (TRAP-positive osteoclasts), dentine matrix resorption and mRNA and protein expression of osteoclast differentiation markers (cathepsin K and integrin β3) induced

by ROS (194). Therefore, C-phycocyanin from blue-green algae showed evidence to promote an equilibrium between the pro-oxidant effects and its antioxidant capacity. Similarly, Polyphenols rosmarinic acid (from Perilla frutescens, lemon balm mint, sage and sweet basil) and arbutin (from Ericaceae, Asteraceae and Vaccinium) inhibited ROS induced osteoclast differentiation (100).

Simvastatin (HMG CoA reductase inhibitors), a lipid-lowering drug, inhibited osteoclast differentiation. In addition, simvastatin reduced TRAP expression and ROS mediated signaling pathways of NF-kB, AKT/PK B, JNK and P38 MAPK. This indicates that simvastatin has potential usefulness on ROS/oxidative stress-induced osteoporosis and bone resorption (98,228).

Thymoquinone is a major compound extracted from black seed oil and was previously shown to regulate the dedifferentiation and inflammation of rabbit articular chondrocytes resulting in osteoarthritis. Thymoquinone increases ROS production, decrease expression of COX-2 and prostaglandin in a dose-dependent manner through increase in p38, p-ERK and PI3K signaling pathway. Interestingly, antioxidant N-acetyl cysteine inhibited the dedifferentiation and inflammation caused by the thymoquinone induced ROS (229).

ALA was also shown to exert a protective effect against primary and secondary osteoporosis. Furthermore, in the type 2 diabetic rat model, *ALA* showed a protective effect over uncontrolled diabetes-induced bone loss. Thus, it is evident that antioxidant supplements provide an effective strategy for secondary bone defect treatment under diabetic conditions (230).

Cadmium is a high toxicity metal, that is most commonly found in the environment. Cadmium induces oxidative stress by various mechanisms such as by displacing Fenton metals from proteins, so that toxic hydroxyl radicals are produced and bind to mitochondrial membrane resulting in the disturbance of oxidative phosphorylation and production of peroxide radicals. Male wistar rats were exposed to cadmium for three months and supplemented with alpha-lipoic acid. ALA rescued Cadmium-Induced oxidative stress, inflammatory process and bone metabolism defects (231).

In vivo experiments with rats investigating glucocorticoid-induced osteoporosis showed osteogenic promoting effect by inhibiting oxidative stress upon treatment with *ALA* acting through NF-kappa B, JNK, NOX4 and PI3K/AKT signaling pathways (232).

Polyphenolic extract from melon (heat-treated melon extract) showed a protective effect against osteoporosis induced by ovariectomy in female rats. In addition, the melon heat-treated extract significantly increased whole-body bone density, femur and lumbar spine and bone metabolism markers (C-telopeptide cross-linked collagen type I as a bone resorption marker and alkaline phosphatase, osteocalcin, and calcium as bone formation marker) in ovariectomized rats (233). Furthermore, selenium supplement reversed hydrogen peroxide-induced inhibition of osteoblast differentiation mediated by ROS and oxidative stress (234,235). Supplement of vitamin C and Vitamin E on clinically diagnosed osteoporosis patients showed a significantly decreased serum MDA, TrACP and a significant increase in serum SOD and erythrocyte GSH after 90 days. In addition, bone status was improved with antioxidant vitamin supplementation. Therefore vitamins C and E can be used as a palliative treatment for osteoporosis (236). *In vivo*, vitamin C showed a protective response on oxidative stress and bone mineral density of ovariectomy rats (237).

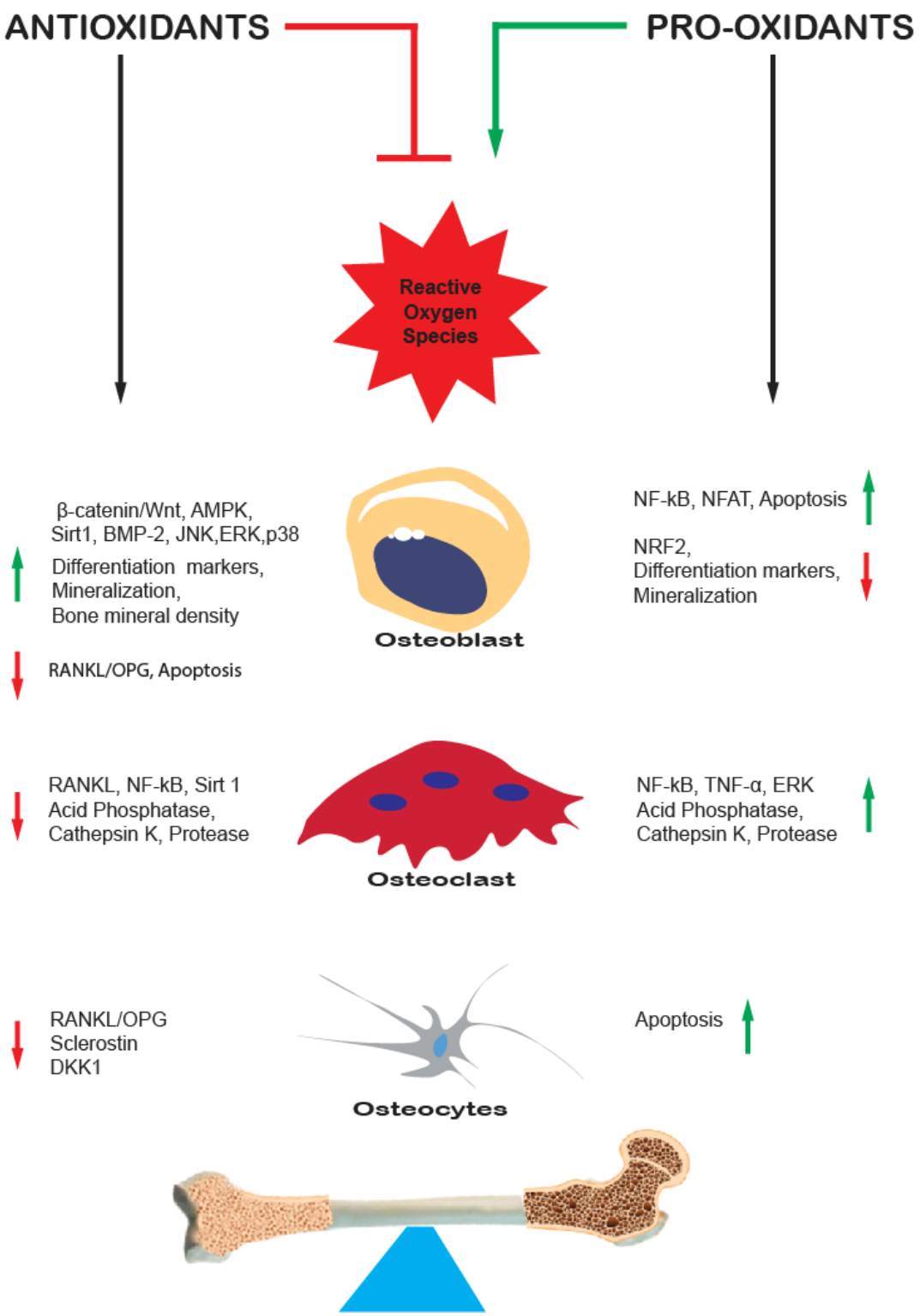

Figure 1.2.2: Effect of Antioxidants and Pro-Oxidants on bone remodeling. Antioxidants inhibit oxidative stress and stimulate bone formations acting on various signaling pathways in the remodeling process. On the other hand, pro-oxidants increase oxidative stress and increase bone resorption, affecting various signaling pathways, cytokines, enzymes, and proteins in bone remodeling.

1.2.7. Fish as a model for oxidative stress in bone

In this decade, small fish models such as zebrafish and medaka are alternatives to classical mammalian models because of several advantages. Due to this unique characteristic of small fish such as large embryo clusters, small size and easy to maintain and manipulated during experiments, rapid development, easily visualized embryonic development and robust in nature. The number of publications reporting fish in medical research has increased tremendously in the last years (238). As a skeletal model, zebrafish and medaka are emerging in biomedical research because of the similar molecular mechanism and signaling pathways on skeletal pathologies and development (239).

The skeleton system among the vertebrates is highly conserved; however, while comparing it with the teleost fish (zebrafish and medaka), most of the skeleton elements are still present on these model animals, which is an advantage for the study of bone formation and remodeling (Figure 1.2.3).

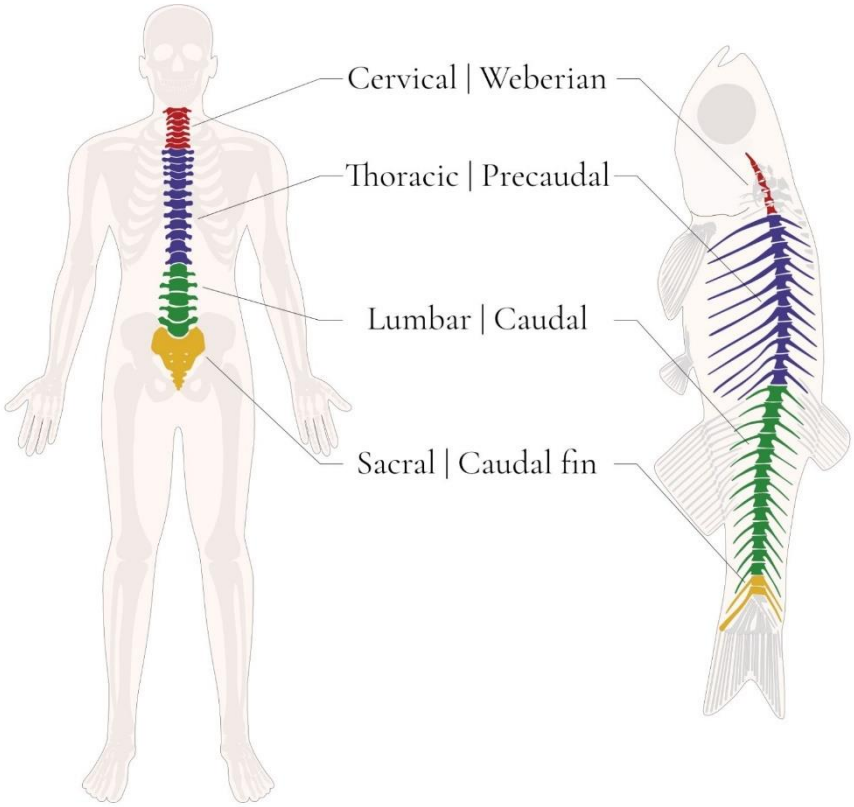

Figure 1.2.3: Comparison between human and fish skeleton system. The Human spine consist of 30 vertebrae starting from the base of skull to the pelvis. The vertebrae are categorized into; cervical vertebrae (red), thoracic vertebrae (blue), lumbar vertebrae (green) and sacral vertebrae (yellow). The zebrafish spine's organization and structure are remarkably similar to that of humans, with 29-33 vertebrae divided as Weberian vertebrae (red), precaudal vertebrae (blue), caudal vertebrae (green), and caudal fin vertebrae (yellow). Adapted from (240,241).

The gene sequencing of zebrafish (242) and medaka (243) has been an advantage for many epigenetics cell signaling research. For example, a comparison between zebrafish and human genome showed 70% similarities of orthologues (238,239,242). Furthermore, the advancement of gene-editing tools such as TALEN and CRISPR/Cas9 has increased research on the human genetic disease by generating transgenic and mutant fish models (238,239,244).

On skeletal research, zebrafish and medaka has been emerging as a powerful models for osteoporosis research with widely used methods on bone formation and development (operculum assay), analyzing deformities on the vertebral column (245), regeneration of skull and fin rays (246–248), ossification and mineralization process as shown in figure 1.2.4.

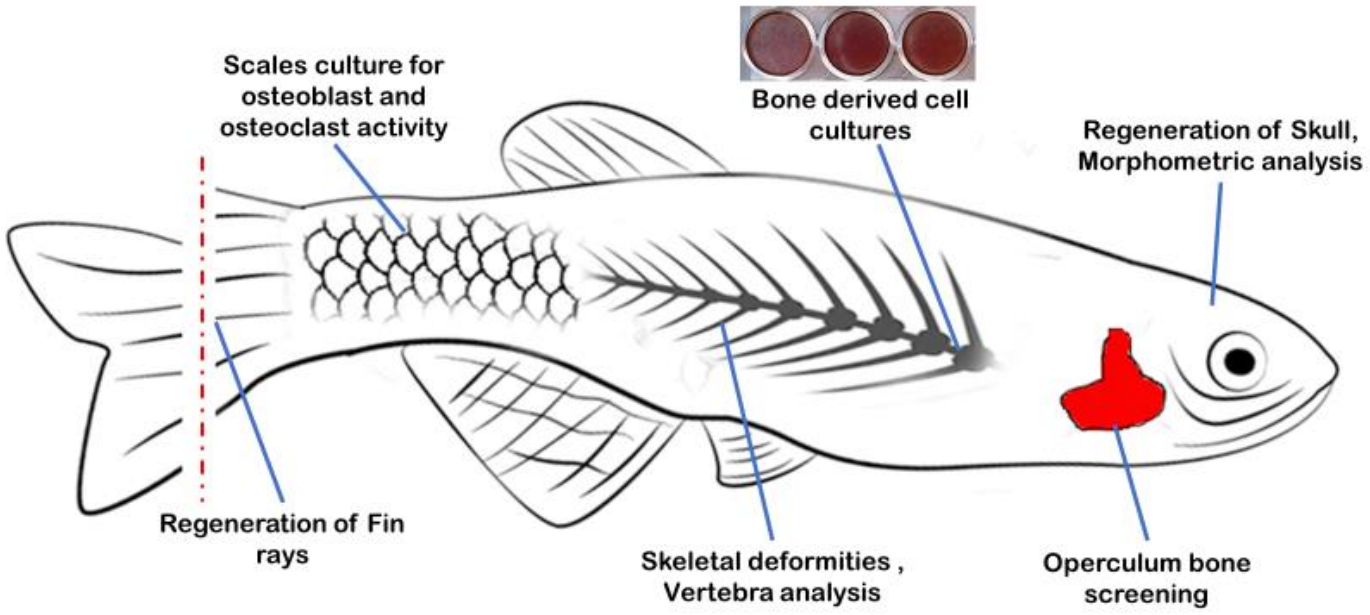

Figure 1.2.4: *In vivo* fish model for skeletal analysis. From Left, fish model for regeneration (caudal fin amputation study), scale *ex vivo* culture, analysis of axial skeleton deformities and vertebrae mineralization, bone derived osteoblast mineralization (*in vitro)*, operculum bone mineralization for screening of bone anabolic compounds.

With the advancement in technology, several *in vitro* systems have been established from mineralizing tissues of fish. The cells derived from the calcified zebrafish tissue are able to differentiate into osteoblast and chondroblasts by expressing differentiation markers, alkaline phosphatase activity, and extracellular matrix mineralization (249). Similarly, the cells derived from *Sparus aurata* calcified tissues (ABSa15, VSa13 and VSa16) showed excellent mineralization capacity and are currently extensively used for mineralization assay (250,251). Furthermore, fish scales are also used for *in vitro* analysis of osteoblast and osteoclast function through histological and biochemical methods (252–254). The screening of bone development in zebrafish morphometric analysis of operculum on the developing larvae through live imaging has shown a great significance on bone studies (255–257).

Impact of oxidative stress on bone remodeling in Fish

Regarding oxidative stress on bone in zebrafish, dexamethasone has been shown to induce osteoporosis by producing ROS. Tanshinol, an antioxidant compound from *Salvia miltiorrhiza Bunge,* showed a protective effect over dexamethasone-induced osteoporosis by scavenging ROS (258). Similarly, RES showed a protective effect against dexamethasone-induced osteoporosis by reducing oxidative stress (225). Another antioxidant, such as Evodiamine from the fruit of *Evodia rutaecarpa* prevents dexamethasone-induced osteoporosis by regulating the RANKL/RANK/OPG signaling pathway (259). Furthermore, salvianolic acid B has increased bone formation and rescued glucocorticoid-induced osteoporosis by preventing oxidative stress and increasing osteoblast-specific gene expression (260).

CHAPTER 1.3

OBJECTIVE

This thesis was developed in the framework of a Marie Sklodowska-Curie Innovative Training Network (MCSA-ITN) [H2020, Marie Skłodowska-Curie Actions Innovative Training Network No 766347] with the primary research aim to create an innovative expertise combining research in skeletal biology of aquaculture fish species with that in biomedical models and humans.

Osteoporosis has become a significant public health issue worldwide, and till now, no gold standard regimes are available. Depending upon the aetiology, various factors responsible for osteoporosis can be categorized as primary and secondary. Oxidative stress has been associated with various metabolic bone diseases through the action of reactive oxygen species (ROS). Pro-oxidant drugs have increased ROS and induced bone loss in patients during chemotherapy. Understanding the role of oxidative stress in the development of primary and secondary osteoporosis could lead to further research towards preventive and therapeutic measures to combat osteoporosis. Furthermore, oxidative stress is a key factor for impaired osteoblastic bone formation, thus protection of osteoblastic activity from oxidative damage or inhibition of osteoclastic activity by antioxidants may have a potential therapeutic value for osteoporosis. The presence of skeletal anomalies is one of the most important bottlenecks in current aquaculture production. Skeletal deformities in farmed teleosts are a persistent problem in aquaculture, posing a high economic burden. Interestingly, ROS have been found in farmed fish to cause specific types of skeleton anomalies with persistent damage to the quality of fish produced. ROS production is regulated by the balance of pro-oxidant and antioxidant nutrients, however the combined effect of these nutrients on bone formation and remodeling has not been studied, neither in human nor in fish.

The main objective of this thesis under this framework is to better understand the role of ROS on bone formation and remodeling, especially on osteoblast and osteoclast activity, as well as the effect of these nutrients in bone mineralization and remodeling on *in vitro* and *in vivo* models.

In general, this work aims to uncover the novel mechanism involved in antioxidant induced bone development and pro-oxidant induced bone impairment. The general objective is further dissected into specific objectives. The first objective of this study is to examine *in vitro* and *in vivo* effect of antioxidants and pro-oxidants in bone mineralization and remodeling. Pro-oxidants are known to induce ROS, reactive nitrogen species and their intermediates, which negatively affects bone, either by limiting osteoblast differentiation or enhancing osteoclast differentiation.

The second objective of the study is to counteract or reverse the pro-oxidant-induced bone impairment both *in vitro* and *in vivo.* We will examine the potency of antioxidants to counteract the pro-oxidant drugs that increase oxidative stress by increasing free radicals, deteriorates osteoblastic differentiation and mineralization, and enhances osteoclastic differentiation and activity. Therefore, these antioxidants can be used as therapeutic agents for osteoporosis or as a supplement to counteract pro-oxidant-induced bone impairment.

In order to achieve the objective of the BIOMEDAQU project on translational research, we interned to use an *in vitro* and an *in vivo* approach using fish models. Specifically, we will test our hypothesis on osteoblast differentiation and mineralization [MC3T3-E1 cells] and osteoclast differentiation [Raw 246.7 cells] derived from murine. The results obtained from our *in vitro* studies will be confirmed by *in vivo* with osteocytic bone model zebrafish as part of biomedical research and with non-osteocytic bone model gilthead seabream as part of aquaculture research.

CHAPTER 2

MOLECULAR MECHANISMS

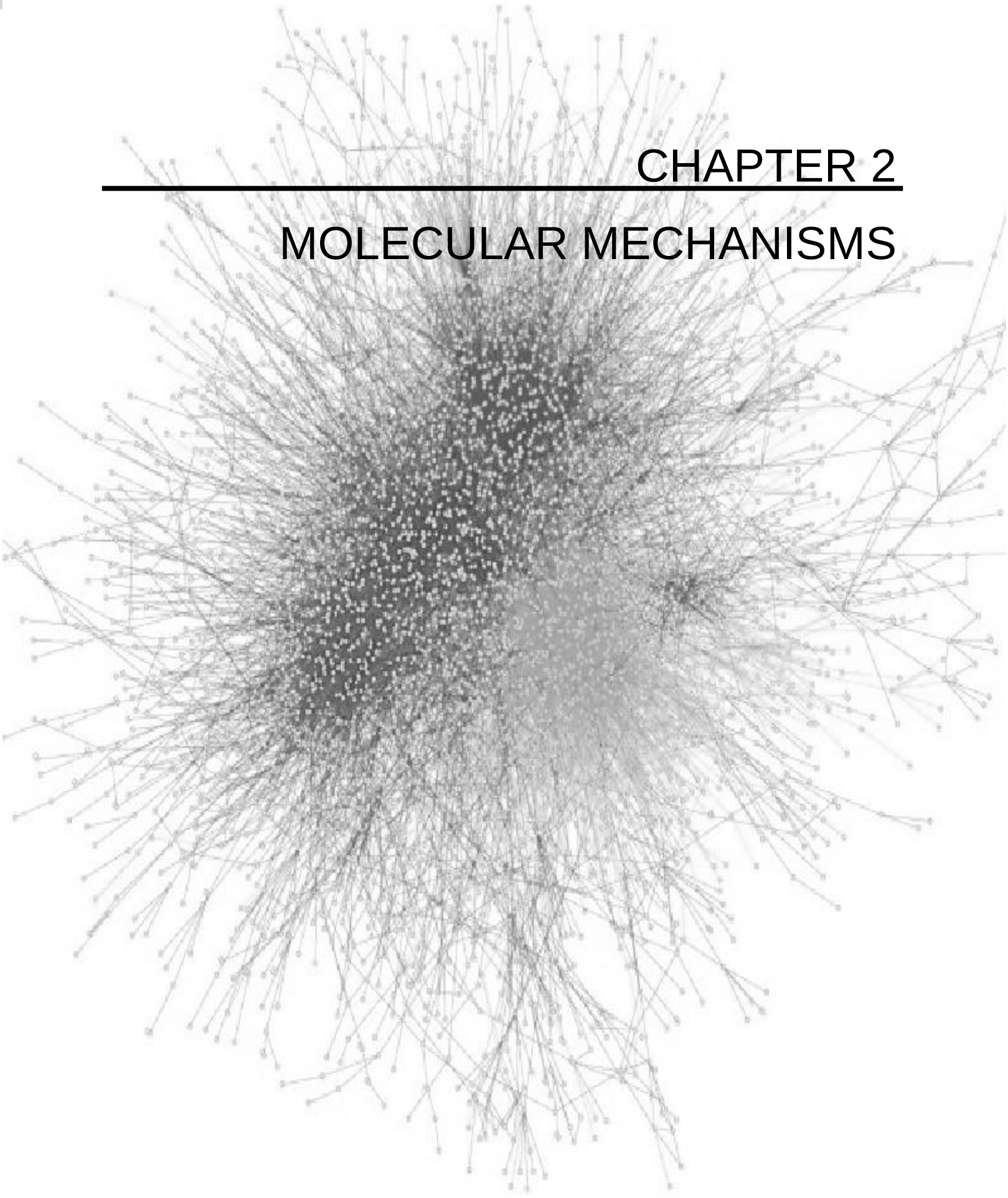

PREAMBLE

This chapter aims to investigate the molecular mechanisms of doxorubicin-induced bone loss and reversal effect by antioxidant supplementation. This chapter explains the molecular mechanism of doxorubicin-induced bone loss on both osteoblast and osteoclast cells. The first part consists of the analysis of doxorubicin induced bone loss and its reversal by the transcriptome analysis of murine osteoblast cells, along with gene ontology analysis and KEGG pathway analysis. The chapter 2.1 is planned to be submitted to BMC genomics. The second chapter consists of osteoclast differentiation during doxorubicin and antioxidant supplementation along with an *in vivo* experiment with transgenic reporter zebrafish [*tg(ctsk-dsRed)*]. Chapter 2.2 is published in the *International Journal of Molecular Sciences* (IJMS) with the title “Resveratrol-mediated reversal of Doxorubicin-induced osteoclast differentiation” [https://doi.org/10.3390/ijms232315160].

CHAPTER 2.1

Transcriptomic analysis of signaling pathways associated with reversal of doxorubicin-induced osteoblastic differentiation of MC-3T3E1 cells

Sunil Poudel

Gil Martins

M. Leonor Cancela

Paulo J. Gavaia

Chapter to be submitted to BMC Genomics

ABSTRACT

Doxorubicin (DOX) has been known as the first-line chemotherapeutic agent causing various toxicity through the accumulation of free radicals causing oxidative stress. The DOX has shown to increase bone loss and reduce osteoblast differentiation. In patients under the DOX regimen, increased risk of bone metastasis and osteolytic injury in patients has been reported. However, the precise cellular and molecular mechanisms of doxorubicin-mediated bone loss are not still fully understood because of the complexity of the cellular, molecular effects of DOX. In this study, we used *in vitro* osteoblast model to evaluated DOX-induced bone loss and its reversal by antioxidants using RNA-sequencing (RNAseq) methods. Analysis of Differential expressed genes with enrichment analysis based on biological process GO terms and KEGG pathways revealed Osteocrin and p53 as key regulators for DOX-induced bone impairment. Whereas, while on co-treatment with resveratrol (RES), we found that Osteocrin mRNA was increase as compared to DOX while p53 associated genes were downregulated. Our RNA-seq data pinpointed the regulatory genes and pathways associated with DOX-induced bone impairment and it's reversal effect by RES as p53 pathways, TNF signalling pathways, calcium signalling pathways, and Osteocrin. In conclusion, RES effectively reverses and prevents DOX-induced bone impairment, thus suggesting that a

combined therapy of using DOX and RES may be beneficial for preventing DOX-induced secondary osteoporosis.

2.1.1. INTRODUCTION

Oxidative stress alters the bone remodelling process, causing an unbalance between osteoclast and osteoblast activity. This can lead to metabolic bone diseases and contribute to the pathogenesis of skeletal system disorders, including osteoporosis characterized by low bone mineral density and decreased bone mass and bone density, inducing a deterioration of bone structure which causes bone fragility and increases the risk of fractures (42,109).

Doxorubicin (DOX) has been known as a first-line chemotherapeutic agent causing cytotoxicity, which is characterized by accumulation of reactive oxygen species (ROS) and reactive nitrogen species (NOS) (212). The current standard practice regimens for anthracyclines are DOX/cyclophosphamide/5-fluorouracil (CAF), DOX/cyclophosphamide (AC), and cyclophosphamide/5-fluorouracil/epidoxorubicin (CEF) (261). The therapeutic activity of DOX is thought to be due to DNA damage, which is the most effective against highly proliferative tumors (262,263). DOX generates free radicals directly and is a potent catalyst for oxygen radical formation by redox cycling (263–265). Furthermore, DOX reduces the amount of endogenous antioxidants, and lead to direct oxidative injury to mitochondria (266), DNA (267,268) and generates lipid peroxidation (269–274). In patients under DOX regimen, increased risk of bone metastasis and osteolytic injury has been reported (213,275). Also, DOX has been shown to increase systemic bone loss and reduce osteoblast differentiation (215–217). The precise cellular and molecular mechanisms of doxorubicin-mediated bone loss are still not fully understood because of the complexity of the cellular, molecular and organelle changes that occurs due to the action of DOX (213).

Resveratrol (RES) is a polyphenolic (3,4′,5-trihydroxystilbene) compound that is naturally found in a variety of plant foods such as grapes, cranberries, and nuts (174). RES has anti-inflammatory, estrogenic, antioxidant and proliferative properties which can influence bone metabolism (175). RES has been shown to improve bone mineralization and counteract glucocorticoid-induced bone damage in zebrafish (225). Similarly, RES also showed to inhibit oxidative stress and prevent mitochondrial damage induced by zinc oxide (276). Additionally, RES was reported to reverse bone

mass density (BMD) reduction and microarchitectural deterioration in a rodent osteoporosis model (277).

To better understand the mechanism behind the DOX-induced bone loss and reversal effect of RES on DOX-induced bone loss, we performed RNA transcriptome analysis on MC3T3 cells treated with DOX and RES alone or in combination. The data obtained were analyzed by bioinformatics tool to organize and integrate differentially expressed genes (DEGs), in order to better understand the molecular mechanism and cell signalling pathways. In this study, genes associated to biological function and pathways associated with both the treatment of DOX and RES alone or in combination in MC3T3-E1 cells were identified.

2.1.2. METHODS

2.1.2.1 Culture and differentiation of MC3T3-E1 cells

Stock cultures of MC3T3-E1 cells (subclone 4; CRL-2593; ATCC) were maintained in α-minimum essential medium (α-MEM; Gibco, Grand Island, NY, USA) supplemented with 10% v/v fetal bovine serum (Gibco), penicillin (100 units/mL) and streptomycin (100 pg/mL) (Gibco) in a humidified 5% CO2 atmosphere at 37°C. For osteoblast differentiation and mineralization, MC3T3 cells were cultured in growth medium, once the cells reach 90% confluency cells were induced for differentiation with osteogenic media i.e. α-MEM supplemented with 10% v/v fetal bovine serum, 5 mM β-glycerol phosphate and 50 µg/mL ascorbic acid (138,139,278,279). In addition, cells were treated with RES along with differentiation media, whereas for co-treatment DOX (TCI, Tokyo, Japan) was incubated with the cells for 3 hours, then media was replaced by osteogenic medium with RES (TCI). The media was replaced every 48 hours. All experiments were done in triplicates.

2.1.2.2. XTT assay

Cytotoxicity was analyzed by XTT assay (Biotium, USA). In short, cells were seeded in 96-well plates and treated with antioxidants or pro-oxidant. Hereafter, XTT activator reagent was mixed with 5 ml XTT reagent and added to fresh media. The mixture of

media and XTT reagent (100ul +50 ul) was added in each well and incubated for 2 - 4 h at 37°C, 5 % CO2. The absorbance was measured at 630 nm using a microplate reader (Biotek synergy 4, Canada). Three separate experiments were performed.

2.1.2.3. Drug treatment

MC3T3-E1 cells were seeded at $5X10^4$ cells/well and grown in 24-well plates. After the plate reached 90% confluence, cells were induced for differentiation and exposed to DOX and RES alone or in-combinations added to the differentiation medium (50 mg/ml of ascorbic acid and 10 mM β-glycerol-phosphate) (138,139,278,279). Cells treated with RES were exposed for 4 days and for co-treatments, DOX was incubated with the cells for 3 hours, then the media was removed and subsequently RES was added. The media was replaced every 48 hours.

2.1.2.4. Alkaline phosphatase activity

MC3T3-E1 cells were differentiated into Osteoblast with the treatment of DOX, RES and MT alone or in combination for 4 days. Alkaline phosphatase (ALP) staining was performed at the early stage of osteoblastic differentiation (after 4 days) by the NBT/BCIP method. Briefly, cells were fixed with 70% ethanol for 10 minutes at room temperature and washed by PBS 3 times. Then the cells were stained with color solution [NBT (75 mg/mL in 70% Dimethylformamide – 30% of H2O), BCIP (50 mg/mL in Dimethylformamide) in the dark until ALP signal is visualized (280).

2.1.2.5. Alizarin red-S staining (AR-S staining)

Matrix mineralization was quantified by AR-S staining as described (280). MC3T3- E1 cells (5X104 cells/well) were seeded into 24-well plates and cultured for 21 days in α-MEM differentiation media with DOX, RES and MitoTEMPO alone or in combination. Cells were fixed with 4% formaldehyde at 4°C for 1 hour, then stained with 40 mM AR-S solution for 15 minutes. The image of the plate was acquired with an Epson Perfection V37 scanner and destained with 10 % cetylpyridinium chloride (Sigma C0732). The extract was collected and absorbance was measured at 550nm (250,281).

2.1.2.6. mRNA isolation

MC3T3-E1 cells were cultured as described in 6 well plates for 11 days as describe on cell culture and differentiation method. Total RNA was extracted from cell cultures as described by Chomczynski and Sacchi (282). QIAGEN RNeasy Mini kit was used to purify RNA samples, which were then treated with QIAGEN RNase-free DNase according to the manufacturer's instructions. The concentration of RNA was measured by spectrophotometry (NanoDrop ND-1000, Thermo Scientific) and the integrity of RNA was evaluated by electrophoresis (2100 Bioanalyzer, Agilent Technologies). Each sample's RNA integrity number (RIN) index was calculated using Agilent 2100 Expert software. Only RNA samples with a RIN >8 were further processed. The construction of cDNA libraries was carried out using the Ribosomal Depletion Library Preparation Kit. DNA fragments were sequenced using the Illumina Novaseq platform, using with 150bp paired-end sequencing reads.

2.1.2.7. Trimming, mapping of the reads, differential gene expression and data quality analysis

Raw sequences were trimmed to generate high-quality data using the CLC Workbench 12.0.3 (283), as follows: quality trimming based on quality scores (0.01), ambiguity trimming (2 nucleotides) and length trimming (minimum of 30bp). Mapping of the reads was performed against the reference genome, GRCm39 (GCF_000001635.27) with length (minimum percentage of the total alignment length that must match the reference sequence at the selected similarity fraction) and similarity (minimum percentage identity between the aligned region of the read and the reference sequence) parameters set to 0.95.

Gene expression was calculated based on the Reads per Kilobase of exon model per Million mapped reads (RPKM) approach (284). Expression levels were calculated using the RPKM values from each sample independently. Differential expression was then calculated using a multi-factorial statistical analysis based on a negative binomial model that used a generalized linear model approach influenced by the multi-factorial EdgeR method (285). The differentially expressed genes were filtered using standard

conditions (285,286), i.e. a False Discovery Rate (FDR) *P*-value <0.05 and a fold change >2 or <-2. The quality of the produced data was ensured by evaluating the Phred quality score at each cycle (position in read; ensuring a minimum Phred score of 20). Further quality control was performed by principal component analysis (PCA), hierarchical clustering (considering Euclidean distance) and heat map analysis.

2.1.2.8. Ontology analyses and Pathway analysis

Gene ontology enrichment analyses are frequently based on lists of Differentially Expressed Genes (DEGs) defined by the use of a hard cut-off, such as an adjusted P-value of 0.05. This is a common approach in RNA-Seq experiments. However, another way of approaching functional evaluation is to use gene set enrichment analyses, that consider all the genes tested in the differential expression analysis. We have used iDEP93 (integrated Differential Expression and Pathway Analysis) (http://bioinformatics.sdstate.edu/idep93/) for the Gene Ontology to identify the upregulated and downregulated DEGs associated biological function, cellular component and molecular function (287) and we have used webgestalt (WEB-based Gene SeT AnaLysis Toolkit) (http://www.webgestalt.org/) Gene set enrichment analysis/pathways/KEGG to identify the cell signalling pathways with upregulated and downregulated genes (288). The calculation of the *P*-value was based on the probability density function. The cut-off threshold was set to FDR (B&Y) < 0.05.

2.1.2.9. Activity of Signalling Pathways

MC3T3-E1 were used to host the reporter constructs of the Cignal 45-pathway reporter array (QIAGEN). Sub-confluent cultures of MC3T3-E1 were reverse-transfected with reporter constructs according to manufacturer protocol. Briefly, each well of the Cignal 96-well plate containing the 45 reporter constructs received sequentially 50 µL of Opti-MEM (Thermo Fisher Scientific), 0.6 µL of Attractene transfection reagent (QIAGEN) diluted in 50 µL of Opti-MEM, and 50 µL of cell suspension (8 × 105 cells per mL of Opti-MEM supplemented with 10% of FBS and 1% of the non-essential amino acid

mixture (NEAA) from Thermo Fisher Scientific). Cells were incubated for 24 h at 37 ◦C under a humidified 5% CO2 atmosphere, then exposed to Resveratrol, MitoTempo and Doxorubicin for 24 h in Opti-MEM supplemented with 0.5% FBS, 1% NEAA, and 100 U/mL of penicillin/streptomycin (Thermo Fisher Scientific). Firefly and Renilla luciferase activities were determined in cell extracts using the Dual-Luciferase Reporter Assay system (Promega) and a BioTek Synergy 4 multi-plate reader.

2.1.3. RESULTS

2.1.3.1. Cytotoxicity and Osteoblast differentiation

To investigate the molecular mechanisms underlying the effects of DOX on osteogenesis differentiation, cell viability assay (XTT-assay) was performed to analyze the potential cytotoxicity of antioxidants (RES, MitoTEMPO) and Pro-oxidants (DOX and H_2O_2) against MC3T3-E1 cells. The result demonstrated that DOX did not show cytotoxicity toward cells at the investigated concentration of 0.1µM for 3 hours of exposure (Figure 2.1.1A). The higher concentrations of DOX were toxic to the cells (supplementary figure 2.1.1A), similarly, different concentrations of H_2O_2 were exposed to MC3T3 cells for 3 hours and 100 µM concertation was used for further experiments since it was nontoxic for the cells (Figure 2.1.1B). The dose of 10 nM was previously defined as the sublethal concentration of BMSCs treated with DOX (289). The higher concentrations of RES (220 µM, 150 µM, 75 µM, 37 µM) were toxic to the cells (supplementary figure 2.1.1B), whereas antioxidants had no cytotoxic effect at the lower concentrations on pre-osteoblastic cells (Figure 2.1.1C, D). Therefore, the non-toxic concentration of 10µM RES (Figure 2.1.1C) and 10µM MitoTEMPO (Figure 2.1.1D) were used for further experimentation.

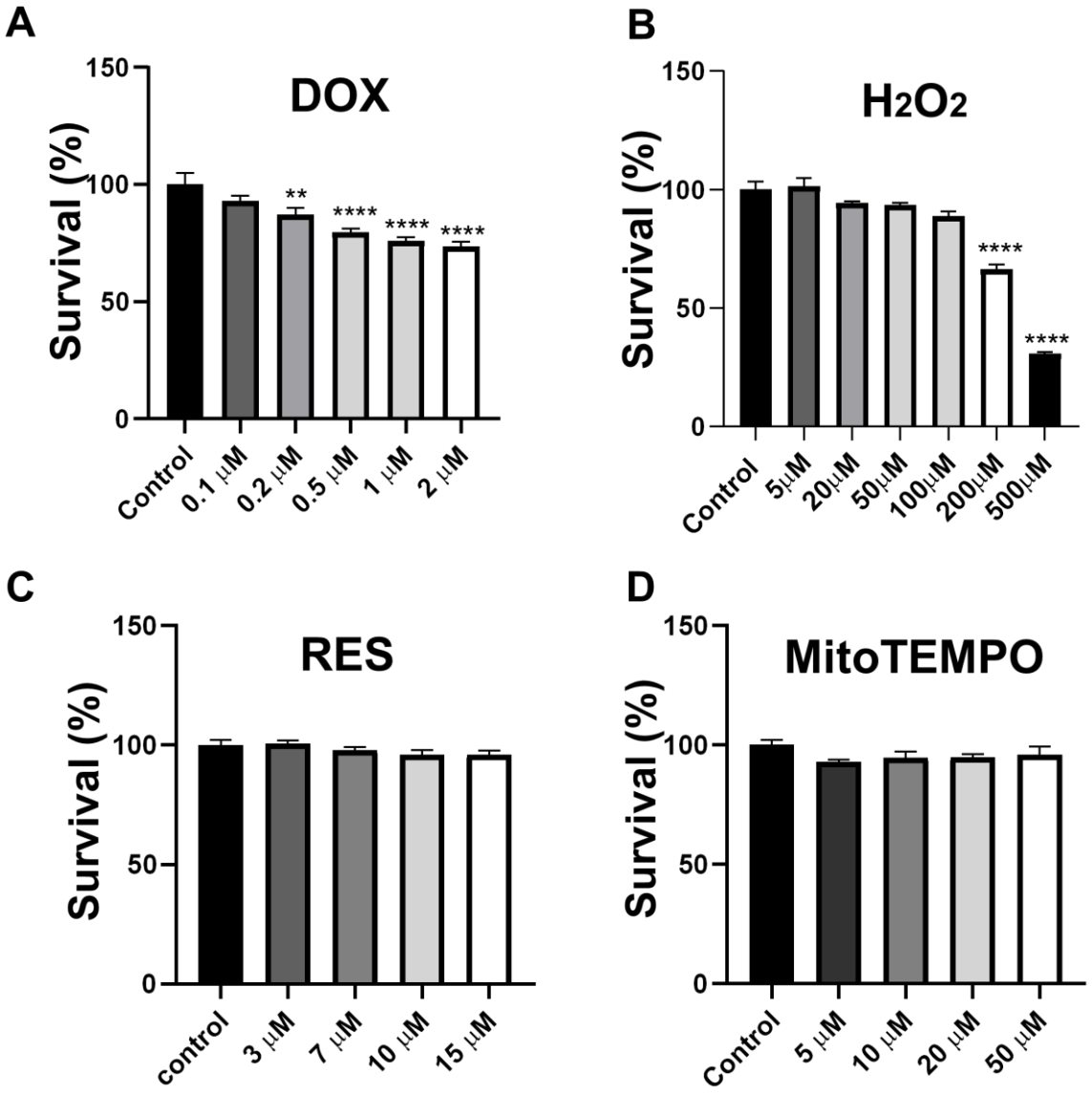

Figure 2.1.1: Cytotoxicity of the compounds on MC3T3-E1 cells. Doxorubicin (A), H_2O_2 (B), Resveratrol (C) and MitoTEMPO (D), MC3T3-E1 cells were cultured for 3 days, RES and MT were treated for 3 days whereas, DOX were treated for 3 hours with the indicated concentrations. XTT reagents were added to each well and the absorbance was read at 450 nm. One-way ANOVA, Tukey's multiple comparisons test, ns- $P>0.05$, *- $P\leq0.05$, **-$P\leq0.01$, ***-$P\leq0.001$, ****-$P\leq0.0001$.

To determine the effect of antioxidants and pro-oxidants on osteogenic differentiation, MC3T3-E1 cells were treated with RES, MitoTEMPO, DOX and H_2O_2 alone or in combination and alkaline phosphatase activity and alizarin red S staining were evaluated. The reduction in the activity of alkaline phosphatase was observed on doxorubicin treatment alone when compared to the osteogenic control. Similarly, in the

co-treatment of DOX with antioxidants (RES and MitoTEMPO), the reduction was more evident as compared to antioxidants alone (RES, MitoTEMPO) (Figure 2.1.2 A,B). Moreover, to investigate the deposition of calcium nodules after 21 days, AR-S staining was performed. DOX significantly deteriorated the mineralization capacity of the cells as compared to osteogenic control and treatments with antioxidants (RES and MitoTEMPO) (Figure 2.1.2 C,D). In contrast, upon combination with RES and MitoTEMPO, the effect of DOX was significantly minimized on osteoblastic activity (Figure 2.1.2 C,D) as confirmed by the increase in mineralization of osteoblasts. Similar results were observed on H_2O_2 treatment on osteoblastic cells, were antioxidants (RES and MitoTEMPO) significantly reversed the negative effects, as shown by H_2O_2 alone on early differentiation marker (ALP stain) and mineralization (AR-S stain) (Supplementary figure 2.1.2).

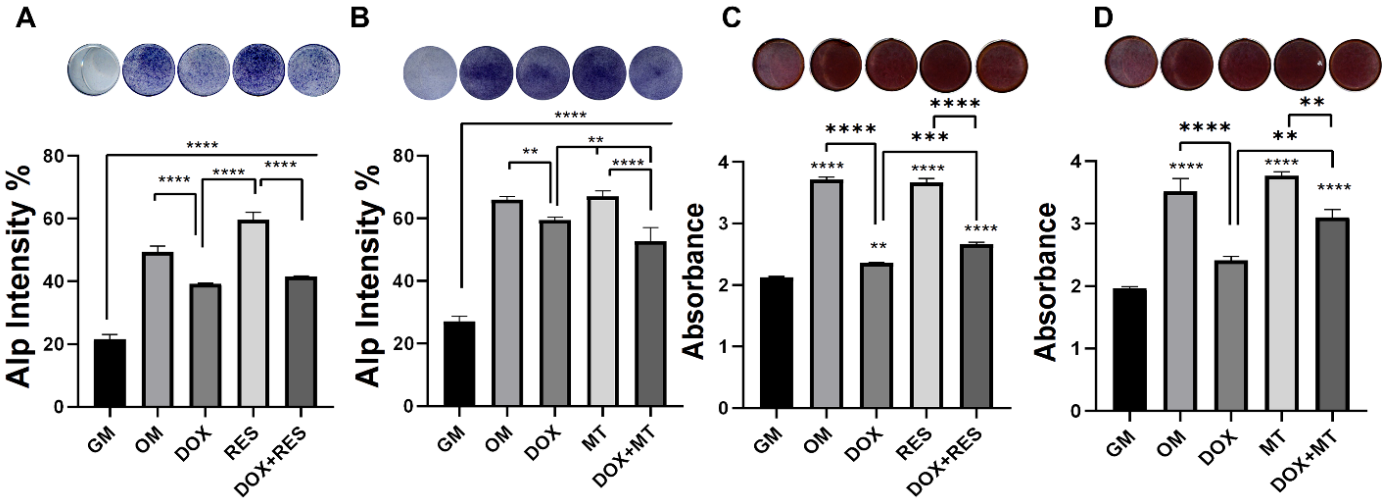

Figure 2.1.2: Reversal effect of RES on DOX-induced osteoblast differentiation and mineralization. MC3T3-E1 cells were cultured for 21 days in Differentiation media (ascorbic acid and β-Glycerophosphate) with RES (10µM), MT (10µM) and DOX (0.10 µM) alone or together. Alkaline phosphatase (ALP) staining on 4th day (A, B). Quantification of ALP staining was sone by ImageJ 1.53c. Alizarin red-S staining done after 21 days of differentiation (C, D). One-way ANOVA, Tukey's multiple comparisons test, ns- P>0.05, *- P≤0.05, **-P≤0.01, ***-P≤0.001, ****-P≤0.0001. Acronyms: Growth Medium (GM), Osteogenic Medium (Growth medium Ascorbic acid and β- Glycerophosphate) (OM), Resveratrol (RES), Doxorubicin (DOX), MitoTEMPO (MT), Doxorubicin+Resveratrol (DOX+RES) and DOX+MT (DOX+MT).

2.1.3.2. RNAseq global transcriptome analysis

We determined transcriptomic alterations in Osteoblast differentiation upon DOX treatment and the reversal effect of RES on DOX-induced bone impairment. Due to difficulty on bioinformatics data analysis with many groups (both antioxidants RES and MitoTempo alone or in combination with DOX) and based on the results from *in vivo* experiment which revealed that MitoTEMPO did not significantly reverse the DOX-induced bone mineralization, we focused on RES and the reversal by RES on DOX-induced bone impairment for RNA-seq analysis. In brief, cells were plated at high density, according to the manufacturer's protocol, and exposed to 0.1 μM of doxorubicin for 3 hours. Total RNA was extracted from osteoblast on day 10 and subjected to RNA sequencing. After trimming and mapping, gene expression levels were calculated based on the RPKM method. To determine data reproducibility across replicate samples we performed principal component analysis (PCA) and hierarchal clustering. The hierarchical clustering was performed using the Manhattan distance, Average linkage and without filtering, the expression levels are visualized in a heat map using a gradient color scheme, where the red color is used for high expression levels and the blue color is used for low expression levels.

PCA and hierarchal clustering clearly show that samples exposed to DOX alone or in combination with RES cluster separately from the control (CON), RES, DOX or combination of DOX and RES (DR) (Figure 2.1.3 A, B). Sample clustering on heatmap shows that data is reproducible across biological replicates (Figure 2.1.3 A).

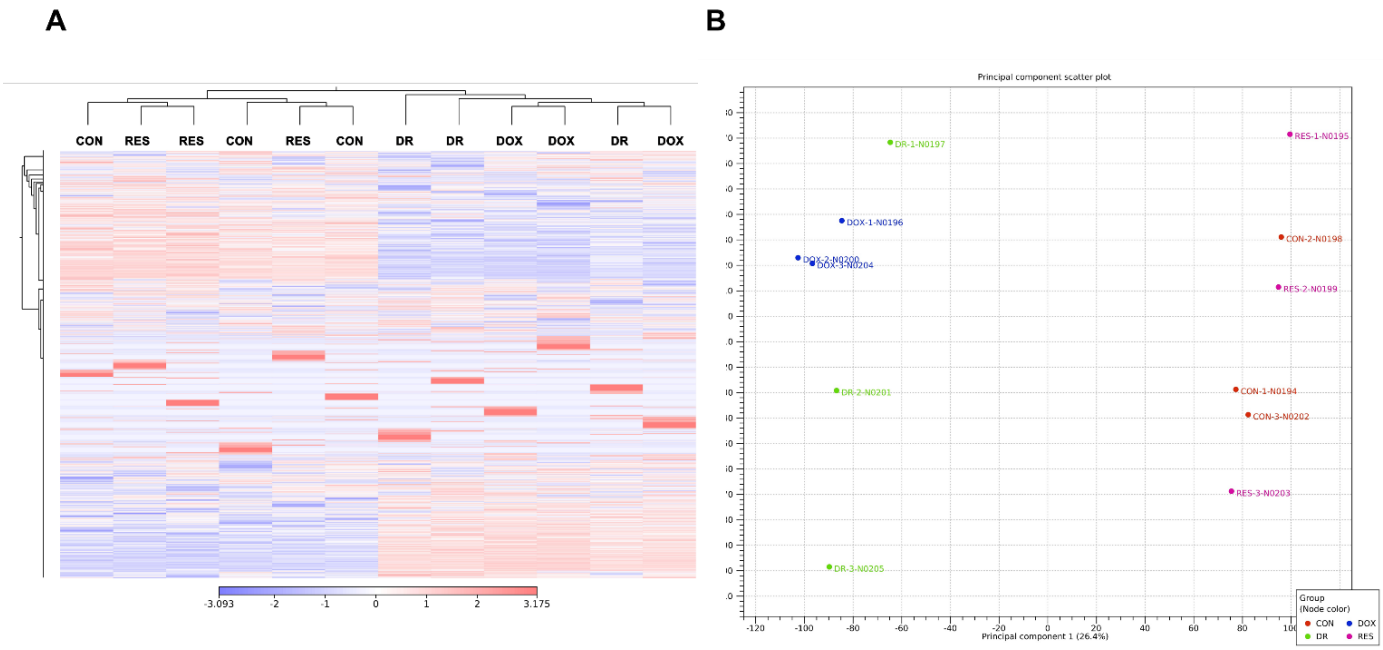

Figure 2.1.3: Hierarchical clustering of samples, heat map and principal component analysis. Heatmap was created with the results of the gene expression (A). The red colour represents over-expression, while the blue colour under-expression. PCA corresponds to the gene expression of the groups of samples (B). The first principal component is shown on the X-axis and the second principal component is shown on the Y-axis. The value after the principal component identifier displays the amount of variance explained by this particular principal component. Acronyms: Control (CON), Resveratrol (RES), Doxorubicin (DOX) and Doxorubicin+Resveratrol (DR).

2.1.3.3. Differential expression analysis

Expression levels were calculated using the RPKM values from each sample independently. Differential expression was then calculated using a multi-factorial statistical analysis based on a negative binomial model that used a generalized linear model approach influenced by the multi-factorial EdgeR method (285). The differentially expressed genes were filtered using standard conditions (285,286), i.e., a False Discovery Rate (FDR) P-value <0.05 and a fold change >2 or <-2.

The significant differentially expressed genes (DEGs) for normalized gene expression among the RES, DOX alone or in combination were identified. The significant DEGs between comparison groups DOX vs CON was 736, CON vs DOX+RES was 594, DOX vs RES was 706, and RES vs DOX+RES was 572 (Figure 2.1.4 A, B). A comparative

analysis was performed to compare between the DEGs, where we found that 329 genes were common on all four comparison groups [CON vs DOX, DOX vs RES, CON vs DOX+RES, RES vs DOX+RES], whereas 116 genes were common in 4 comparison groups [(CON vs DOX, DOX vs RES, CON vs DOX+RES=39),(CON vs DOX, DOX vs RES, RES vs DOX+RES=41),(CON vs DOX, CON vs DOX+RES, RES vs DOX+RES=20), (DOX vs RES, CON vs DOX+RES, RES vs DOX+RES=16)], similarly, 317 genes were common on following 2 group sets [(DOX vs RES, RES vs DOX+RES=69),(CON vs DOX+RES, RES vs DOX+RES=41),(CON vs DOX, DOX vs RES=116), (CON Vs DOX, CON vs DOX+RES=89), (CON vs DOX, RES vs DOX+RES=1) (DOX vs RES, CON vs DOX+RES=1)], finally, there were altogether 431 genes which were unique on the comparison groups [CON vs DOX (130), DOX vs RES (130), CON vs DOX+RES (84), RES vs DOX+RES (87)] as shown in Venn diagram (Figure 2.1.4A, B).

736 genes were differentially expressed between the DOX vs CON, and out of those 508 genes were upregulated and 257 genes were down-regulated. On the comparison, CON vs DOX+RES 400 DEGs were upregulated and 219 DEGs were downregulated. Similarly, 460 DEGs were upregulated and 281 DEGs were downregulated on RES vs DOX and in the comparison group RES vs DOX+RES 253 DEGs were upregulated and 351 DEGs were down-regulated (Figure 2.1.4C).

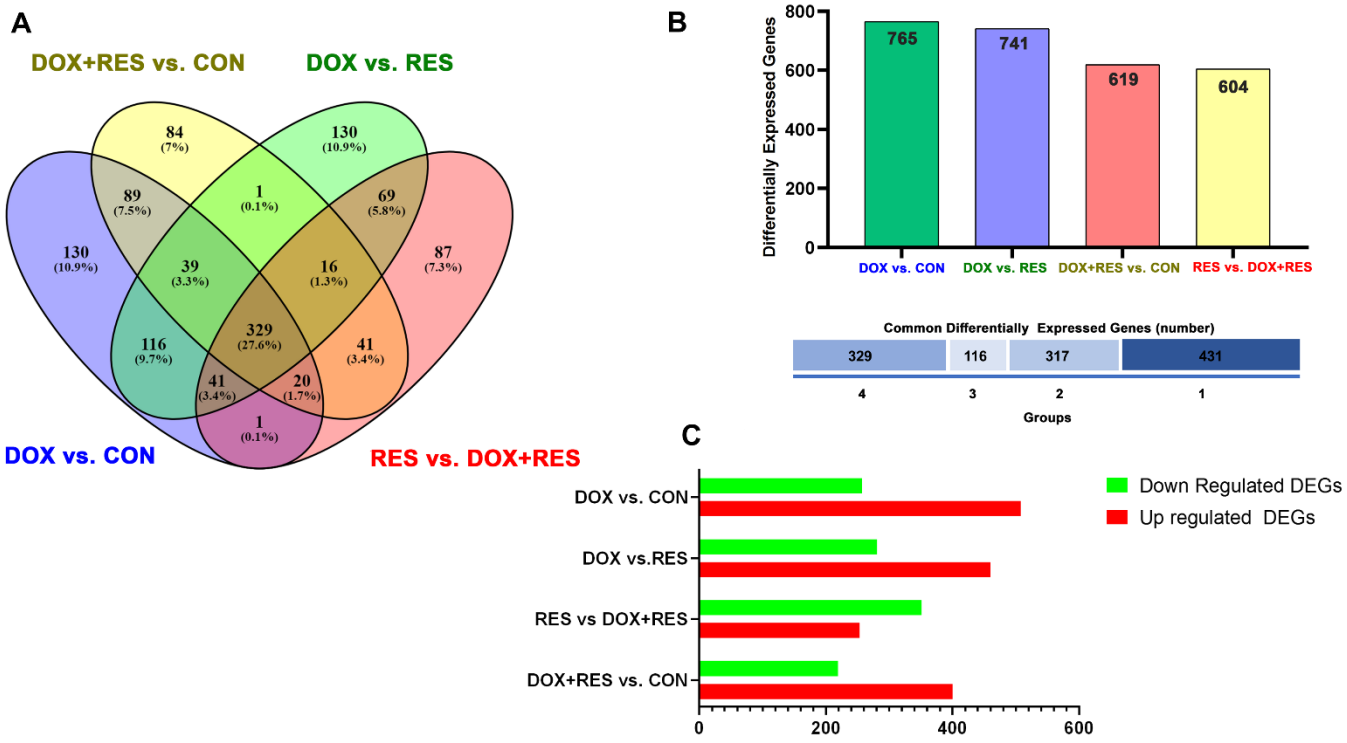

Figure 2.1.4: Venn diagrams of differentially expressed genes on different compared groups. Venn diagram of DEGs on different compared groups (A). Number of DEGs on compared groups and number of genes shared between the compared groups (B). The number of up regulated and down regulated DEGs between the compared groups (C). Acronyms: Control (CON), Resveratrol (RES), Doxorubicin (DOX), and Doxorubicin+Resveratrol (DOX+RES).

2.1.3.4. Gene Ontology analysis

To gain further insight into the molecular processes on reversal of DOX-induced osteoblast by RES, functional enrichment analysis was performed (based on biological process GO terms and KEGG pathways) using up- and down-regulated genes.

Differentially expressed genes were analyzed and functionally classified according to their Gene Ontology (GO) in relation to biological process (BP), cellular component (CC) molecular function (MF) and using the iDEP93 and DAVID Classification System. To highlight gene clusters, the upregulated and downregulated gene sets were analyzed using Idep93, and a Pie-chart was prepared on jvenn (290), overall bar graph was prepared on webgestalt (288). From these DEGs, in the DOX-treated group

compared to the RES group, the following hit numbers (unigenes) were returned for BP/CC/MF: 711/198/175 were downregulated and BP/CC/MF: 849/181/370 were upregulated. In the Biological process, 312 (43.8%) unigenes associated with the developmental biological process and 113 (15.8%) unigenes associated with cell differentiation were downregulated, whereas 295 (34.7%) unigenes were associated with immune response and 228 (26.8%) unigene associated to response to stimulus were upregulated (Figure 2.1.5).

Similarly, the following hit numbers (unigenes) were returned for BP/CC/MF: 672/202/136 were downregulated and BP/CC/MF: 828/207/509 were upregulated for the doxorubicin-treated group compared to the control group. In the biological process, 225 unigenes (33.4%) of the downregulated genes related to the development biological process, 189 unigenes (28.1%) were downregulated genes related to the cellular response. Among the upregulated genes related to biological process, 249 (30%) unigenes were associated with response to stimulus and 235 (28.38%) unigenes were associated with immune response (Supplementary figure 2.1.3).

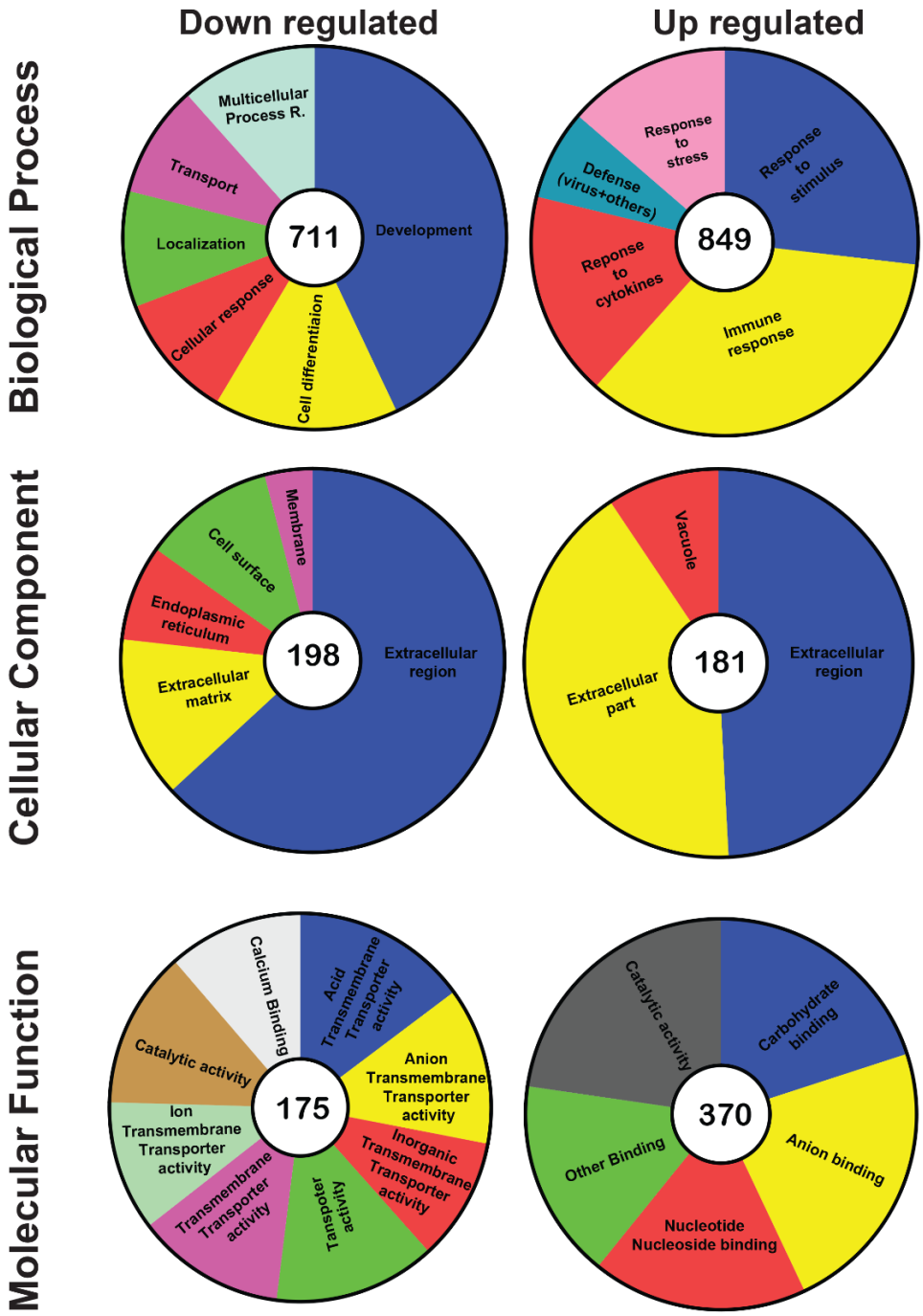

Figure 2.1.5: Pie chart representations of GO entries occurrence among the DEGs categorized as up-regulated and downregulated between DOX vs. RES. Pie charts represent biological processes, cellular components and molecular function GO entries occurrence among differentially expressed genes in doxorubicin vs resveratrol. The number in the center indicates

the hit number. Additional information on GO definition is available in supplementary table 2.1.1-2.1.4.

While analyzing the groups treated with DOX and co-treated RES with CON, BP/CC/MF: 537/229/104 unigenes were downregulated and BP/CC/MF: 604/600/509 unigenes were upregulated. 122 (22.7%) unigenes were associated with development and 200 (37.2%) unigenes associated with cellular response were downregulated. Whereas 204 (33.6%) unigenes associated with the cell cycle process and 130 (21.4%) unigenes associated with response to stimulus were upregulated (Supplementary figure 2.1.4).

While analyzing the groups treated with RES with DOX co-treated RES, BP/CC/MF: 610/146/363 unigenes were downregulated and BP/CC/MF: 542/216/149 unigenes were up-regulated. 184 (30.1%) unigenes associated with responses to stimulus and 159 (26%) unigenes associated with immune response were downregulated. Whereas 236 (43.5%) unigenes associated with development and 59 (10.8%) unigenes associated with cell differentiation were upregulated (Supplementary figure 2.1.5).

In a general manner, the proportion of molecular functions and cellular components were maintained between the different subsets of genes. Differences were more evident for the biological process to be specific on development and cell differentiation-associated genes. Therefore, to illustrate the specific genes related to the biological process, Gene set enrichment analysis (GSEA) was analyzed on WebGestalt.

GSEA furthermore revealed genes that positively regulated cell cycle (*Apex1, Asns, Calr, Ccn2, Ccne1, Cd28, Cdc6, Cenpe, E2f8, Eif4ebp1, Fam83d, Fap, Fzd9, Gper1, Igf1, Kif23, Nusap1, Orc1, Pidd1, Rab1,1fip4, Rxfp3, Slc6a4, Smoc2, Tert, Tfap4 and Wnt5a*), similarly genes related to lymphocyte differentiation (*Nfam1, Rsad2*) and G-coupled receptor (*Ccl5, Htr2b, Ptgdr2*) were upregulated. Genes related to cell growth (*Ostn, Pi16, Tfcp2l1*) were downregulated on the DOX-treated group compared to the CON group (Supplementary figure 2.1.6 and supplementary table 2.1.1).

The pro-inflammatory genes (*Oas1a, Oas1b, Oas1g, Oas2, Oas3, Oasl1* and *Oasl2*),, genes associated to response to type I interferon (*Irf7, Isg15, Mx2, Nlrc5, Oas2* and

Zbp1), interferon-beta (F830016B08Rik, Gbp3, Gm4841, Gm4951, Ifi203, Ifi205, Ifi207, Ifi208, Ifit1, Ifit1bl1, Ifit3, Ifit3b, Igtp, Iigp1 and *Tgtp2*) were upregulated. While the gene associated to ossification (*Ostn*) was highly downregulated (-133 fold). Genes for cell growth (*Ostn, Pi16, Tfcp2l1),* Biomineralization (*Ostn, Klf15*), genes associated with negative regulation of immune system (*Bst2, Ccn3, Cd300a, Cd74, Gper1, Hspa9, Igf1, Il1rl1, Il33, Kitl, Lag3, Nlrc3, Nlrc5, Parp14, Prdm16, Ptk2b, Siglecg, Sox11, Spn* and *Tnfrsf21*) were down-regulated on DOX -treated group as compared to RES (Figure 2.1.6 and supplementary table 2.1.2).

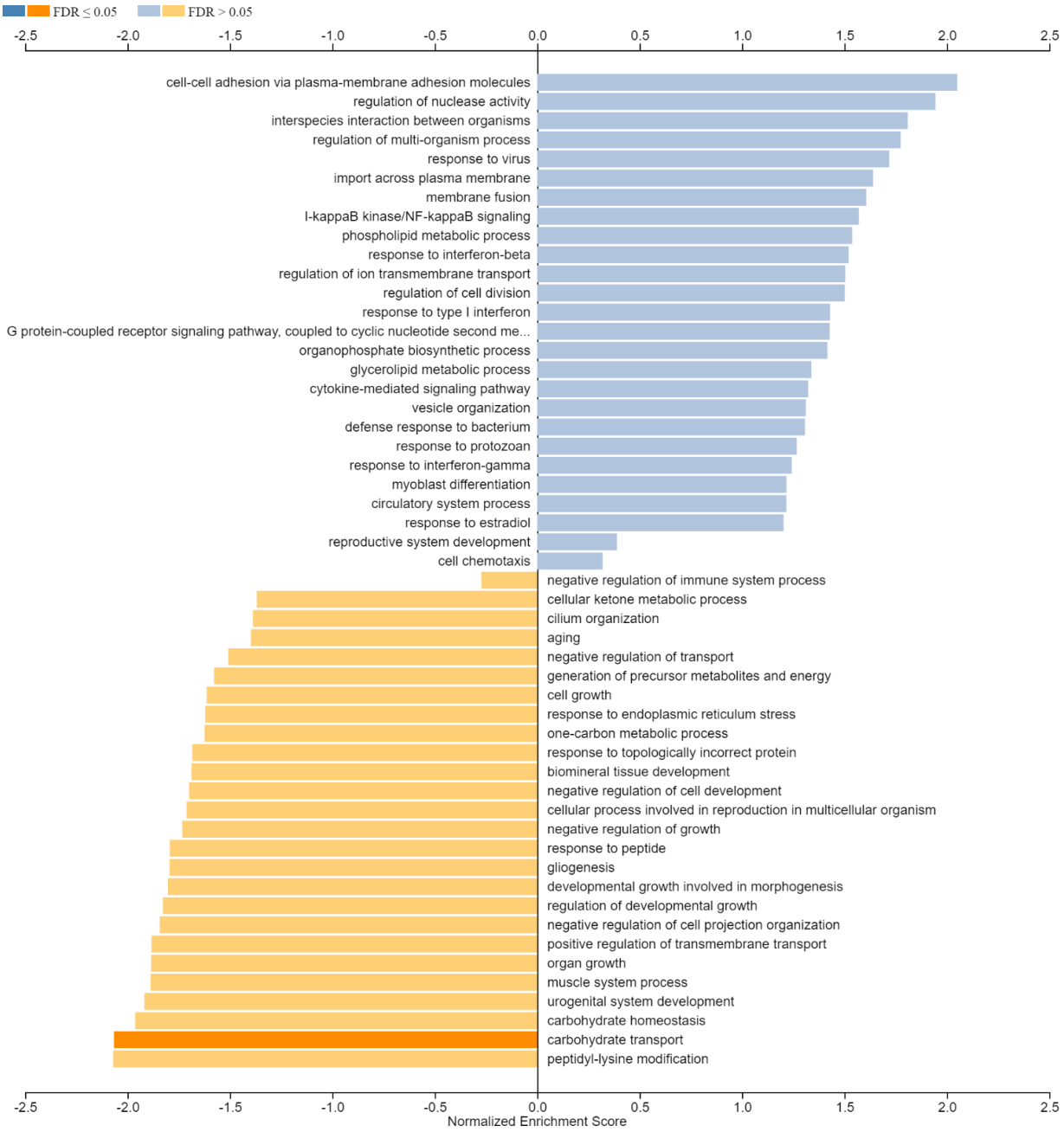

Figure 2.1.6: Over-represented biological processes between the DOX and RES. Gene set enrichment analysis was done in webGestalt/geneontology/biological process noRedundant. Top-ranked categories based on FDR were ranked for each positive and negative related category. Additional information on other comparison groups are available on supplementary figures 2.1.6-8 on biological processes and supplementary table 2.1.1-2.1.4.

Similarly, while analyzing the GSEA between RES and DOX+RES, genes associated with epithelial cell development (*Pdzd7, Sox8* and *Tfcp2l1),* nervous system development (*Artn, Egr2, Egr3, Lgi4, Ntrk3* and *Sox8*), biomineralization [*Ostn* (137-

fold)], developmental growth (Ostn, *Pi16* and *Sema6d*) were upregulated. However, pro-inflammatory genes (*Oas1a, Oas1b, Oas2, Oas3* and *Oasl2*), response to interferon-gamma (*Ccl7, Ccl8, Gbp10, Gbp2, Gbp3, Gbp4, Gbp6, Gbp7, Gbp9, Nlrc5* and *Tgtp2*), response to interferon-beta (*Gbp3, Gm4951, Ifi205, Ifi207, Ifit1, Ifit1bl1, Ifit3, Ifit3b, Iigp1* and *Tgtp2*) and regulation of cell division (*Htr2b, Rxfp3 and Txnip*) were downregulated (Supplementary figure 2.1.7 and supplementary table 2.1.3).

Lastly, while examine GSEA among the DOX+RES with CON, reproductive system development (*Brip1, E2f8, Esr2, Hoxb13, Igf1, Nanog, Ptger4* and *Wnt7b*), negative regulation of cellular component movement (*Adgrg1, Angpt4, Bst2, Cd300a, Fas, Il33, Nrg1, Pdgfb, Ptger4, Sema3e, Sema7a, Slit1, Sp100* and *Tmeff2*), negative regulation of locomotion (*Adgrg1, Angpt4, Bst2, Cd300a, Fas, Il33, Nrg1, Pdgfb, Ptger4, Sema3e, Sema7a, Slit1, Sp100* and *Tmeff2*) and response to interferon-alpha (*Ifit1, Ifit3, Ifit3b* and *Tgtp2*) were upregulated. On the other hand, positive regulation of response to external stimulus (Artn Calr Cd74 F7 Ntrk3 Pdgfb Pgf Smoc2), developmental process on neural stem cells (gliogenesis) (*Adgrg1, Aspa, Atf5, Egr2, Enpp2, Fas, Id4, Il33, Lgi4, Lif, Nrg1, Ntrk3, Pdgfb, Ptk2b* and *Sox11*), response to leukaemia inhibitory factor (*Cth, Egln3, Fzd4, Spp1* and *Tfrc*), Connective tissue development (*Axin2, Ccn1, Ccn2, Col7a1, Gdf6, Id4, Igf1, Mmp13, Pdgfb, Vit* and *Wnt7b*), homeostasis of number of cells (Hspa9 Slc7a11 Tnfrsf13c) and response to steroid hormone (*Artn, Calr, Cd74, F7, Ntrk3, Pdgfb, Pgf* and *Smoc2*) were downregulated (Supplementary figure 2.1.8 and supplementary table 2.1.4).

2.1.3.5. KEGG signalling network analysis

To gain further insight into the molecular processes on reversal of DOX-induced negative effects on osteoblasts by RES, in addition to Gene set enrichment analysis based on biological process, GO terms using up-and downregulated DEGs and KEGG pathways based on upregulated and downregulated pathways between the treatment groups were analyzed.

NOD-like receptor pathways associated genes were upregulated on DOX treatment, DEGs were upregulated on DOX as compared to control and RES (Supplementary figure 2.1.9, and 2.1.10) (supplementary table 2.1.5 and 2.1.6). While co-treating DOX

with RES, NOD-like receptor pathways associated genes were downregulated. mTOR signalling pathway was downregulated on DOX as compared to RES (Supplementary figure 2.1.9, and 2.1.10) (supplementary table 2.1.5 and 2.1.6). PI3-AKT pathway was upregulated with DOX treatment as compared to control (Supplementary figure 2.1.9 and supplementary table 2.1.6) wereas they were downregulated on RES as compared to DOX+RES (Supplementary figure 2.1.12 and supplementary table 2.1.7). RAS signalling pathway responsible for cell growth, division and differentiation was downregulated on DOX treatment as compared to CON and RES (supplementary table 2.1.6 and Supplementary figure 2.1.9 and 2.1.10). Similarly, RAS pathway was upregulated on RES as compared to combined treatment of DOX+RES (supplementary figure 2.1.12 and supplementary table 2.1.7). Calcium signalling pathway was upregulated on DOX treatment as compared to CON, RES (Supplementary figure 2.1.9 and 2.1.10, supplementary table 2.1.4, 2.1.6) and on the combined treatment of DOX and RES as compared to CON (Supplementary figure 2.1.11 and supplementary table 2.1.8). However, it was downregulated on RES treatment as compared to DOX+RES (Supplementary figure 2.1.12 and supplementary table 2.1.7). Pathways associated with the cell cycle were upregulated while combining DOX with RES as compared to CON (Supplementary figure 2.1.11 and Supplementary table 2.1.8).

Tumour necrosis factor (TNF) plays an important role in bone remodelling, TNF regulates the differentiation of cell lineages involved in bone remodelling, including both osteoclasts and osteoblasts, and associated coupling factors. Genes associated with TNF signalling pathway were upregulated on DOX treatment as compared to RES (Supplementary figure 2.1.12 and supplementary table 2.1.8). TNF signalling is also known to influence the WNT signalling pathway (291). Wnt signalling pathway was upregulated on DOX treated osteoblasts as compared to CON (Supplementary figure 2.1.9 and supplementary table 2.1.5) and RES (Supplementary figure 2.1.10 and supplementary table 2.1.6), while it was downregulated on DOX+RES as compared to RES (Supplementary figure 2.1.12 and supplementary table 2.1.8).

Focal adhesion pathways are associated with the signals that mediate cancer cell resistance to cytotoxic agents. Here, Focal adhesion pathways were upregulated on

DOX treated groups as compared to CON (Supplementary figure 2.1.9 and supplementary table 2.1.5). However, the signalling pathway was downregulated on RES as compared to DOX and DOX+RES (Supplementary figure 2.1.12 and supplementary table 2.1.8).

MAPK signalling pathway was upregulated upon DOX exposure, alone or in combination with RES, as compared to CON (Supplementary figure 2.1.9, 2.1.11 and supplementary table 2.1.5 and 2.1.6). However, MAPK signalling pathway was downregulated on DOX exposure as compared with RES (Supplementary figure 2.1.10 and supplementary table 2.1.6). Similarly, Hif-1 signalling pathway was also down-regulated on DOX exposure as compared to RES (Supplementary figure 2.1.10 and supplementary table 2.1.6).

p53 signalling is an important tumour-suppressor protein that activates various responses, including cell-cycle arrest and apoptosis (292). We found that p53 signalling pathway was upregulated on DOX exposure alone or in combination with RES as compared to CON (Supplementary figure 2.1.9, 2.1.11 and supplementary table 2.1.5 and 2.1.7).

Several genes associated with metabolic pathways were downregulated on DOX exposure as compared to RES and CON (Supplementary figure 2.1.9, 2.1.10 and supplementary table 2.1.5 and 2.1.6). While comparing RES with DOX co-treated with RES, the genes associated with metabolic pathways were upregulated (Supplementary figure 2.1.12 and supplementary table 2.1.8), however comparing DOX co-treated RES compared to CON these genes associated with metabolic pathways were downregulated (Supplementary figure 2.1.11 and supplementary table 2.1.7). Figure 2.1.7 shows the summary of the KEGG pathways associated with the all-treatment groups.

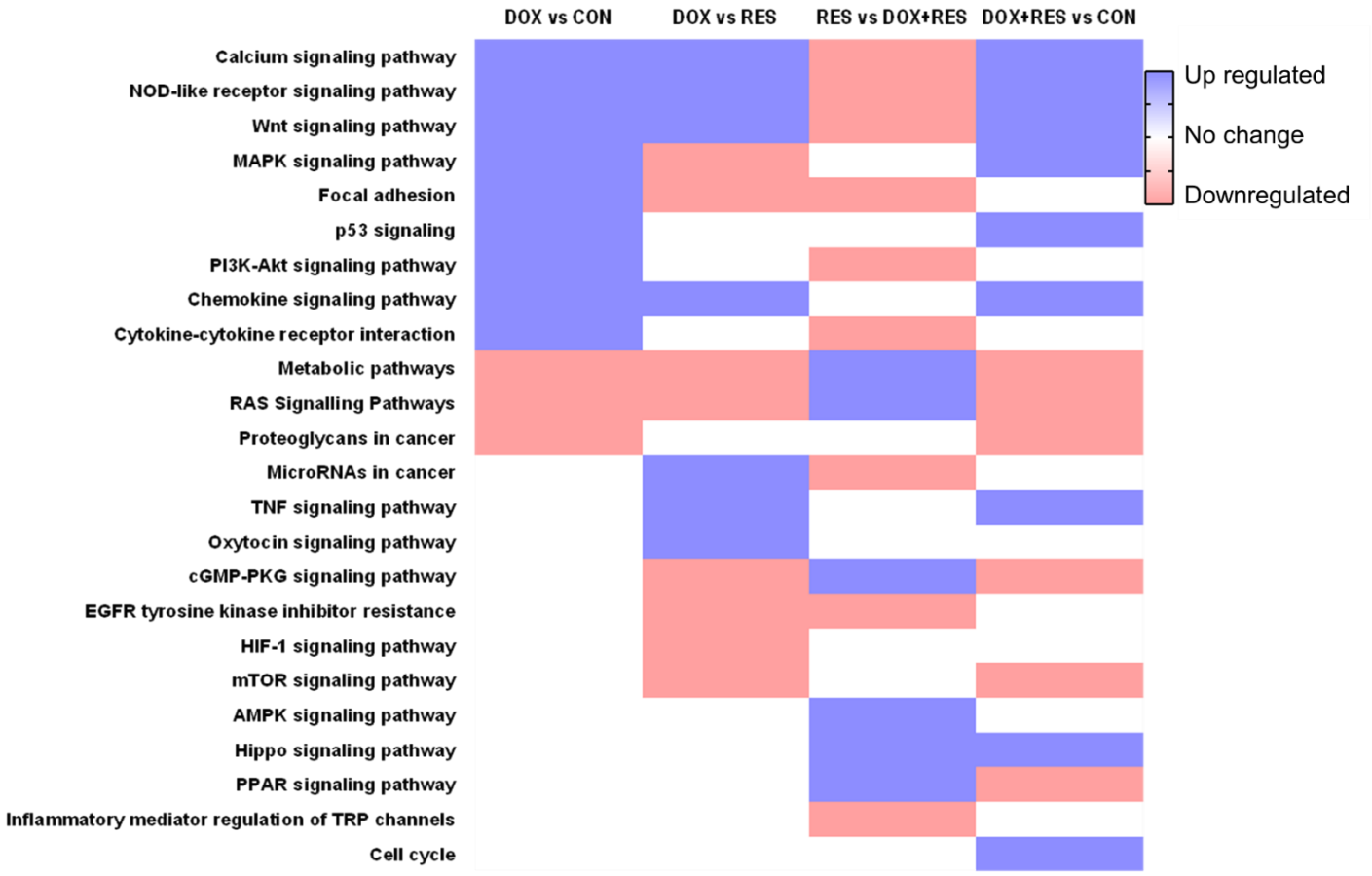

Figure 2.1.7: Summary of KEGG pathways analysis between the comparison groups. Gene set enrichment analysis was done in webGestalt/pathway/KEGG. Top-ranked categories based on FDR were ranked for each positive and negative related category. Detail information on comparison groups is available on supplementary figure 2.1.9-12 and supplementary table 2.1.5-2.1.8. Acronyms: Control (CON), Resveratrol (RES), Doxorubicin (DOX), and Doxorubicin+Resveratrol (DOX+RES).

2.1.3.6. Confirmation of Cell signalling pathway using reporter activity.

To confirm the cell signalling pathways behind the DOX-induced impairment of osteoblast differentiation and mineralization and the reversal of DOX-induced effect by RES, Cell-based reporter assay (Cignal-45) was used to pinpoint the transcriptional factors and signalling pathways with the help of double-luciferase reporter assay during the treatment with RES, MitoTEMPO (used as antioxidant control) and DOX.

Firstly, we analyzed pathways involved in the developmental process. RES exposure showed to increase MAPK/ERK, C/EBP, C-MYC and EGR1 pathways as compared to

CON, whereas TGF-β, Notch, NF-kB, GATA, FoxO and MAPK/JNK were downregulated. However, Notch, WNT, Myc/mac, TGF-β, cAMP/PKA and MAPK/JNK pathways were upregulated upon DOX exposure (Figure 2.1.8 A). In immune signalling pathways, RES treatment was shown to upregulate C/EBP and PKC/Ca++ pathways, and DOX upregulated TGF-β and cAMP/PKA pathways (Figure 2.1.8 B). RES exposure in osteoblastic cells showed to increase major stem cell signalling pathways such as KLF4, Hedgehog, MEF2, Myc/max, Sox2 as compared to MitoTEMPO and DOX (Figure 2.1.8 C). Regarding the toxicity and stress signalling, RES exposure upregulated antioxidant response, heat shock, hypoxia and MAPK/ERK pathways as compared to MitoTEMPO and DOX (Figure 2.1.8 D). On cancer signalling, most of the pathways such as FOXO, STAT3, MAPK/JNK, Myc/max, Notch, p53, TGF-β and wnt were upregulated upon DOX exposure as compared to RES and MitoTEMPO (Figure 2.1.8 E).

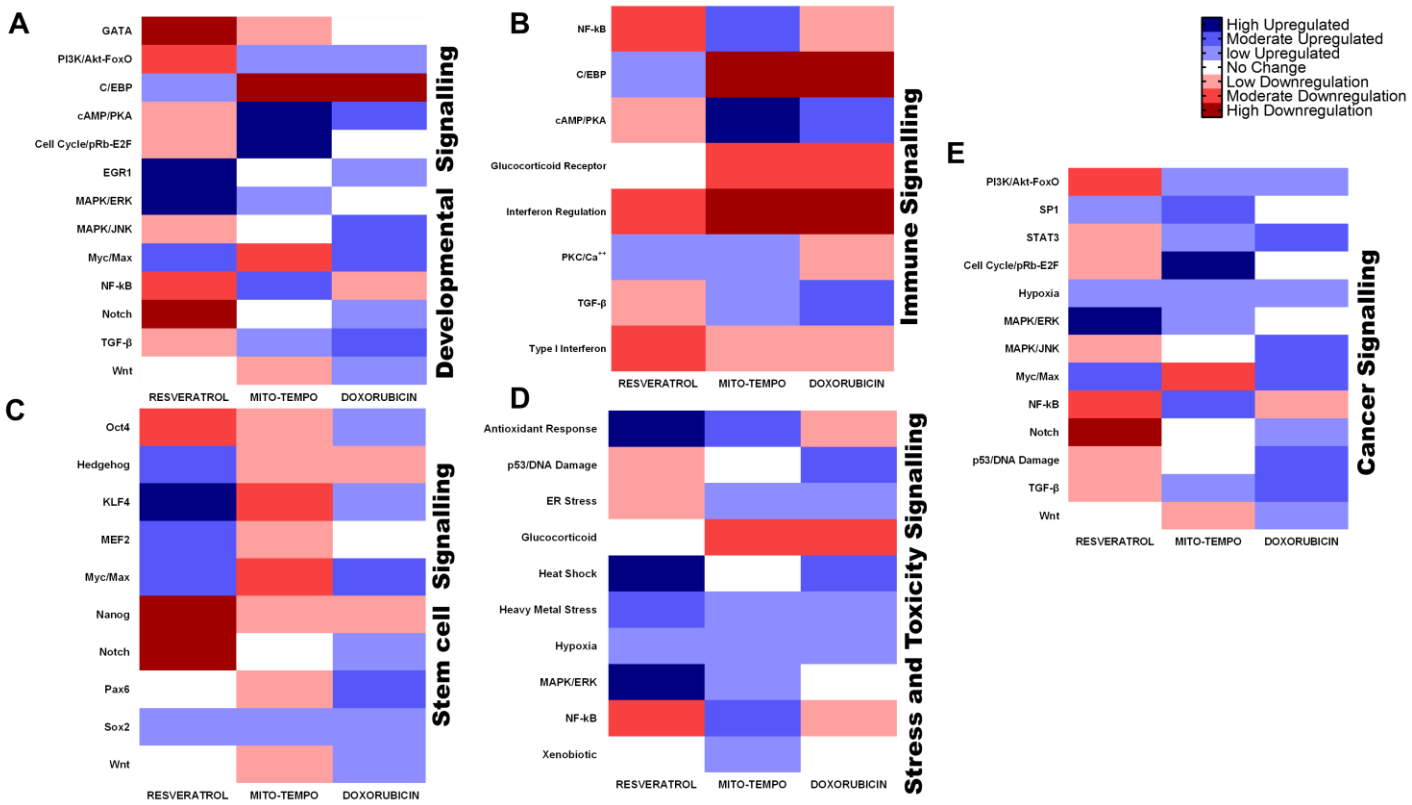

Figure 2.1.8: Activity of cell signalling pathways between RES, MT and DOX. Developmental signalling pathway (A), Immune signalling (B), Stem cell signalling (C), Stress and Toxicity signalling (D) and Cancer signalling (E) was analyzed using Cignal 45-pathway reporter array. Cells were incubated for 24 h then exposed to Resveratrol, MitoTEMPO and Doxorubicin for 24 h. Firefly and Renilla luciferase activities were measured.

2.1.4. DISCUSSION

Osteoporosis is a skeletal disorder characterized by decreased bone mass and skeleton microarchitecture degradation, which leads to bone fragility and risk of fracture (117). In the context of medication or specific diseases, the alteration of bone microarchitecture and low bone mass resulting in bone fragility and risk of fracture is termed as secondary osteoporosis (293). 50-80% of males and 30% of post-menopausal females are found to have secondary osteoporosis (294). Several therapeutic regimens including DOX in chemotherapy carry the risk of causing or favoring the development of secondary osteoporosis (295). DOX/cyclophosphamide combined regimen showed to induce low bone mineral density and significant bone loss (215), and DOX exposure caused a 60% reduction in bone formation in normal rats (216,217). RES has been shown to reverse

the osteoporosis associated bone mass density reduction and microarchitecture deterioration (277). In this study, we are addressing the molecular mechanisms behind DOX-induced bone impairment and effects of RES on the reversal of DOX-induced bone impairment by RNA sequencing and bioinformatic analysis.

2.1.4.1. p53 signalling pathways as a mediator of DOX and RES exposure

In this study, KEGG pathways associated with DOX and RES exposure, alone or in combination, the target genes were identified and analyzed using bioinformatics tools. Among these, the common upregulated and downregulated pathways on all comparison groups were grouped and analyzed. We found that AMPK, Calcium, Cell cycle, cGMP-PKG, Chemokine, Cytokine-cytokine receptor interaction, EGFR tyrosine kinase inhibitor resistance, Focal adhesion, HIF-1, Hippo, Inflammatory mediator regulation of TRP channels, MAPK, Metabolic, mTOR, NOD-like receptor, Oxytocin, p53, PI3K-Akt, PPAR, Proteoglycans in cancer, RAS, TNF and Wnt signalling pathway were either upregulated or downregulated between the treatment of DOX or RES or both.

McSweeney *et al.* (296), has shown that p53 pathways is a key regulator of transcriptomic changes induced by doxorubicin, with expression of death receptor (DR) and apoptotic pathways significantly increased and associated with DOX-induced toxicity (296). In this study, we found that p53 was upregulated on DOX exposure on osteoblastic cells (Figure 11). Activation of p53 increases two pathways, death receptors and stalling of cell cycle progression which intend to repair minor DNA damage and restore genomic stability. If the DNA damage is unrepairable apoptosis is activated (297).

In this study, Cyclin E1 (*Ccne1*), cyclin B2 (*Ccnb2*), *Fas* (TNF receptor superfamily member 6), G two S phase expressed protein 1 (*Gtse1*), p53 induced death domain protein 1 (*Pidd1*) and *Tnfrsf26*, *Tnfrsf21* (tumour necrosis factor receptor superfamily, member 21 and 26) gene were influenced by DOX. Death receptors are part of the TNF-receptor superfamily that initiate apoptosis or necroptosis signal in target cells upon activation by ligands such as Fas ligand, TNF-related apoptosis-inducing ligand (TRAIL) and TNFα (298). These TNF associated cytokines are secreted by normal cells as an innate immune response (299). Increased death receptor expression, TNF-

receptor superfamily in response to the exposure to DOX on osteoblasts also showed to increase cytokine-cytokine receptor interaction and chemokine signalling pathways observed in this study and as suggested by McSweeney *et.al.* (296). p53 gene is associated to both activation of the death receptor apoptotic pathways and repression of cell cycle progression (296,297,300). The downregulation of genes associated with metabolic pathways on DOX-exposure and increased on RES exposure might be a strong indication of p53 activation downregulated several glycolytic pathways and glucose transporters (301). Similar to our result, Yu *et al.*, also showed that RES exposure exhibit protective effects against osteoporosis that were associated with p53 signalling pathway prostate cancer pathway, cell cycle signalling pathway and glioma pathway, and concluded that the anti-osteoporosis effect of RES is associated with the inhibition of the p53 signalling pathway (302).

Calcium is a versatile second messenger regulating cellular processes such as cell proliferation and apoptosis (303). Many chemotherapy agents remodel intracellular Ca2+ homeostasis on various cells, such as the effect of DOX on mitochondrial Ca^{2+} in cardiomyocytes (304). DOX (1 μM) showed to induce alterations in intracellular calcium signalling (305). On MC3T3 cells exposed to DOX, genes associated with calcium signalling pathway (*Cacna1b, Htr2b, Mylk3, Plcd4* and *Tbxa2r*) were upregulated by 10-14 folds as compared to control and 19 folds as compared to RES, whereas, while comparing RES with the combination of DOX+RES, these genes were downregulated by 10 folds.

2.1.4.2. Osteocrin as an activity-regulated factor on DOX-induce bone impairment

Interestingly, we found that Osteocrin (*Ostn*), peptidase inhibitor 16 (*Pi16*) and transcription factor CP2-like 1 (*Tfcp2l1*) were downregulated by 239.9, 53.8 and 34.9-fold respectively as compared to CON on DOX exposure. Osteocrin is also known as musclin, is a novel secretory peptide released mainly from the bone and skeletal muscle, and plays critical roles in regulating bone growth (306–309). Our results showed that osteocrin gene was downregulated on MC3T3 cells upon DOX exposure as compared to control and RES. Conversely, Osteocrin gene was upregulated on RES

as compared to DOX+RES. This suggests that Osteocrin can be one of the candidates for DOX-induced bone impairment and its reversal by RES. Osteocrin showed to increase cGMP levels and PKG which is required for controlling inflammation and oxidative stress (310,311). In our study, we have found that the cGMP-PKG signalling pathway (*Adra1b, Atp2a3, Prkg2*) was down-regulated after DOX exposure as compared to RES, which further confirms the involvement of Osteocrin on reversal of DOX-induce bone impairment. El-Mowafy *et al.*, has shown that RES increase cGMP levels (312). It is proposed that Osteocrin binds to natriuretic peptide receptor NPR3/NPR-C, which prevents binding between NPR3/NPR-C and natriuretic peptides, resulting in increased cGMP production (313). Activation of natriuretic peptide receptors has shown to protect against oxidative stress on vascular smooth muscle (314). Foxo1 was shown to downregulate Osteocrin mRNA expression both *in vitro* and *in vivo* in mice models (315). In this study, we have shown that RES exposure on MC3T3 cells downregulated Foxo1. Osteocrin also has showed to attenuate inflammation, oxidative stress, apoptosis on doxorubicin-induced cardiotoxicity (316). Collectively, our data suggests Osteocrin as one of the responsible factors for DOX-induced bone impairment and that RES could reverse the effect of DOX by influencing Osteocrin (Figure 2.1.9).

Our data provides evidence on key molecular partners of DOX-induced bone loss and the reversal effect of RES on DOX-induced bone loss. Some of the limitations in this study should be considered. Firstly, the interpretation of the large data set with limited bioinformatics tools and comparing different conditions was challenging. Finally, we were able to identify Osteocrin as one of the key players on DOX-induced bone impairment, however, an additional study with qPCR or western blotting is needed to know exactly how DOX-inhibits Osteocrin.

In conclusion, the RNA-seq data revealed that the protective effect of RES against DOX-induced bone impairment was associated with p53 pathways, TNF signalling pathways calcium signalling pathways, and Osteocrin. Our results showed that RES effectively prevents DOX-induced bone impairment, thus suggesting that a combined therapy using DOX and RES may be beneficial for preventing DOX-induced secondary osteoporosis in humans.

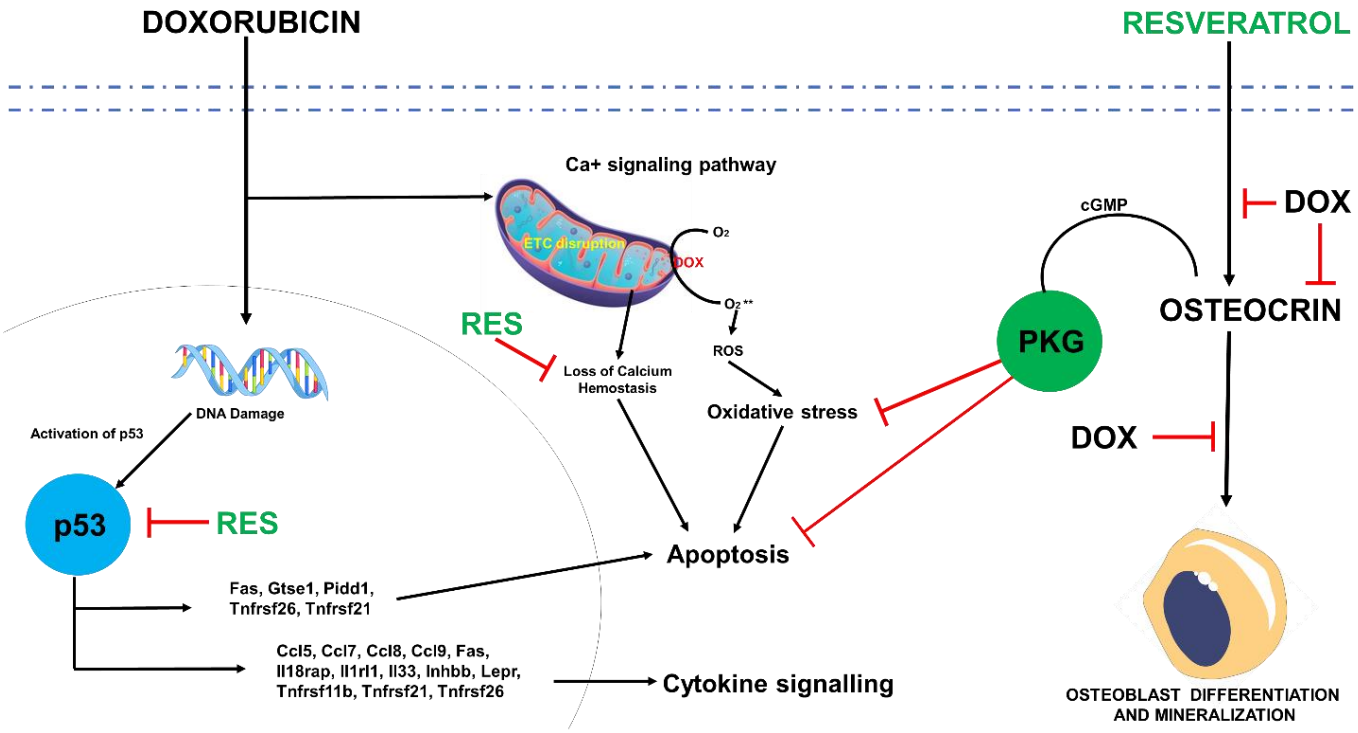

Figure 2.1.9: Proposed mechanism for doxorubicin-induced bone impairment.
Doxorubicin shows several mechanisms for bone impairment including DNA damage which activates p53, activation of p53 increases transcription of genes associated with apoptotic pathway, activation of calcium signalling disrupting calcium hemostasis of the cell, increase ROS and decrease transcription of Osteocrin. While Resveratrol reverses DOX-induced bone impairment by inhibiting p53 and activating transcription of Osteocrin.

CHAPTER 2.2

Resveratrol-mediated reversal of Doxorubicin-induced osteoclast differentiation

Sunil Poudel
Gil Martins
M. Leonor Cancela
Paulo J. Gavaia

International Journal of *Molecular Sciences*

Chapter published in *International Journal of Molecular Sciences* (IJMS). [https://doi.org/10.3390/ijms232315160].

ABSTRACT

Secondary osteoporosis has been associated to cancer patients on Doxorubicin (DOX) as a drug regimen. However, the molecular mechanism behind DOX-induced bone loss has not been fully elucidated. Furthermore, molecules that can protect against the adverse effects of DOX are still a challenge in chemotherapeutic treatments. In this study, we investigated the effect and mechanism of DOX in osteoclast differentiation and used the *Sirt 1* activator resveratrol (RES), to counteract DOX-induced effects on osteoclastogenesis. RAW 264.7 cells were differentiated into osteoclasts under cotreatment with DOX and RES, alone or combined. RES treatment inhibited DOX-induced osteoclast differentiation showing reduction in TRAP-positive cells, in osteoclast fusion marker *Oc-stamp* and on expression of osteoclast differentiation markers *Rank, Trap, Ctsk* and *Nfatc1*. Conversely, RES induced an increase in expression of antioxidant genes *Sod 1* and *Nrf 2*. *FoxM1* expression was significantly

increased by RES, which deregulates ROS levels by stimulating mRNA expression of ROS scavenger genes, such as *Sod 1* and *Nrf 2*. In contrast, DOX significantly reduced *FoxM1* expression resulting in oxidative stress. Treatment with the antioxidant MitoTEMPO did not influence DOX-induced osteoclast differentiation. DOX-induced activation and differentiation of osteoclasts was also studied using the zebrafish *cathepsin*-K reporter line (*Tg[ctsk:DsRed*]). DOX significantly increased *ctsk* positive signal, while cotreatment with RES resulted in a significant reduction of *ctsk* positive cells. Interestingly, RES also significantly rescued DOX-induced mucositis in this model. In addition, zebrafish exposed to DOX displayed altered locomotor behaviour and locomotory pattern, while RES significantly reversed these effects. Our research suggests that RES prevents DOX-induced osteoclast fusion and activation *in vitro* and reduces DOX-induced *ctsk* positive cells and mucositis while improving locomotion parameters *in vivo.* Therefore, these results suggest that RES is an excellent candidate to counteract DOX-induced osteoporosis, which might be highly beneficial for chemotherapeutic regimens.

2.2.1. INTRODUCTION

Doxorubicin (DOX), a first-line chemotherapeutic agent, is known for its cytotoxic effects, characterized by accumulation of reactive oxygen species (ROS) and reactive nitrogen species (NOS) (212). DOX has been shown to increase systematic bone loss and reduce osteoblast differentiation [2,3,4]. Bone homeostasis depends on the cross-talk between bone-forming by osteoblasts and bone resorption by osteoclasts. Any imbalance of this coupled process results in diseases, such as osteopenia and osteoporosis. The presence of ROS can result in increased reduction-oxidation reactions and cause interruption of normal biological functions, leading to oxidative stress and disrupting bone homeostasis (94). Cytokine receptors like TNF-α, IL-1, TGF-β and G protein-coupled receptors have been shown to generate ROS, that will serve as a mediator for the activation of downstream signaling pathways (317). This receptor-mediated generation of ROS plays a crucial role in RANKL-RANK induced osteoclastogenesis (91). ROS produced by macrophages plays a critical role in cellular defence as well as in receptor-mediated pathways such as PI3K, NF-kB and AKT (317,318). During osteoclast differentiation, ROS acts as a secondary messenger in RANKL-RANK dependent signaling pathways such as TRAF, NFATC1, AKT and MAPKS (319–322). Similarly, the NADPH oxidase system (Nox) plays a major role in ROS mediated bone resorption; however, the knockdown mouse model of Nox did not show any reduction of ROS or any bone abnormalities (323,324). ROS produced at various subcellular sites of macrophages, such as the mitochondria electron transfer chain, are responsible for the differentiation of osteoclasts (201). Likewise, NFATC1, a master regulator for osteoclast differentiation, could be a crucial downstream modulator of RANKL-mediated ROS signaling (325).

FoxM1 is a member of the forkhead box transcription factor family, like the FoxO transcription factors. However, in contrast to those, which are activated in quiescent cells and inhibit proliferation, FoxM1 is only expressed in proliferating cells and has a critical role in cell-cycle progression (326–328). Chemotherapeutic agents such as DOX, epirubicin, paclitaxel, lapatinib, gefitinib, imatinib and cisplatin, have been referred to exert their cytotoxic and cytostatic capacities through FoxO3 and FoxM1 (329). The expression of FoxM1 is induced by increased oncogenic stress requiring ROS, that

upregulates FoxM1 in a negative feedback loop. This counteracts elevated intracellular ROS levels by stimulating the expression of antioxidant enzyme genes to protect dividing cells and tumour cells from oxidative stress (326). In addition, FoxM1 has been shown to be a downstream target of p38 MAPK, which is also downregulated in response to DOX and epirubicin exposure (330,331).

Sirt1 inhibits bone resorption by inhibiting Nf-kb signaling in osteoclast lineage cells [24–26] and promotes bone formation via deacetylation of FoxOs (332). Activation of Sirt1 with the natural polyphenol resveratrol (RES) has been proven to attenuate loss of bone mass caused by ovariectomy (333,334), hind limb unloading (335,336), or ageing in mice (337). Additionally, RES also inhibits osteoclast formation *in vitro* through inhibition of ROS (338–340), increases catalase and superoxide dismutase (SOD) activity (341) and protects mitochondria against oxidative stress (342).

Similarly, the mitochondrial superoxidase scavenger, (2-(2,2,6,6-Tetramethylpiperidin-1-oxyl-4-ylamino)-2-oxoethyl) triphenylphosphonium chloride (MitoTEMPO, MT) protects against mitochondrial dysfunction by scavenging ROS (197) (198). N-acetyl Cysteine, an antioxidant widely used as a nutritional supplement, and free radical scavenging enzymes such as superoxide dismutase and diphenyleneiodonium were shown to inhibit osteoclast formation (343,344). Mitochondrial ROS (mtROS) are essential for hypoxic enhancement of osteoclast differentiation (200). Although, on osteoclasts, pyruvate dehydrogenase is not affected during hypoxia, which facilitates the entry of pyruvate to TCA cycle and allows mitochondrial metabolic flux, a continuation of hypoxic oxidative phosphorylation results in the accumulation of mitochondrial ROS in osteoclasts (200,345). Mitochondrial antioxidants have been shown to reverse the effect of mtROS on osteoclast differentiation (201,344) as it was referred for mitochondria-specific antioxidant MitoQ, that was shown to prevent hypoxic induction of NF-kB, NFAT pathway, CREB and HIF signalling molecules during osteoclast differentiation and suppressed the RANKL-induced differentiation of RAW264.7 cells into multinucleated and TRAP positive osteoclasts (201). Tafazzin is a mitochondrial enzyme crucial for cardiolipin remodeling. Knocking down tafazzin in cardiac myocytes decreased levels of cardiolipin and increased mtROS resulting in mitochondrial dysfunction. MitoTEMPO

treatment normalized tafazzin knockdown-induced mtROS production and counteracted the resultant apoptosis (346).

DOX has also been shown to increase bone loss by restraining osteoblastogenesis (213) and increasing osteoclastogenesis (347). In addition, DOX and epirubicin exposure were shown to downregulate FoxM1 (330,331), leading to activation of osteoclast differentiation (348). We hypothesized that the involvement of FoxM1 on DOX-induced osteoclast differentiation is a contributing factor for DOX-induced bone loss. Therefore, in this study, we investigated the involvement of FoxM1 on DOX-induced osteoclast differentiation and examined the potential of antioxidants to reverse these negative effects of DOX on bone. In addition, we used a *cathepsin*-K reporter zebrafish transgenic line (*Tg[ctsk:DsRed*]) (349) to investigate the effects of DOX, RES and MT on the activation of osteoclasts and to investigate the capacity of antioxidants to counteract the effect of DOX *in vivo*.

2.2.2. MATERIALS AND METHODS

2.2.2.1. Cells and cell culture

RAW 264.7 cells were cultured in Dulbecco's Modified Eagle Medium (DMEM; Gibco, Grand Island, NY, USA) supplemented with 10% fetal bovine serum (FBS), incubated in humidified air atmosphere containing 5% CO_2 at 37 °C. In addition, all culture media were supplemented with 1% penicillin/streptomycin, 2 mM L-Glutamine and 0.2% fungizone. FBS, Penicillin and streptomycin and L-Glutamine were obtained from Gibco (Gibco).

2.2.2.2. XTT assay

Cytotoxicity was analyzed by XTT assay (Biotium, Fremont, USA). In short, RAW 264.7 cells were seeded in 96-well plates and treated with antioxidants or pro-oxidant. RAW 264.7 cells were treated with RES (TCI, Tokyo, Japan) and MT (Sigma-Aldrich, Darmstadt, Germany) for 4 days, whereas cells were treated with DOX (TCI) for 3 hours. Hereafter, 25µl of XTT activator reagent was mixed with 5 ml XTT reagent and mixed. Next, 50 µl of freshly prepared XTT reagent (activator + reagent) was added to 100 µl of fresh media 100. Finally, 150 µl of media + XTT was added to each well and incubated for 2 - 4 h at 37°C, 5 % CO_2. The absorbance was measured at 630 nm using a microplate reader (Biotek synergy 4, Winooski, USA). Three isolated experiments were performed.

2.2.2.3. Osteoclast Differentiation

RAW 264.7 cells were differentiated into osteoclasts by induction with M-CSF (30 ng/ml) (Peprotech, London, UK) and RANKL (50 ng/ml) (Peprotech). All differentiation experiments were done with a Control- (Growth medium), a Control+ [cytokines (RANKL and M-CSF)] and with treatment using RES (Cytokines + Resveratrol), MT (Cytokines + MT), DOX (Cytokines + DOX), and in combinations of antioxidants with DOX (Cytokines+ antioxidants + DOX). The cells were exposed to RES or MT continuously for 4 days, whereas exposure to DOX was done for 3 hours, every 72 hours. Treatment

media was replaced every 72 hours. Three isolated experiments were performed. For *in vitro* treatments, RES was dissolved in pure ethanol and stored at a concentration of 220 mM, and a working solution was prepared at 10mM. MT was dissolved and stored at a concentration of 50 mM in distilled water and the working solution was prepared by diluting the stock solution to 1mM. DOX was dissolved in distilled water and stored at 100 mM, and a working solution was prepared at 100µM. All antioxidants and pro-oxidant solutions were stored at -20°C covered with aluminum foil to protect from direct light, and all experiments were conducted at low light conditions.

2.2.2.4. Tartrate-resistant acid phosphatase staining (TRAP Staining)

For TRAP staining, RAW 264.7 cells (2.5×10^4 cells/well) were seeded on 24 well plates. Following that, cytokines, M-CSF (30 ng/ml) and RANKL (50 ng/ml) were used for treatment together with antioxidants and pro-oxidant. First, RAW 264.7 cells were treated with antioxidants (RES and MT) for 4 days whereas, cells were treated with pro-oxidant (DOX) for 3 hours. Then, RES, MT, DOX and cytokines were added to the wells, and the medium was renewed after 2 days. Finally, TRAP staining was performed after 4 days of treatment following the Burstone (350) method using Naphthol AS-MX phosphate (Sigma-Aldrich) and Fast Red stain (Sigma-Aldrich). Briefly, cells are fixed with 4% paraformaldehyde for 10 minutes. Then, cells were incubated on buffer containing 50 mM di-sodium tartrate dehydrate on 0.1M acetate buffer, 0.04% $MgCl_2$ at pH to 4.4 for 15 minutes, then the samples were stained with TRAP-staining buffer [(Incubation buffer+ Naphthol AS-MX phosphate (0.1 mg/ml) and Fast Red Violet LB (0.3 mg/ml)] in the dark until TRAP signal was visible. All the experiments were done in triplicates.

2.2.2.5. RT-PCR and real-time PCR

RNA was isolated from the cultures using the Nzyol reagent (Nzytech, Lisbon, Portugal) according to the manufacturer's instructions. The concentration of RNA was measured by Nanodrop (Thermo Scientific, Waltham, USA). cDNA synthesis was reverse transcribed to cDNA using a kit (Thermo Scientific). 1 µg total RNA from the cells was

used cDNA synthesis. DNA digestion was done with DNase I treatment (Promega, Madison, USA) for 30 min at 37ºC and reverse-transcribed for 1 h at 37°C using M-MLV reverse transcriptase (Invitrogen, Waltham, USA), oligo-d(T) universal primer [5'-ACGCGTCGACCTCGAGATCGATG(T)13-3'] and RNaseOUT (Invitrogen). Quantitative real-time PCR (qPCR) assays were performed using the Bio-Rad CFX system (Bio-RAD, Hercules, USA). Gene expression was normalized using β-actin as a housekeeping gene (281), and relative quantification was determined using the ΔΔCt method (351). Primers used in this study are listed in Table 2.2.1.

Table 2.2.1: Primer sequences. All sequences in 5´ to 3´orientation.

Gene		Sequences
Beta-actin	Forward primer	CCTGACCCTGAAGTACCCCATTGA
	Reverse primer	GTCATCTTTTCACGGTTGGCC
Oc-stamp	Forward primer	TGGGCCTCCATATGACCTCGAGTAG
	Reverse primer	TCAAAGGCTTGTAAATTGGAGGAGT
Rank	Forward primer	TGCCTCTGGGAACGTGACTG
	Reverse primer	AGGTCTGGCTGACATACACCAC
Trap	Forward primer	CAGCTGTCCTGGCTCAAAA
	Reverse primer	ACATAGCCCACACCGTTCTC
Nfatc1	Forward primer	CAAGTCCTCACCACAGGGCTCACTA
	Reverse primer	GCGTGAGAGAGGTTCATTCTCCAAGT
Ctsk	Forward primer	CTGAAGATGCTTTCCCATATGTGGG
	Reverse primer	GCAGGCGTTGTTCTTATTCCGAG
Nf-kb p105	Forward primer	TGTCAACAGATGGCCCATACCT
	Reverse primer	TTGTGACCAACTGAACGATAACCT
Sod 1	Forward primer	GGACAATACACAAGGCTGTACCA
	Reverse primer	CAGTCACATTGCCCAGGTCTC
Nrf 2	Forward primer	AAAGTTCAGTCTTCACTGCCC
	Reverse primer	TCGGTATTAAGACACTGTAATTCGG
FoxM1	Forward primer	GTCTCCTTCTGGACCATTCACC
	Reverse primer	GCTCAGGATTGGGTCGTTTCTG

2.2.2.6. Osteoclast activation *In vivo*

To examine osteoclast activation *in vivo*, a *cathepsin*-K (*ctsk*) reporter zebrafish transgenic line (*Tg[ctsk:DsRed*]) (349) was used. A working solution of RES was prepared at 75mM and 100mM in ethanol, MT was prepared at 20mM and DOX was

prepared at 1mM. Triplicate groups of 15 zebrafish post-larvae at 25 days post-fertilization (dpf) were waterborne exposed to RES (75µM and 100µM), MT (20µM) and DOX (17.2µM) alone and in combinations as follows: DOX+RES 75 (17.2µM+ 75µM), DOX+RES 100 (17.2µM+ 75µM) and DOX+MT (17.2µM+ 20µM) for 24 hours. After 24 hours of exposure, 6 post-larvae were randomly selected from each group to analyze locomotor behavior, where each fish was placed in a well of a 12-well plate for behaviour analysis using a Zantiks MWP larvae tracking system (Zantiks Ltd, Cambridge, UK). The post-larvae were acclimated for 15 minutes in the tracking system, before locomotor behaviour was analyzed for 5 minutes. *Ctsk* signal was identified by fluorescence microscopy using a Leica Mz7.5 stereomicroscope (Leica, Wetzlar, Germany) equipped with an mcherry filter (550-650 nm) and a DFC7000T color camera (Leica). Images were further analyzed using ImageJ1.53c. To measure the fluorescence intensity, the RBG image was split into single channels and converted into grayscale. First, the threshold was adjusted to highlight the fluorescence signal on the head and abdominal region. Then, the intensity was measured, and relative intensity was calculated.

2.2.2.7. Statistical analysis

Statistical analysis was performed using Graphpad prism 8 software, and results are expressed as mean ± SEM. The data sets presenting a normal distribution were evaluated by student's t-test or one-way analysis of variance (ANOVA) test. Significance of results was considered for $p \leq 0.05$ (ns- $P>0.05$, *- $P\leq0.05$, **-$P\leq0.01$, ***-$P\leq0.001$, ****-$P\leq0.0001$). All graphics were drawn using GraphPad prism 8.

2.2.3. RESULTS

2.2.3.1. Cytotoxic effect of Resveratrol, Doxorubicin and MitoTEMPO

To investigate the molecular mechanisms underlying the effect of RES, MT and DOX on osteoclast differentiation we first performed an XTT assay to analyze the potential cytotoxic concentration of these compounds on RAW 264.7 cells. As shown in Figure 2.2.1A, all concentrations tested, up to 10 µM of RES, did not produce any toxic effect on the cells after 4 days of treatment. DOX exposure at a concentration range of 0.1 µM- 0.5 µM DOX did not show any toxicity (Figure 2.2.1B). MT did not show any toxic effect on cells after 4 days of treatment at concentrations from 5 µM to 20 µM (Figure 2.2.1C). Therefore 10 µM RES, 10 µM MT and 0.1µM DOX (3 hours exposure with 72 hours intervals) were determined as non-toxic and selected for further experiments with RAW 264.7cells.

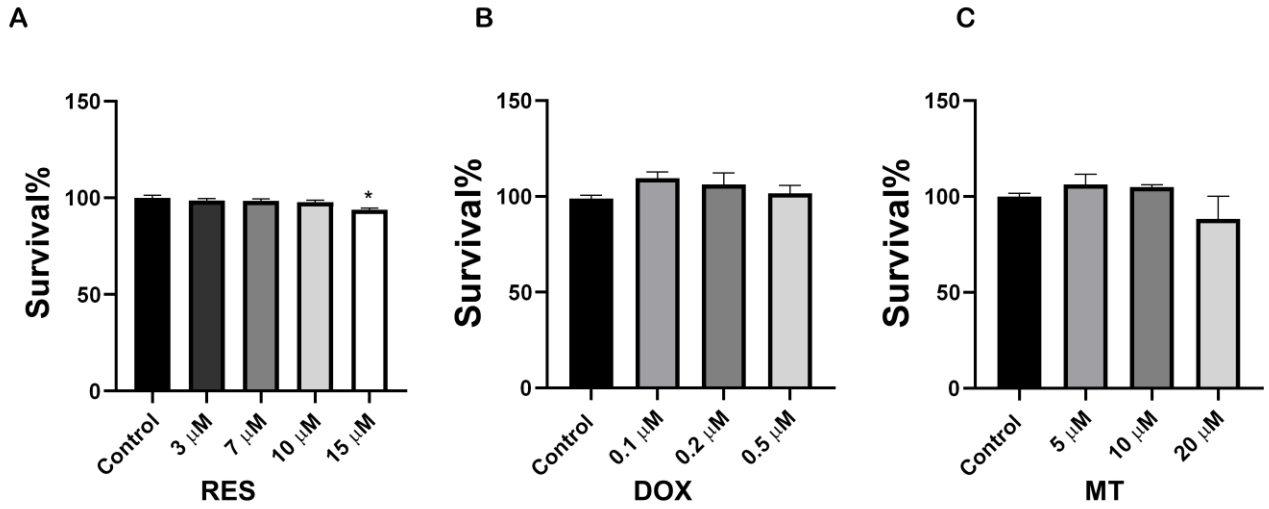

Figure 2.2.1: Cytotoxicity of doxorubicin and antioxidants on RAW 264.7 cells. RAW 264.7 cells were exposed to Doxorubicin (DOX) (A), Resveratrol (RES) (B) and MitoTEMPO (MT) (C) and XTT assay was performed. Cells were treated for 3 days with RES and MT, and for 3 hours with DOX. One-way ANOVA, Tukey's multiple comparisons test, *- $P \leq 0.05$.

2.2.3.2. Inhibition of Doxorubicin-induced osteoclastogenesis by RES

Raw 264.7 cells were differentiated into the osteoclastic lineage by induction with M-CSF (30 ng/ml) and RANKL (50 ng/ml) in co-treatment with DOX and RES to verify the effect of exposure to these molecules, alone or in combination, over osteoclastogenesis (Figure 2.2.2A). DOX treatment showed a significant increase in the number of tartrate-

resistant acid phosphatase (TRAP)-positive cells compared to a positive control (with M-CSF and RANKL). However, while co-treating with DOX and RES simultaneously, the number of TRAP-positive osteoclastic cells was significantly reduced compared to DOX alone (Figure 2.2.2B). In addition, the number of multinucleated osteoclasts was significantly increased in the DOX treatment compared to the RES and control groups (Figure 2.2.2C).

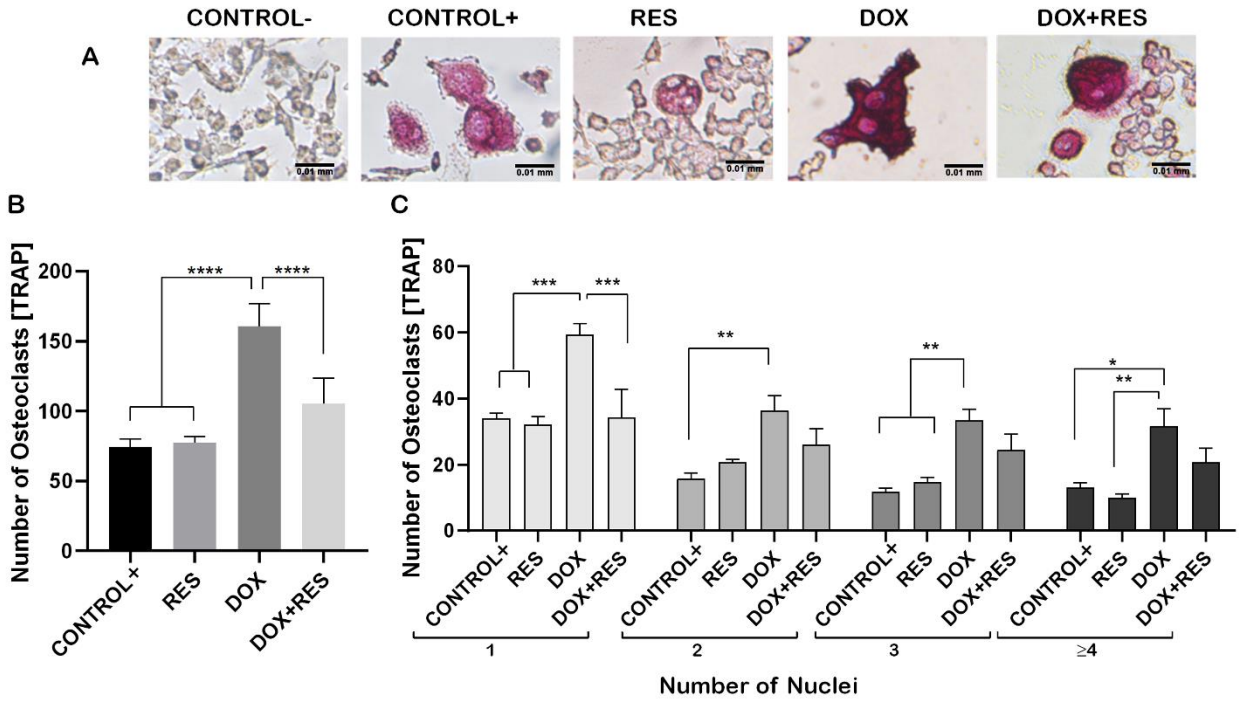

Figure 2.2.2: Resveratrol prevents Doxorubicin-induced osteoclast differentiation. RAW 264.7 cells were cultured for 4 days with M-CSF (30 ng/ml) and RANKL (50 ng/ml) and treated with Resveratrol (RES) and Doxorubicin (DOX) alone or combined. TRAP positive osteoclastic cells (A). Number of TRAP-positive cells (B). Number nuclei in TRAP-positive cells from the different treatments (C). One-way ANOVA, Tukey's multiple comparisons test, *- P≤0.05, **-P≤0.01, ***-P≤0.001, ****-P≤0.0001.

2.2.3.3. Resveratrol inhibits Doxorubicin-induced osteoclast differentiation marker genes

During osteoclast differentiation, Oc-stamp, *Rank, Trap, Ctsk*, *Nf-kb* and *Nfatc1* play essential roles. The mRNA expression of these differentiation markers of osteoclastogenesis was examined after 96 hours of differentiation in Raw 264.7 cells. DOX treatment showed increased multinucleated osteoclasts, whereas when combined with RES, the number of multinucleated osteoclasts decreased (Figure 2.2.2).

Therefore, we hypothesized that DOX increases the fusion of the osteoclast. As expected, the mRNA levels of the osteoclast fusion marker osteoclast stimulatory transmembrane protein (Oc-stamp) were significantly increased on DOX treatment, while in combination with RES, Oc-stamp was significantly downregulated (Figure 2.2.3A). Similarly, DOX treatment significantly increased *Rank* expression compared to negative control; however, on co-treatment with RES, *Rank* expression was significantly reduced compared to DOX (Figure 2.2.3B). Similarly, *Trap* expression was reduced upon RES treatment as compared to positive control and on combined treatment, and *Trap* mRNA expression was significantly reduced by RES as compared to DOX alone (Figure 2.2.3C). *Ctsk* mRNA expression was significantly increased upon DOX treatment as compared to other groups; however, RES significantly decreased the DOX-induced expression of *Ctsk (*Figure 2.2.3D).

Furthermore, RES significantly reduced the expression of *Nfatc1* as compared to positive control whereas, when combining RES with DOX, RES significantly reduced *Nfatc1* expression as compared to DOX alone (Figure 2.2.3E). *Nf-kb p105* was significantly upregulated upon RES treatment, whereas when combining DOX with RES, the expression of *Nf-kb p105* was significantly reduced as compared to RES alone (Figure 2.2.3F). This indicates that RES inhibits *Nf-kb* induced osteoclast differentiation.

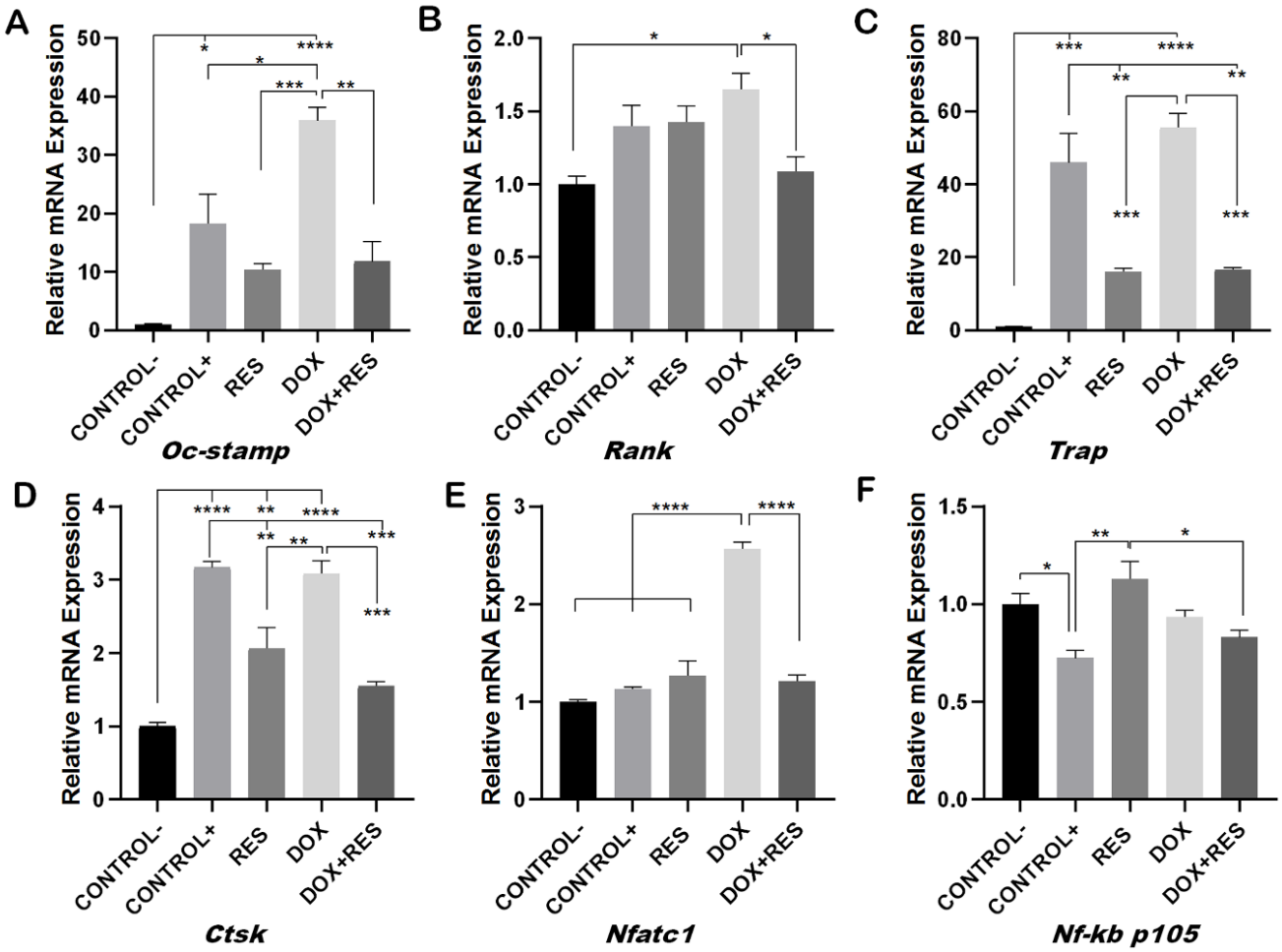

Figure 2.2.3: Inhibition of Doxorubicin-induced osteoclast differentiation by Resveratrol. RAW 264.7 cells were cultured for 4 days with M-CSF (30 ng/ml) and RANKL (50 ng/ml) and treated with Resveratrol (RES) and Doxorubicin (DOX) alone or combined. Levels of mRNA expression for *Oc-stamp* (A), *Rank* (B) *Trap* (C), *Ctsk* (D), *Nfatc1* (E) and *Nf-kb p105* (F) were analyzed by qPCR. One-way ANOVA, Tukey's multiple comparisons test, *- P≤0.05, **-P≤0.01, ***-P≤0.001, ****-P≤0.0001.

2.2.3.4. Involvement of FoxM1 on osteoclast differentiation and Oxidative stress

FoxM1 transcription factor controls cell proliferation by promoting cell cycle progression and is a critical regulator of oxidative stress. Elevated *FoxM1* levels downregulate ROS by stimulating the expression of ROS scavenger genes such as *Sod 1*, *Nrf 2,* among others (326,352,353). The expression of *FoxM1* was significantly reduced on osteoclasts (positive control) as compared to the undifferentiated cells (negative

control), suggesting a high involvement of ROS in the differentiation processes (Figure 2.2.4A).

The expression of *FoxM1* was significantly upregulated on the RES group relative to the positive control and DOX, whereas in the group co-treated with DOX and RES, the expression of *FoxM1* showed only a slight increase which was not significantly different from DOX or the other groups (Figure 2.2.4A). The expression of antioxidant gene *Sod 1* was significantly reduced on the DOX group as compared to RES treated cells and positive control, however co-treatment group showed a small rescue of Sod 1 expression (Figure 2.2.4B). RES also significantly upregulated *Nrf 2* mRNA expression as compared to the positive and negative controls. However, DOX and DOX+RES also upregulated *Nrf 2* mRNA as compared to positive control (Figure 2.2.4C).

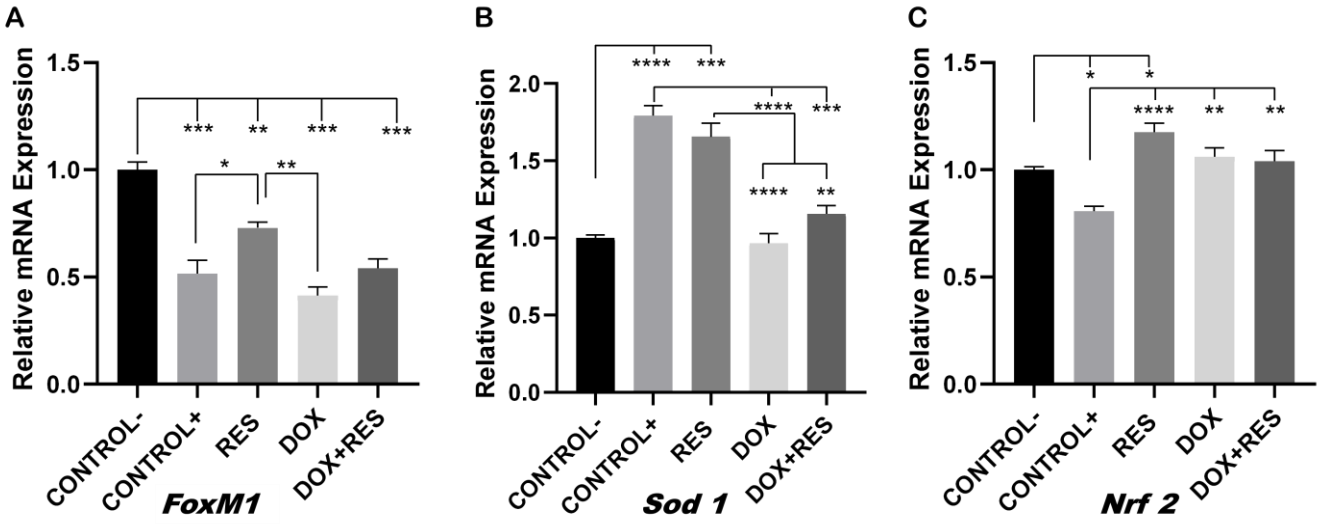

Figure 2.2.4: Involvement of FoxM1 on osteoclast differentiation and oxidative stress. RAW 264.7 cells were cultured for 4 days with M-CSF (30 ng/ml) and RANKL (50 ng/ml) and treated with Resveratrol (RES), MitoTEMPO (MT) and Doxorubicin (DOX) alone or together. RNA from the cells was obtained, and mRNA expressions for *FoxM1* (A), *Sod 1* (B) and *Nrf 2* (C) were analyzed by qPCR. One-way ANOVA, Tukey's multiple comparisons test, *- P≤0.05, **- P≤0.01, ***-P≤0.001, ****-P≤0.0001.

2.2.3.5. Effect of Mitochondrial antioxidant on Doxorubicin-induced osteoclast differentiation.

To investigate the involvement of ROS during osteoclast differentiation, we used MT (MitoTEMPO, triphenylphosphonium chloride), a mitochondrial superoxide scavenger, which blocks mitochondrial ROS and intracellular ROS generation (354,355). MT was shown to significantly reduce DOX-induced osteoclast differentiation, as observed by the TRAP-positive cells (Figure 2.2.5 A, B). No significant difference was observed on the number of TRAP-positive cells on MT treatment compared to positive control. While when combining DOX with MT, the number of single nucleated osteoclasts was significantly lower on the combined treatment with DOX and MT compared to DOX alone. However, the number of multinucleated osteoclasts (with 3 or 3+ nuclei) was not significantly different on DOX compared to DOX and MT (Figure 5C). The number of multinucleated TRAP positive cells (with 3 or 3+ nuclei) were significantly increase on the combined treatment with DOX and MT as compared to MT alone and control (Figure 2.2.5C). Therefore, MT showed a limited effect in counteracting the DOX-induced osteoclast differentiation.

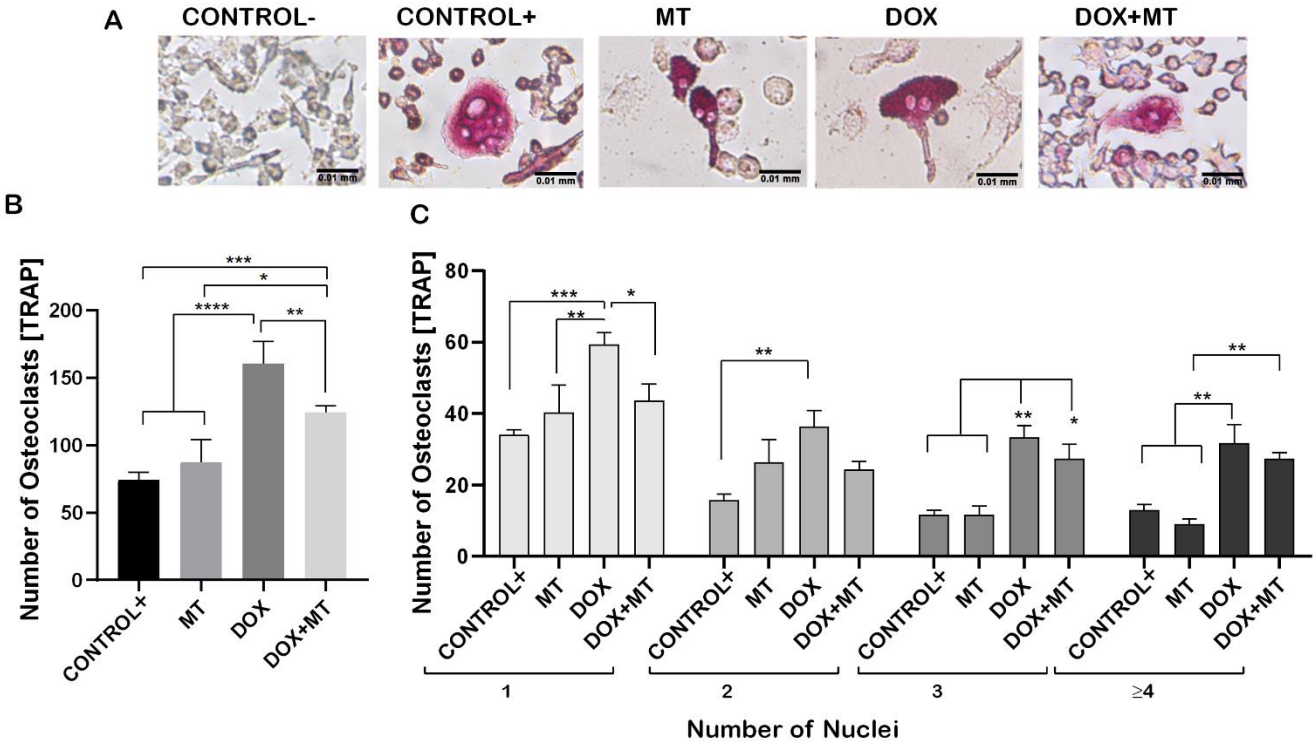

Figure 2.2.5: Effect of MitoTEMPO on Doxorubicin-induced osteoclast differentiation. RAW 264.7 cells were cultured for 4 days with M-CSF (30 ng/ml) and RANKL (50 ng/ml) and treated

with MitoTEMPO (MT) and Doxorubicin (DOX) alone or together. Cells were stained for TRAP (A). The number of TRAP-positive cells (B). The number of TRAP-positive cells with multiple nuclei (C). One-way ANOVA, Tukey's multiple comparisons test, *- P≤0.05, **-P≤0.01, ***-P≤0.001, ****-P≤0.0001.

2.2.3.6. MitoTEMPO is unable to reverse Doxorubicin-induced osteoclast markers genes

To investigate if MT was able to reverse the DOX-induced osteoclast differentiation, we investigated osteoclast fusion and differentiation markers on MT and DOX alone and in combination. The DOX-induced expression of the osteoclast fusion marker *Oc-stamp* was not reduced when combined with MT (Figure 2.2.6A). The DOX-induced expression of differentiation markers of osteoclastogenesis *Rank, Trap, Ctsk* and *Nfatc1* were unaffected when combined with MT (Figure 2.2.6 B, C, D and E). *Trap* and *Nfatc1* were significantly reduced upon MT treatment as compared to positive control (Figure 2.2.6, C and E). The DOX-induced expression of *Nf-kb p105* was also not affected by MT cotreatment (Figure 2.2.6F). The mRNA expression of *FoxM1* was significantly reduced on all treatment groups as compared to the negative control (Figure 2.2.6G). Since MT, a mitochondrial superoxide scavenger, blocks mitochondrial ROS and intracellular ROS generation (354,355), the mRNA expression of *Sod 1* was significantly lower as compared to positive control. However, also DOX and DOX+MT treatments showed a downregulation of *Sod1* (Figure 2.2.6H). *Nrf 2* mRNA expression was upregulated in all treatments as compared to positive control. However, it showed no significant differences between MT and DOX alone or in combination (Figure 2.2.6I).

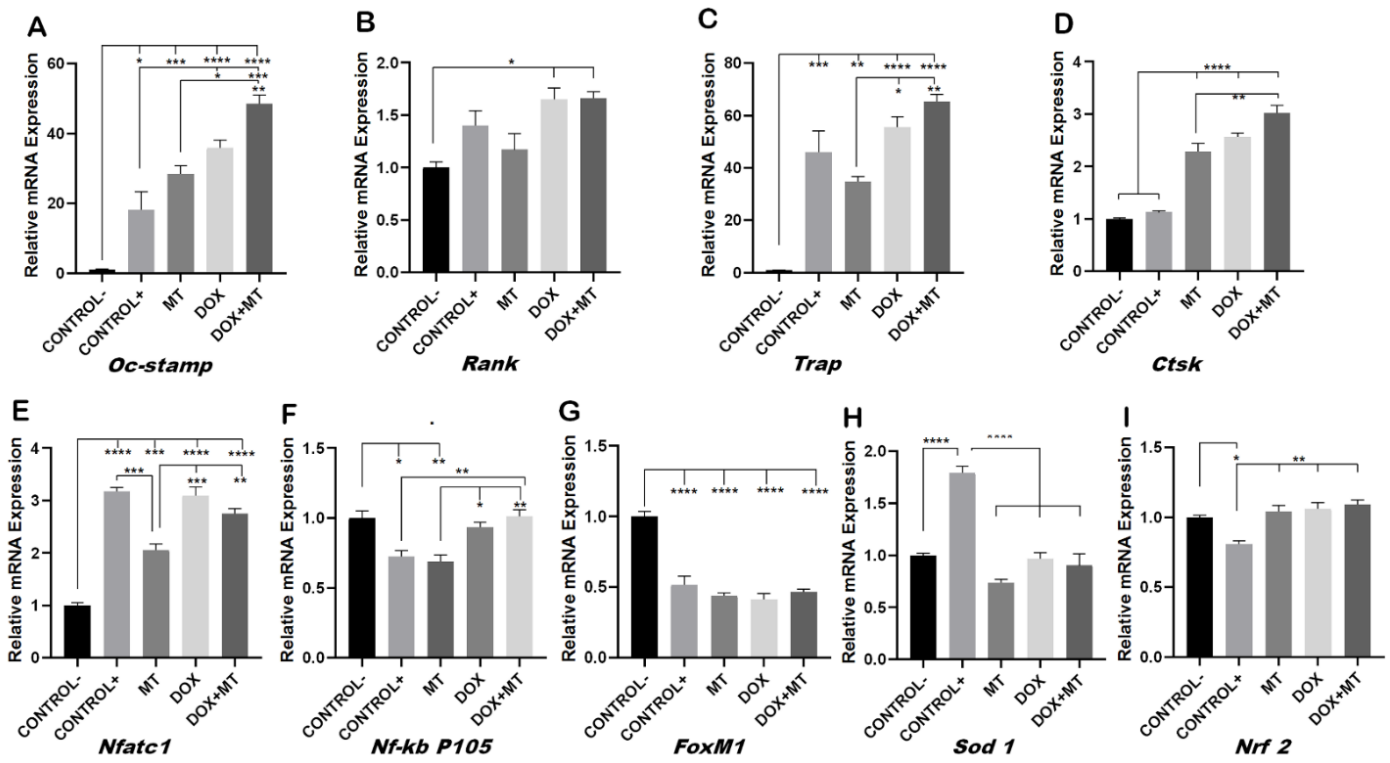

Figure 2.2.6: Effect of MitoTEMPO on Doxorubicin-induced osteoclast differentiation and oxidative stress markers. RAW264.7 cells were cultured for 4 days with M-CSF (30 ng/ml) and RANKL (50 ng/ml) and treated with MitoTEMPO (MT) and Doxorubicin (DOX) alone or together. Levels of mRNA expression for *Oc-stamp* (A), *Rank* (B), *Trap* (C), *Ctsk* (D), *Nfatc1* I *Nf-kb p105* (F), *FoxM1* (G), *Sod1* (H) and *Nrf2* (I) were analyzed by qPCR. One-way ANOVA, Tukey's multiple comparisons test, *- P≤0.05, **-P≤0.01, ***-P≤0.001, ****-P≤0.0001.

2.2.3.7. *In vivo* reversal of Doxorubicin-induced osteoclast differentiation by Resveratrol

We investigated the effect of DOX and RES, alone or in combination, in a *ctsk* reporter zebrafish transgenic line (*Tg[ctsk:DsRed*]) (349). At 25 dpf zebrafish were exposed to DOX (17.2 µM) alone, RES (75 µM and 100 µM) alone or in combination for 96 hours. After 96 hours, *ctsk* positive cells on the head area were identified by fluorescence microscopy; *ctsk* positive cells were significantly higher on DOX treated groups (Figures 2.2.7A, and B). While when combining DOX with RES, the number of *ctsk* positive cells was significantly reduced as compared to DOX alone (Figure 2.2.7B), suggesting that RES significantly prevented DOX-induced osteoclast differentiation *in vivo*.

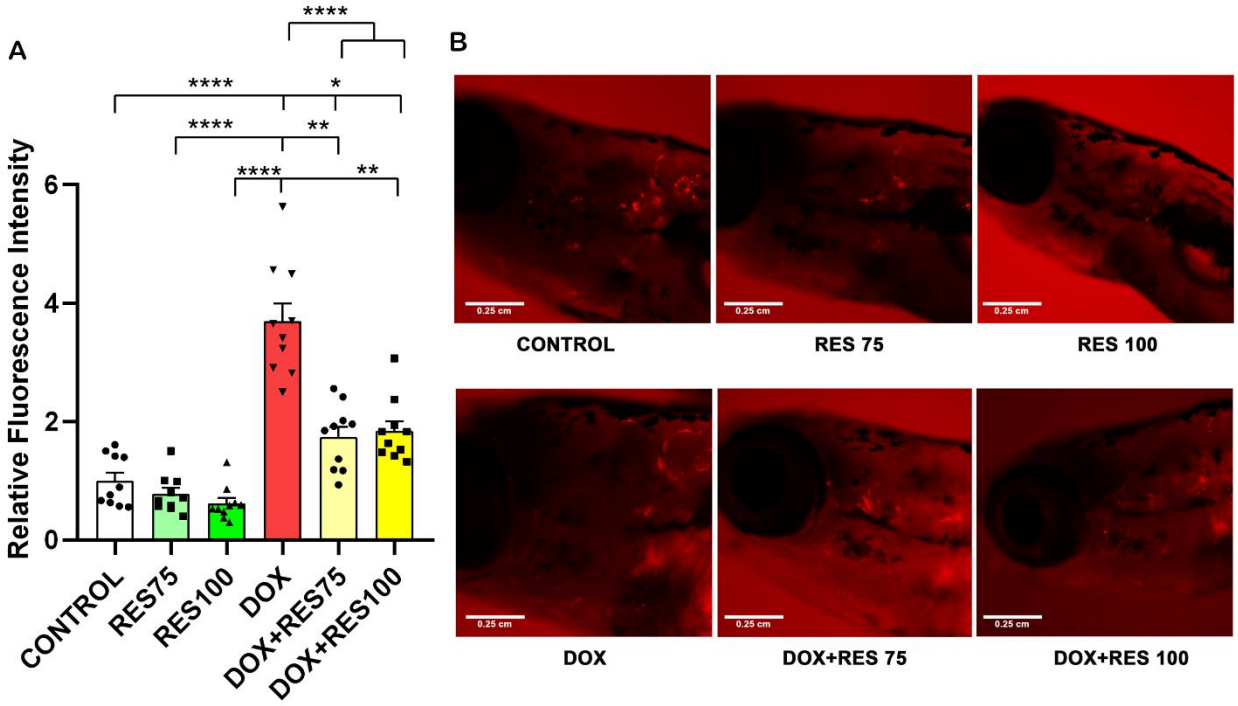

Figure 2.2.7: Inhibitory effect of Resveratrol on Doxorubicin-induced stimulation of osteoclasts. The *ctsk* reporter zebrafish transgenic line (*Tg[ctsk:DsRed*]) at 25 dpf was exposed to different concentrations of Resveratrol (RES, 75 µM and 100 µM) alone or together with Doxorubicin (DOX, 17.2 µM) for 96 hours and *ctsk* signal was measured in the head area. Quantification of fluorescence intensity between the treatment groups (A), *ctsk* positive cells (B). One-way ANOVA, Tukey's multiple comparisons test, *- P≤0.05, **-P≤0.01, ****-P≤0.0001.

2.2.3.8. *In vivo* reversal of Doxorubicin induced mucositis by Resveratrol

Our results revealed that DOX increased mucositis on zebrafish. The expression of *ctsk* on the abdominal region was extremely high on DOX treated groups as compared to control and RES groups (Figure 2.2.8 A and B). While when combining DOX with 75 µM or 100 µM RES, the mucositis was significantly reversed, as shown by the reduction in fluorescence signal on the abdominal region (Figure 2.2.8B).

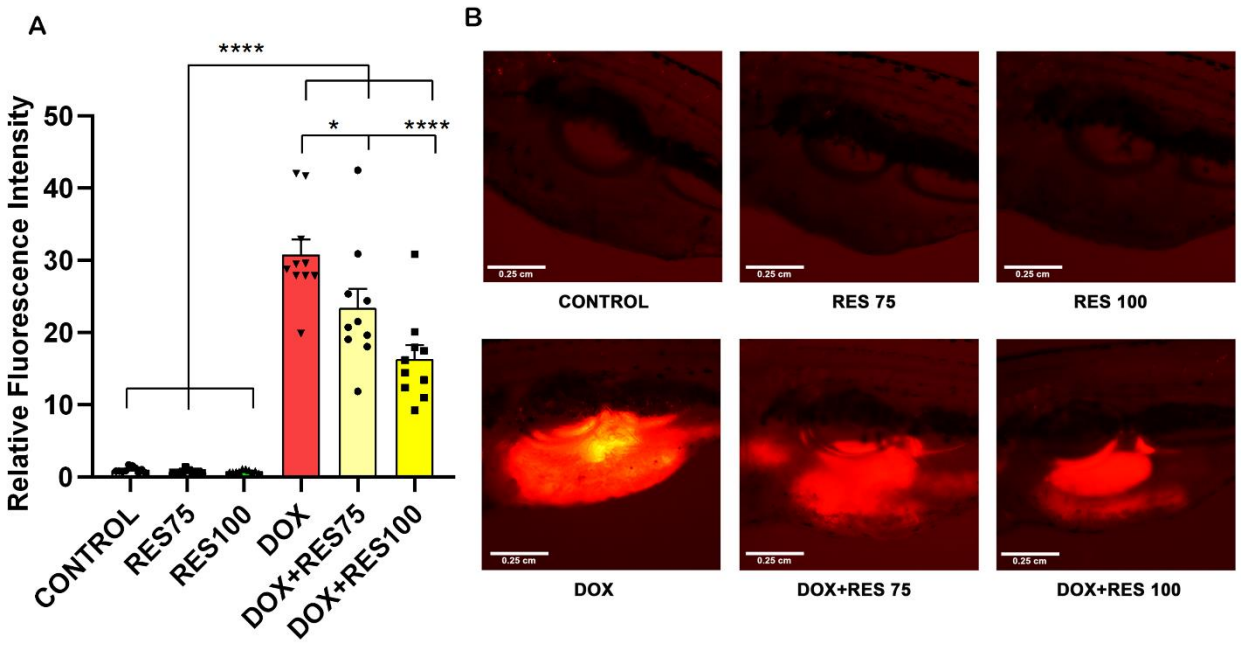

Figure 2.2.8: Reversal of Doxorubicin-induced mucositis by Resveratrol. The *ctsk* reporter zebrafish transgenic line (*Tg[ctsk:DsRed*]) was exposed to different concentrations of Resveratrol (RES, 75 µM and 100 µM) alone or together with Doxorubicin (DOX, 17.2 µM) for 96 hours. Quantification of fluorescence intensity between the treatment groups (A), *ctsk* signal in the abdominal area of the fish (B). One-way ANOVA, Tukey's multiple comparisons test, *-P≤0.05, ****-P≤0.0001

2.2.3.9. MitoTEMPO is unable to reverse Doxorubicin-induced osteoclast differentiation *in- vivo.*

We investigated the effect of DOX and MT, alone or in combination, in a *ctsk* reporter zebrafish transgenic line (*Tg[ctsk:DsRed*]). Our results showed that when combining MT with DOX, the *ctsk* positive cell's fluorescence signal was not significantly altered compared to the DOX treatment group (Figure 2.2.9 A,B). Therefore, MT at 20 µM concentration was unable to reverse the DOX-induced osteoclast differentiation as indicated by *ctsk* positive cells.

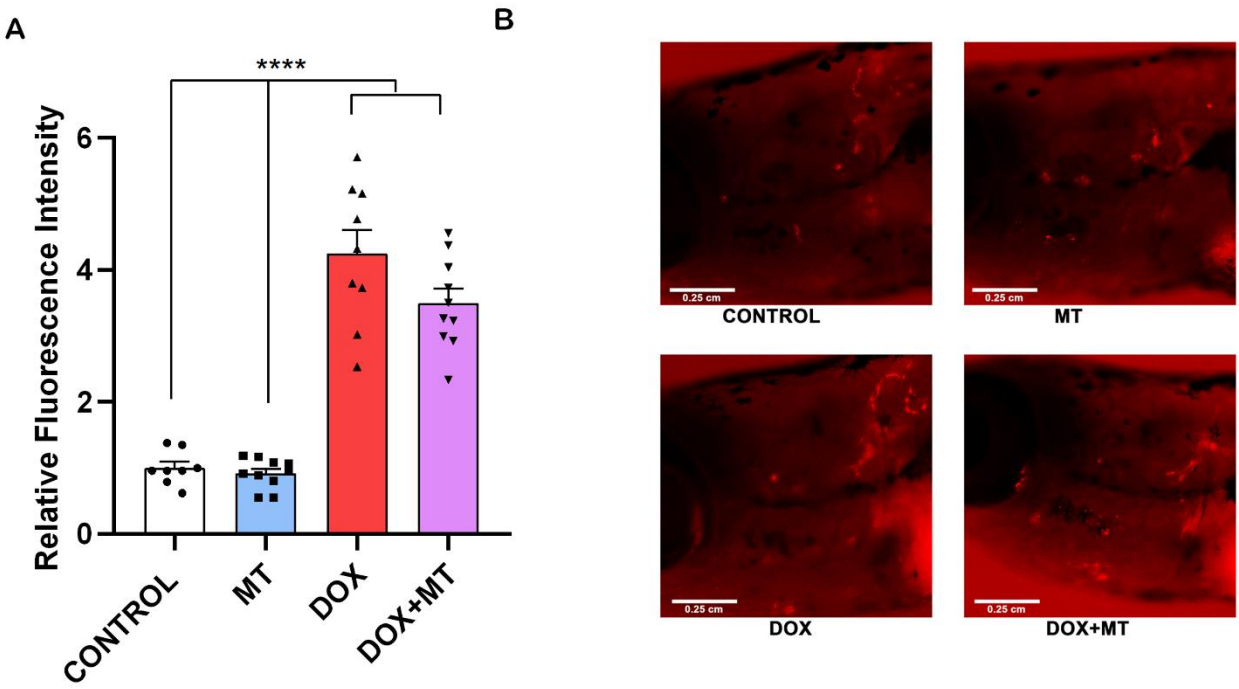

Figure 2.2.9: Effect of MitoTEMPO on Doxorubicin-induced stimulation of *ctsk* cells. The *ctsk* reporter zebrafish transgenic line (*Tg[ctsk:DsRed*]) at 25 dpf were exposed to MitoTEMPO (MT, 20µM) alone or together with Doxorubicin (DOX, 17.2µM) for 96 hours. Quantification of fluorescence intensity between the treatment groups (A) and the *ctsk* signal in the head area (B). One-way ANOVA, Tukey's multiple comparisons test, ****-P≤0.0001.

2.2.3.10. Doxorubicin decreases locomotor activity of zebrafish

Zebrafish at 25 dpf were exposed to RES (100µM), MT (20µM) and DOX (17.2µM) alone or in different combinations for 24 hours, and the locomotor activity were analyzed using a Zantiks MWP. Figure 2.2.10A show the total travelled distance of the post-larvae treated with RES, MT and DOX. The travelled distance was significantly reduced by Doxorubicin compared to the control treatment and to both antioxidants alone (RES and MT). The locomotion pattern of these groups is shown in Figure 2.2.10B. In the combination treatments with DOX and RES or DOX and MT, the distance travelled did not show any significant differences between DOX alone or in combination. However, in the fish under co-treatment with RES and DOX there was an improvement on locomotive pattern as compared to DOX.

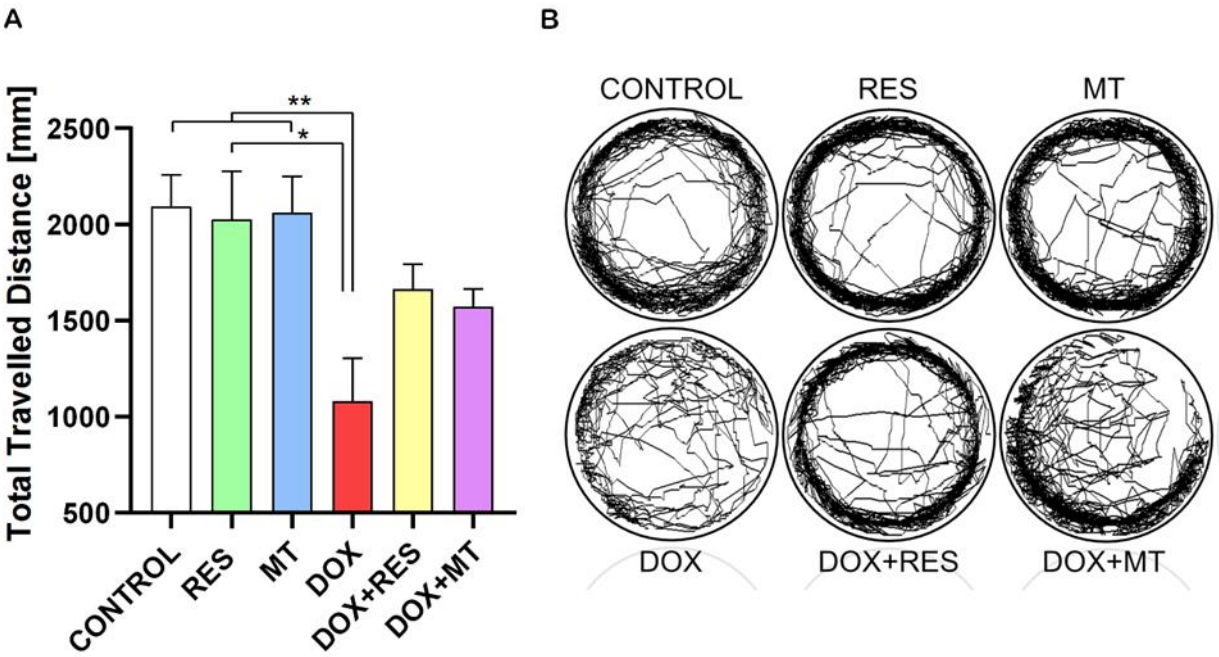

Figure 2.2.10: Effect of Doxorubicin on locomotor activity of zebrafish post-larvae. *Ctsk* reporter zebrafish transgenic line (*Tg[ctsk:DsRed*]) were exposed to different concentrations of Resveratrol (RES), MitoTEMPO (MT) alone or together with Doxorubicin (DOX) for 24 hours. Locomotor activity was measured on Zantiks MWP system. Total distance travelled with RES (100µM), MT (20µM) and DOX (17.2µM) alone or together (A). The locomotory pattern of fish between the treatment groups(B). One-way ANOVA, Tukey's multiple comparisons test, *-P≤0.05, **-P≤0.01.

2.2.4. DISCUSSION

Doxorubicin (DOX) is a chemotherapy agent that increases reactive oxygen species (ROS) and is known to decrease *FoxM1* expression, which is required for the proliferation of cells (212). FoxO3 and FoxM1 function downstream of PI3K-Akt, Ras-ERK and JNK/p38MAPK signalling pathways are crucial for cell survival, proliferation, differentiation, and cell cycle control. This chemotherapeutic agent influences cellular toxicity through FOXO3 and FoxM1 signalling affecting cell survival, proliferation, differentiation via cell cycle control resulting in cell termination by apoptosis or senescence (329). Patients under DOX treatment showed increased systemic bone loss during chemotherapy (215), and a significant depletion of bone mass was observed upon DOX exposure in rats (216,217). This depletion of bone mass was established to be caused by an imbalance between osteoblast and osteoclast activity. Here, we have shown that osteoclast activity was significantly increased upon DOX exposure as shown by increased numbers of TRAP-positive cells. Number of multinucleated osteoclasts were significantly higher on DOX treatment, which is suggestive evidence of increased resorption resulting on systematic bone loss during chemotherapy [2]. However, co-treatment with DOX and RES decreased TRAP-positive cells and osteoclast markers. *Oc-stamp* encodes for a transmembrane protein required for the fusion of osteoclasts (356) that was highly expressed on DOX treated RAW 264.7 cells differentiation, suggesting that DOX promoted an increased fusion of the macrophage/monocyte lineage during osteoclastogenesis, forming larger, and therefore, more active osteoclasts. Interestingly, when combining DOX with RES, there was a significant reduction of *Oc-stamp* mRNA expression, suggesting that RES prevents the fusion of macrophages.

Resveratrol (RES) is known to influence a broad range of signalling pathways including sirtuins, kinases, steroid receptors, lipo- and cyclooxygenases [32,49]. Sirt1 signalling is an important mediator of stress resistance and antiaging effects (358). By activating Sirt1, RES epigenetically modifies the expression of mesenchymal stem cells, favoring osteoblast differentiation and decreasing adipocyte formation. Similarly, RES-mediated apoptosis of osteosarcoma cells involves Sirt1 activation. RES induced apoptosis in osteosarcoma cells in a dose-dependent manner but did not significantly affect normal

osteoblasts [51,52]. Gehm *et al.* (1997) have shown that RES functions as an agonist for estrogen receptor-mediated transcription due to its similar structure to diethylstilbestrol, a synthetic estrogen (361). Similarly, β-estradiol dose-dependently decreased M-CSF and RANKL-induced osteoclast differentiation in myelomonocytic precursors (362). The inhibition of osteoclast differentiation by RES might be due to its similar structure to estrogen (361). RelA/p65 is responsible for the NF-κB heterodimer formation, nuclear translocation and signal activation. RES has been shown to inhibit RANKL-induced osteoclast differentiation by deacetylation of RelA/p65 at lysine 310 subunit of NF-κB (363,364). Similarly, *Nf-kb p105* serve as *Nf-κb* precursors and inhibitors of NF-κB dimers (363). In this study, RES significantly increased *Nf-kb p105* suggesting that RES inhibits NF-kB dimer formation, thus inhibiting nuclear translocation and subsequent inhibiting NF-kB signalling. Similarly, receptor-mediated ROS generation plays a crucial role in RANKL induced osteoclast differentiation. RANKL stimulation increases ROS in pre-osteoclasts via NADPH oxidase or increased mitochondrial ROS (96,201,319). Taken together, this study provides evidences of an increased DOX-induced osteoclast differentiation and fusion, and shows the ability of RES to counteract DOX-induced osteoclast activation. Previously, DOX was shown to be able to activate the immune system with an increase in inflammatory cytokines (IL-1β, IL-6 and TNFα) (365). The osteoclast differentiation markers *Rank, Trap, Ctsk* and *Nfatc1* were significantly upregulated by DOX exposure, confirming the results observed in the DOX treatment regimen, with a significant increase in osteoclast differentiation. On the other hand, RES treatment was shown to decrease the expression of osteoclast fusion marker (*Oc-stamp*) and differentiation markers (*Trap* and *Ctsk*) compared to the positive control with M-csf and Rankl induction. It has been shown that inhibition of *Oc-stamp* completely inhibits fusion and multinucleation of osteoclasts, resulting in reduced resorption (366). These results are in line with the experimental data presented in our work, with a reduction of multinucleated osteoclasts and a downregulation of differentiation markers upon treatment with RES, as observed both *in vivo* and *in vitro*. Taken together, our results show that RES significantly reduces DOX-induced osteoclast fusion and differentiation. Therefore, it is possible to suggest that a combined

therapy of DOX with supplementation of RES would significantly help on preventing DOX-induced bone resorption.

In our study, DOX exposure significantly reduced *FoxM1* expression during osteoclastic differentiation of RAW 264.7 cells. Proliferating cells express *FoxM1*, that has been shown to have an essential role in cell cycle progression (326–328). However, upon RES treatment of these differentiating cells, the expression of *FoxM1* increased. This translates in an increment on *FoxM1* expression that will inhibit osteoclast differentiation and increase proliferation of RAW 264.7 cells. Taken together, our data shows the involvement of *FoxM1* on osteoclast differentiation during RES and DOX treatment.

As FoxM1 is a critical regulator of oxidative responses (353), the upregulation of FoxM1 expression reduces ROS by stimulating the expression of ROS scavenger genes such as *Sod 1* and *Nrf 2* (326,352,353). During osteoclast differentiation, the expression of *FoxM1* was significantly reduced, suggesting a high involvement of ROS in this process. RES exposure inhibits osteoclast differentiation and negatively regulates intracellular ROS by stimulating the expression of detoxifying enzymes, such as *Sod 1* and *Nrf 2* (341,342). In this study, DOX treatment increased osteoclast differentiation and decreased expression of *Sod 1,* suggesting *FoxM1* involvement as a regulator of DOX-induced osteoclast differentiation, as previously described by Yao *et al.* (329) and Olano *et al.* (330). Since FoxM1 is a crucial regulator of oxidative stress, DOX and MT (326) both reduced the expression of *FoxM1* in combined treatments, while MT alone or in combination was unable to protect against DOX-Induce oxidative stress and osteoclast differentiation.

In this study, we confirmed the *in vitro* osteoclast differentiation results through an *in vivo* experiment using the *ctsk* reporter zebrafish transgenic line (*Tg[ctsk:DsRed*]). DOX treatment significantly increased the *ctsk* positive cells in the head of zebrafish, further confirming our *in vitro* results on DOX-induced activated osteoclast differentiation on RAW 264.7 cells. On the other hand, exposure to RES decreased the osteoclast differentiation as shown by *ctsk* positive cells on zebrafish (*Tg[ctsk:DsRed*]). In combination with DOX, RES significantly counteracted the DOX-induced osteoclast differentiation as indicated by *ctsk* positive cells. Apart from osteoclasts, *Ctsk* is present

in other tissues such as the ovary, heart, skeletal muscle, lung, placenta, testis, small intestine and colon (367). The presence of *ctsk* on the intestine has been associated with pathological conditions of the intestine, e.g., chronic inflammatory disease (368,369). Similarly to data previously described by Kaczmarek *et al*. (370), we observed that DOX strongly induced mucositis on our fish model. Interestingly, combining DOX with RES significantly decreased the *ctsk* signal, suggesting that RES could reverse DOX-induced mucositis significantly. The results obtained from the *in vivo* experiment show that the combination of DOX with RES provides a positive approach that can be implemented in the future to counteract DOX-induced intestinal inflammation.

Furthermore, DOX exposure in 25 dpf zebrafish post-larvae decreased locomotor behaviour and unsynchronized swimming pattern. DOX induced locomotor activity might result from impaired sleep-wake rhythms as described by Savard et al. (371,372). Similarly, DOX treatment during chemotherapy was associated with disturbances of sleep, sleep efficiency and poor sleep quality (372,373). The experiments performed with 24 hours of exposure to DOX showed unsynchronized swimming behaviour as compared to the RES and MT treatments. However, the unsynchronized swimming behaviour improved when combining DOX with RES or with MT. These results suggest that RES and MT confer protection against DOX-induced stress on sleep-wake rhythms, although the mechanisms involved are still not fully understood and require further investigation.

2.2.5. CONCLUSION

In this study, DOX-induced oxidative stress and osteoclast differentiation are mediated through FoxM1. DOX showed increased osteoclast fusion, differentiation *in vitro* and *in vivo,* increased mucositis and changed locomotory behaviour and pattern whereas these phenomena significantly reduced Sirt1 activator exposure. Furthermore, while combining DOX with Sirt1 activator (RES), the Sirt1 activator significantly rescues DOX-induced alteration on osteoclast activation, mucositis and locomotory behaviour *in vitro* and *in vivo*. Therefore, our observations suggest that activation of osteoclast differentiation is one of the critical factors for DOX-induced bone loss, where FoxM1

plays a crucial role, and that the Sirt1 activator RES was shown to be able to reverse these negative effect.

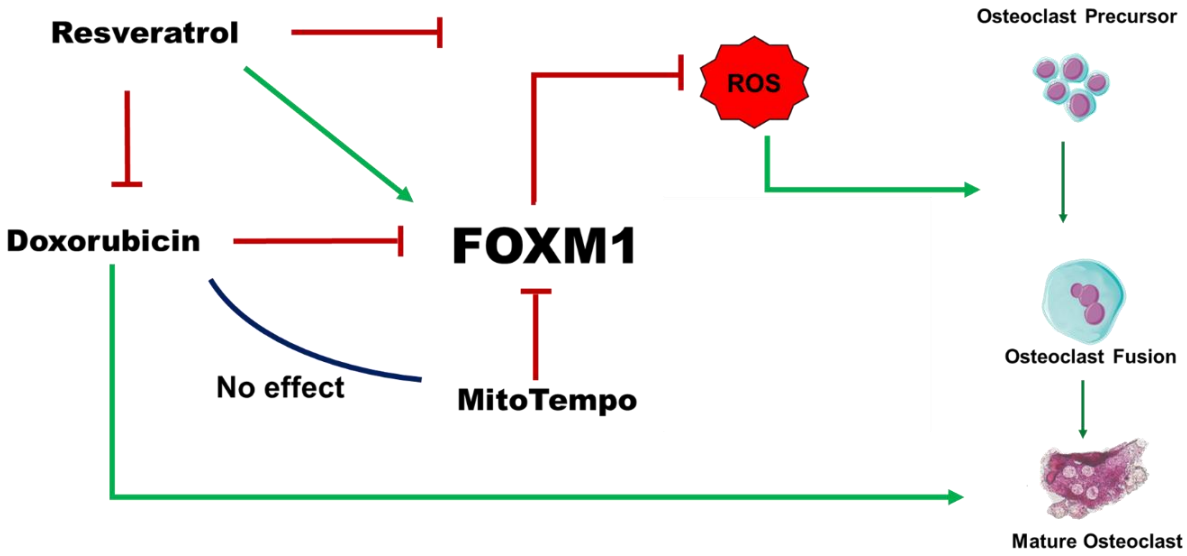

Graphical Abstract 2.2: Doxorubicin (DOX) increases osteoclast differentiation by inhibiting FoxM1 signalling, increasing intracellular ROS and Oxidative stress. Sirt1 activator (Resveratrol) reverse Doxorubicin-induced osteoclast differentiation. Whereas MT did not show any effect on DOX-induced osteoclast differentiation.

CHAPTER 3

IN VIVO OSTEOCYTIC BONE MODEL

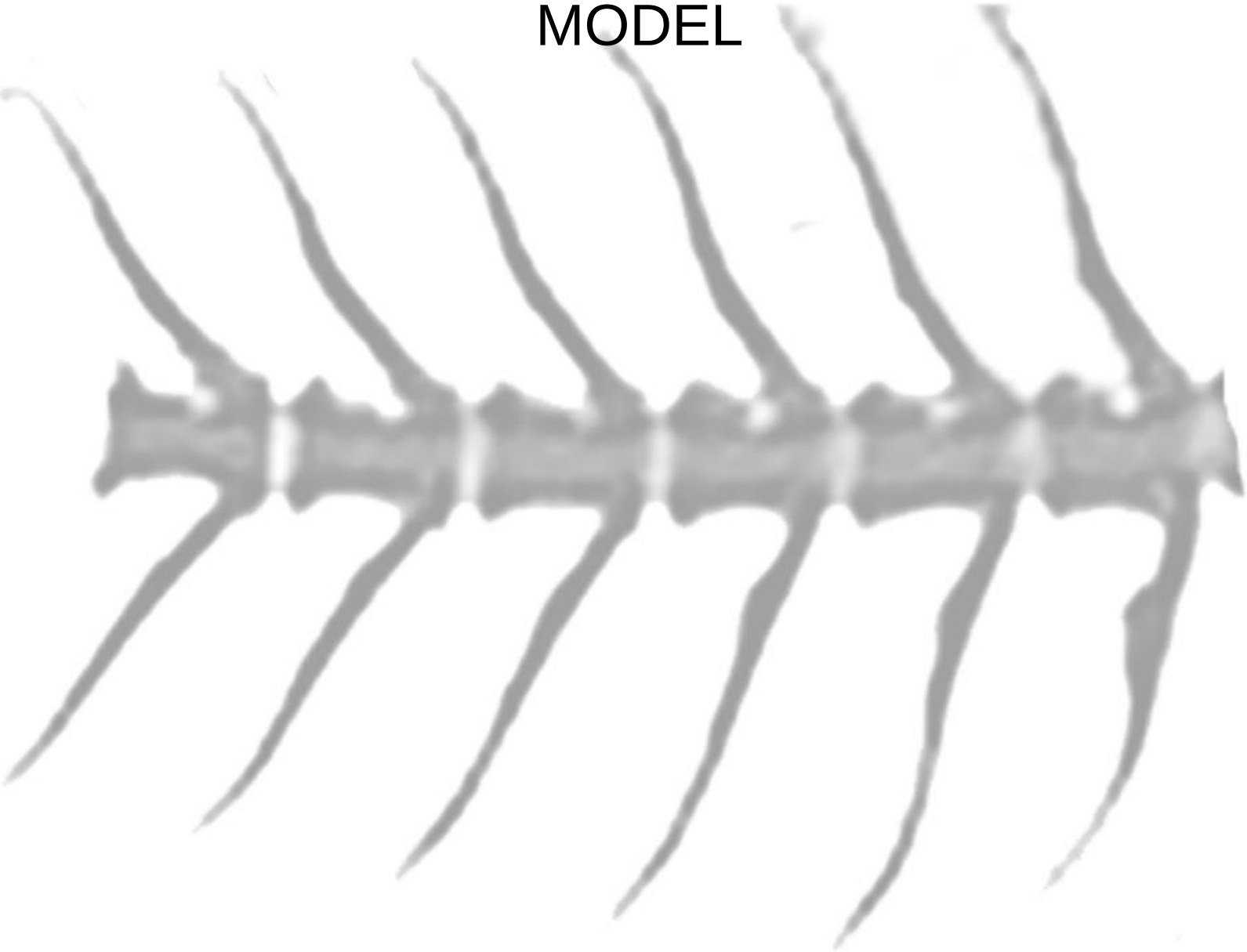

PREAMBLE

The BIOMEDAQU project aims to translate research from *in vitro* to *in vivo*. This chapter contains the translational experiment on osteocytic bone model (zebrafish) with doxorubicin and antioxidants, which will provide insights on doxorubicin-induced bone loss, further strengthening biomedical research. This chapter aims to translate the results obtained on murine cells (osteoblast and osteoclast) to zebrafish model. This chapter is published to the *Nutrients* with the title “Regular supplementation with antioxidants rescues Doxorubicin-induced bone deformities and mineralization delay in zebrafish” [https://doi.org/10.3390/nu14234959].

Regular supplementation with antioxidants rescues Doxorubicin-induced bone deformities and mineralization delay in zebrafish

Sunil Poudel
Gil Martins
Leonor Cancela
Paulo J. Gavaia

Chapter published in *Nutrients*. [https://doi.org/10.3390/nu14234959]

ABSTRACT

Osteoporosis is characterized by abnormal bone structure with low bone mass and degradation of skeleton microarchitecture leading to bone fragility and risk of fracture. Oxidative stress induces an imbalance in osteoblast and osteoclast activity that leads to bone degradation, a primary cause of secondary osteoporosis. Doxorubicin (DOX) is a widely used chemotherapy drug for treating different cancers, known to induce secondary osteoporosis. The mechanism underlying DOX-induced bone loss is still not fully understood, but one of the relevant mechanisms is through massive accumulation of reactive oxygen and nitrogen species (i.e., ROS and NOS) leading to oxidative stress. We investigated the effects of antioxidants Resveratrol (RES) and MitoTEMPO (MT) on DOX-induced bone impairment using the zebrafish as a model. Skeletal deformities, lipid peroxidation, mineral analysis and bone related molecular markers were analyzed. DOX was shown to increase mortality, induce alterations on intestinal villi, and impair growth and mineralization of zebrafish. The lipid peroxidation was also significantly increased in DOX supplemented groups as compared to control and antioxidants, suggesting that ROS formation is one of the key factors for DOX-induced bone loss. The osteoblast differentiation markers *osteocalcin 2* and *osterix/sp7* were significantly downregulated upon DOX supplementation. Furthermore, DOX affected mineral contents (calcium, phosphorus, sodium, potassium, and magnesium) of zebrafish, suggesting that it affected mineral metabolism. However, upon regular supplementation of antioxidants, DOX-induced effects on mineral content were rescued.

Our data show that supplementation with antioxidants effectively improves the overall growth and mineralization in zebrafish and counteracts DOX-induced bone anomalies.

3.1. INTRODUCTION

Osteoporosis is a common metabolic skeletal disorder characterized by abnormal bone structure, low bone mass and degradation of skeleton microarchitecture, leading to bone fragility and increased risk of fracture (117,293). Oxidative stress induces an imbalance in osteoblast and osteoclast activity, leading to imbalances in bone metabolism, a primary cause of secondary osteoporosis caused by specific medications such as doxorubicin (DOX) (109,295). Several clinical studies have revealed that antioxidant and/or pro-oxidant mechanisms are involved in bone pathologies such as osteoporosis (44–47). DOX has long been recognized among the most toxic anticancer agents, causing large accumulations of reactive oxygen and nitrogen species (i.e. ROS and NOS) that negatively impact on bone cell metabolism (212). NADPH-dependent reductases are capable of producing a one-electron reduction of DOX to DOX-semiquinone free radicals (374,375). Under aerobic conditions, quinone-semiquinone derived from adriamycin undergoes redox cycling and generates superoxide radicals (376). Adriamycin free radicals are formed by a non-enzymatic mechanism involving iron. The Fe_2^+-DOX free radical complex formed by the redox interaction of adriamycin with Fe_3^+ reduces oxygen to hydrogen peroxide and ROS (375,377,378). This mechanism produces a free radical that induces DNA damage by oxidative injury (267,268) and causes lipid peroxidation (269–274) upon DOX exposure. Previously, postmenopausal breast cancer patients under DOX regimen have shown decreased bone mineral density and bone loss [23]. Similar effects were also observed in DOX exposed rats (216,217).

Teleost fish, such as the zebrafish (*Danio rerio*), are recognized models for biomedical research, including skeletal development, due to its similarities in molecular mechanisms and signaling pathways with humans (238,239). In fish, skeletal anomalies are linked with oxidative stress, genetics, epigenetics, and nutritional factors, such as vitamins, minerals, and lipids, which are considered the main influencing nutrients on skeleton development. Antioxidant defense mechanisms of the cells are constantly counteracting ROS produced by endogenous or exogenous sources (379,380) with catalase, superoxide dismutase and glutathione peroxidase acting by scavenging hydrogen peroxide, superoxide and hydroperoxides, respectively (381).

Resveratrol (RES) is a naturally occurring polyphenolic (3,4′,5-trihydroxystilbene) compound found in grapes, cranberries, and nuts (174), with antioxidant, anti-inflammatory, estrogenic, and proliferative properties, which can influence bone metabolism (175). Previously, it has been shown that RES can counteract glucocorticoid induced bone damage (225) and zinc oxide induced oxidative stress (276) on zebrafish. RES has also been shown to improve lipid metabolism homeostasis in zebrafish (382). Mito-TEMPO [MT] is a mitochondria-targeted antioxidant which scavenges mitochondri-al superoxide and alkyl radical (197,198). MT has shown to be able to reverse tafazzin knockdown-induced mitochondrial ROS production (346). This suggests MT as a potential compound for counteracting mitochondrial-induced oxidative stress.

Previously, we have shown the reversal effect of RES and MT on DOX-induced bone impairment on gilthead seabream (Sparus *aurata*) (383). In this study, taking advantage of the zebrafish as an *in vivo* model with osteocytic bone, we investigated the effects of DOX-induced bone impairment and aimed to reverse DOX-induced negative effects by regular supplementation with antioxidants. As far as we know, no studies have been performed on DOX-induced bone loss in this model. Therefore, this study will further strengthen the previous results obtained *in vitro* on the effects of DOX, Res and MT on bone development and mineralization and on the reversal of DOX-induced bone impairment by antioxidants.

3.2. MATERIALS AND METHODS

3.2.1 Housing conditions

Wild-type zebrafish [AB-strain (ZFIN ID: ZDB-GENO-960809-7)] were maintained at zebrafish facility of the Centre of Marine Sciences (CCMAR, Portugal). Adults were crossed to obtain the necessary larvae for this study. The photoperiod of the room was controlled with a 14-h/10-h light/dark cycle and air humidity maintained at 60% (384). Fish were kept in 3.5L plastic tanks connected to a 980L recirculating housing system (ZebTEC®; Tecniplast, Buguggiate VA, Italy). Water quality was ensured by a daily water renewal of 10% of total volume in recirculation through an automated pump.

Water quality was ensured through filtration: mechanical (pleated cartridge filters, 50 µm), biological (ceramic beads), carbon filter (granular activated), and ultraviolet sterilization (180, 000 µWs/cm2). The circulating water temperature (28°C ± 1°C), pH (7.5 ± 0.2) and conductivity (750 ± 30 µs) of circulating water were maintained and controlled through an integrated computerized system, and the pH and conductivity were stabilized through the addition of a sodium bicarbonate solution (S5761, Sigma Aldrich, Madrid, Spain) and Instant Ocean® salt concentrated solution (35g/L; Aquarium systems, Sarrebourg, France). NO_2^- and NH_4^+ values were maintained <0.1mg/L and NO_3^- <50mg/L, with weekly monitoring (385).

3.2.2. Micro diet preparation

Microdiets were prepared according to Poudel *et al.* (383). Briefly, the microdiets supplemented with antioxidants and pro-oxidant were prepared manually by mixing squid flour, water-soluble components and subsequently with fat and lipid-soluble vitamins, and finally, on warm water with gelatin dissolved. RES (34mg/kg) (TCI, Tokyo, Japan) (225,383,386) and DOX (30mg/kg) (TCI) (383,386) were dissolved on polar molecules whereas MT (5mg/kg)(Sigma-Aldrich) (383,386,387) was dissolved in water. The dough was first compressed and then made into pellets using a grinder (Severin, Suderm, Germany). Then the pellets were dried for 24 hours at 38 °C in an oven (Ako, Barcelona, Spain). Finally, dried pellets were crushed and placed through sieves (Filtra, Barcelona, Spain) in order to get varied particle sizes (i.e., 500 µm, 250 µm, and 125 µm) (380).

3.2.3. Feeding trial

A zebrafish broodstock group of AB strain with 4-5 months, females (n = 20) and males (n = 20), was crossed and about 2500 eggs were collected and incubated at 28 °C±0.5°C in 1L tanks (Tecniplast) at a density of 200 eggs/L in E2 (embryo medium) with 50 ppt methylene blue (Sigma-Aldrich) to reduce bacterial and fungal growth (388,389). At 5 days post fertilization (dpf), 2400 larvae were pooled and divided into quadruplicates (100 larvae/L) for each treatment group. The rearing density was gradually decreased every 5 days by increasing the volume of water in the tank i.e., 5-10 dpf: 100 larvae/liter, 10-15 dpf: 66 larvae/L, 15-30 dpf: 33 larvae/L. A volume

corresponding to 90% of water was renewed every day with fresh water collected from the zebrafish recirculating system, since the trial was conducted in static conditions. The feeding trial was conducted until 30 dpf (post-larvae), when all skeletal structures were predicted to be completely formed (385).

The zebrafish larvae were fed with microdiets supplemented with antioxidant and pro-oxidants alone or combined. The fish were fed three times a day with antioxidant microdiets, whereas pro-oxidant diets were only fed to the fish every 72 hours and continued with a combination of control or antioxidant diets. The microdiet combinations were done by mixed feeding with the pro-oxidant and antioxidant diets. The total amount of diet fed daily per tank was 15 mg and increased 5 mg each week. For the first 2 days of feeding, 150 rotifers/ml were added to the experimental tanks during the morning (390). On the 5^{th} day microdiet uptake was checked by microphotographic observation (385). A spatula was prepared with a 3D printer with capacity of 5 mg per scoop to standardize the feeding.

3.2.4. Whole-mount staining and evaluation of skeletal anomalies

To assess skeletal abnormalities and vertebral mineralization in the post-larvae, whole-mount double staining was done using an acid-free protocol for bone and cartilage adapted from Gavaia *et al*. (391) and Walker and Kimmel (392). A group of 20 post-larvae/replicate were stained, for cartilage whole mount stain alcian blue 8GX (Sigma-Aldrich) and for mineralized structure alizarin red S (AR-S) (Sigma-Aldrich) was used (392). Briefly, 30 dpf post-larvae were stained with alcian blue solution (0.1% W/V) in MgCl2 (60 mM) dissolved in 70% ethanol for 3 hours followed by rehydration steps for 2 hours in a decreasing concentration gradient of ethanol (96% to 25%). Samples were then stained with 0.05% AR-S in 0.5% potassium hydroxide solution (KOH, Sigma-Aldrich) for overnight. Clearing was done with 1% KOH and larvae were consequently transferred through increasing glycerol concentrations (25% to 100%) and stored in 100% glycerol (Merk Milli-pore, Massachusetts, USA) until examination. Whole-mount sample were examined and analyzed under a stereomicroscope (MZ10F Leica, Wetzlar, Germany). Detection of skeletal anomalies was performed following the nomenclature by Bird NC. *et al.* (393). For assessing the mineralization of vertebrae, 20

individuals per group were analyzed. The vertebrae were categorized according to the degree of mineralization as: unmineralized, mineralizing and mineralized according to the intensity of AR-S staining observed, using ImageJ1.53c.

3.2.5. Mineral contents

Samples of zebrafish post larvae (30 dpf) (N= 8/tank) were dried for 72 hours in an oven at 60°C. Dried and weighted samples were followed with a 65% nitric acid digestion, and microwave (Discover SP-D 80, CEM, North Carolina, USA) with magnetic beads for 9 minutes was used extraction of minerals. The samples were then diluted in a 1:5 ratio with milli-Q water. Calcium standard (Agilent, California, USA), which also contains Fe, Mg, Na and K, and Phosphorus standard (Agilent), were prepared on 5% nitric acid. The mineral contents were measured by Microwave plasma-atomic emission spectrometry (MP-AES 4200, Agilent, California, USA) at 393.366 and 213.318 nm wavelength for Calcium and Phosphorus, respectively. The intensity values obtain from samples were compared with the standard curve.

3.2.6. Lipid Peroxidation (MDA) analysis

Lipid peroxidation was measured using the malondialdehyde (MDA) assay kit (Sigma-Aldrich), by reacting MDA with thiobarbituric acid substance (TBARS). Approximately 25–30 mg of larval sample was homogenized on 20% trichloroacetic acid (w/v) (1.5 mL) with 0.05 mL of 1% BHT in methanol. To the primary solution, 2.95 mL of 50 mM thiobarbituric acid was added, then mixed and heated for 10 minutes at 100 °C. The protein precipitates were extracted by centrifugation at 2000g, and the absorbance was measured using the Evolution 300 spectrophotometer (Thermo Scientific, Loughborough, UK) at 532 nm. MDA standard curve was plotted, and the absorbance of samples was compared against the standard. TBA-MDA concentration was expressed as nmol MDA/mg of tissue (394).

3.2.7. RNA extraction and qPCR

NZYol Reagent (NZYtech, Lisbon, Portugal) was used to extract total RNA from 10 whole specimens at 30 dpf using. DNase I treatment (Promega, Wisconsin, USA) was done on RNA (1 µg) for 30 min at 37ºC and the sample was reverse-transcribed at at

37°C for one hour using M-MLV reverse transcriptase (Invitrogen, Waltham, USA), RNaseOUT (Invitrogen) and oligo-d(T) universal primer [5'-ACGCGTCGACCTCGAGATCGATG(T)13-3']. qPCR assays were carried out using a Bio-Rad CFX thermocycler (Bio-RAD, Hercules, USA). Gene expression levels were normalized using *eef1a1l1* as housekeeping gene (395) and the ΔΔCt method was applied to determine relative quantification (351,383). The sequence of primers used in this study are listed in Table 3.1.

Table 3.1. Sequences of primers used. All sequences in 5'–3' orientation.

Gene	primer sequence		GenBank (accession no.)
oc2/bglapl	Fw:	CCAACTCCGCATCAGACTCCGCATCA	NM_001291889
	Rev:	AGCAACACTCCGCTTCAGCAGCACAT	
sp7	Fw:	GCTAAGTCCAGGGCAGGCTCAG	NM_212863
	Rev:	CAATGGCGTGAAATCAGGAGTGTAAC	
runx2b	Fw:	TCAGGAATGCCTCAGGGGTTATG	NM_212862
	Rev:	CTTGCGGTGGGTTTGTGAATACT	
eef1a1l1	Fw:	TTGAGAAGAAAATCGGTGGTGCTG	NM_131263
	Rev:	GGAACGGTGTGATTGAGGGAAATTC	

3.2.8. Histology

Sample preparation and tissue process for the histological protocol were performed as previously described in Cardif *et al.* (396). Prior to paraffin inclusion, decalcification was done with 10% EDTA and 1% PFA. 5 µm Tissue sections were prepared using rotary microtome Microm HM 315 (Microm International GmbH, Walldorf, Germany). Slides were then stained following hematoxylin and eosin staining protocol as described by Fischer *et al*. (397). Blind evaluation of histological parameters was performed for analyzing intestinal *villi* length (398,399). VisiCam 3 Plus (Avantor VWR, Pennsylvania,

USA) was used to capture the images from a standard light microscope (Zeiss, Dresden, Germany) and length of *villi* was measured using ImageJ1.53c software.

3.2.9. Statistical analysis

The data obtained from the skeletal anomalies analysis followed the nomenclature adapted from Gavaia *et al*. (391) and Walker and Kimmel (392), and was coded according to the typology of the deformities. The data for the mineralization of the vertebrae were coded as mineralized, mineralizing, and unmineralized and then the cumulative percentage was calculated. Partial Least-Squares Discriminant Analysis (PLS-DA) was analyzed using MetaboAnalystR 3.0 R package and MetaboAnalyst (400,401), The significance of class discrimination was verified by performing a permutation test ($p < 0.001$; 0/1000), and the performance was measured using the "B/W ratio" as indicated by Bijlsma et al (402). MetaboAnalystR 3.0 R package and MetaboAnalyst 5.0 was used to analyze univariate and multivariate analysis (400,401). Level of significances was analyzed using Student's t-test, One-way ANOVA and Two-way ANOVA on Graphpad prism 8 and IBM SPSS 16. Bar graphs are presented as mean ± SEM. Homogeneity of variance was analyzed with Levene's test. Differences in p-value ≤ 0.05 were considered significant (ns- $P>0.05$, *- $P\leq0.05$, **-$P\leq0.01$, ***-$P\leq0.001$, ****-$P\leq0.0001$).

3.3. RESULTS

3.3.1. Fish growth and survival

The antioxidant supplementation (RES, MT) on microdiets showed to significantly increase the fish standard length at both 15 and 30 dpf, as compared to control and DOX. However, no significant differences in length were observed between DOX and control at 15 and 30 dpf (Figure. 3.1 A,B). However, while combining treatment with combination of DOX with antioxidants RES and MT, both antioxidants significantly increased the standard length of the larvae on both time points. No significant differences were observed on dry weight between the groups supplemented with RES, MT and DOX alone or in combination. However, a significant increment on body weight was observed between control and all other microdiet supplemented groups at 30 dpf (RES, MT, DOX, DOX+RES, DOX+MT) (Figure 3.1C). Although the DOX diet significantly reduced the survival of larvae at 30 dpf as compared with MT, the DOX-induced mortality of the larvae was significantly rescued by antioxidant supplementation (Figure 3.1D). Moreover, the microdiets prepared manually were compared with commercially available standard diet for zebrafish (ZEBRAFEED®, Sparos Lda, Portugal), and no significant difference was observed in growth performance (Supplementary figure 3.1A).

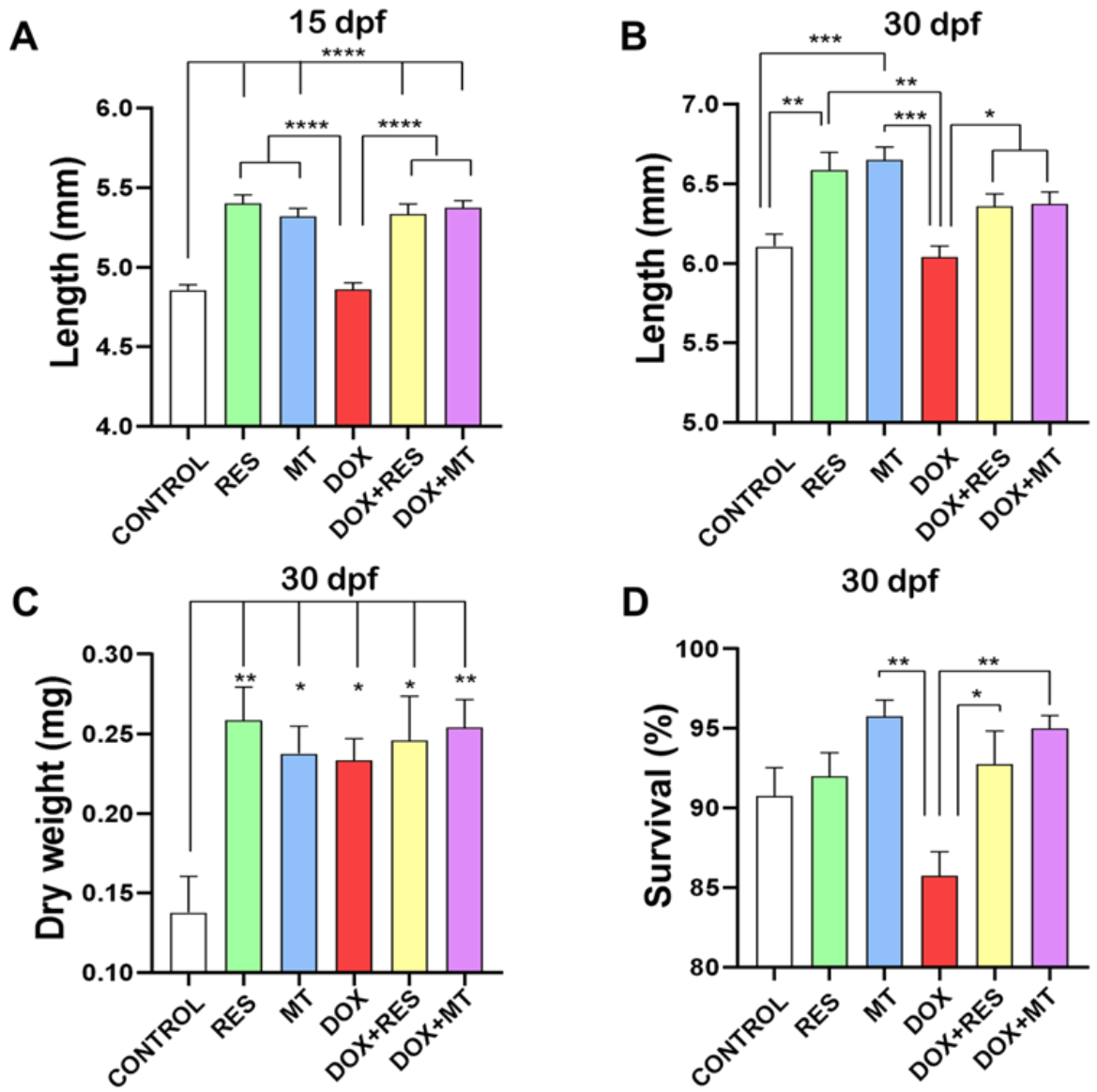

Figure 3.1: Growth and survival parameters during the trial. Larvae were fed with RES, MT and DOX alone or in combination for 30 days. Total length of zebrafish at 15 days post fertilization (dpf) (A) and 30 dpf (B), Dry weight at 30 dpf (C) and Survival at 30 dpf (D). Level of significance were calculated using Tukey's multiple comparison (one-way ANOVA) [* $p \leq 0.05$, ** $p \leq 0.01$, *** $p \leq 0.001$, **** $p \leq 0.0001$]. Acronyms: Days post fertilization (dpf).

3.3.2. Intestinal *villi* morphology on antioxidant and pro-oxidant supplemented groups

The histological sections were stained with hematoxylin and eosin (H&E stain) (Figure 3.2 A), and villi length was measured (Figure 3.2 B). Histological examination revealed that regular supplementation of antioxidants RES and MT significantly increased the villi length as compared to DOX and control. Similarly, supplementation of antioxidants

combined with DOX significantly increased the length of villi compared to DOX alone (Figure 3.2 A and B). Therefore, supplementation of antioxidants (RES and MT) significantly protects against the DOX-induced negative effects on the intestinal mucosa of zebrafish.

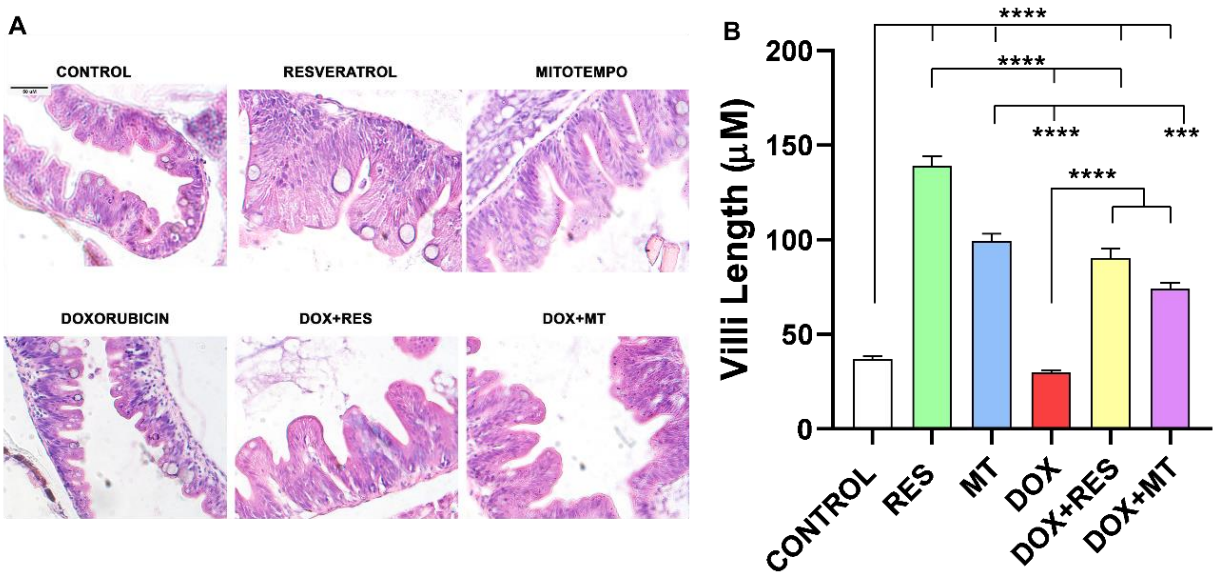

Figure 3.2: Histology of zebrafish gut. 30 dpf zebrafish guts sections were stained with H&E stain observe the villi (A). Length of villi (B). Level of significance were calculated using Tukey's multiple comparison (one-way ANOVA) [* $p \leq 0.01$ and *** $p \leq 0.001$].

3.3.3. Antioxidants rescued DOX-induced skeletal deformities

Skeletal deformities were analyzed at 30 dpf. RES supplementation significantly reduced the incidence of skeletal deformities as compared to control. In contrast, MT did not show any significant difference in incidence compared to control. As expected, DOX showed a significantly increased incidence of skeletal deformities compared to antioxidant supplemented groups and control groups. However, in the fish fed a combination of DOX with antioxidants (RES or MT), there was a significant reduction on incidence of deformities as compared to DOX treatment was observed (Figure 3.3A).

Partial Least-Squares Discriminant Analysis (PLS-DA score) (402) was used to examine the discriminant and similarities on the incidence of skeletal deformities on zebrafish at 30 dpf enriched with RES, MT and DOX alone or in combination (Figure 3.3B). The cluster analysis showed that the DOX supplemented group was distinct and completely separated from other groups, while [control, antioxidants (RES and MT) and combination of antioxidants and DOX] formed a grouping cluster (Figure 3.3B). The region-specific skeletal deformities between the microdiets supplemented groups are presented on Figure 3.3C. A higher incidence of skeletal anomalies was observed in the caudal fin vertebrae region, followed by the caudal vertebrae and pre-caudal regions. Low incidence of deformities was observed on the head as compared to the axial skeleton. DOX supplementation showed a significantly increased incidence of axial skeleton deformities compared to RES and MT, while combining DOX with antioxidants, RES and MT, significantly rescued DOX-induced deformities on the axial skeleton. The heatmap depicts the distribution of skeletal deformities, where the DOX supplemented group was completely different from other groups (Figure 3.3D). The red color indicates the high incidence of deformities observed on individuals supplemented with DOX, whereas zebrafish supplemented with antioxidants (RES and MT) showed low incidence intensity as indicated by blue color. The most common skeletal deformities observed in this study were vertebral fusions, compressions, lordosis, scoliosis, and shortened vertebrae (supplementary figure 3.1B).

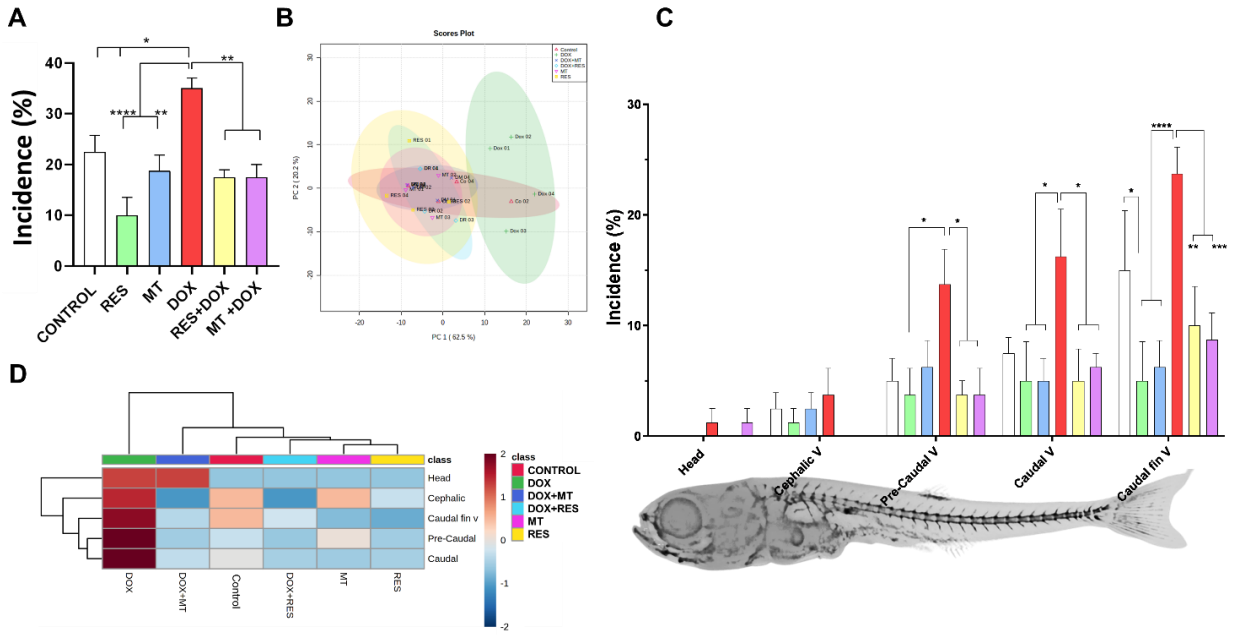

Figure 3.3: Incidence and distribution of skeletal deformities. Incidence of skeletal deformities (A). Partial Least-Squares Discriminant Analysis (PLS-DA score) on the incidence of deformities of zebrafish supplemented with antioxidants and pro-oxidants (B). Distribution of skeletal deformities (C) and heatmap of distribution of skeletal deformities (D). Level of significance were calculated using Tukey's multiple comparison (one-way ANOVA) [* $p \leq 0.05$, ** $p \leq 0.01$, *** $p \leq 0.001$, **** $p \leq 0.0001$]

3.3.4. Antioxidants improve mineralization of the axial skeleton

To investigate the effect of the tested antioxidants and pro-oxidant on mineralization of the axial skeleton, whole-mount double stained larvae were analyzed for mineralization pattern and malformations of the skeleton. The mineralization pattern was categorized as fully mineralized, mineralizing and unmineralized, according to the intensity of AR-S stain. The RES supplemented group showed a significantly increased mineralization of the vertebrae (fully mineralized- 38%, and mineralizing- 37%) as compared to control (fully mineralized- 9%, and mineralizing- 20%) and DOX (fully mineralized-7%, and mineralizing- 16%). The MT treatment also significantly increased the mineralization of vertebrae (fully mineralized- 20%, and mineralizing- 38%) compared to control and DOX groups (Figure 3.4 A,B). The extent of fully mineralized vertebrae was increased significantly upon RES supplementation as compared to MT. Similarly, while combining DOX with antioxidants, the mineralization of the vertebrae was significantly increased [DOX+RES (fully mineralized- 20%, and mineralizing- 33%), DOX+MT (fully

mineralized- 15%, and mineralizing- 37%)] as compared to DOX alone (Figure 3.4 A,B). The heatmap depicts the mineralization pattern of the axial skeleton among the microdiets supplemented groups. The clustering analysis on the heatmap shows that mineralization of the vertebrae is categorized into two distinct groups: control, DOX and RES, MT, DOX+RES, DOX+MT. Control and DOX groups were different from the remaining, displaying a lower mineralization of vertebral bodies. Similarly, on the second cluster, RES also showed distinct mineralization pattern, with stronger mineralization as compared to MT, DOX+RES and DOX+MT (Figure 3.4C).

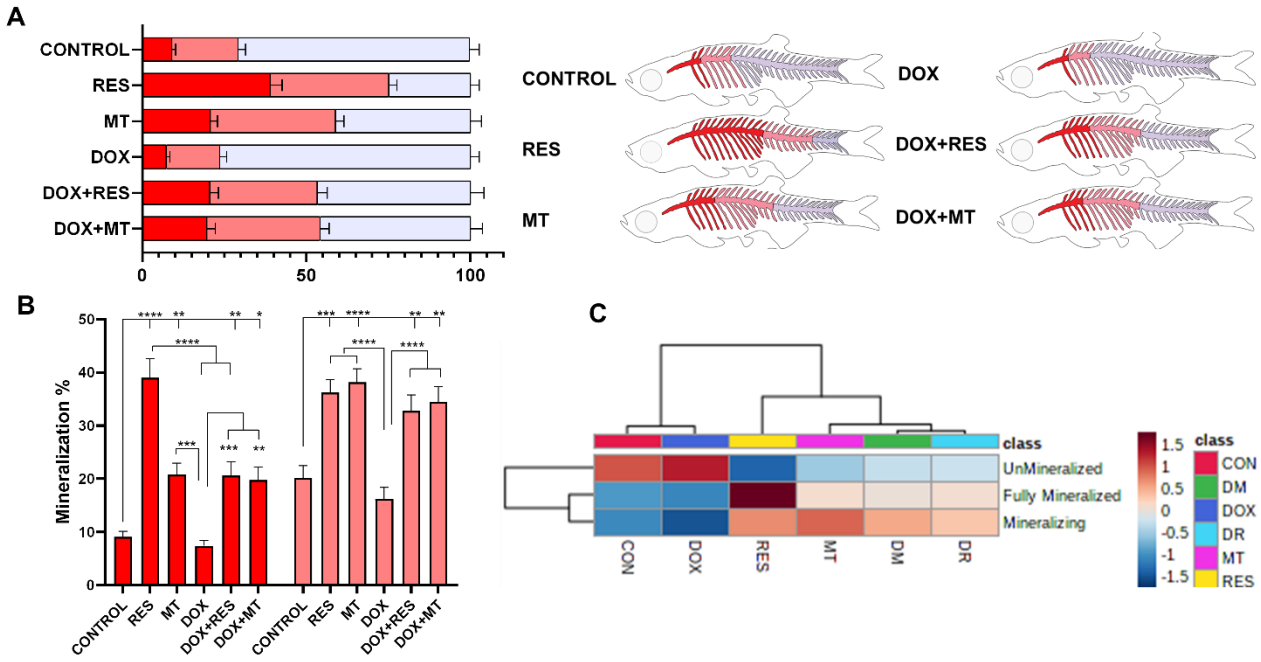

Figure 3.4: Mineralization of zebrafish vertebral column. Percentage of mineralized (red), mineralizing (pink), unmineralized (blue) vertebrae (A) and graphical representation of the mineralization status of the zebrafish. Mineralization status of the vertebrate (B), (red represents mineralized vertebrae and pink represents mineralizing vertebrate). Heat map of mineralization of vertebrae of zebrafish feed with RES, MT and DOX supplemented microdiets (C). Level of significance were calculated using Tukey's multiple comparison (one-way ANOVA) [* $p \leq 0.05$, ** $p \leq 0.01$, *** $p \leq 0.001$, **** $p \leq 0.0001$]

3.3.5. Doxorubicin affects minerals content

DOX supplementation significantly reduced contents in calcium (Figure 3.5A), phosphorus (Figure 3.5B), sodium (Figure 3.5D), potassium (Figure 3.5E) and

magnesium (Figure 3.5F) as compared to antioxidants (RES and MT) treated groups. However, the calcium/phosphorus ratio (Figure 3.5C) was not significantly altered between the groups, since both minerals varied at comparable extents. While combining DOX with antioxidants (DOX+RES and DOX+MT) the calcium and phosphorus content was increased significantly as compared to DOX alone. Similarly, sodium (Figure 3.5D), potassium (Figure 3.5E) and magnesium (Figure 3.5F) contents were significantly increased while co-supplementing DOX and MT.

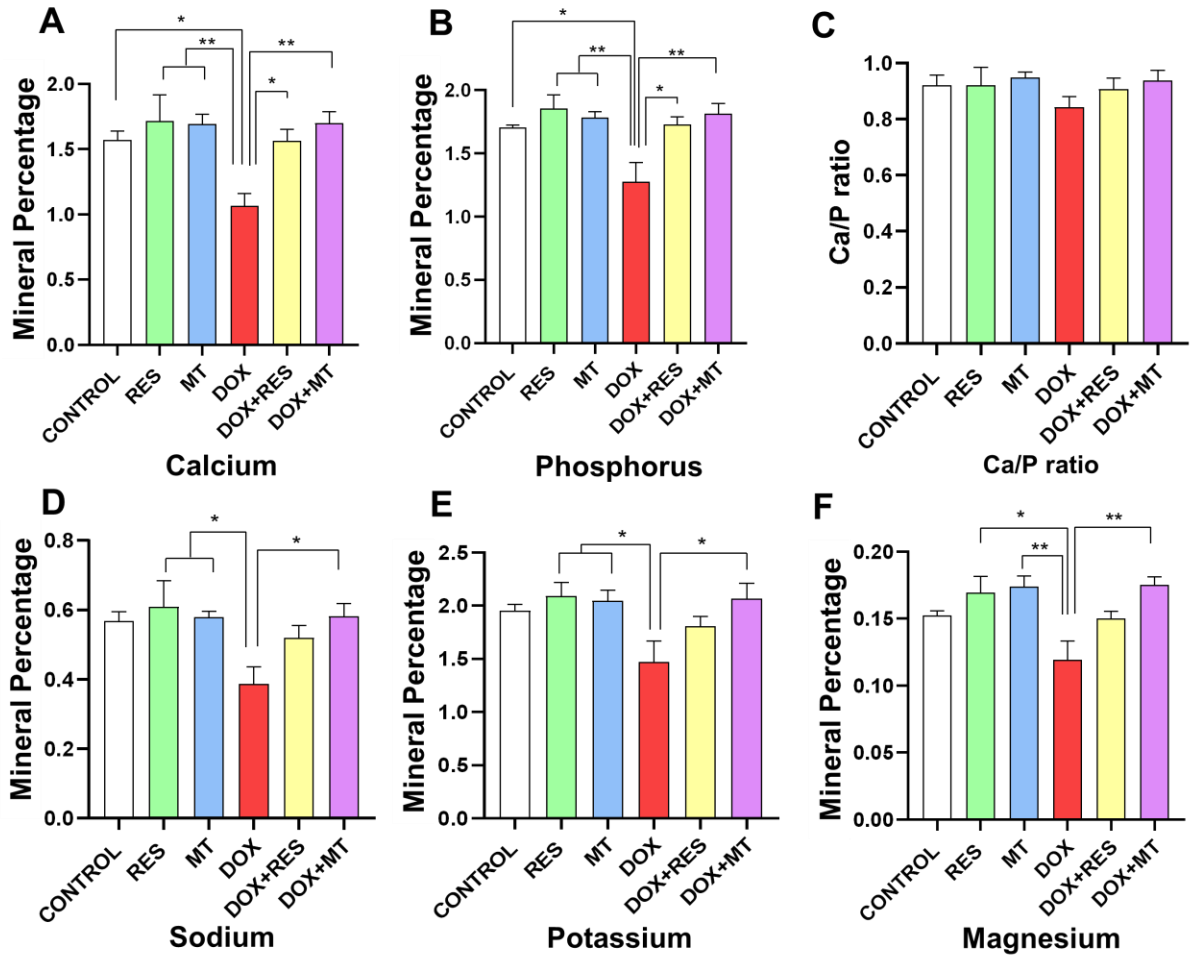

Figure 3.5: Mineral analysis of zebrafish fed with microdiets supplemented with antioxidants and pro-oxidant. Mineral content of Calcium (A), Phosphorus (B), Calcium/Phosphorus ratio (C), Sodium (D), Potassium (E), and Magnesium (F). Level of significance were calculated using Tukey's multiple comparison (one-way ANOVA) [* $p \leq 0.05$ and ** $p \leq 0.01$].

3.3.6. Antioxidants reverse Doxorubicin-induced oxidative stress.

Malondialdehyde (MDA) is the end product of lipid peroxidation, commonly used as a marker for assessing oxidative damage due to the increase of free radicals. The MDA

level was significantly higher on DOX-supplemented as compared to RES and control at 15 dpf (Figure 3.6A). Similarly, at 30 dpf the lipid peroxidation was significantly increased on DOX supplemented groups compared to RES and DOX+RES (Figure 3.6B).

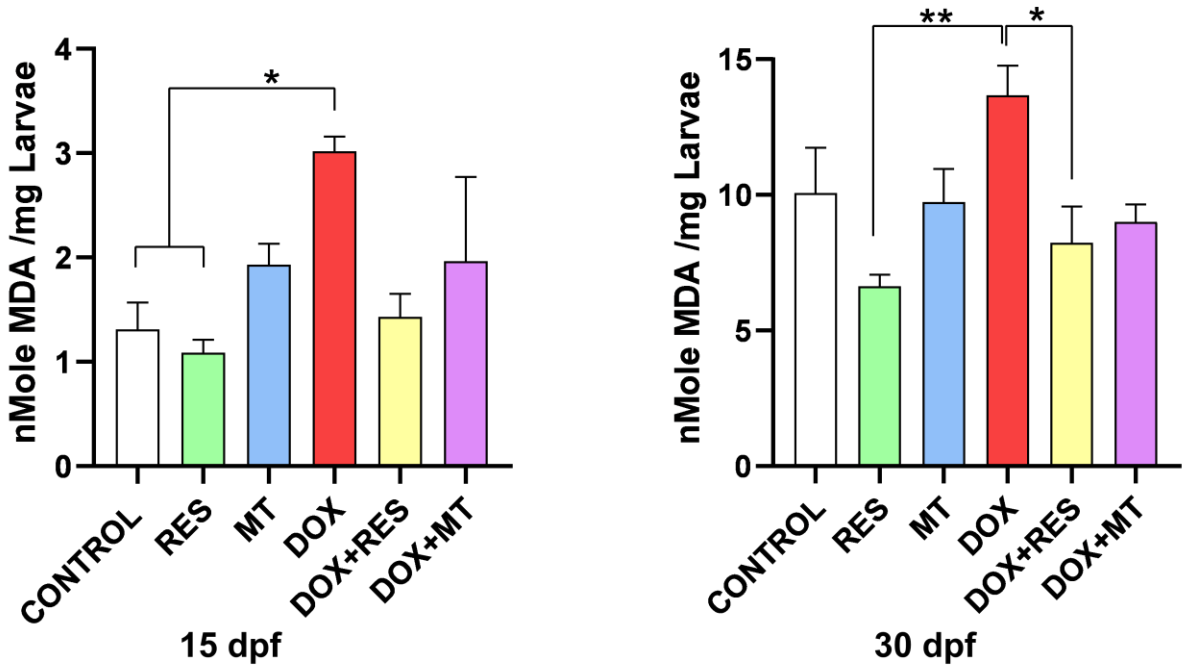

Figure 3.6: Lipid peroxidation on zebrafish fed with microdiets enriched with antioxidant and pro-oxidant. Lipid peroxidation of the zebrafish larvae at 15 dfp (A) and 30 dpf (B). Level of significance were calculated using Tukey's multiple comparison (one-way ANOVA) [* $p \leq 0.05$ and ** $p \leq 0.01$].

3.3.7. Doxorubicin-induced effects on osteoblast differentiation markers

In the group supplemented with DOX, it was observed a significant reduction on osteoblastic differentiation marker mRNAs, including the mature osteoblast marker *osteocalcin 2 (*Figure 3.7 A) and the immature osteoblast marker *osterix/sp7 (sp7)* (Figure 3.7B) as compared to RES and MT. However, no significant differences were observed on the mRNA expression of early differentiation marker *runx2b (*Figure 3.7C).

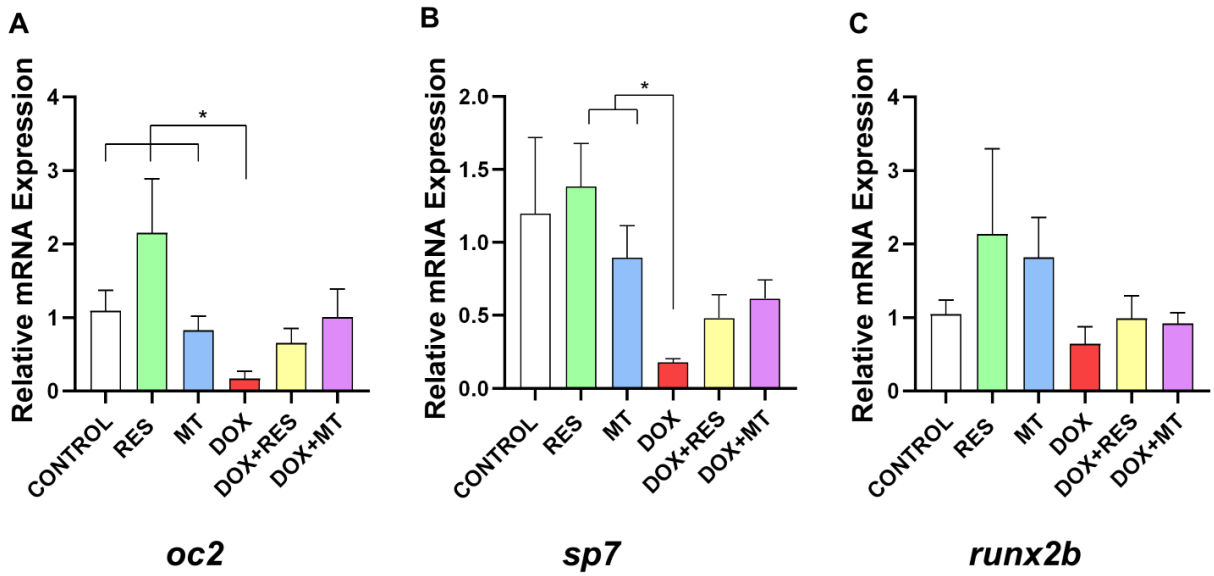

Figure 3.7: Doxorubicin affects osteoblastic markers. mRNA expression of osteoblast differentiation markers on zebrafish supplemented with antioxidants (RES and MT) and Pro-oxidant (DOX) microdiets alone or in combination; *osteocalcin* 2 (*oc2*) (A), *osterix/sp7 (sp7)* (B) and *runx2b* (C). Level of significance were calculated using students t-test [* $p \leq 0.05$].

3.4. DISCUSSION

Resveratrol (RES) was previously shown to have antioxidant, anti-inflammatory, estrogenic-like and cell proliferative properties (174,175). Several *in vivo* and *in vitro* studies have investigated the effect of RES on bone differentiation and remodeling (174,175,225,276). In the zebrafish model, RES was shown to protect against the glucocorticoid-induced bone damage (225), zinc oxide-induced oxidative stress (276), and also improved lipid metabolism homeostasis in zebrafish (382). Previously DOX has also shown to increase systematic bone loss and reduce osteoblast differentiation

(215–217). Furthermore, during DOX treatment in patients, an increased risk of bone metastasis and osteolytic injury has been reported (213,275).

In our study it was demonstrated that RES positively affected growth, with fish presenting a significantly increased length as compared to control and the group supplemented with the pro-oxidant doxorubicin (DOX). Dietary RES supplementation also significantly increased the standard length of zebrafish larvae compared to commercially available standard diets (ZEBRAFEED®, supplementary figure 3.1A). DOX has been known to be a highly toxic anticancer drug (403). DOX-induced developmental toxicity has been studied on various animal models such as dogs (404), rats (405) and zebrafish (406–408). Chang *et al*. (408) previously reported DOX-induced developmental toxicity on zebrafish, where fish subjected to higher concentration of DOX (≥ 25 mg/L) showed acute lethal effects, while fish on lower concentrations (≤ 0.1 mg/L) showed sublethal effects as well as multiple malformations (408). Our results revealed no significant differences on standard length between the DOX-supplemented group and the control, however, the standard length was significantly decreased compared to RES and MitoTEMPO (MT). Furthermore, the survival of the larvae was adversely affected by DOX, whereas co-supplementation of RES and MT had a protective effect over DOX-induced mortality. Several other studies have also indicated that, in agreement with our observations, the antioxidants RES (225,409,410) and MT (411) significantly improve overall health and promote growth of both mammalian and fish models. Retardation in growth is also considered as a marker of chronic stress (412), where antioxidants (RES and MitoTEMPO) have been shown to confer protection against these effects.

Metabolism and absorption of the dietary nutrients occurs in the jejunumprocetes. The jejunum is responsible for absorbing most of the nutrients such as carbohydrates, fats, minerals, proteins, and vitamins. The intestinal villi increase the surface area for food absorption and add digestive secretions. In this study, we have shown that antioxidant supplementation significantly increased the length of intestinal villi, which contributes to higher nutrient absorption resulting in enhanced fish growth. Several reports have pointed out that DOX administration caused severe damage on the intestine by

increasing apoptosis of jejunal epithelium (413), increased influx of leukocytes and reduced villi length (414), which was also observed in our study. Besides that, in this study, antioxidants (RES and MT) induced an increase in the villi length and conferred protection against DOX-induced damage on the intestinal villi of larval and juvenile zebrafish. Zhou *et al*. (415) has reported similar findings, showing that antioxidants protects against free radical-induced intestinal injury and counteracts oxidative stress by modulating the p53 mRNA expression. The negative effect on intestinal villi is suggested as an explanation for the growth retardation of the larvae fed with DOX supplemented microdiets.

As previously described, higher concentrations of DOX showed acute lethal effects, while lower concentrations (≤ 0.1 mg/L) showed sublethal effects such as developing multiple malformations (416). The concentration of DOX used in this study was 30mg/kg of diet, which is high compared to previous studies performing oral administration of DOX (10 mg/kg orally) on mice (416). According to pharmacokinetics analysis, the maximum concentration (Cmax) and max-imum time (Tmax) of plasma DOX concentration, were 0.2062 µl/ml and 2 hours, respec-tively (416). Considering that the leaching of micronutrients from the diet in the aquatic environment is 30-35 percent (417,418), the amount of DOX supplemented on the microdiets (30mg/kg) is sufficient for an effective concentration after the leaching.

The dietary supplementation with DOX at 30mg/kg that we have used induced an increase in larval mortality by 15%, which is significantly different from other groups. Moreover, this concentration showed a significantly higher incidence of skeletal deformities as compared to the other experimental groups. In contrast, co-supplementation with the antioxidants RES and MT was able to rescue the adverse effects of DOX and reduce the incidence of deformities, increasing survival and mineralization. In this study, the incidence of skeletal anomalies was more concentrated on caudal vertebrae and on the caudal fin vertebrae regions, which is in agreement with previous findings in zebrafish (385) and other aquaculture species (i.e. *Sparus aurata*) (383,419–424). The deformities in the caudal region can lead to secondary vertebral deformities as a result of insipid swimming behavior that affects the growth and

conversion index of the fish (420,425). Therefore, our data indicate that RES and MT supplementation in the diet would be beneficial for counteracting the DOX-induced bone deformities and for the overall development of the fish.

Mineralization and differentiation of the bone fully depend upon the osteoblast population, which are tightly regulated by osteocytes (426). In our study, the larvae supplemented with DOX, has shown decreased mineralization of the vertebrae compared to groups fed antioxidants (RES and MT). Development and mineralization of axial skeleton on zebrafish starts from the calcified centra of Weberian region and is followed by rays of caudal fin, simultaneously (393,427). Here, the effect of antioxidants on mineralization of the vertebrae are expected to be due to increased osteoblast proliferation and differentiation.

The other factor responsible for the mineralization of bone is mineral metabolism (428). Bone is the main calcium and phosphate reservoir in higher vertebrates (429). However, fish absorb different mineral elements from the medium, since water contains abundant calcium. Therefore, calcium deficiency is uncommon in fish. However, the only source for phosphorus is food, where a reduction in phosphorus results in low bone mineralization, development of skeletal abnormalities and reduced growth (430,431). The significant reduction of calcium, phosphorus, sodium potassium and magnesium on the DOX-supplemented groups indicates that DOX alter overall mineral metabolism. Calcium and phosphorus are associated to bone mineralization, the inorganic phase of the bone is composed of calcium phosphates predominantly as hydroxyapatite [$Ca_{10}(PO_4)_6(OH)_2$] (432). Calcium homeostasis maintains the absorption of calcium and phosphorus from the intestine and maintain levels in bone (432). In addition to bone metabolism, phosphorus as phosphate (HPO_4^{2-}) is a crucial signaling molecule, an important component on cell wall and is essential for RNA and DNA structure, and termed as the currency of energy metabolism as (ATP, ADP and AMP) (428–432). The lower calcium and phosphorus content suggests that overall bone metabolism is affected by DOX. Therefore, based on our results, we hypothesize that reduced capacity for mineral absorption leads to the lower bone mineral content observed,

resulting in lower mineral deposition and contributes to the increased incidence of skeletal deformities observed in DOX supplemented zebrafish larvae.

An increase in ROS is one of the working mechanisms of action of DOX-induced toxicity (212,213,403,433). The increased ROS production results in lipid peroxidation, which is a crucial mechanism for DOX-induced toxicity (269–274). Under normal conditions, ROS produced by the cell are balanced by the antioxidant defense mechanism of the cells (381,434). Here, when zebrafish was supplemented with DOX alone or in combination for 30 days, MDA concentration was significantly increased on DOX supplementation, but co-supplementation with RES and MT could prevent this effect on lipid peroxidation, in accordance with previously reported results (269–274). This signifies that antioxidants supplementation on feed would protect against ROS induced oxidative stress and lipid peroxidase (435,436).

Osteocalcin (Bglap or osteocalcin) is essential in skeletal development and calcium metabolism. Osteocalcin is a Ca2+-binding vitamin K-dependent protein produced by osteoblasts, essential for the differentiation and the mineralization of extracellular matrix (15). Osterix/Sp7 is a zinc finger transcription crucial for osteoblastogenesis during skeletal development (437). Similarly, to the mammalian osteoblast differentiation transcription factors, *runx2 and osterix* has demonstrated shown to regulate osteoblast differentiation during zebrafish bone formation (438). The significant decrease on the osteoblast differentiation markers induced on the DOX supplementation groups indicates that DOX impairs bone formation and mineralization processes on zebrafish. Osteocalcin plays an essential role in bone mineralization due to its ability to bind with high-affinity bone hydroxyapatite (439) and *osterix* on osteoblast differentiation (438), the mRNA expression of *osteocalcin* and *osterix* was downregulated by DOX, which correlates with the lower mineralization of the vertebrae observed in zebrafish at 30 dpf.

Our data provide evidence that regular supplementation with antioxidants could rescue DOX-induced bone deformities and mineralization in zebrafish. However, some of the limitations in this study should be considered. Firstly, the concentration provided on the microdiets have partially leached in the aquatic environment and must be quantified. The amount of the diet each fish consumed is also unknown; therefore, and despite the

effects observed, measuring the DOX concentration in larvae should be considered for further studies.

3.5. CONCLUSION

In conclusion, our data indicate that antioxidants supplementation effectively improves overall growth, increases mineralization, and rescues pro-oxidant-induced deformities in zebrafish. Antioxidants (RES, MT) may serve as a supplementation that can prevent and treat primary or secondary osteoporosis by counteracting pro-oxidant induced ROS production and oxidative stress. Thus, the present study indicates the potential to introduce antioxidants as a candidate drug/supplement for studies in mammalian models to prove their potential use in osteoporosis treatment.

CHAPTER 4

IN VIVO NON-OSTEOCYTIC BONE MODEL

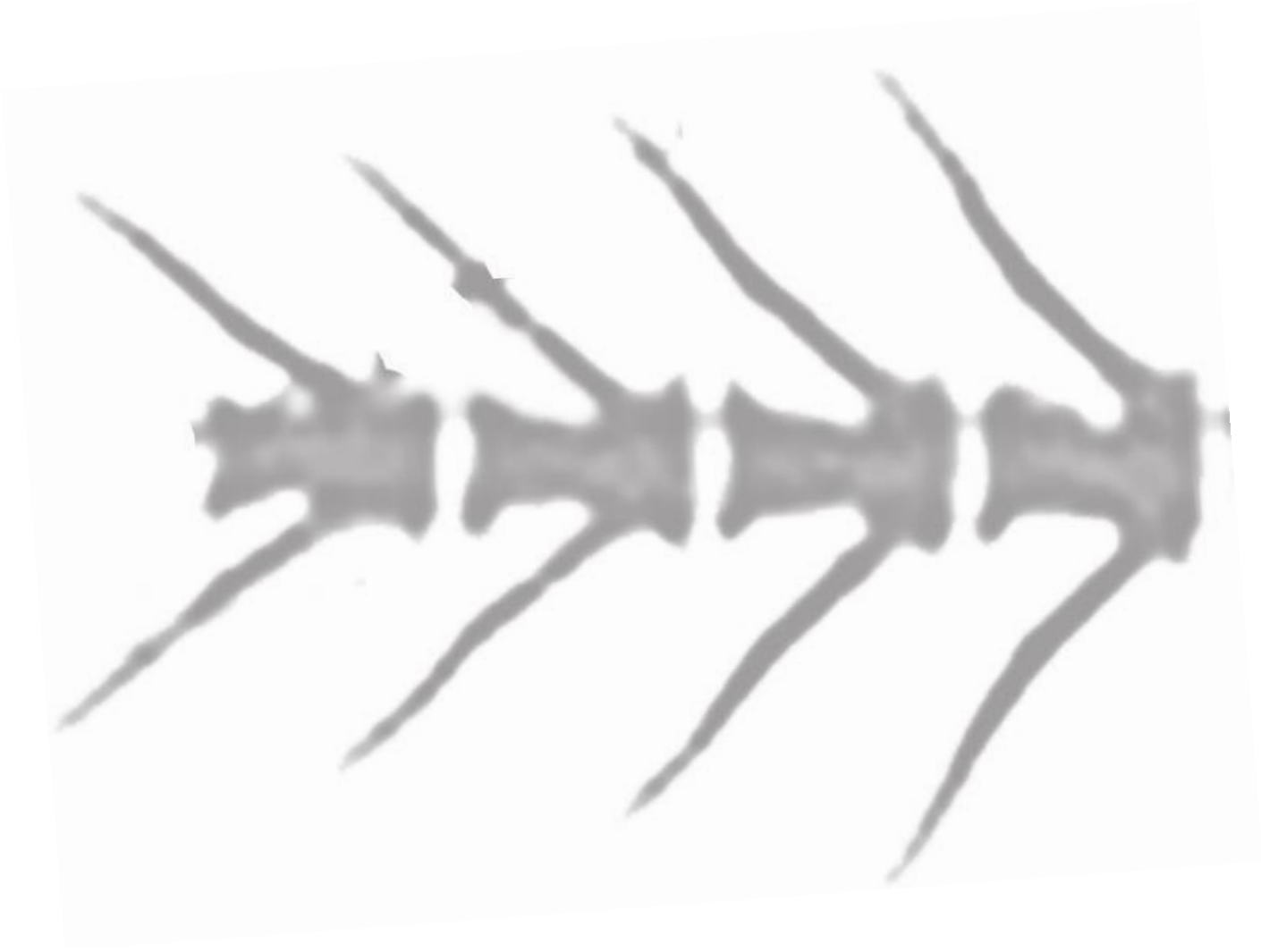

PREAMBLE

The BIOMEDAQU project aims to translate research from *in vitro* to *in vivo* models. This chapter contains the translational experiment on non-osteocytic bone model (seabream) with doxorubicin and antioxidants which will provide insights on the effect of antioxidant and pro-oxidant on aquaculture. This chapter aims to translate the results obtained on murine cells (osteoblast and osteoclast) and osteocytic bone model to non- osteocytic-aquaculture model. This chapter is published in *Nutrients* first-authored by Sunil Poudel.

Reversal of Doxorubicin-induced bone loss and mineralization by supplementation of Resveratrol and MitoTEMPO in the early development of *Sparus aurata*

Sunil Poudel
Marisol Izquierdo
Maria Leonor Cancela
Paulo J. Gavaia

nutrients

Chapter published in *Nutrients.* [https://doi.org/10.3390/nu14061154]

ABSTRACT

Doxorubicin is a widely used chemotherapeutic drug known to induce bone loss. The mechanism behind doxorubicin-mediated bone loss is unclear, but oxidative stress has been suggested as a potential cause. Antioxidants that can counteract the toxic effect of doxorubicin on the bone would be helpful for the prevention of secondary osteoporosis. We used resveratrol, a natural antioxidant, and MitoTEMPO, a mitochondria-targeted antioxidant, to counteract doxorubicin-induced bone loss and mineralization on *Sparus aurata* larvae. Doxorubicin supplemented microdiets increased bone deformities, decreased mineralization, and lipid peroxidation, whereas Resveratrol and MitoTEMPO supplemented microdiets improved mineralization, decreased bone deformities, and reversed the effects of doxorubicin *in-vivo* and *in-vitro*, using osteoblastic VSa13 cells. Partial Least-Squares Discriminant Analysis highlighted differences between groups on the distribution of skeletal anomalies and mineralization of skeleton elements. Calcium and Phosphorus content was negatively affected in the doxorubicin supplemented group. Doxorubicin reduced the mRNA expression of antioxidant genes, including *catalase*, *glutathione peroxidase 1*, *superoxide dismutase 1*, and *hsp90* suggesting that ROS are central for Doxorubicin-induced bone loss. The mRNA expression of antioxidant genes was significantly increased on resveratrol alone or combined treatment. The length of intestinal villi was increased in response to antioxidants and reduced on doxorubicin. Antioxidant supplements effectively prevent bone deformities and mineralization defects, increase antioxidant response and reverse doxorubicin-

induced effects on bone anomalies, mineralization, and oxidative stress. A combined treatment of doxorubicin and antioxidants was beneficial in fish larvae and showed the potential for use in preventing Doxorubicin-induced bone impairment.

Keywords: oxidative stress; resveratrol; MitoTEMPO; doxorubicin; bone deformities; mineralization

4.1 INTRODUCTION

Oxidative stress is caused by reactive oxygen species (ROS) that are normally generated as by-products of aerobic metabolism during oxidative phosphorylation in mitochondria (440). The major forms of ROS include the superoxide anions (O_2^-), hydrogen peroxide (H_2O_2) and free radicals such as hydroxyl radicals (OH·). Oxidative stress caused by ROS alters the bone remodeling process, causing an unbalance between osteoclast and osteoblast activity (441). This can lead to metabolic bone diseases and contribute to the pathogenesis of skeletal system disorders including osteoporosis, characterized by low bone mineral density, decrease in bone mass and density, and deterioration of bone structure, which causes bone fragility and risk of fracture (42,109). Several clinical studies suggested the involvement of antioxidant and/or pro-oxidant systems in the pathology of bone osteoporosis (44–47). Osteoporosis can be classified into various types: primary osteoporosis or idiopathic osteoporosis, age-related osteoporosis and secondary osteoporosis, where bone loss results from a specific disease or medication (109).

Gilthead seabream (*Sparus aurata*) is a highly valuable commercial species widely cultivated in Europe. Due to its extensive cultivation, the presence of skeletal anomalies is one of the most important bottlenecks in current aquaculture production. Skeletal deformities in farmed teleosts are a persistent problem in aquaculture, posing a high economic burden. Deformed fish are manually sorted out from the production on a regular basis, which results in lower profit (419,442,443). Previous works showed that 15 -50% of seabream juveniles possess severe anomalies detected already at early stages (419,442). Skeletal anomalies, altered meristic characters and delayed development can be considered as developmental disturbances which are the indication of inappropriate nutrition and associated oxidative stress (379,444), inappropriate rearing conditions (419,443) and genetics (443,445). However, early assessment of skeletal anomalies is often difficult, since the presence of slight anomalies is hard to diagnose at early larval stages, but these can later develop into more severe abnormalities affecting the external body shape (445–447).

With the advancements in technology, several *in-vitro* systems have been established from mineralizing tissues of fish. Cells derived from zebrafish calcified tissues can be differentiated into osteoblastic and chondroblastic lineages, as was detected by the analysis of expressing differentiation markers, alkaline phosphatase activity and extracellular matrix mineralization (448). Similarly, cells derived from gilthead seabream calcified tissue (ABSa15, VSa13 and VSa16) proved to have excellent mineralization capacity and are currently extensively used for mineralization assays (250,251).

Many factors such as oxidative stress, genetics, epigenetic and nutritional factors have been linked to skeletal abnormalities in teleost fishes under culture conditions. Among the nutritional factors, vitamins, minerals, dietary lipids have also been recognized to influence the development of skeletal malformations (379). Lipid peroxidation produces toxic compounds such as fatty acid hydroxides, fatty acid hydroperoxides, hydrocarbons and aldehydes, which damage cellular and subcellular membranes, causing several pathological conditions (379,380). An endogenous antioxidant defense system is responsible for counteracting this oxidative risk on fish (434). To maintain the antioxidant defense mechanism, radical scavenging enzymes such as catalase, superoxide dismutase and glutathione peroxidase scavenge hydrogen peroxide, superoxide and hydroperoxides, respectively (381). Therefore, a diet with a high level of polyunsaturated fatty acid, such as docosahexaenoic acid (22:6 *n*−3) and with an imbalanced content in antioxidant compounds results in oxidative stress, where production of intracellular reactive oxygen species (ROS) increases, negatively affecting proteins, lipids and DNA (380).

Resveratrol (RES) is a polyphenolic (3,4′,5-trihydroxystilbene) compound naturally found in a variety of plant foods such as grapes, cranberries, and nuts (174). RES has anti-inflammatory, estrogenic, antioxidant and proliferative properties which can influence bone metabolism (175). This compound was shown to improve bone mineralization and counteract glucocorticoid-induced bone damage in zebrafish (225). Similarly, resveratrol also inhibits oxidative stress and prevents mitochondrial damage induced by zinc oxide (276).

MitoTEMPO [MT, (2- (2,2,6,6-Tetramethylpiperidin -1-oxyl-4-ylamino)-2-oxoethyl) triphenylphosphonium chloride] is a mitochondria targeted antioxidant (197). MT is a superoxide scavenger and a physicochemical compound mimicking superoxide dismutase from mitochondria. It can easily pass through the lipid bilayers and accumulate in the mitochondria (198). The mitochondria metabolic activity is the primary source of ROS and the principal site of ROS-induced damage. Mitochondrial dysfunction influences osteoblasts through the regulation of mitophagy, apoptosis, and mitochondrial DNA damage. Therefore, improving mitochondrial functions through the application of antioxidants can prevent cytotoxicity and dysfunction in osteoblasts (199). Mitochondrial ROS are also essential for hypoxic enhancement of osteoclast differentiation (200). In zebrafish, MT was shown to revert the effect of tafazzin knockdown induced cellular mitochondrial ROS production and cellular ATP decline thus suggesting that it can potentially counteract mitochondrial oxidative stress (346).

Doxorubicin (DOX) has been used as an anticancer drug which causes cellular toxicity by inducing massive accumulation of ROS and reactive nitrogen species (212). DOX promotes a direct oxidative injure to DNA (267,268) and generates lipid peroxidation (269–274). By the action of NADPH-dependent reductase it produces semiquinone free radicals by reducing DOX to DOX semiquinone (374,375). Under aerobic conditions, redox cycling of adriamycin-derived quinone-semiquinone produce superoxide radicals (376). On the other hand, adriamycin free radicals are produced by a non-enzymatic mechanism involving iron. Redox reaction of adriamycin with Fe^{3+} produces Fe^{2+}-DOX free radical complex which reduces oxygen to hydrogen peroxide and ROS (375,377,378). A recent study indicated that premenopausal breast cancer patients treated with a combination of DOX/cyclophosphamide exhibited low bone mineral density and significant bone loss (215), suggesting a relationship between DOX treatment and systemic bone loss. Accordingly, exposure to DOX caused a 60% reduction in bone formation in normal rats, suggesting a potential for reduced osteoblast differentiation (216,217). Zebrafish has been used as a model for investigation the molecular mechanism on DOX induced cardiotoxicity (406) and as a screening tool to study toxic profile of DOX (407). When exposed to DOX at different concentrations, zebrafish embryos showed serious developmental toxicity. Zebrafish embryos between

4 to 120 hours post fertilization were exposed to different concentrations of DOX. The higher concentrations showed acute lethal effect while lower concentrations showed sublethal effects as well as multiple malformations on larvae and embryos. As the concentration of DOX increased, malformation rate was also increased (408). Based on these findings, we hypothesized that supplementation of antioxidants could reverse DOX-induced bone loss.

The aims of this study were to investigate the effects of DOX, RES and MT on bone development and mineralization and to determine the capacity of antioxidants to counteract the potentially negative effects of doxorubicin on the developing skeleton of *Sparus aurata.*

4.2 MATERIALS AND METHODS

4.2.1 Microdiet preparation

The microdiets with antioxidants and pro-oxidant were prepared by manually mixing squid powder first with water-soluble components, then with fat and lipid-soluble vitamins, and finally, on gelatin dissolved warm water. 150µM (34 mg/kg) of RES based on Luo et al. 2019 (225) and 10 µM (5 mg/kg) of MT based on Peterman *et al.* (449) was used for the preparation of microdiets. While for DOX, non-toxic concentrations were determined by treating of larvae with different concentrations (i.e., 5, 15, 30, and 60 µg/kg) and analyzing the effects on mortality. Lower concentrations (i.e., 5, 15, and 30 µg/mL) did not show toxic effects up to 48 h, while 60 µg/kg of DOX were toxic and showed to increase mortality of larvae at 24 h of exposure. Therefore, 30 µg/kg supplementation of DOX was chosen to use in the trial (Supplementary figure 4.1). RES and DOX were dissolved on polar molecules, whereas MT was dissolved in water. With the help of a grinder (Severin, Suderm, Germany) the dough was compressed, and pellets were prepared. The pellets were dried in an oven at 38 °C for 24 hours (Ako, Barcelona, Spain). To obtain different particle sizes (i.e., 500 µm, 250 µm, and 125 µm), the dried pellets were ground (Braun, Kronberg, Germany) and sieved (Filtra, Barcelona, Spain) (380). The proximate composition of basal diet (control) was Protein—64.46%, Lipid—20.44%, Ash—7.27%, Moisture—9.78% (380,436,450) (Table 4.1 and 4.2).

Table 4.1: Ingredient's formulation in the experimental microdiets

Ingredients (g/kg)	*Control*	*Resveratrol*	*MitoTEMPO*	*Doxorubicin*
Squid powder	702.00	702.00	702.00	702.00
Gelatin	30.00	30.00	30.00	30.00
Krill oil	130	130	130	130
Mineral premix	45.00	45.00	45.00	45.00
SelPlex	3.00	3.00	3.00	3.00
Vitamin premix	60.00	60.00	60.00	60.00
Attractants	30.00	30.00	30.00	30.00
Resveratrol	---	0.034	---	---

MitoTEMPO	---	---	0.005	---
Doxorubicin	---	---	---	0.030

Table 4.2: Vitamins, minerals and attractants formulation in the experimental microdiets

Vitamin premix		Mineral premix	g/kg
Hydro-soluble Vitamin	g/kg	NaCl	2.15133
Cyanocobalamin B12	0.0003	MgSO4.7H2O	6.77545
Astaxanthin	0.05	NaH2PO4.H2O	3.81453
Folate	0.0544	K2HPO4	7.58949
Pyridoxine B6	0.1728	Ca(H2PO4).2H2O	6.7161
Thiamine B1	0.2177	FeC6H5O7	1.46884
Riboflavin B2	0.7253	C3H5O3.1/2Ca	16.1721
Pantothenata calcium B5	1.0159	Al2(SO4)3.6H2O	0.00693
4-Aminobenzoic acid	1.45	ZnSO4.7H2O	0.14837
Nicotinic acid B3	2.9016	CuSO4.5H2O	0.01247
Inositol	14.509	MnSO4.H2O	0.02998
Sub Total	21.097	KI	0.00742
		CoSO4.7H2O	0.10706
Lipo-soluble Vitamin	g/kg	Total	45.00007
Retinoic acid Vit A	0.0024		
Cholecalciferol Vit D3	0.0365	Attractants	g/kg
Menadione Vit K	0.1728	Inosine-5-monophosphate (Inosinc acid)	5
α-Tocopherol acetate (Vit E Acetate)	1.5	Betaine (Trimethylglycine)	6.6
Sub total	1.7117	L-Serine	1.7
		L-Tyrosine	1.7

Ascorbyl polyphosphate (V.C)	1.8	L-Phenylalanine	2.5
Choline Chloride	29.658	DL-Alanine	5
		L-Aspartic acid	3.3
Vitamin premix Total	54.2667	L-Valine	2.5
		Glycine	1.7
		Total	30

4.2.2 Feeding trial

Gilthead seabream larvae were obtained from natural spawns from a broodstock kept at the facilities of the Grupo de Investigación en Acuicultura (GIA) (EcoAqua Institute, Las Palmas de Gran Canaria, Spain). Larvae were previously fed with rotifers (*Brachinous plicatilis*) enriched with Ori-Green (Skretting, France) and *Artemia* nauplii. At 30 days after hatching (dah) the larvae were randomly stocked into 18 experimental tanks (200 L light grey color cylinder fiberglass tanks) at a density of 2100 larvae/tank. The larvae were fed with experimental microdiets with added antioxidants and pro-oxidant, either alone or in combination. The antioxidant supplemented microdiets were fed every hour from 8:00 to 20:00, whereas pro-oxidant supplemented microdiet was fed at intervals of 72 hours and was continued with a respective combination of control or antioxidant diets. The microdiet combinations were Control (CON), Resveratrol (RES), MitoTEMPO (MT), Doxorubicin + Control (DOX), Doxorubicin + Resveratrol (DOX+RES), Doxorubicin + MitoTEMPO (DOX+MT). The combinations were prepared by combining the feeding with both diets for each group. After 5 days of feeding, microdiet uptake was checked by microphotographic studies. All 18 tanks were supplied with filtered seawater (37 g/L salinity) at an increasing rate of 0.3–1 L/min along the experimental period. Water entered the tank from the bottom and exited from the top; water quality was tested daily, and no deterioration was observed. Water was continuously aerated (125 ml/min), attaining 6.0–6.2 g/L dissolved O_2, saturation ranging between 84% and 90%. Water temperature was kept between 20.5 ± 0.5°C throughout the whole trial.

Growth was determined in larvae at 30 dah by measuring the total length in a stereomicroscope (Leica MZ10F, Leica, Germany) with an attached camera (Leica DFC7000T, Leica, Germany) and dry weight in a precision analytic balance (larvae were dried at 105°C until constant weight). Final survival was calculated by individually counting all the live larvae at the beginning and the end of the experiment.

At the end of the trial, microdiets and larvae samples were washed with distilled water and stored at -80 °C for oxidative stress assessment and mineral content analysis. A group of 100 larvae/tank were collected and fixed with PBS buffered 4% formaldehyde solution for 24 hours at 4 °C. Then samples were washed with PBS and preserved in 70% ethanol at room temperature to analyze skeletal anomalies and developmental status. For the analysis of skeletal gene markers and oxidative stress-related gene expression, 30 larvae/tank were kept on RNA later solution and stored at -80 °C. For histology, a group of 15 larvae/ tank were fixed with PBS buffered 4% formaldehyde.

4.2.3 Whole-mount staining of the skeleton

To evaluate larvae skeletal anomalies and developmental status, 100 larvae/tank were stained with an acid-free double staining protocol for cartilage and bone adapted from Gavaia *et al*. (391) and Walker and Kimmel *et al*. (392). Whole-mount acid-free double staining was performed using alcian blue 8GX (Sigma-Aldrich, Madrid, Spain) for cartilage and alizarin red S (AR-S) (Sigma-Aldrich, Madrid, Spain) for mineralized tissues (392). Samples were stained in 0.1% alcian blue 8GX solution (dry weight/volume) with 60 mM $MgCl_2$ in 70% ethanol for 3 hours and rehydrated with a decreasing concentration of ethanol (96% to 25%) for 2 hours. Then, the samples were stained overnight with 0.05% AR-S in 0.5% potassium hydroxide (KOH) (Sigma-Aldrich, Spain). Stained samples were cleared with 1% KOH and subsequently transferred through an increasing concentration of glycerol (25% to 100%). Samples were stored in 100% glycerol (Merk Millipore, Billerica, MA, USA) until observation.

4.2.4 Skeletal anomalies

Specimens stained for cartilage and bone were observed under a stereomicroscope (MZ10F Leica, Wetzlar, Germany). Skeletal anomalies were classified using a dichotomic indicator, where the letter indicates skeletal element affected and the number indicates typology of the anomaly (Table 3: List of considered anomalies) adapted from Gavaia *et al*. [59] and Prestinicola *et al*. [9].

The following derived variables were computed for each experimental treatment.

I. Incidence of skeletal anomalies.
II. Deformities charge.
III. The average number of affected areas.
IV. Incidence (%) of skeletal anomalies according to the number of areas affected (severity).
V. Incidence (%) of each skeletal anomaly typology according to the region affected.

Table 4.3: List of considered anomalies

Regions affected
A. Cephalic (1^{st}–2^{nd} vertebra; carrying epipleural ribs)
B. Pre-haemal or Pleural (With open haemal arches carrying epipleural or pleural ribs, without haemal spines)
C. Haemal or pre caudal (With haemal and neural arches closed by spines)
D. Caudal (With haemal and neural arches closed by modified spines)
E. Pectoral fin
F. Anal fin
G. Caudal fin
H. Dorsal fin
Anomalies Considered
1. Scoliosis
2. Lordosis

3. Kyphosis
4. Vertebral fusion
5. Vertebral body malformation
6. Malformed neural arch and/or spine
7. Malformed haemal arch and/or spine and/or rib
8. Malformed ray (deformed, absent, fused, supernumerary)
9. Malformed pterygiophores (deformed, absent, fused, supernumerary)
10. Malformed hypural (deformed, absent, fused, supernumerary)
11. Malformed epural (deformed, absent, fused, supernumerary)
12. Others
13. Jaw deformities
14. Reduced dental/ malformed Pre-maxillary and/or maxillary
15. Cephalic deformities (glossohyal, neurocranium, etc.)
16. Vertebral slipping
17. Deformed or reduced opercle
18. Supernumerary vertebra
19. Ectopic mineralization
20. Absent

4.2.5 Meristic characters

Meristic character count was carried out on the following elements on 300 larvae/group: total mineralized vertebrae, cranial vertebrae, abdominal/pre-haemal vertebrae, haemal vertebrae, caudal fin vertebrae including urostyle, dorsal fin and anal fin (pterygiophores and lepidotrichia), and caudal fin (hypurals, epurals and rays).

The meristic count was carried out based on the following assumptions:

I. Supernumerary bones were included in the meristic count.
II. Non-completely fused bone elements were counted as distinct elements.

4.2.6 Developmental stage of the skeleton

For evaluating the skeletal developmental stage, 300 larvae/group were stained with an acid-free double staining protocol for cartilage and bone adapted from Gavaia *et al*. (391) and Walker and Kimmel (392) and the skeletal elements were observed under a stereomicroscope (MZ10F Leica, Germany). Vertebrae, neural arches and spines, ribs, parhypural, urostyle, hypurals, and caudal-fin rays were examined and were categorized according to the degree of mineralization as mineralized, mineralizing, cartilaginous, and absent.

4.2.7 Mineral contents

Samples were dried in the oven at 65°C for 72 hours. After complete drying, samples were weighted and mineral content was determined by microwave plasma-atomic emission spectrometry (MP-AES 4200, Agilent, Santa Clara, CA, USA). Samples were digested with 65% of nitric acid, and extraction was facilitated with magnetic beads on microwave (Discover SP-D 80, CEM, Matthews, NC, USA) for 9 minutes. The samples were diluted in 1:10 ratio with milli-Q water. The standards for Calcium and Phosphorus were prepared on 5% nitric acid. The extracted samples were measured by atomic emission spectrometry, and intensity values of the samples were compared against the standard curve.

4.2.8 Cell culture and ECM Mineralization assay

Vsa13 cells derived from the vertebra of gilthead seabream (*Sparus aurata*), were maintained as previously described (250,281). Briefly, cells were cultured in Dulbecco's modified eagle medium (DMEM) supplemented with 10% fetal bovine serum (FBS), 1% penicillin-streptomycin, 1% fungizone, and 2 mM L-glutamine, and incubated at 33ºC in a 10% CO_2 humidified atmosphere. Confluent cultures were sub-divided 1:3 every 3-4 days using 0.2% trypsin-EDTA solution.

ECM mineralization was performed as previously described (250,281). Confluent Vsa13 cells were supplemented with osteogenic medium containing 50 µg/mL of L-ascorbic acid, 10 mM β-glycerophosphate and 4 mM calcium chloride. The cells were treated with antioxidants (RES and MT) throughout 21 days with renewal of treatment medium

twice a week. Treatment with pro-oxidant (DOX) was performed for 3 hours twice a week. After 21 days, mineral deposition was examined through AR-S staining as described (451). AR-S staining was quantified by solubilizing calcium-bound dye in 10% (w/v) cetylpyridinium chloride and absorbance was measured by spectrophotometry at 550 nm using a microplate reader (250,281).

4.2.9 RNA extraction and qPCR

Total RNA was extracted from cell cultures using NZYol Reagent (NZYtech, Lisbon, Portugal). Total RNA (1 µg) was submitted to Dnase I treatment (Promega, Madison, WI, USA) for 30 min at 37ºC and reverse-transcribed for 1 h at 37°C using M-MLV reverse transcriptase (Invitrogen, Waltham, MA, USA), oligo-d(T) universal primer [5'-ACGCGTCGACCTCGAGATCGATG(T)13-3'] and RNaseOUT (Invitrogen, Waltham, MA, USA). Quantitative real-time PCR (qPCR) assays were performed using the Bio-Rad CFX system (Bio-RAD, Hercules, CA, USA). Gene expression was normalized using β-actin as housekeeping gene (281) and relative quantification was determined using the ΔΔCt method (351). Primers used in this study are listed in Table 4.4.

Table 4.4: Primer sequences

Gene	GenBank (accession no.)	5'–3' primer sequence
catalase (cat)	Q308823.1	Fw: TGGTCGAGAACTTGAAGGCTGTC
		Rev: AGGACGCAGAAATGGCAGAGG
glutathione peroxidase 1 (gpx1)	KC201352.1	Fw:GAAGGTGGATGTGAATGGAAAAGATG
		Rev: CTGACGGGACTCCAAATGATGG
superoxide dismutase 1 (sod1)	XM_030439011.1	Fw:TGACGCTCACAGGAGAAATCAAAGGG
		Rev:CAGTAGGACCGCCATGATTCTTACCA
heat shock protein 90 kDA alpha 1 (hsp90)	KM522802.1	Fw: TGCCTGGAACTCTTCACCGAACTG
		Rev:CGCAGCAGATCAGACAACTTCTTCCT
osteopontin (spp1)	AY651247.1	Fw:TACCATCGTCACGGACACAGAGACAG
		Rev:GCTCGTAGGACTTGTAGGGAACAGG
ß-actin (actb)	AF384096.1	Fw: CTTCCTCGGTATGGAGTCCTGCGG

Rev:TCCTGCTTGCTGATCCACATCTGCT

4.2.10 Lipid Peroxidation (MDA) analysis

Lipid peroxidation was determined by the reaction of MDA with thiobarbituric acid substance (TBARS) using Lipid Peroxidation (MDA) Assay Kit from Sigma-Aldrich. Briefly, approximately 20–30 mg of larval tissue per sample was homogenized in 1.5 mL of 20% trichloroacetic acid (w/v) containing 0.05 mL of 1% BHT in methanol. For this, 2.95 mL of freshly prepared 50 mM thiobarbituric acid solution was added before mixing and heating for 10 min at 100 °C. After cooling, protein precipitates were removed by centrifugation (Sigma-Aldrich 4K15, Taufkirchen, Germany) at 2000g, and the absorbance was measured at 532 nm in a spectrophotometer (Evolution 300, Thermo Scientific, Loughborough, UK). The absorbance was normalized against a blank at the same wavelength and was compared with the MDA standard curve. The concentration of TBA-malondialdehyde (MDA) was expressed as nmol MDA per mg of tissue (394).

4.2.11 Histology

Histological procedures were performed as previously described in Cardif *et al*. (396). The larvae were decalcified with 10% EDTA and 1% PFA prior to paraffin inclusion. Sections were prepared at 5 µm using a rotary microtome (Microm HM 315 Rotary Microtome, Microm International GmbH, Walldorf, Germany) and stained using Harris hematoxylin and eosin as described by Fischer *et al*. (397). Blind evaluation of histological preparation was performed analyzing intestinal *villi* length (398,399). Images were acquired with wave image software were processed and length was measured using ImageJ1.53c software.

4.2.12 Statistical analysis

Data obtained from the analysis were plotted on an Excel sheet. For the skeletal anomalies, the data were coded according to the typology of the anomaly (Table 4.3:

List of considered anomalies) according to the affected regions and relative frequency of the anomalies, incidence of anomalies, deformities charge, the relative frequency of affected areas was calculated and analyzed. For the numeric value such as the number of mineralized vertebrae, length, weight and survival were directly calculated. The data were coded for the analysis of developmental stage as mineralized, mineralizing, cartilaginous, and absent, the numeric value was entered and finally, the cumulative percentage was calculated. For the meristic count absolute true value was entered and mean, median, and range (maximum and minimum value) was calculated. Partial Least-Squares Discriminant Analysis (PLS-DA), the performance is measured using prediction accuracy or group separation distance using the "B/W ratio" as suggested by Bijlsma et al (402).Univariate and multivariate analyses were performed using the MetaboAnalystR 3.0 R package and MetaboAnalyst 5.0 (400,401). Statistical analysis was performed using IBM SPSS 16 and Graphpad prism 8. Results are expressed as mean ± SEM. Levene's test was performed for the homogeneity of variance. Significances were evaluated by student's t-test, One-way, and Two-way Anova. Difference in value $p \leq 0.05$ was considered significant (ns- $P>0.05$, *- $P\leq0.05$, **-$P\leq0.01$, ***-$P\leq0.001$, ****-$P\leq0.0001$).

4.3 RESULTS

4.3.1. Doxorubicin affects growth and survival

The toxic dose of DOX was determined by exposing gilthead seabream larvae to different concentrations of DOX for up to 48 h. 60µg/mL of DOX were toxic for the larvae already at 24 h of exposure, while lower concentrations (i.e., 5, 15, and 30 µg/mL) did not show toxic effects up to 48 h. Therefore, 30 µg/mL concentration of DOX was chosen for the trial (supplementary figure 4.1). The prepared microdiets showed no toxic effects on larvae (supplementary figure 4.1). Temperature, oxygen, and O_2 saturation were stable throughout the trial period (supplementary table 4.1).

After 15 days of feeding trial (at 45 dah), the overall survival of the larvae was not significantly different between the groups (Figure 4.1A). The treatment with DOX supplemented diet significantly reduced the total length, but this effect was significantly reversed by co-treatment with RES (Figure 4.1B). No significant differences were observed in other groups. No significant differences between the groups were found on dry weight (Figure 4.1C).

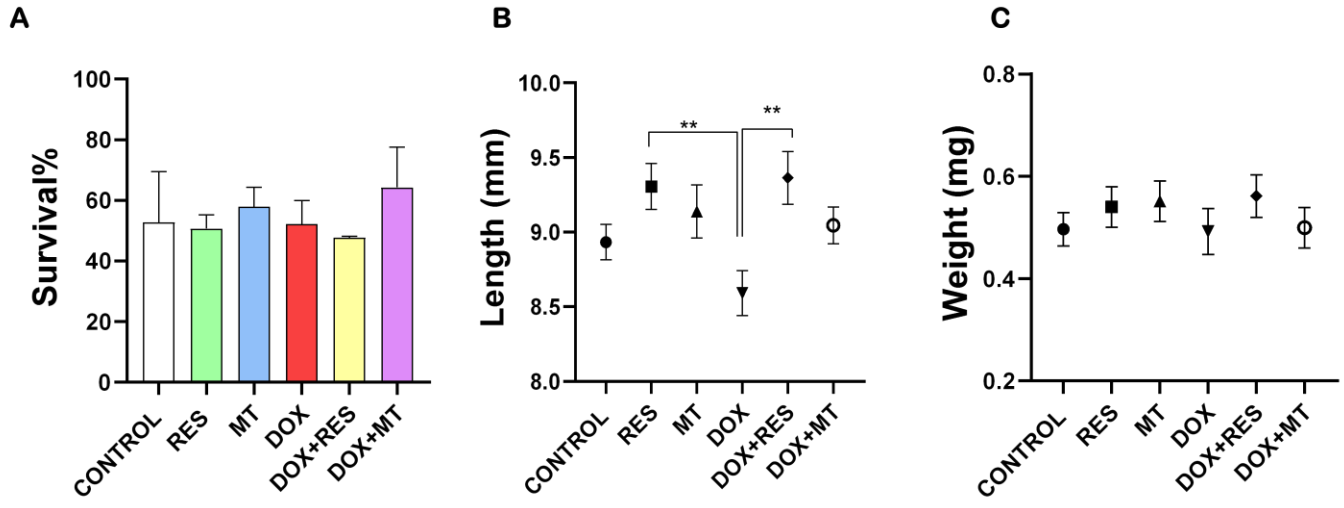

Figure 4.1: Survival and growth parameters of gilthead seabream larvae at the end of the trial. Survival of seabream (A), total length (B), dry weight (C). One-way ANOVA, Tukey's multiple comparisons test, *- P≤0.05, **-P≤0.01. Acronyms: Resveratrol (RES), Doxorubicin (DOX), MitoTEMPO (MT), Doxorubicin+Resveratrol (DOX+RES) and Doxorubicin+MitoTEMPO (DOX+MT).

4.3.2. Histological changes on antioxidant and pro-oxidants supplemented groups

Histological sections stained with hematoxylin and eosin (Figure 4.2A) revealed that DOX supplementation significantly reduced the length of *villi* as compared to control and antioxidants (RES and MT). In contrast, RES supplementation increased the length of the villi as compared to the control (Figure 4.2B). The length of the *villi* on co-treatment of DOX with antioxidants (RES and MT) was not significantly different from the control group but was significantly different from DOX treated group. Therefore, supplementation with both antioxidants significantly protected against the DOX-induced impact on the intestinal mucosa.

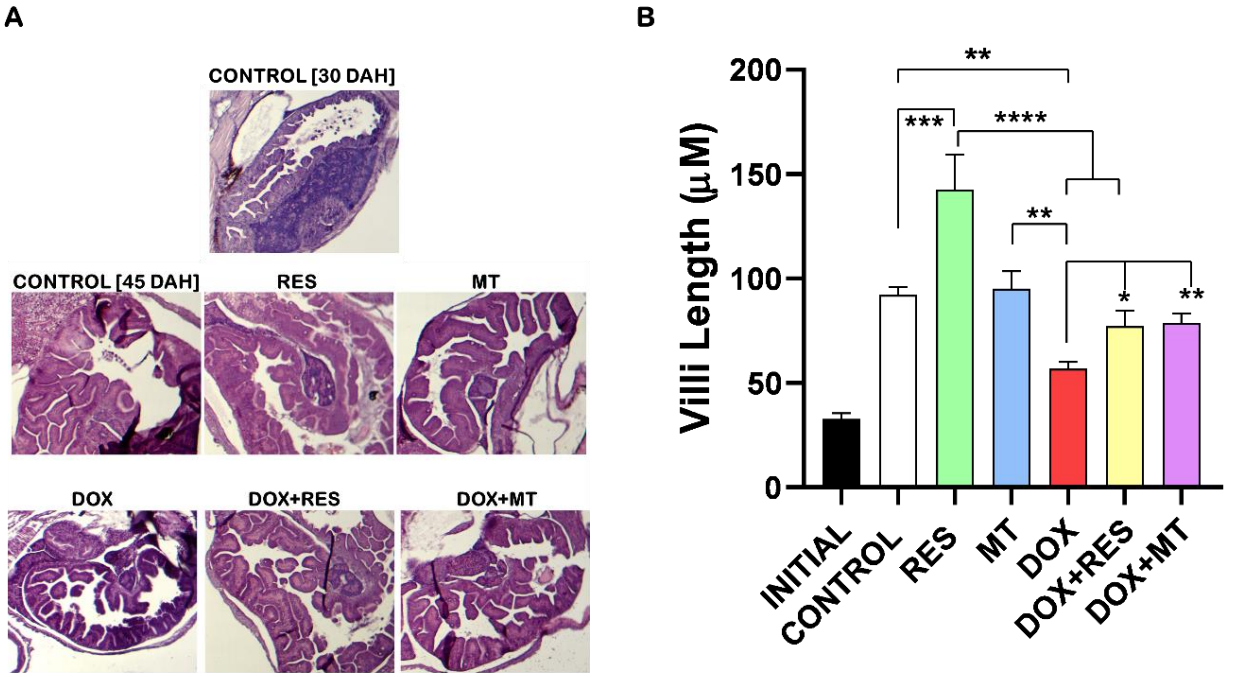

Figure 4.2: Histology of gut of gilthead seabream supplemented with antioxidants and pro-oxidants microdiets at 45 DAH (days after hatched). Stained with hematoxylin and eosin (10x) initial-initial larvae of 20 dah (A). Length of villus measured on ImageJ (B). One-way ANOVA, Tukey's multiple comparisons test, *- P≤0.05, **-P≤0.01, ***-P≤0.001, ****-P≤0.0001. Acronyms: Resveratrol (RES), Doxorubicin (DOX), MitoTEMPO (MT), Doxorubicin+Resveratrol (DOX+RES) and Doxorubicin+MitoTEMPO (DOX+MT).

4.3.3. Antioxidants reversed the incidence of skeletal deformities

The similarities and discriminant analysis on the distribution of skeletal deformities between the treatment groups were done using Partial Least-Squares Discriminant Analysis (PLS-DA score). The PLS-DA cluster analysis showed three distinct clusters, with the control groups being completely isolated, another cluster with antioxidants (RES and MT) and the third cluster with DOX alone or in combination (Figure 4.3A). The heatmap shows the distribution of skeletal deformities between the treatment group. The control and DOX treated groups showed a high number of skeletal deformities whereas the RES treatment group showed a smaller number of skeletal deformities on specific regions. The combination of DOX with either RES or MT prevented DOX-induced skeletal deformities (Figure 4.3B).

The incidence of skeletal anomalies was significantly decreased on RES supplemented group as compared to other groups while the incidence of skeletal anomalies was significantly higher on DOX supplemented group as compared to RES and MT groups (Figure 4.3C). Similarly, deformities charge and affected areas were significantly increased in the presence of DOX supplementation. But those effects were significantly rescued when DOX was combined with antioxidants (RES and MT) (Figure 4.3D and 4.3E). Thus, supplementation of antioxidants significantly reduced, while pro-oxidant (DOX) significantly increased, the incidence of skeletal deformities, deformities charge and severity. When analyzing the number of areas affected, it is clearly shown that DOX has induced higher numbers of multiple skeletal deformities. Upon antioxidants treatment, alone or in combination, a significantly higher number of fish presented a less severe phenotype (a smaller number of deformities/affected areas) as compared to DOX treatment (Figure 4.3F). The larvae supplemented with DOX presented a relatively higher severity of malformations affecting three regions as compared to the groups supplemented with RES and MT. However, DOX supplemented with a combination of antioxidants RES and MT significantly reduced these negative effects. A similar effect was also observed on the severity of malformations affecting four and more regions with the DOX group showing a significantly higher number of fish with malformations as compared to antioxidants RES and MT (Figure 4.3F).

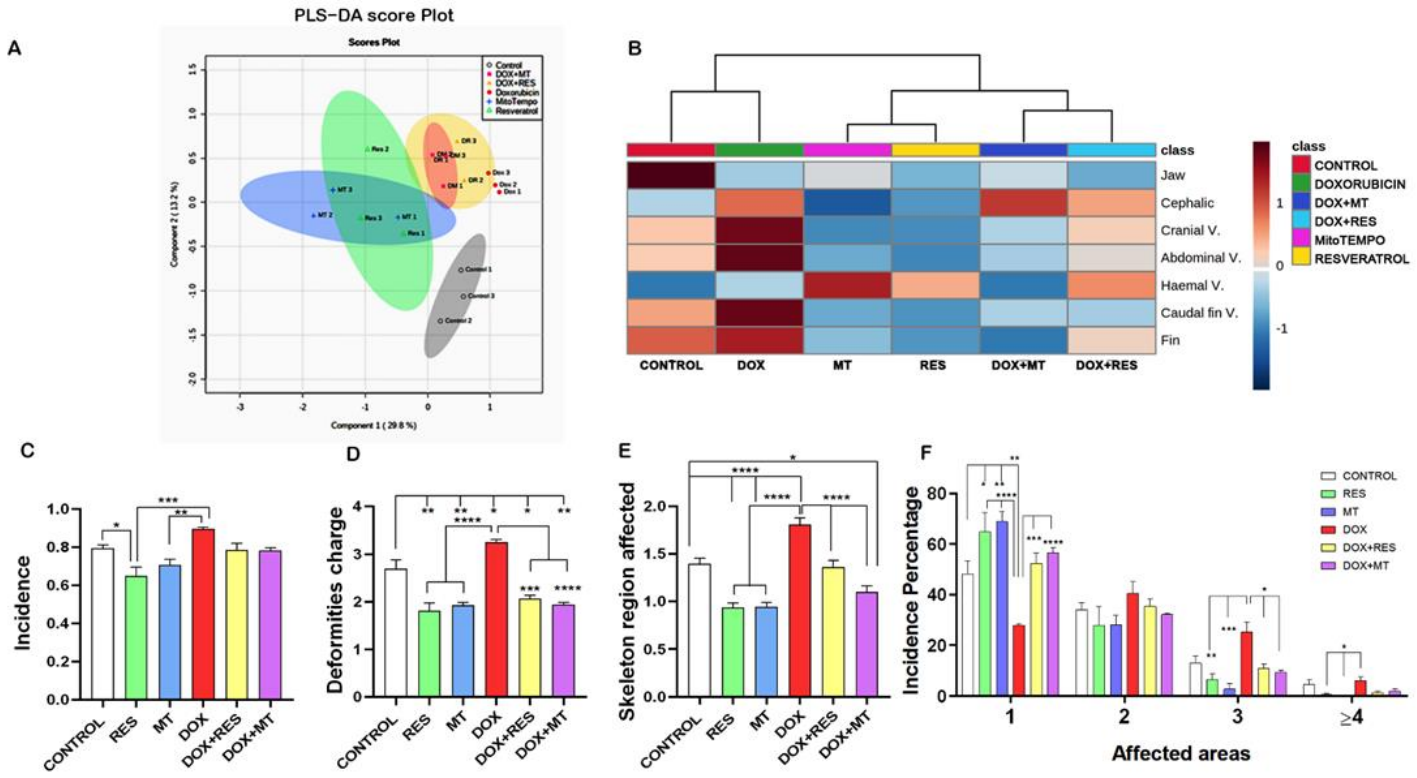

Figure 4.3: Incidence of Skeletal deformities. Partial Least-Squares Discriminant Analysis (PLS-DA score) between the antioxidants and pro-oxidants groups (A), heatmap of distribution of skeletal deformities (B), incidence of Deformities (C), deformities charge (D), number of affected areas (E), severity of malformation (number of affected areas) (G). One-way ANOVA, Tukey's multiple comparisons test, *- P≤0.05, **-P≤0.01, ***-P≤0.001, ****-P≤0.0001. Acronyms: Resveratrol (RES), Doxorubicin (DOX), MitoTEMPO (MT), Doxorubicin+Resveratrol (DOX+RES) and Doxorubicin+MitoTEMPO (DOX+MT).

The incidence of specific skeletal anomalies was analyzed in the different groups (Figure 4.4). The incidence of jaw deformities showed a significantly lower level on RES supplemented groups as compared to Control. A higher number of cephalic deformities was observed on DOX supplemented groups, compared to RES and MT supplemented groups (Figure 4.4A). DOX supplemented group showed a substantially higher number of incidence of deformities on cephalic neural arches and/or spines (Figure 4.4B, A6) as compared to Control, RES and MT. The incidence of skeletal malformations on these structures was significantly decreased on antioxidant supplemented groups as compared to Control and the number of deformities significantly reversed when DOX was combined with antioxidants (RES and MT). Similarly, to the observed in the

cephalic region, larvae supplemented with DOX showed a significantly higher incidence of malformations on pre-haemal neural arches and/or spines (B6) as compared to Control and to the groups supplemented with antioxidants RES and MT (Figure 4.4C). Also, the incidence of skeletal malformations of the neural arches and/or spines on the pre-haemal region was significantly decreased on antioxidant supplemented groups as compared to Control. The higher incidence of deformities recorded in the caudal region was on the neural arches and/or spines (D6) and on haemal arches and/or spines (D7). The incidence of malformations on D6 was significantly reduced upon RES and MT supplementation as compared to Control, while it was significantly higher upon supplementation with DOX as compared to Control, RES and MT (Figure 4.4D). However, the combination of DOX with antioxidants, RES and MT substantially reversed the effect of DOX alone. The incidence of malformed epurals (deformed, absent, fused, supernumerary) (G11) and ectopic mineralization (G19) was higher as compared to other deformities in this region. The RES treatment significantly decreased the incidence of malformed epurals as compared to Control. The incidence of malformed epurals was significantly increased by DOX supplementation as compared to RES and MT and the supplementation with antioxidants significantly reversed that effect (Figure 4.4E). Ectopic mineralized structures (G19) on the caudal fin region were significantly higher on DOX group as compared to Control, RES and MT (Figure 4.4E). A comparatively low incidence of skeletal malformations was observed on the haemal vertebrae region (Figure 4.4F) and on the anal and dorsal fins (Figure 4.4G). The heat map showed an overall distribution of skeletal anomalies between the groups with two distinct clusters with control and DOX groups being different from the other groups (Figure 4.4H).

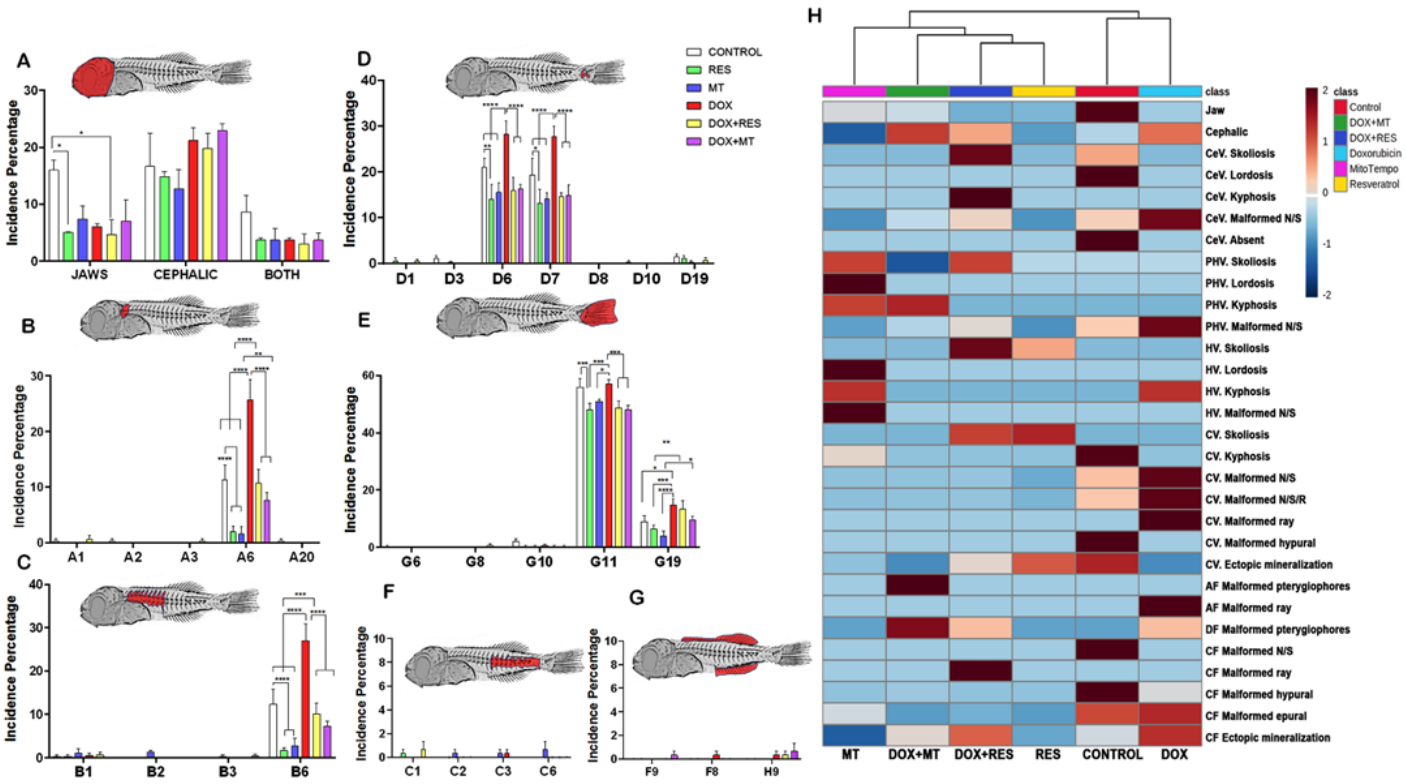

Figure 4.4: Distribution of skeletal deformities. Incidence of deformities in between the antioxidant and pro-oxidant supplemented groups. Head region (A), cephalic region (B), prehaemal region (C), caudal region (D), caudal fin (E), haemal or pre-caudal region (F), anal fin (F), dorsal fin (G) and heat map of the specific deformities between the antioxidant and pro-oxidant supplemented groups (H). Two-way ANOVA, Tukey's multiple comparisons test, ns-P>0.05, *- P≤0.05, **-P≤0.01, ***-P≤0.001, ****-P≤0.0001. Acronyms: Resveratrol (RES), Doxorubicin (DOX), MitoTEMPO (MT), Doxorubicin+Resveratrol (DOX+RES), Doxorubicin+MitoTEMPO (DOX+MT), Cephalic vertebrae (CeV), Pre-haemal vertebrae (PHV), Haemal vertebrae (HV), Caudal vertebrae (CV), Anal fin (AF), Dorsal fin (DF) and Caudal fin (CF).

The analysis of the results on skeletal deformities clearly demonstrates that the incidence of malformations was higher in the DOX group than in the RES and MT groups. Similarly, when the antioxidants RES and MT were combined with the pro-oxidant, the DOX-induced negative effects on the incidence of particular malformations were significantly reversed (Figures 4.3 and 4.4).

4.3.4. Antioxidants prevent Dox-induced mineralization and development delays

To illustrate the differences on skeleton mineralization we performed Partial Least-Squares Discriminant Analysis between the treatment groups on the mineralization pattern of skeletal elements on whole-mount stained larvae. The cluster analysis revealed that mineralization of the skeleton elements between control, antioxidant, pro-oxidant and antioxidants plus pro-oxidant groups were distinctly different from one another (Figure 4.5A). Acid-free double staining using alcian blue and alizarin red showed that RES supplementation significantly increased mineralization of vertebrae as compared to Control. Whereas MT supplementation did not show any difference on the mineralization of vertebrae and DOX supplementation significantly decreased the mineralization of vertebrae as compared to RES. Interestingly, the combined treatment with DOX and RES significantly reversed the effect of DOX on the mineralization of vertebrae, providing levels comparable to DOX treatment alone (Figure 4.5B). The mineralization pattern of skeletal elements between the antioxidants and pro-oxidants supplemented groups observed in the larvae was confirmed with an *in vitro* extracellular matrix mineralization assay using VSa13 cells. AR-S staining was performed to investigate extracellular matrix mineralization. The exposure of VSa13 cells to DOX significantly impaired the mineralization capacity of the cells as compared to treatments with RES and MT. In contrast, upon treatment in combination with RES or MT, the effect of DOX was significantly reversed (Figure 4.5C) as confirmed by the increase in mineralization of osteoblastic cells.

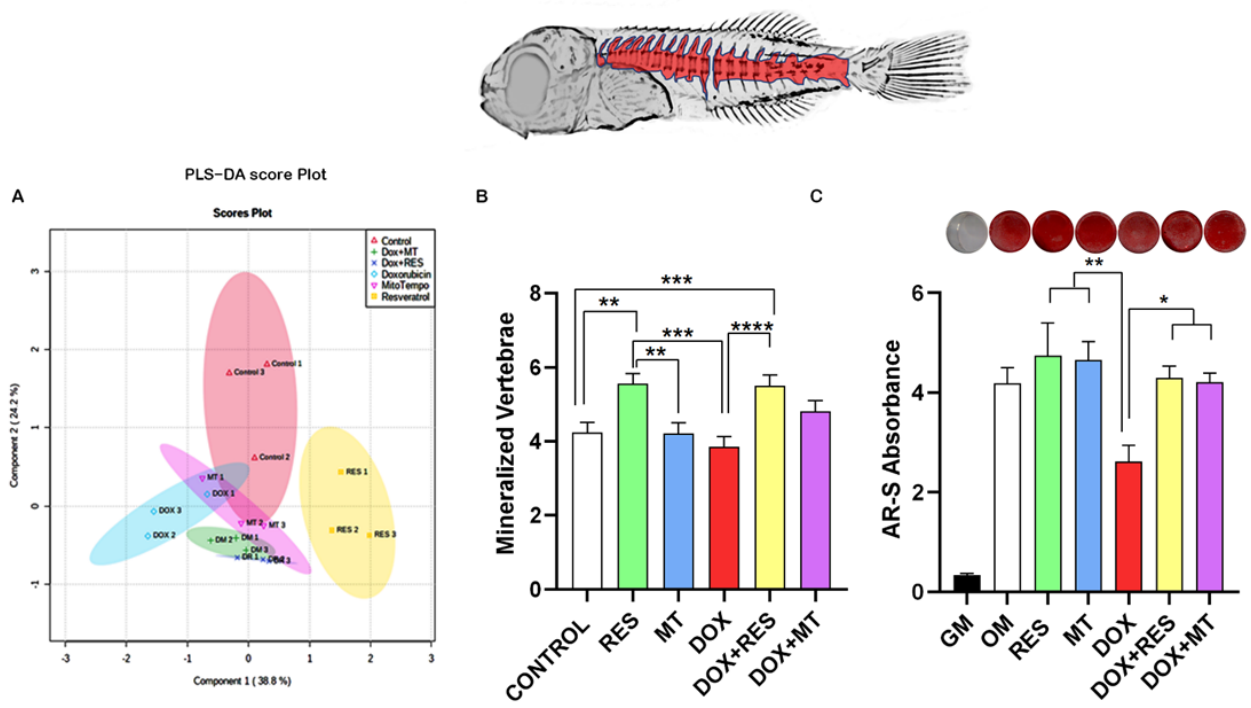

Figure 4.5: Mineralization of the skeletal elements. Partial Least-Squares Discriminant Analysis (PLS-DA score) between the antioxidants and pro-oxidants groups on the mineralization of the skeleton elements (A), Mineralized vertebrae of seabream fed with Microdiets (B) and Extracellular matrix mineralization assay of VSa13 cells (C). One-way ANOVA, Tukey's multiple comparisons test, *- P≤0.05, **-P≤0.01, ***-P≤0.001, ****-P≤0.0001. Acronyms: Alizarin red-S (AR-S), Growth medium (GM), Osteogenic medium (OM), Resveratrol (RES), Doxorubicin (DOX), MitoTEMPO (MT), Doxorubicin+Resveratrol (DOX+RES) and Doxorubicin+MitoTEMPO (DOX+MT).

The RES supplementation increased mineralization in neural arches of cranial vertebrae (27% mineralized and 45% mineralizing) as compared to other groups (Figure 4.6A). The MT treated group showed a higher percentage of cartilaginous (46%) and mineralizing (49%) structures, while only 5% were already mineralized. The DOX supplemented group showed delayed mineralization with a large portion of the structures still cartilaginous (43%) or mineralizing 55% (Figure 4.6A). Similarly, in pre-haemal neural arches and ribs, RES supplementation was shown to increase the percentage of mineralizing (RES- 41%, MT- 30%) and mineralized (RES- 5%, MT- 3%) structures, while in the DOX treatment no mineralized arches were observed (Figure 4.6B). Haemal vertebrae neural arches and spines were still under formation on 45 dah

seabream larvae. All groups showed 90% and more cartilaginous neural arches and spines. (Figure 4.6C). In caudal fin vertebrae, the groups treated with antioxidants (RES and MT) showed an increased number of mineralizing neural arches and modified haemal arches compared to the DOX supplementation group where the number of cartilaginous (45%) structures was higher (Figure 4.6D). RES and MT increased the mineralized, as well as mineralizing state of urostyle and hypurals. DOX supplementation increased cartilaginous elements whereas in combination with antioxidants the percentage of mineralizing and mineralized urostyle was increased compared to DOX alone (Figure 4.6E). Antioxidant supplementation showed a slight increment in mineralizing caudal-fin rays. The DOX supplementation did not show any difference in mineralizing rays percentage (Figure 4.6F). The heatmap shows the pattern of mineralization of the skeletal elements between the treatment groups. The control and DOX treated groups showed lower intensity of mineralization whereas the RES treatment groups show a high intensity of mineralization of skeletal elements. The combination of DOX with RES or with MT partially prevented DOX-induced reduction of mineralization (Figure 4.6G).

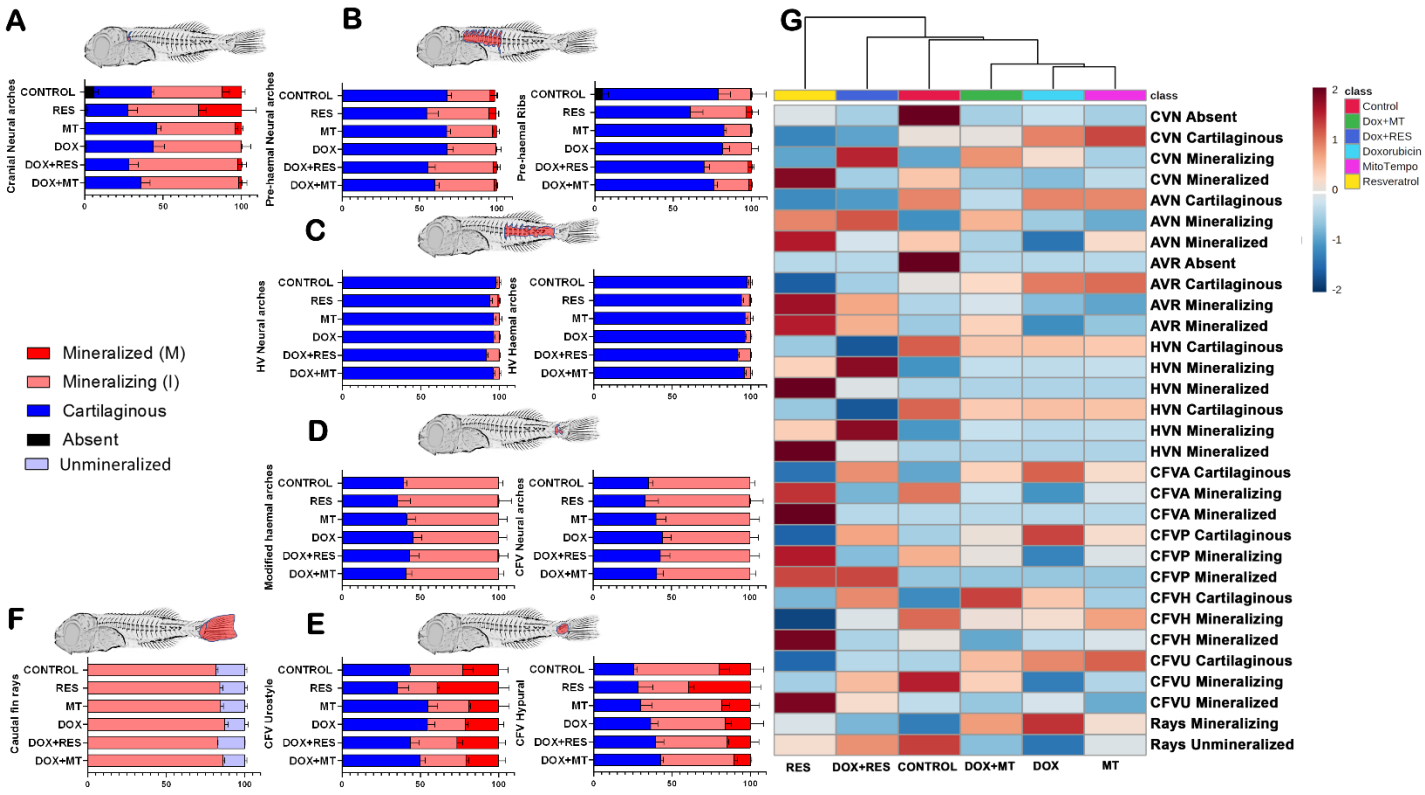

Figure 4.6: Developmental status and mineralization patterns of gilthead seabream fed different microdiets. Percentage of mineralized, mineralizing, cartilaginous, unmineralized and absent; cranial vertebrae neural arch (a), prehaemal vertebrae neural arches and ribs (b), haemal vertebrae neural (c), modified haemal arch and caudal vertebrae neural arches (d), caudal fin vertebrae (CFV), urostyle and hypural (e), caudal fin rays (f). Heat map of mineralization pattern of skeleton element between the antioxidant and pro-oxidant supplemented groups (G). Graph: percentage +/- SEM. Acronyms: Resveratrol (RES), Doxorubicin (DOX), MitoTEMPO (MT), Doxorubicin+Resveratrol (DOX+RES) and Doxorubicin+MitoTEMPO (DOX+MT), Cephalic vertebrae neural arches (CVN), Pre-haemal vertebrae neural arches (PVN), Pre-haemal vertebrae ribs (PVR), Haemal vertebrae neural arches (HVN), Haemal vertebrae haemal arches (HVH), Caudal vertebrae Modified haemal arches (MHA), Caudal fin vertebrae neural arches (CFVN), Caudal fin vertebrae hypural (CFVH), Caudal fin vertebrae urostyle (CFVU) and Caudal fin rays (Rays).

4.3.5. Antioxidant and pro-oxidants alter the meristic characters

The meristic character counts are shown in table 4.5, with a comparison of observed mean, median and range values between the groups supplemented with antioxidant, pro-oxidant and the combination of both. The number of mineralized vertebrae were different among the groups with a higher number observed on RES supplemented group and a decreased number in DOX supplemented group (Table 4.5 and Figures

4.5A and 4.5B). The mean number of mineralized cranial vertebrae was significantly different on RES group compared to DOX and control groups (one-way ANOVA p-<0.0001). The number of pre-haemal vertebrae and the haemal vertebrae showed no differences between the groups. In the caudal region, the number of epurals was increased in DOX supplemented group whereas in other groups there were no differences. Significant differences were observed on ectopic cartilage in hypuralia between the groups as well as in the number of caudal-fin rays. In the dorsal fin, both the number (mean and median) of cartilaginous pterygiophores and of unmineralized lepidotrichia were higher on the DOX group as compared to other groups. The number (mean and median) of cartilaginous pterygiophores on the anal fin as well as the number of unmineralized lepidotrichia were also higher on DOX as compared to other groups.

Table 4.5: Meristic Count

		Cranial vertebrae		Pre-haemal vertebrae		Haemal vertebrae		Caudal fin				Dorsal fin			Anal fin		
		Mineralized	Mineralizing	Mineralized	Mineralizing	Mineralized	Mineralizing	Epural	Ectopic C. in hypuralia	Mineralizing	Unmineralized	Pterygiophores (Cartilaginous)	Lepidotrichia (Mineralizing)	Lepidotrichia (Unmineralized)	Pterygiophores (Cartilaginous)	Lepidotrichia (Mineralizing)	Lepidotrichia (Unmineralized)
CONTROL	Mean	0.3667*	0.2367*	2.0633*	1.28*	0.0533*δ	0.15*	3.53*	0.7567*	13.78*	2.58*	11.92*	0.87*-	6.4533*	7.6967*	0.8133*δ	5.1933*δ
	Std.	0.4827	0.42575	3.08074	1.55014	0.37987	0.56737	0.67623	0.81	3.24552	2.18774	9.08085	2.87064	6.88422	5.24624	2.72947	5.36955
RES	Mean	0.5304*	0.1791*	3.1993*	1.3311*	0.1824*	0.1723*	3.4561*	0.6723*	14.6723*	2.0676*	12.0946*	1.4899*	5.8277*	7.9122*	1.375*	4.5946*
	Std.	0.49992	0.38405	3.42238	1.37724	0.88327	0.62222	0.58056	0.78	2.98085	1.96981	8.98272	3.50785	5.91413	5.01784	3.08379	4.88975
MT	Mean	0.4047*	0.1271*δ	2.4314*	0.9699*δ	0.1271*	0.1271*	3.5017*	0.5585*	12.903*	2.9431*	10.5786*	0.9264*δ	5.9331*	6.6656*	0.8361*δ	4.5786*
	Std.	0.49165	0.33363	3.27762	1.38148	0.75345	0.53461	0.51406	0.708826785	3.11318	2.1253	9.51913	2.79524	6.15479	5.50246	2.52967	4.88076
DOX	Mean	0.4392*	0.125*δ	2.3547*	0.8851*	0.0541*δ	0.0507*	3.4662*δ	0.5946*δ	13.9189*	2.2399*	13.5878*	1.2568*	8.2061*	8.3649*δ	1.0878*	6.1723*
	Std.	0.49713	0.33128	3.14279	1.3405	0.46989	0.27457	0.63689	0.677361159	2.97564	2.04688	9.15251	3.15717	7.18577	5.07055	2.84737	7
DOX+RES	Mean	0.5973*	0.1107*	3.4497	0.9564*δ	0.1242*	0.2483*	3.4732*δ	0.5906*δ	14.4832*	2.1745*	13.1745*	2.2483*	6.6946*	8.3289*δ	1.8658*	5.151*
	Std.	0.49126	0.31434	3.49205	1.16115	0.6777	0.68565	0.55135	0.756684446	2.78187	1.59009	8.81324	4.49452	6.41946	4.96173	3.73654	4
DOX+MT	Mean	0.5498*	0.0859*	2.9416*	1.055*	0.0893*	0.1649*	3.4777*	0.7595*	14.0344*	2.5636*	12.2337*	1.488*	7.0172*	7.7629*	1.2749*	5.5326*
	Std.	0.49837	0.28071	3.24622	1.22773	0.62056	0.5933	0.52063	0.781602051	3.05109	1.68929	9.20871	3.71702	6.71358	5.29822	3.03429	5.36285

[δ] No significant differences between the group, * Significant differences between the groups (one-way ANOVA, Tukey's multiple comparisons test, $p \leq 0.05$). Acronyms: Std.: Standard deviation, resveratrol (RES), doxorubicin (DOX), MitoTEMPO (MT), doxorubicin + resveratrol (DOX+RES), doxorubicin + MitoTEMPO (DOX+MT), and Ectopic C. in hypuralia (Ectopic cartilage in hypuralia).

4.3.6. Doxorubicin affects minerals content

Although the mineral formulation of the microdiets was similar (Table 4.1 and 4.2), analysis of mineral content showed that the DOX group had significantly lower calcium and phosphorus contents compared to RES and MT groups (Figure 4.7A and 4.7B). The calcium/phosphorus ratio was also significantly reduced in the group supplemented with DOX as compared to other groups except for DOX+MT (Figure 4.7C). Similarly, potassium content was significantly reduced in the group supplemented with DOX as compared to the groups supplemented with RES and MT alone or in combination with DOX (supplementary figure 4.2). Sodium, magnesium, and iron contents were also decreased in the groups supplemented with DOX alone or in combination with antioxidants (supplementary figure 4.2).

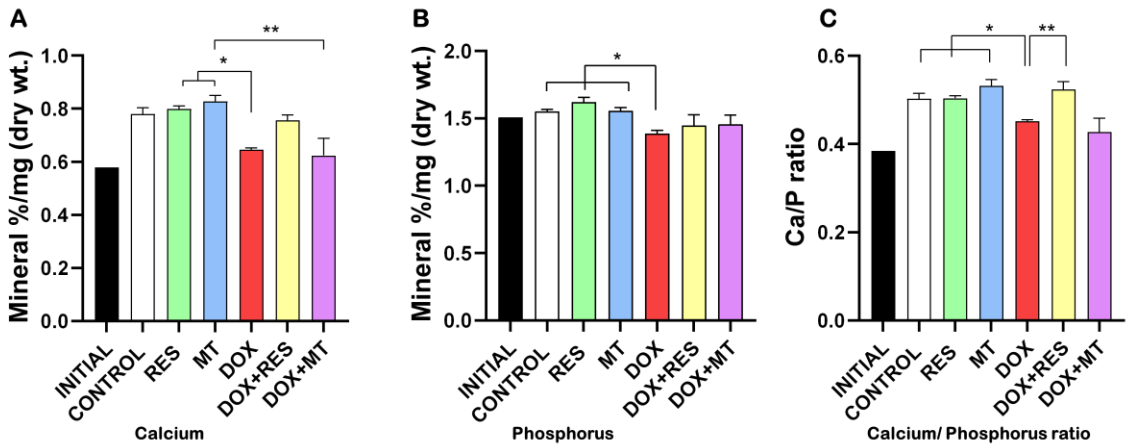

Figure 4.7: Mineral analysis of gilthead seabream fed with microdiets. Calcium (A), phosphorus (B), calcium/phosphorus ratio (C). One-way ANOVA, Tukey's multiple comparisons test, *- P≤0.05, **-P≤0.01, ***-P≤0.001, ****-P≤0.0001. Acronyms: Resveratrol (RES), Doxorubicin (DOX), MitoTEMPO (MT), Doxorubicin+Resveratrol (DOX+RES) and DOX+MT (DOX+MT).

4.3.7. Doxorubicin-induced oxidative stress was reversed by antioxidants

An increase in free radicals causes overproduction of Malondialdehyde (MDA), a common marker of oxidative stress and antioxidant status. The degree of lipid peroxidation was significantly higher on DOX supplemented group as compared to RES and MT groups. No significant difference was seen between DOX and

control group. RES supplementation significantly reduced the lipid peroxidation as compared to control group. Similarly, in the groups combining DOX with antioxidants, the MDA level was significantly reduced as compared to DOX alone (Figure 4.8A). In the DOX treated groups, a significant reduction was observed in mRNAs transcribed from antioxidant genes, including *catalase - cat* (Figure 4.8B), *superoxide dismutase 1 - sod1* (Figure 4.8C) *glutathione peroxidase 1* - gpx1 (Figure 4.8D), and *heat shock protein 90 - hsp90* (Figure 4.8E) as compared to RES. *Osteopontin* (*spp1*), a gene responsible for the mineralization and highly expressed by mature osteoblasts, was significantly upregulated upon RES treatment, whereas *spp1* expression was significantly reduced on DOX treated group as compared to RES (Figure 4.8F).

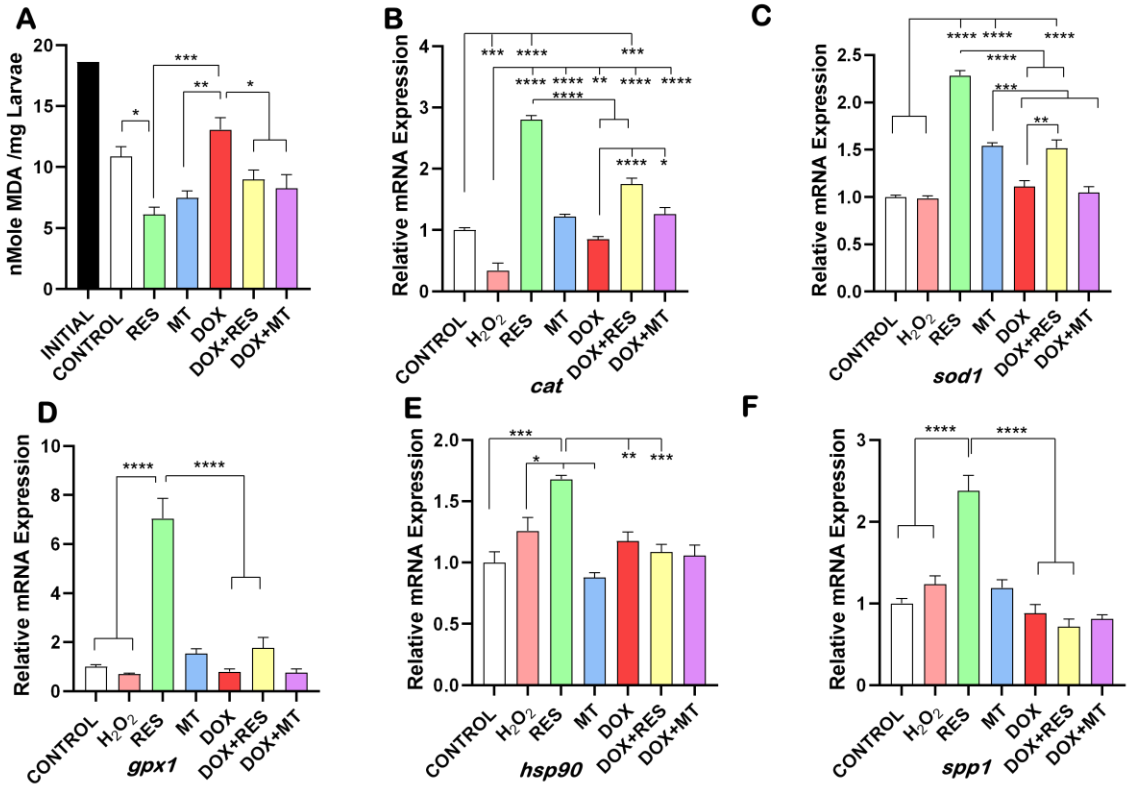

Figure 4.8: Oxidative stress and antioxidant status on antioxidant and pro-oxidant treatment. Lipid peroxidation of the gilthead seabream larvae feed with antioxidant and pro-oxidant diets, initial- initial larvae of 20 days (A). mRNA expression of expression of antioxidants genes on VSa13 cells treated with Antioxidants and Pro-oxidants (Resveratrol, MitoTEMPO, Hydrogen peroxide and Doxorubicin); Catalase (*cat*) (B), superoxide dismutase 1 (*sod1*) (C), glutathione peroxidase 1 (*gpx1*) (D), heat shock protein 90 kDA alpha 1 (*hsp90*) (E) and osteopontin (*spp1*) (F). One-way ANOVA, Tukey's multiple comparisons test, *- P≤0.05, **-P≤0.01, ***-P≤0.001, ****-P≤0.0001.

Acronyms: Resveratrol (RES), Doxorubicin (DOX), MitoTEMPO (MT), Doxorubicin+Resveratrol (DOX+RES), Doxorubicin+MitoTEMPO (DOX+MT).

4.4 DISCUSSION

Doxorubicin is one of the main anticancer drugs, causing high toxicity characterized by massive accumulation of ROS (403) and reactive nitrogen species (ROS) as its central working mechanisms (212,213,433). As a result, DOX promotes a direct oxidative damage to DNA (267,268) and increases lipid peroxidation (269–274). DOX treated patients exhibit significant bone loss (215), and a reduction by 60% of bone mass was also observed in normal rats treated with DOX (216,217).

The developmental toxicity associated with DOX has been previously studied in various models including rats (405) dogs (404) and zebrafish (406–408). In zebrafish, DOX induces developmental toxicity, with higher concentrations (≥ 25 mg/L) causing acute lethal effects and lower concentrations (≤0.1 mg/L) showing sublethal effects with multiple malformations (408). In this study, we aimed to counteract the DOX-induced bone loss by antioxidant supplementation. Our data shows that DOX supplementation (30 mg/kg) promoted a delay in growth when compared to RES supplementation, as indicated in total length; however, the weight of the larvae did not show any difference. Reduction of growth is considered a marker for chronic stress in teleost fish (412) and antioxidant supplementation has been shown to improve growth on rainbow trout and southern flounder and rescue the glucocorticoid-induced negative effects on growth in zebrafish (225,409,410). Similarly, MT had been shown to improve development in re-implanted porcine embryos (411).

The dietary nutrients are metabolized and absorbed in the jejunum with intestinal *villi* increasing the surface area of absorption (452). Up to 75% of RES is absorbed by passive diffusion after oral administration, accumulating in numerous organs, such as the stomach, intestines, or liver, where it is significantly absorbed and metabolized (453). Previously, it was observed that DOX administration increased apoptosis of the jejunal epithelium (413),

demonstrated by severe intestinal damage, reduction of *villus* length and increased influx of leukocytes (414). The pharmacokinetics examination of plasma DOX concentration after oral administration revealed that the maximum concentration (Cmax) was 0.2062 l/ml and the maximum time (Tmax) was 2 hours (416). Therefore, in the present study, we examined the effect of DOX on intestinal *villi* and investigated if antioxidants were able to protect them against pro-oxidant-induced oxidative stress. Comparable to the results reported by Zhou *et al*. (415), the *villi* length were increased in response to antioxidants treatment. The absorption and pharmacokinetics of these compound can be speculated as a factor responsible for the effects. The negative impact of DOX on intestinal *villi* may thus be the reason for the delayed growth of larvae fed with DOX supplementation.

Skeletal anomalies are detectable at very early stages and can develop into sub-lethal anomalies in subsequent life stages (443). They are more prone to occur in animals having fast growth rates (454,455), since 90% of the bone's organic content are represented by collagen, responsible for maintaining stability and mechanical function (455). Ascorbic acid deficiency in fish has been shown to decrease bone collagen content and increase the incidence of skeletal anomalies (456). Skeletal anomalies established during early stages were characterized by disorganized connective tissue, abnormal mineralization and muscle bundles (429,457). The anomalies in the skull, jaw, pre-maxillary, glossopharyngeal and opercular plate affect the efficient nourishment of the larvae due to their inability of feeding which results in slower growth and weaker larvae (423,424). Our results showed that antioxidants significantly decreased the incidence of jaw anomalies resulting in better nourished and stronger larvae. In the current study, the caudal (vertebrae and fin) region was found to be the most strongly affected on all groups, confirming what had previously been reported by some authors for this species (419,421,423,424). Anomalies affecting the vertebral arches and ribs are considered insignificant since they have no impact on the external shape (443). However, the presence of these anomalies is a sign of altered osteogenic processes, and since neural arches protect the spinal cord and provide an entry

point for dorsal musculature, severe anomalies in neural arches and spines will affect the overall performance of the larvae (442,443). The haemal arches protect the arteria and *venae caudalis*, therefore severe anomalies in these structures could interfere with normal blood flow resulting in chondrogenesis influenced by low oxygen levels (458). Santamaria *et al*. (457) observed gilthead seabream larvae with lordosis at early stages, before the vertebrae differentiate, due to disorganized mineralization process. In European seabass and red seabream, lordosis are associated with failure to inflate the swim bladder, resulting in increased swimming activity which can overall affect the development of the larvae (459). Due to high swimming activity, the larvae overall energy expenditure is increased, and consequently its demand for food intake (460). The caudal vertebrae and the caudal fin were the most affected region in this study with a higher incidence of skeletal anomalies, as previously reported for *S. aurata* (419–421). The incidence of skeletal anomalies on caudal vertebrae and caudal fine were found to be significantly higher upon DOX supplementation, whereas when combined with antioxidants (RES and MT), the incidence was significantly reduced compared to DOX alone. Divanach *et al.* (425) and Koumoundouros *et al.* (420) have indicated that incidence of the caudal deformities can induce secondary vertebral deformities or reduce the biological performance (growth, conversion index) of the fish due to their effect on swimming efficiency. Accordingly, we found that vertebral arches/ribs and neural arches were significantly affected upon DOX supplementation, which may be the result of altered osteogenic process and mineralization. These effects were significantly rescued with the co-supplementation of antioxidants (RES and MT) suggesting that it can effectively prevent pro-oxidant induced bone deformities.

Studies by Boglione *et al.* (442,443) showed that skeleton anomalies detected at early ontogenetic stages (poorly or not differentiated skeletal tissue), can develop into sub-lethal skeletal anomalies at later stages. In addition, even if some vertebrae and related anomalies can develop at an older age, many skeletal anomalies arise during chondrogenic and osteogenic differentiation during early larval stages (15,442,443,461). The mineralization pattern of the skeletal

elements was analyzed in this study and found to be altered between the antioxidant and pro-oxidant supplemented groups *in vivo*, a result also confirmed with *in vitro* experiments. Mineralization and development of the axial skeleton of seabream larvae are simultaneous to posterior notochord dorsal flexion and sequentially posterior to the hypural complex and urostyle (446). RES supplementation significantly increased the mineralization of the skeletal elements in the larvae which can be the result of increased osteoblast differentiation and mineralization, as confirmed by VSa13 mineralization assay. Osteopontin (Spp1) plays an important role in the regulation of biomineralization (462,463). Preosteoblastic cells express Spp1 mRNA at early bone differentiation stages, while the highest expression of *spp1* is observed in mature osteoblasts (464). The expression of *spp1* mRNA is directly proportional to the ALP activity and calcium deposition level (465) and *Spp1* is upregulated by growth, differentiation factors and by mechanical stress, which promotes bone formation (380,464,466). Down regulation of *spp1* is associated with low mineralization in mechanically stimulated mice (466). VSa13 cells showed a decrease in the expression of *spp1* upon DOX treatment compared to RES. These data on VSa13 cells EC mineralization assay further strengthen the *in vivo* mineralization of seabream vertebrae on DOX-induced bone loss.

The diversity of mineralization patterns during development of skeletal elements in teleosts indicates the complexity of the mechanisms involved (446). Previously, Prestinicola *et al.* (419) and Russo *et al.* (467) have shown that the variability on the meristic counts is directly related to the occurrence of skeletal anomalies. In this study, we observed the alteration on meristic characters between the antioxidant and pro-oxidant treated groups of seabream larvae. Furthermore, antioxidant supplementation increased mineralization and reversed the pro-oxidant induced negative effects on mineralization, both *in vitro* and *in vivo,* suggesting that RES (225,276,468) and MT (469) supplementation would be beneficial, not only for enhancing bone development and mineralization, but also for the overall development of larvae.

In higher vertebrates, the skeleton serves as the main reservoir for calcium and phosphate (429). Skeletal system development and vertebrae stability are related to the mineral content. Fish absorb various elements from water, including calcium, therefore calcium deficiency is uncommon in fish. In contrast, food is the main source of phosphorus for fish, with low phosphorus intake resulting in reduced bone mineralization, skeletal abnormalities and reduced growth (430,431). Several *in vitro* and *in vivo* studies have shown that DOX reduces mitochondrial calcium uploading capacity (470–473). Indeed, the increased induction of mitochondrial permeability transition pore resulted in a loss of calcium loading capacity (471,474). Antioxidants are able to protect against DOX-induced mitochondrial toxicity (470). Our results showed that DOX significantly reduced the Ca/P ratio as compared to control and antioxidant supplementation, whereas combined treatment with RES significantly rescued Ca/P ratio. In addition, treatment with DOX decreased the calcium and phosphorus content of the larvae, suggesting its interference with mineral metabolism. Similarly, a decrease in the levels of potassium has been shown to increase bone resorption activity (475). In our study, DOX significantly decreased potassium content as compared to antioxidants supplementation (Figure S2), suggesting that DOX might increase osteoclast differentiation.

One of the objectives of this study was to illustrate the mechanism of DOX-induced bone loss. Our data indicate that supplementation of DOX reduced the expression of antioxidant genes including *cat*, *gpx1*, *sod1* and *hsp90* (468,476), which was significantly increased upon RES supplementation, alone or in combination with DOX. These results suggest that DOX-induced bone loss is the result of oxidative stress (213) which was rescued upon RES supplementation. Similarly, Meng *et al*. (477) also observed the improvement of antioxidant status regulating antioxidant genes when RES was supplemented through diet in sows and piglets (477). The DOX treatment induced an increase in lipid peroxidase, a decrease in antioxidant gene expression and in osteoblastic-associated mineralization. The ability of RES (276,468) and MT (469,478) to counteract those effects strongly indicates that oxidative stress is a major player in DOX-

induced bone loss (403). Skeletal deformities, altered meristic characters, and delayed development can be considered developmental disturbances that indicate inappropriate nutrition and associated oxidative stress (379,444). Malondialdehyde (MDA) concentration is the hallmark for lipid peroxidation resulting from oxidative stress by exogeneous production of ROS by food containing high polyunsaturated fatty acid, ionizing radiation ageing and environmental factors (435,436). This study shows that dietary supplementation with antioxidants is beneficial to overcoming the oxidative stress resulting from dietary external sources. Our results show that inclusion of antioxidants in larval diets for *S. aurata* can help prevent skeletal problems during early development, with benefits for the production of this species.

In the present study, supplementation with antioxidants resulted in improved protection against DOX-induced peroxidation, as evidenced by the significant reduction of MDA concentration. This demonstrates the importance of RES and MT to reduce oxidative stress by reducing hydroperoxides (435,436). Rana *et al*. reported that SOD1 is a molecular target of DOX mediated bone loss (213). In the present study, the phenotype induced by DOX on both *in vitro* and *in vivo* experiments has been reversed by performing a co-treatment with antioxidants. We hypothesized that RES induced reversal of DOX-induced bone deformities in seabream larvae is related to increased osteoblast differentiation/mineralization and protection against oxidative stress, as indicated by our *in vitro* studies. DOX has previously shown to reduce bone mass in humans and mice (215–217), as a result of decreased osteoblastogenesis (213) or increased osteoclastogenesis (347). Oxidative stress is one of the major players in DOX-induced bone loss, in agreement with data previously published in which SOD1 was identified as a molecular target of DOX mediated bone loss (213). Our *in vitro* study shows that the decrease in the mRNA of *sod1* was significantly reversed by RES. Transcriptomic analysis had revealed p53 as a key regulator of doxorubicin-induced toxicity in mice (296). In addition, p53 was shown to induce expression of pro-oxidants genes to further increase ROS, resulting on apoptosis and senescence of the cells (479). In contrast, RES was shown to increase

osteoblastogenesis by inhibiting p53 signaling pathway on human bone marrow-derived mesenchymal stem cells (302). Altogether, the reversal of the negative effects of DOX upon bone cell differentiation and mineralization, and the increase in expression of antioxidant genes by RES, suggests that p53 is a major player involved in the mechanism of DOX-induced bone loss. Further studies should be carried to confirm the proposed role of p53 on the mechanism of bone differentiation.

4.5 CONCLUSION

In conclusion, our data indicate that DOX-induced mineralization, bone deformities, and bone loss are a result of oxidative stress. Antioxidant supplementation effectively prevented the incidence of bone anomalies and mineralization defects induced by pro-oxidants in both *in-vivo* and *in-vitro* models. RES and MT supplementation were able to reverse pro-oxidant-induced effects on bone anomalies, mineralization, and oxidative stress. Further testing in other models will reinforce our findings. Our data further suggest that antioxidants supplementation of fish diet would be beneficial to overcome oxidative stress-induced bone deformities.

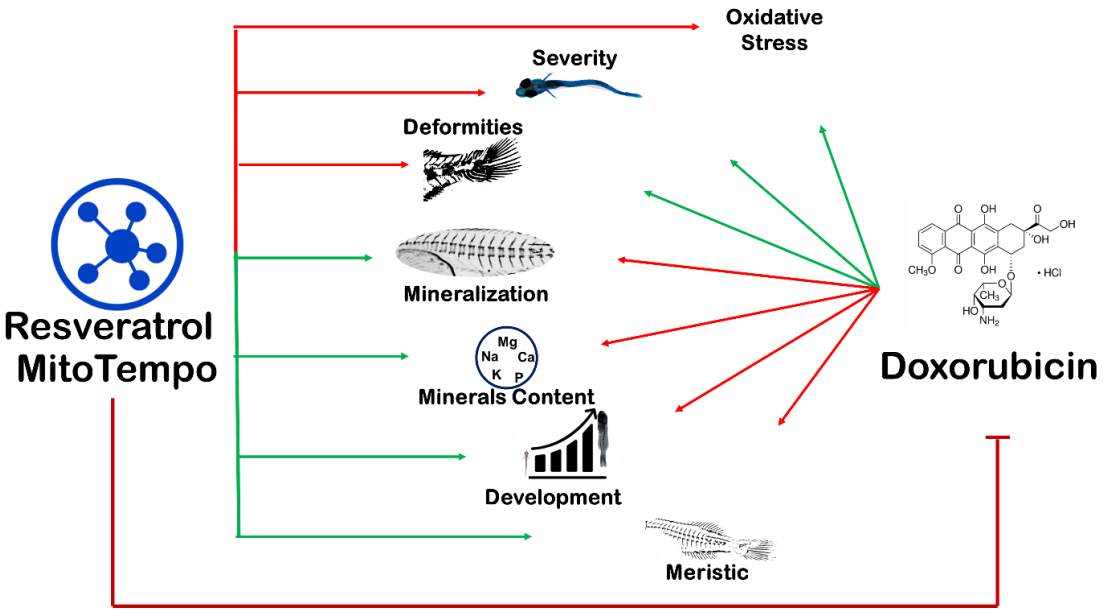

Figure 4.9. Graphical Abstract. Antioxidants (Resveratrol and MitoTempo) supplementation improved skeletal health and the Doxorubicin-induced effect on skeletal anomalies were reversed by the supplementation of Antioxidants.

CHAPTER 5

CONCLUSIONS AND FUTURE PERSPECTIVES

5.1. CONCLUSION

Clinically doxorubicin (DOX) is used in a wide range of chemotherapy applications, such as soft tissue and bone sarcomas and cancers of the breast, bladder, thyroid, ovary, acute lymphoblastic/myeloblastic leukemia, small cell lung cancer and Hodgkin lymphomas. Several therapeutic regimens including DOX in chemotherapy carry the risk of causing or favoring the development of secondary osteoporosis (295). DOX/cyclophosphamide combined regimen showed low bone mineral density and significant bone loss (215) in patients, while DOX exposure caused a 60% reduction in bone formation in normal rats (216,217). The use of the antioxidants, such as resveratrol (RES), has been shown to reverse the osteoporosis associated reduction in bone mass and density and microarchitecture deterioration (277).

Previously, the adverse effects of DOX on bone have been reported. In humans, recipients of DOX suffer long term bone damage in the form of reduced adult height and increased fracture risk (214). As in humans, in this thesis, zebrafish (Chapter 3) and gilthead seabream (Chapter 4) also showed reduced standard length. Furthermore, Hadji *et al.* (215) showed that premenopausal breast cancer patients treated with DOX exhibited low bone mineral density and significant bone loss, suggesting a cause and effect relationship between DOX treatment and systemic bone loss. Similar to the results described by Hadji *et al.* (215), in this study (Chapter 3 and 4), the calcium and phosphorus contents of zebrafish and gilthead seabream were significantly reduced by the DOX supplementation, showing that the effects on the skeletal system are similar across vertebrates.

DOX exposure caused a 60% reduction in bone formation in normal rats, suggesting a potential for reduced osteoblast differentiation (216) (217). DOX has also been shown to negatively regulate trabecular bone volume and cortical bone thickness in rabbits (218). Van Leeuwen *et al*. (216), Friedlaender *et al.* (217), and Glackin *et al.* (219) have showed that DOX inhibits osteoblastic cells and diminish bone formation, Similar to these results, we found that MC3T3-E1 cells treated with DOX showed a decreased osteoblast differentiation and ECM

mineralization (Chapter 2.1). This depletion of bone mass was established to be caused by an imbalance between osteoblast and osteoclast activity. Here (Chapter 2.2), we have shown that osteoclast activity was significantly increased upon DOX exposure as shown by increased numbers of TRAP-positive cells and cathepsin K positive cells in the head areas of the reporter zebrafish line (*tg(ctsk:dsRed*)). The number of multinucleated osteoclasts was significantly higher on DOX treatment, suggesting that the resorption of bone increases during DOX treatment. The co-treatment with RES revealed a decrease in osteoclast differentiation.

Oc-stamp encodes for a transmembrane protein required for the fusion of osteoclasts (356) that was highly expressed on DOX treated RAW 264.7 cells differentiation, suggesting that DOX promoted an increased fusion of the macrophage/monocyte lineage during osteoclastogenesis, forming larger, and therefore, more active osteoclasts. Interestingly, when combining DOX with RES, there was a significant reduction of *Oc-stamp* mRNA expression, suggesting that RES prevents the fusion of macrophages. The upregulation of FoxM1 expression reduces ROS by stimulating the expression of ROS scavenger genes such as *Sod 1* and*, Nrf 2* (326,352,353). Rubiolo e*t al.* and Shin SM *et al.* (341,342) have showed that RES protects cells against ROS-induced oxidative stress damage by the increment of antioxidant enzymes in transcriptional level. Similar to this results, In this study, RES exposure inhibited osteoclast differentiation and negatively regulates intracellular ROS by stimulating the expression of detoxifying enzymes, such as *Sod 1* and *Nrf.* Furthermore, DOX treatement showed increased osteoclast differentiation and decreased expression of *Sod 1*, suggesting FoxM1 involvement as a regulator of DOX-induced osteoclast differentiation. Similar to this results, several studies have indicated that DOX exposure leads to downregulation of *FoxM1* expression (330,331).

Kaczmarek *et al*. (370) has described that DOX treatment on mice showed to increase development of mucositis. Similar to this indication, we observed that DOX strongly induced mucositis on our fish models (zebrafish and seabream).

Interestingly, combining DOX with RES significantly decreased the cathepsin K signal, suggesting that RES was able to significantly reverse DOX induced mucositis on zebrafish. The results presented in this thesis show that antioxidant supplementation significantly increased the length of intestinal villi of zebrafish (Chapter 3) and gilthead seabream (Chapter 4), which contributes to higher nutrient absorption, resulting in enhanced fish growth. Several reports have pointed out that DOX administration induced severe damage on the intestine, with increased apoptosis of jejunal epithelium (413), increased influx of leukocytes and reduced villi length (414), which was also observed in our models (zebrafish and seabream).

The concentration of DOX (30mg/kg) that we have used caused an increase by 15% larval mortality in zebrafish (Chapter 3). In addition, this concentration also prompted a significantly higher incidence of skeletal deformities as compared to other supplemented groups on both models, zebrafish (Chapter 3) and gilthead seabream (Chapter 4). In contrast, antioxidants (RES and MT) were able to rescue the adverse effects of DOX and reduce the incidence of deformities, increasing survival and mineralization on both fish models. Also, in both zebrafish and gilthead seabream the incidence of skeletal anomalies was mostly located on the caudal vertebrae and the caudal fin vertebrae regions, which is in agreement with our previous findings in other aquacultured species (419–424). The deformities in the caudal region can lead to secondary vertebral deformities as a result of insipid swimming behaviour that affects the growth and conversion index of the fish (420,425). Therefore, our data indicate that antioxidants (RES and MT) supplementation in the diet would be beneficial for counteracting DOX-induced bone deformities and favors the overall development of the fish.

Mineralization and differentiation of bone fully depend upon the osteoblast population, which are tightly regulated by osteocytes (426). In this thesis, DOX has shown decreased mineralization of the vertebrae compared to antioxidants (RES and MT) of zebrafish and seabream. We have shown that DOX inhibits murine osteoblast differentiation and mineralization (Chapter 2.1) and activates

osteoclast differentiation (Chapter 2.2). Here, the effect of antioxidants on the mineralization of the vertebrae can be the result of increased osteoblast proliferation and differentiation (Figure 2.1.2, Chapter 2).

Another factor responsible for the mineralization of bone is the mineral metabolism (428). The significant reduction of mineral content on zebrafish (Chapter 3) [calcium, phosphorus, sodium, potassium and magnesium] and gilthead seabream (Chapter 4) [calcium and phosphorus] on the DOX-supplemented groups implies that DOX alter overall mineral metabolism. Calcium and phosphorus are associated to bone mineralization, the inorganic phase of the bone is composed of calcium phosphates predominantly as hydroxyapatite [$Ca_{10}(PO_4)_6(OH)_2$] (432). Calcium homeostasis maintains the absorption of calcium and phosphorus from the intestine and maintain levels in bone (432). The lower calcium and phosphorus content suggests that overall bone metabolism is affected by DOX on both models (Chapter 3 and 4). Therefore, based on our results, we hypothesize that reduced capacity for mineral absorption leads to the lower bone mineral content observed, resulting in lower mineral deposition and contributes to the increased incidence of skeletal deformities observed in DOX supplemented zebrafish and seabream larvae.

An increase in ROS is one of the working mechanisms of action of DOX-induced toxicity (212,213,403,433). The increased ROS production results in lipid peroxidation, which is a crucial mechanism for DOX-induced toxicity (269–274). In both models (zebrafish and seabream), DOX supplemented alone or in combination significantly increased MDA concentration, similarly to what was previously observed on murine models (269–274). This signifies that antioxidants supplementation on feed would protect against ROS induced oxidative stress and lipid peroxidase (435,436).

Similar to the results obtained from *in vitro* osteoblast and osteoclast differentiation (Chapter 2), DOX significantly reduced *in vivo* expression (Chapter 3 and 4) of osteoblastic differentiation markers, bone Gla protein (Bgp or osteocalcin) and osterix/sp7. Osteocalcin plays an essential role in bone

mineralization due to its ability to bind with high-affinity bone hydroxyapatite (439). *Osterix* is an osteoblast specific transcriptional factor which regulates other differential genes during osteoblast differentiation (438). The mRNA expression of *osteocalcin* and *osterix* was significantly reduced by DOX, which might be the evidence for low mineralization of the vertebrae of zebrafish and seabream.

Although DOX is clinically widely used that causes cellular toxicity to various cells such as cardiomyocytes, osteoblasts and etc., a lot of effort to understand the precise mechanism of DOX-induced toxicity, that remains unclear. Previously, it was reported that DOX increases free radicals and increases oxidative stress of the cells and therefore induces toxicity (262–274). In this work (Chapter 2.1), we have identified a gene potentially responsible for DOX-induced bone impairment. We have found that Osteocrin (*Ostn*) a novel secretory peptide mRNA was highly downregulated by DOX. Recently, some studies have been performed to better understand the function of *Ostn* on bone growth, and showed that it plays a causal role in the regulation of bone growth (306–309). However, the receptor to which osteocrin binds on osteoblast is still unidentified (311). In our study during osteoblast differentiation, RES showed to increase Osteocrin expression as compared to DOX. Thus, these results suggests involvement of Osteocrin on DOX-induce bone impairment and its reversal by RES. However, further research is needed to find out the exact mechanism of osteocrin during DOX-induced bone impairment and its reversal.

5.1.1. Osteocrin as a marker for DOX-induced bone loss

Osteocrin is also known as musclin, is a novel secretory peptide released mainly from the bone and skeletal muscle, and plays critical role in regulating bone growth (306–309). We observed that osteocrin gene was downregulated on MC3T3 cells exposed to DOX and upregulated upon RES exposure. This suggests that osteocrin is involved for DOX-induced bone impairment and its reversal by RES. Similar to our results, osteocrin has been previously associated with DOX-induced cardiotoxicity in mice (316). In our experiments with zebrafish

and seabream, we observed that DOX supplementation impaired growth with reduction of the total length of larvae when compared to the RES supplemented group. We think that Osteocrin can be one of the responsible factors for this alteration, since it has previously been shown that Osteocrin facilitated long bone formation in mice (306) and elongation of bone in zebrafish (311). Furthermore, the data obtained from DOX-induced bone deformities on zebrafish and seabream and the reduction of *in vitro* ECM mineralization by DOX exposed VSa13 cells is suggestive of involvement of osteocrin on bone formation and remodelling process. Previously, it has been reported that endogenous osteocrin serves as a physiological regulator of endochondral ossification in mice. Osteocrin-deficient mice was shown to reduce osteoblastic activity on long bone and murine periosteal derived cell culture treated with osteocrin showed to increase differentiation and mineralization (480). It is still unclear how DOX downregulated and RES upregulated the osteocrin gene on osteoblastic cells. To the best of our knowledge, no studies have been published on the role of osteocrin on DOX-induced bone impairment. These results will further help to understand the mechanism of DOX-induced bone loss and would be helpful to overcome the DOX-induced toxicity.

5.1.2. Osteocrin; crosstalk between bone and other tissues

The role of osteocrin has been still not fully understood. Osteocrin, being a secretory protein expressed in bone and skeletal muscles (306–309), might facilitate the cross-talk between other tissues and bone. Chiba *et al.* have shown that osteocrin secreted from the heart and other tissues contributes to cranial development and chondroblast differentiation in zebrafish (311). Kanai *et al. 2007* (306) has reported that an increase in circulating osteocrin is directly proportional to skeleton overgrowth. DOX has shown to induce cardiotoxicity, nephrotoxicity, hepatotoxicity, etc. (404–408). In our study, we have found that bone deformities were increased, and bone mineralization was decreased on zebrafish and seabream on DOX supplementation.

Taking together all the results achieved, we hypothesize that the effect of DOX on muscles, heart, kidney, liver and brain can affect the expression of osteocrin, which will affect the crosstalk between bone and these tissues. On the other hand, antioxidants can also influence muscle, heart etc. to increase the production of osteocrin which facilitates bone development. We hypothesize that osteocrine has autocrine, endocrine and paracrine function on bone development.

Furthermore, osteocrin was found to regulate neuronal function and physical endurance (481,482). Osteocrin mRNA are also expressed in the human cortex. Ataman *et al.* has showed that *MEF2* regulates osteocrin expression and regulates dendritic growth in primate's cortex, playing a crucial role in the organization of dense primate neocortical networks (313). Previously, it was been reported that DOX induce locomotor activity and disturb circadian rhythm in mice (371,372), and during chemotherapy patients were associated with sleep disturbances, sleep efficiency and poor sleep quality (372,373). In this study, we also found that the locomotor activity and synchronicity of swimming behaviour on zebrafish was affected by DOX and was significantly reversed by antioxidants. With these results, it is suggested that DOX-induced cognitive function impairment is associated with osteocrin.

DOX is a known inducer of free radicals, and accumulation of free radicals (ROS and RNS) serves as mechanism for cytotoxicity through oxidative stress (262–274). DOX-induced toxicity is also associated with the disruption of calcium homeostasis due to the destruction of cell membrane permeability. Previously, it has been shown that DOX treatment affects several genes involving calcium signalling such as calcium/calmodulin-dependent protein kinase 2 (*CaMK II*). The calcium overload in cells results in oxidative stress, mitochondrial damage, structural deterioration of cells, apoptosis and death (305,483). In this study, during murine *in vitro* osteoblast differentiation (Chapter 2) we have shown that calcium signaling pathway markers (*Cacna1b, Htr2b, Mylk3, Plcd4* and *Tbxa2r*) were upregulated upon DOX treatment. The *Cacna1b* gene is associated calcium

channel complex in the brain (484,485). Which can be the result of disturb locomotory activity of zebrafish treated with DOX affecting the cognitive behaviour. However, RES treatment was able to significantly rescue the locomotory pattern.

In this study, DOX downregulated zinc finger protein 385c. Zinc finger proteins are also responsible for modulating the antioxidant status of the cell. DOX was shown to deteriorate the antioxidant defence of the cells leading to oxidative stress. The antioxidant genes such as cytochrome c oxidase subunit 6A2 (*Cox6a2*), acyl-Coenzyme A oxidase 2, branched-chain (*Acox2*) were also downregulated on DOX treatment which clearly signifies that DOX induces oxidative stress on osteoblast cells. Osteocrin had shown to reduce DOX-induced oxidative stress on the cardiomyocytes (316). In our study, the exposure of RES showed to upregulate osteocrin expression and to reverse DOX-induced toxicity in *in vitro* and *in vivo* experiments, therefore it is indicative that osteocrin is one of the responsible genes to the DOX-induced toxicity and involved in the reversal of its negative effects.

Furthermore, our findings suggest that Osteocrin has a new autocrine/ endocrine/ paracrine role in bone metabolism and is a significant molecular component in the crosstalk between bone and other tissues. This study has discovered a new component and opened up previously unknown territory in what regards the significance of Osteocrin in bone metabolism and crosstalk, both of which should be investigated further.

5.2. FUTURE PERSPECTIVES

This study was carried out under the scope of BIOMEDAQU project [H2020Marie Skłodowska-Curie Actions Innovative Training Network No 766347], with the research aim to create expertise combining research in skeletal biology of aquaculture fish species with that in biomedical models and humans. In this work, it is important to address both aspects of BIOMEDAQU projects i.e., aquaculture and biomedicine so that both fields will get the benefit from it.

5.2.1. Aquaculture

Skeletal anomalies are a persistent issue in farmed fish, compromising the welfare, performance, and quality of the aquaculture products. In aquaculture, nutrition plays an important role in the overall quality of the fish, however nutrition research in aqua culture comprise of some restrictions and limitations. With the advancement of the techniques related to transcriptomics, metabolomics and bioinformatics these limitations and issues can be addressed easily. In this research, we studied the effect of antioxidants and pro-oxidants on bone development. Here we tried to translate our *in vitro* results to both the osteocytic fish model zebrafish, and to the non-osteocytic model seabream. The results obtained from the *in vitro* studies were translated to zebrafish and those results obtained from zebrafish were translated to seabream, showing that the studies carried out on the *in vitro* models and zebrafish are possible to be translated to aquaculture produced fish. In this work, we studied the effect of antioxidants and pro-oxidants on zebrafish and seabream by performing nutritional trials using custom designed microdiets. The adverse effects of the pro-oxidant on bone were reversed by the antioxidants, however in future studies it should be considered that pro-oxidant and antioxidant molecules can influence a large number of molecular mechanisms associated with immunity, metabolism, transcriptional regulation and epigenetics, that can influence the overall performance and growth of the fish.

5.2.2. Biomedicine

Clinically DOX is used in a wide range of chemotherapy applications with the risk of causing or favoring the development of secondary osteoporosis. In this study, we counteracted DOX-induced bone impairment with antioxidants supplementation, performing experiments with both *in vitro* and *in vivo* models. The effects shown *in vitro* by DOX exposure were translated to *in vivo* models, establishing zebrafish as a valuable tool for research of the effects of these molecules on bone. In the present work, we have provided evidences for the role of osteocrin as a key molecular candidate for DOX-induced bone impairment and the reversal of DOX-induced effects by RES. Furthermore, our data indicates a new autocrine/paracrine role for Osteocrin which should be investigated further. In this work, we have shown that DOX-induced bone impairment can be reversed with antioxidant supplements which would be beneficial for preventing secondary osteoporosis during chemotherapy, however in future autocrine/paracrine role of Osteocrin should be studies using a better model. The mechanism by which RES increases Osteocrin should be studied in detail and RES can be introduced as a dietary supplement to prevent secondary osteoporosis.

APPENDIX

Supplementary Data

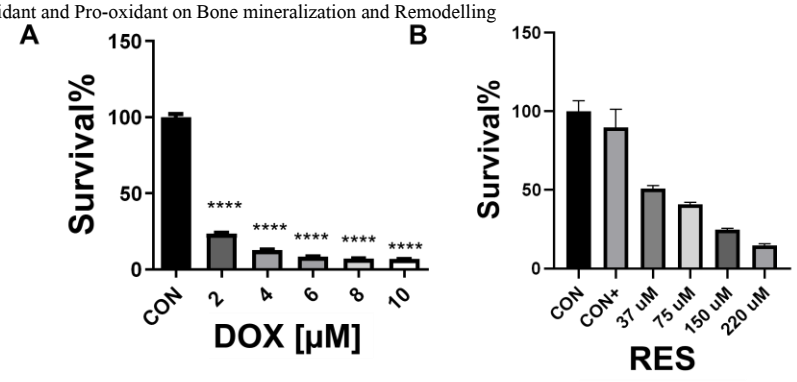

Supplementary figure 2.1.1: Cytotoxicity of the compounds on MC3T3-E1 cells. Doxorubicin (A), and Resveratrol (B). MC3T3-E1 cells were cultured for 3 days, DOX and RES treated for 3 days. XTT reagents were added to each well and the absorbance was read at 450 nm. One-way ANOVA, Tukey's multiple comparisons test, ns- P>0.05,

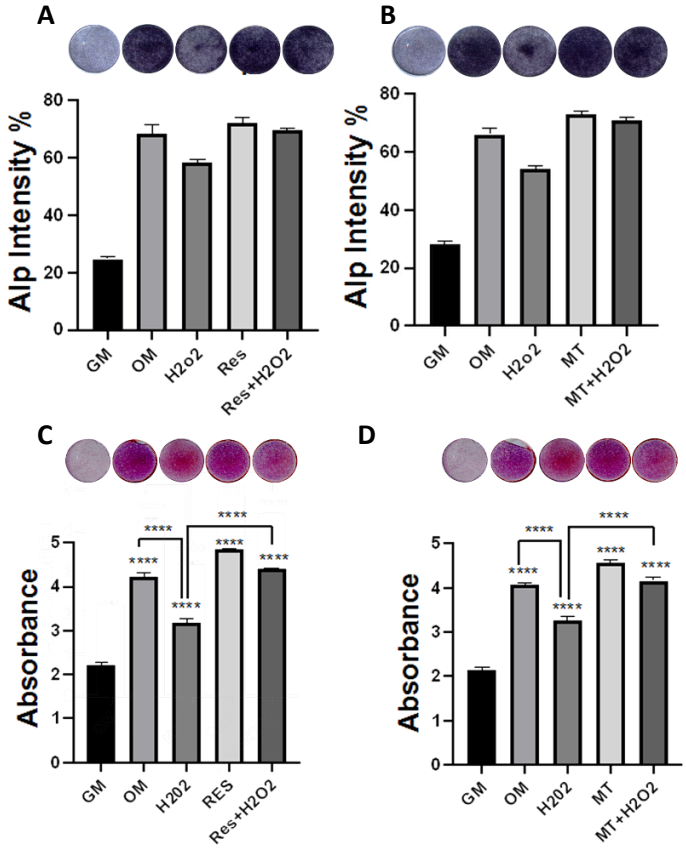

*- P≤0.05, **-P≤0.01, ***-P≤0.001, ****-P≤0.0001

Supplementary figure 2.1.2: Reversal effect of RES on H_2O_2-induced osteoblast differentiation and mineralization. MC3T3-E1 cells were cultured for 21 days in Differentiation media (ascorbic acid and β-Glycerophosphate) with RES, MitoTEMPO and H_2O_2 alone or together. (A, B) Alkaline phosphatase staining on 4th day. (C, D) Alizarin red-S staining done after 21 days of differentiation. One-way ANOVA, Tukey's multiple comparisons test, ns- P>0.05, *- P≤0.05, **-P≤0.01, ***-P≤0.001, ****-P≤0.0001.

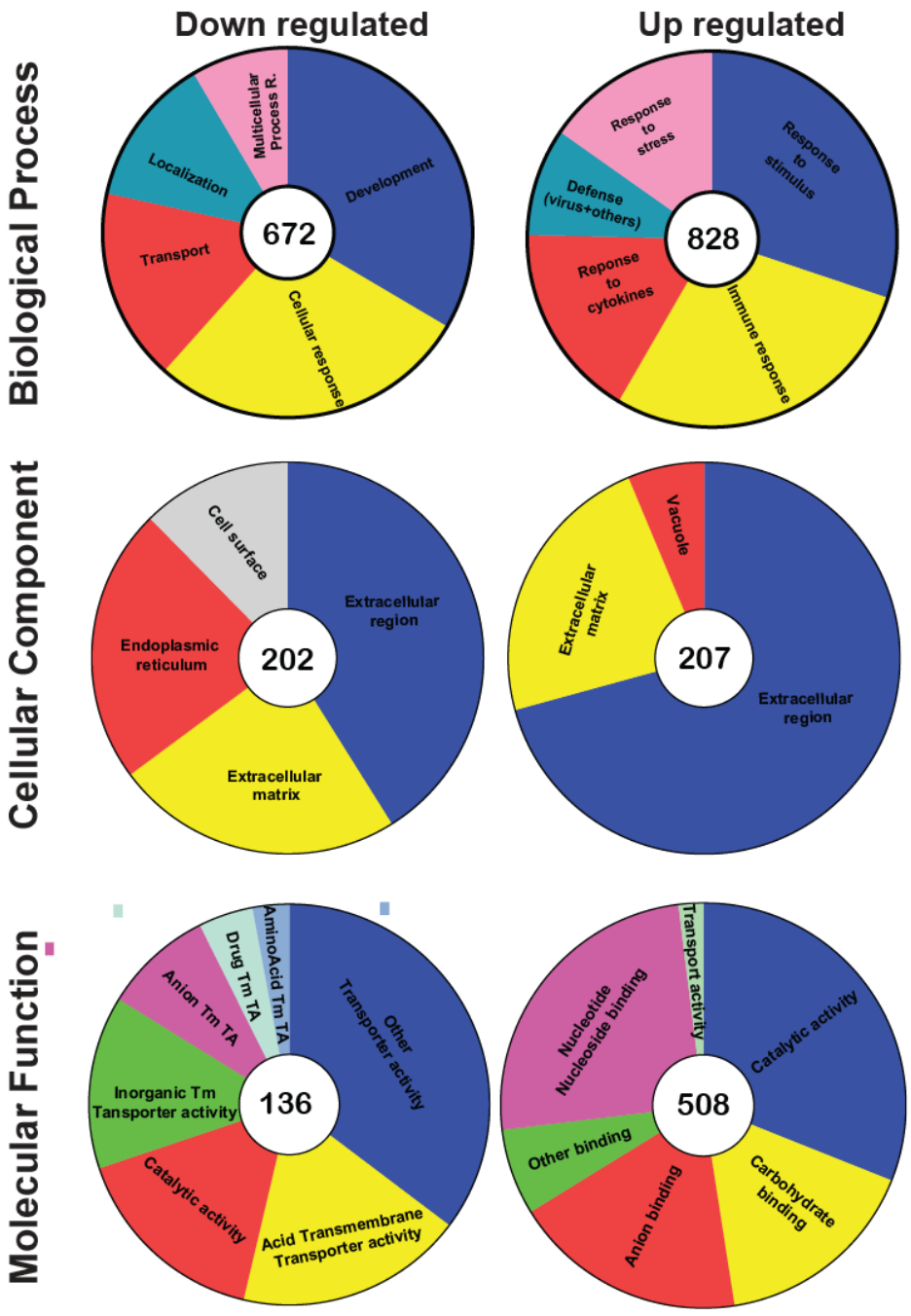

Supplementary figure 2.1.3: Pie chart representations of GO entries occurrence among the DEGs categorized as up-regulated and downregulated between DOX vs. CON. Pie charts represent biological processes, cellular components and molecular function GO entries occurrence among differentially expressed genes in doxorubicin vs control. The number in the center indicates the hit number. Additional information on GO definition is available in supplementary table 2.1.1-2.1.4.

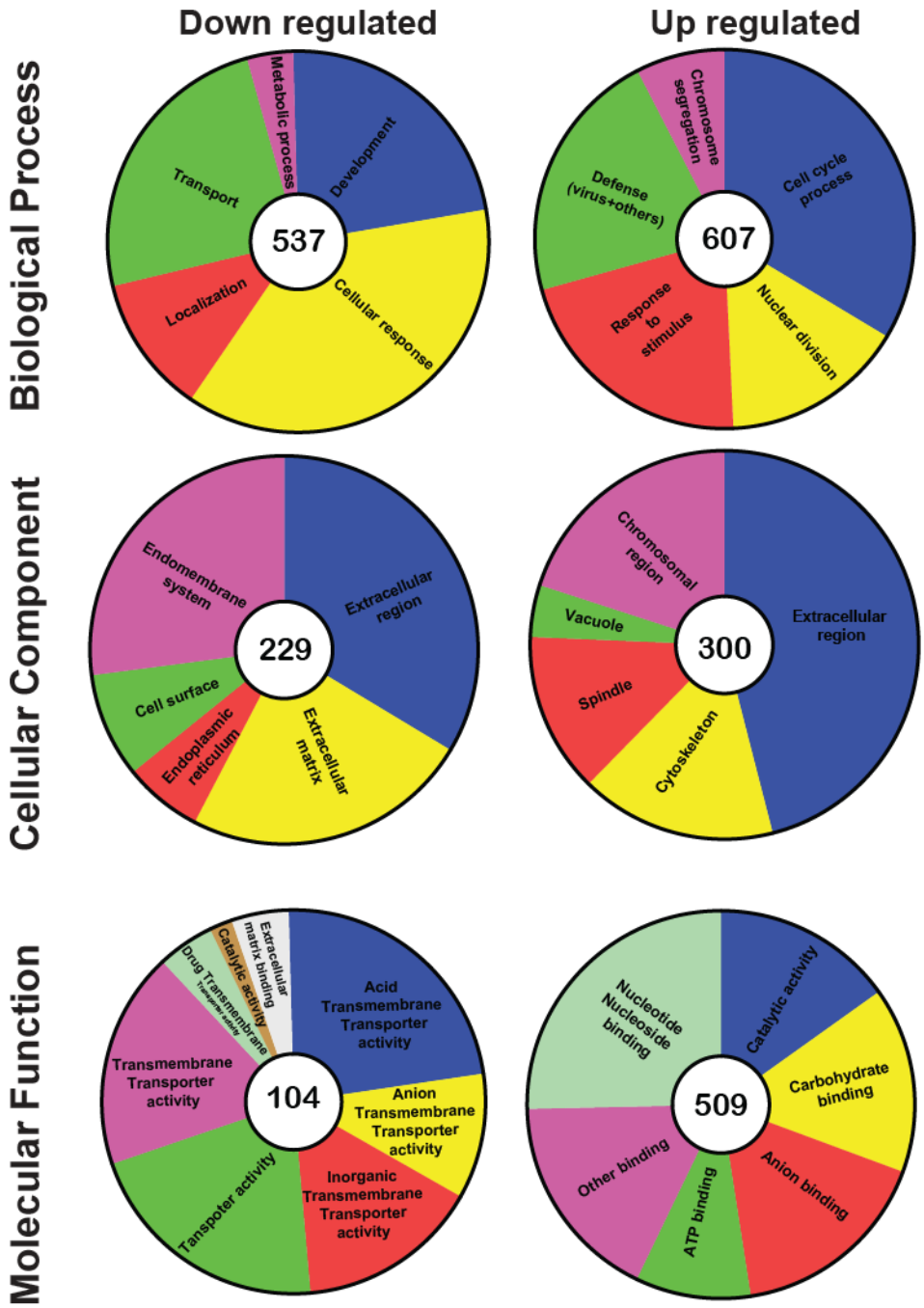

Supplementary figure 2.1.4: Pie chart representations of GO entries occurrence among the DEGs categorized as up-regulated and downregulated between DOX+RES vs. CON. Pie charts represents biological processes, cellular components and molecular function GO entries occurrence among differentially expressed genes in doxorubicin with resveratrol versus control. The number in the center indicates the hit number. Additional information on GO definition is available in supplementary table 2.1.1-2.1.4.

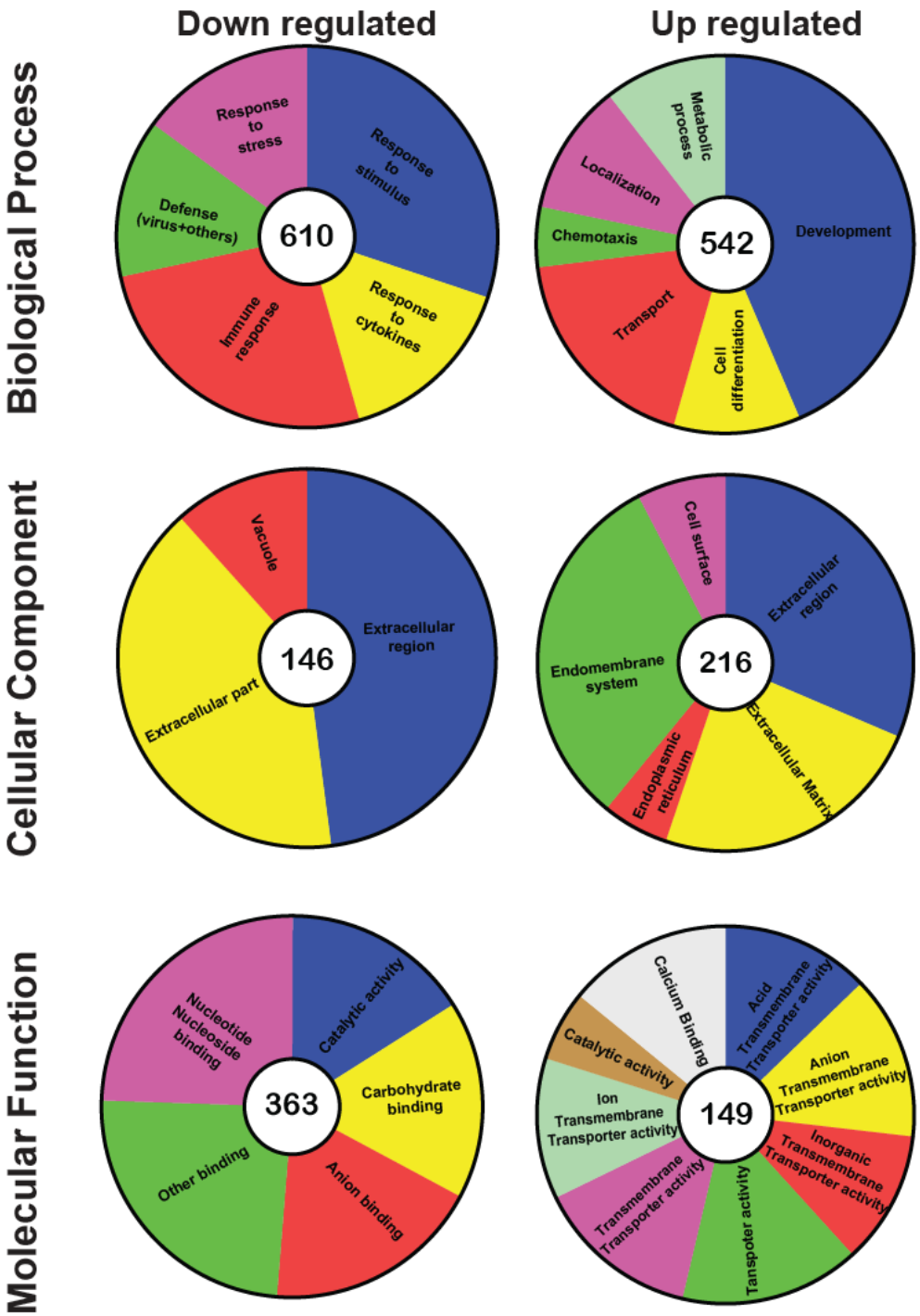

Supplementary figure 2.1.5: Pie chart representations of GO entries occurrence among the DEGs categorized as up-regulated and downregulated between RES vs DOX+RES. Pie charts represent biological processes, cellular components and molecular function GO entries occurrence among differentially expressed genes in resveratrol vs doxorubicin with resveratrol. The number in the center indicates the hit number. Additional information on GO definition is available in supplementary table 2.1.1-2.1.4.

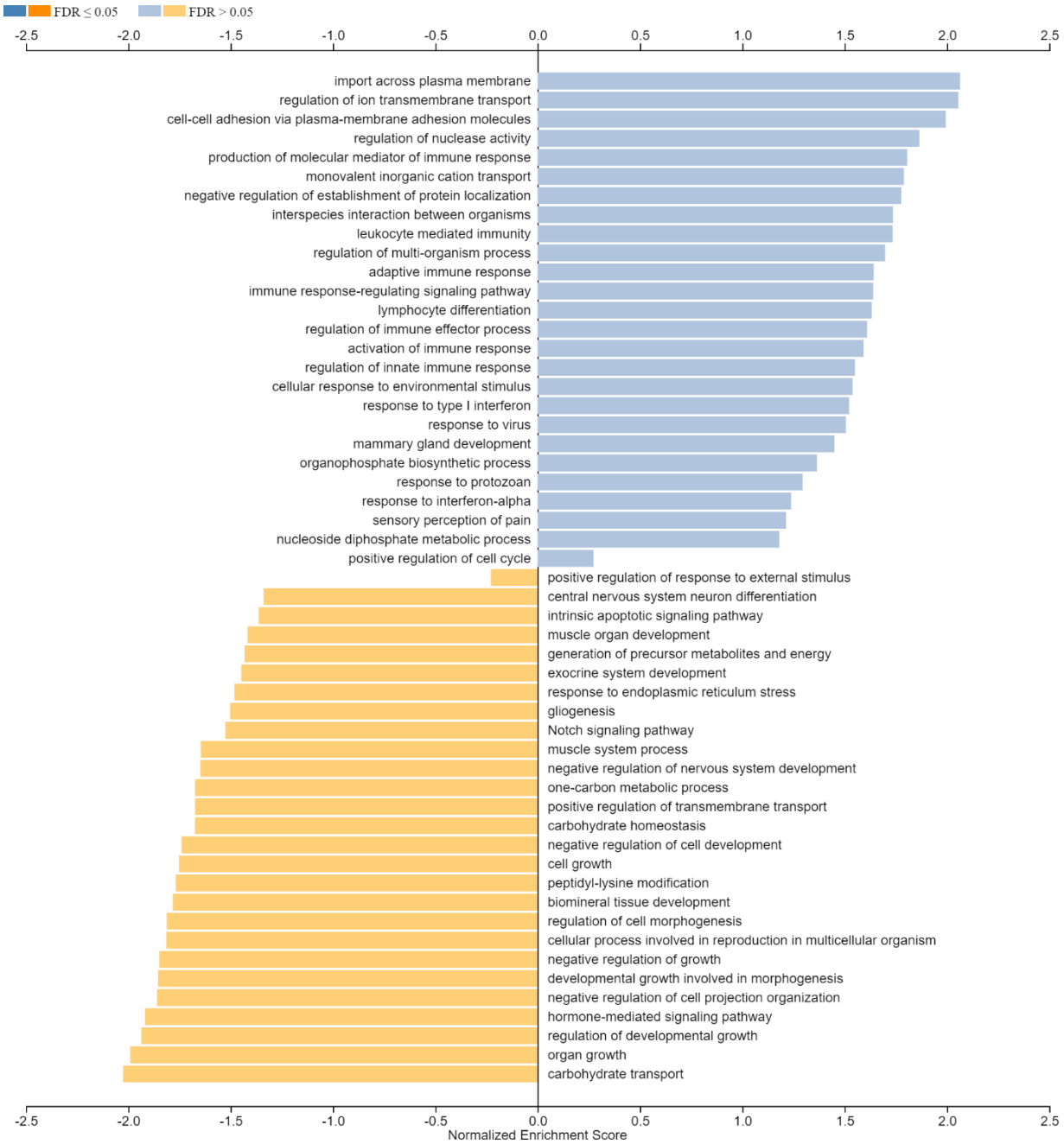

Supplementary figure 2.1.6: Over-represented biological processes between the DOX and CON. Gene set enrichment analysis was done in webGestalt/geneontology/biological process noRedundant. Top-ranked categories based on FDR were ranked for each positive and negative related category. Additional information on other comparison groups is available on supplementary figures 2.1.6-8 on biological processes and supplementary table 2.1.1-2.1.4.

Supplementary figure 2.1.7: Over-represented biological processes between the RES vs. DOX+RES. Gene set enrichment analysis was done in webGestalt/geneontology/biological process noRedundant. Top-ranked categories based on FDR were ranked for each positive and negative related category. Additional information on other comparison groups is available on supplementary figures 2.1.6-8 on biological processes and supplementary table 2.1.1-2.1.4.

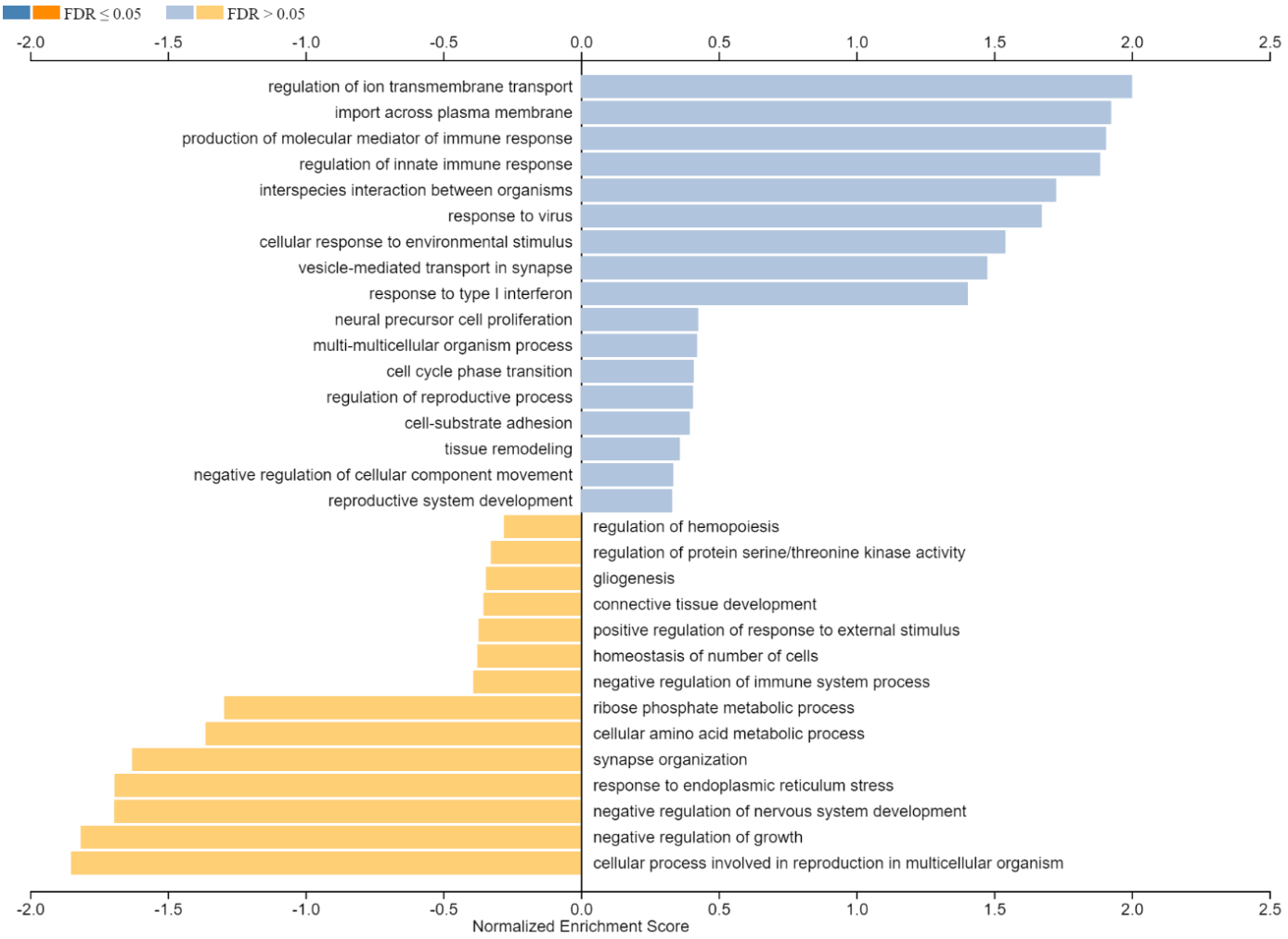

Supplementary figure 2.1.8: Over-represented biological processes between the DOX+RES and CON. Gene set enrichment analysis was done in webGestalt/geneontology/biological process noRedundant. Top-ranked categories based on FDR were ranked for each positive and negative related category. Additional information on other comparison groups is available on supplementary figures 2.1.6-8 on biological processes and supplementary table 2.1.1-2.1.4.

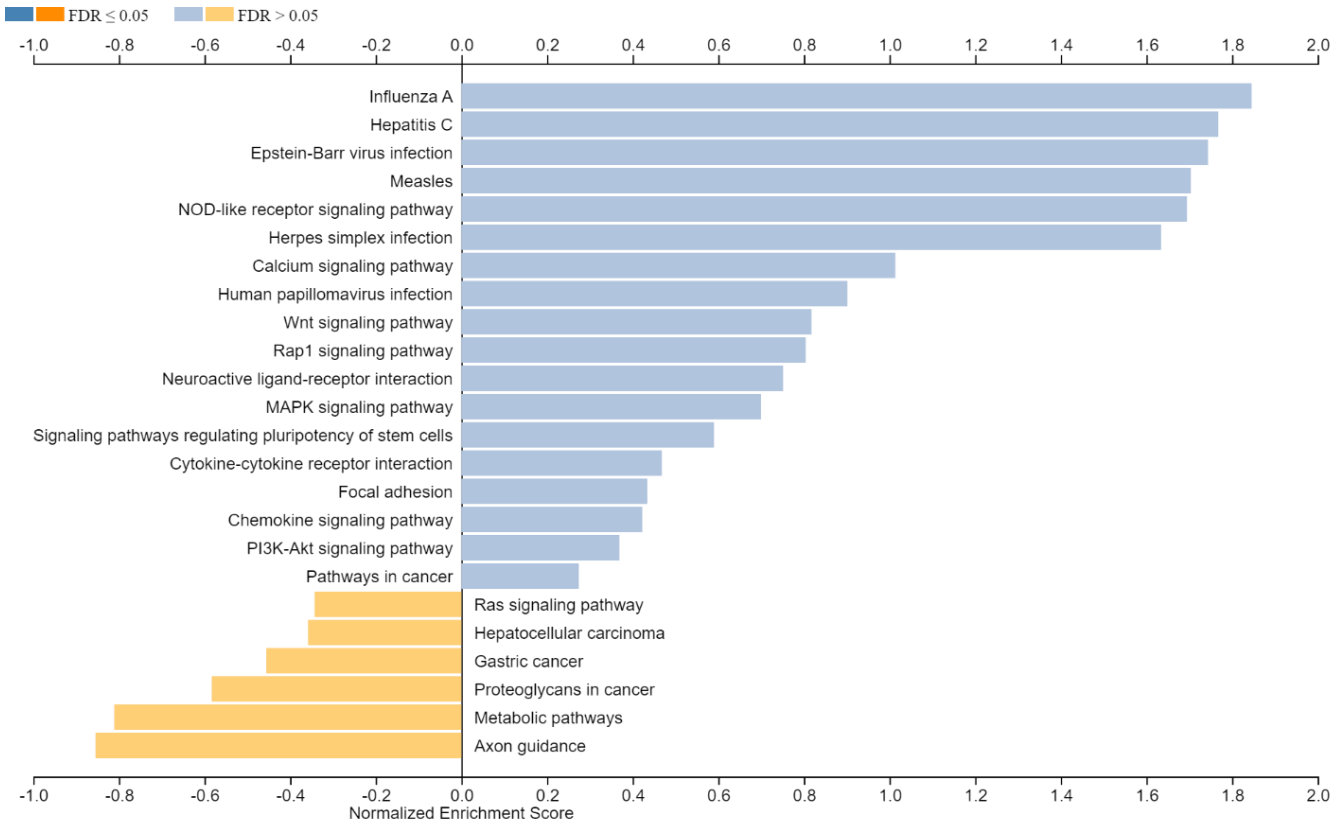

Supplementary figure 2.1.9: KEGG pathways analysis between DOX and CON. Gene set enrichment analysis was done in webGestalt/geneontology/biological process noRedundant. Top-ranked categories based on FDR were ranked for each positive and negative related category. Additional information on other comparison groups is available on supplementary figures 2.1.6-8 on biological processes and supplementary table 2.1.1-2.1.4.

Supplementary figure 2.1.10: KEGG pathways analysis between DOX and RES. Gene set enrichment analysis was done in webGestalt/geneontology/biological process noRedundant. Top-ranked categories based on FDR were ranked for each positive and negative related category. Additional information on other comparison groups is available on supplementary figures 2.1.6-8 on biological processes and supplementary table 2.1.1-2.1.4.

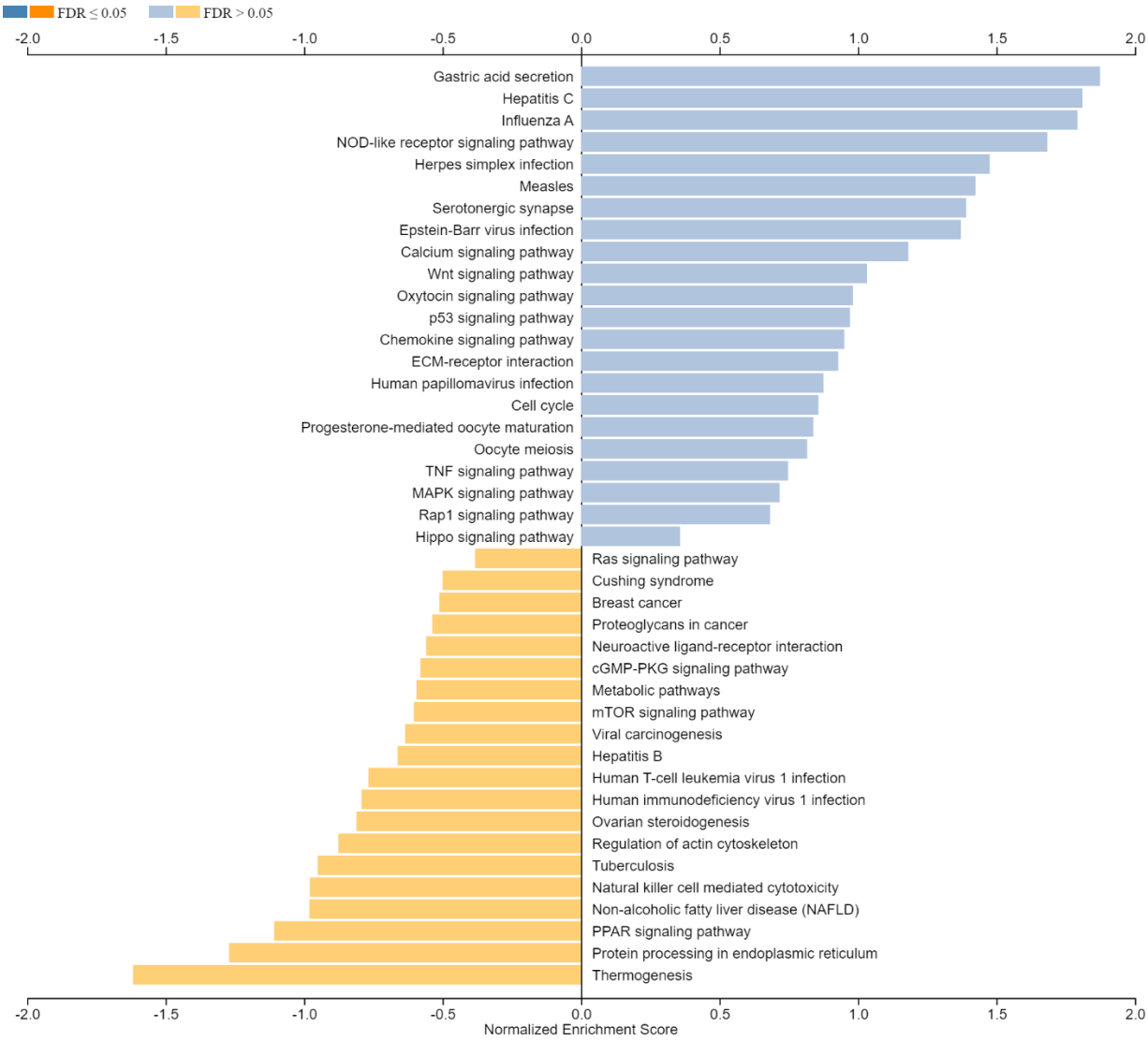

Supplementary figure 2.1.11: KEGG pathways analysis between DOX+RES and CON. Gene set enrichment analysis was done in webGestalt/geneontology/biological process noRedundant. Top-ranked categories based on FDR were ranked for each positive and negative related category. Additional information on other comparison groups is available on supplementary figures 2.1.6-8 on biological processes and supplementary table 2.1.1-2.1.4.

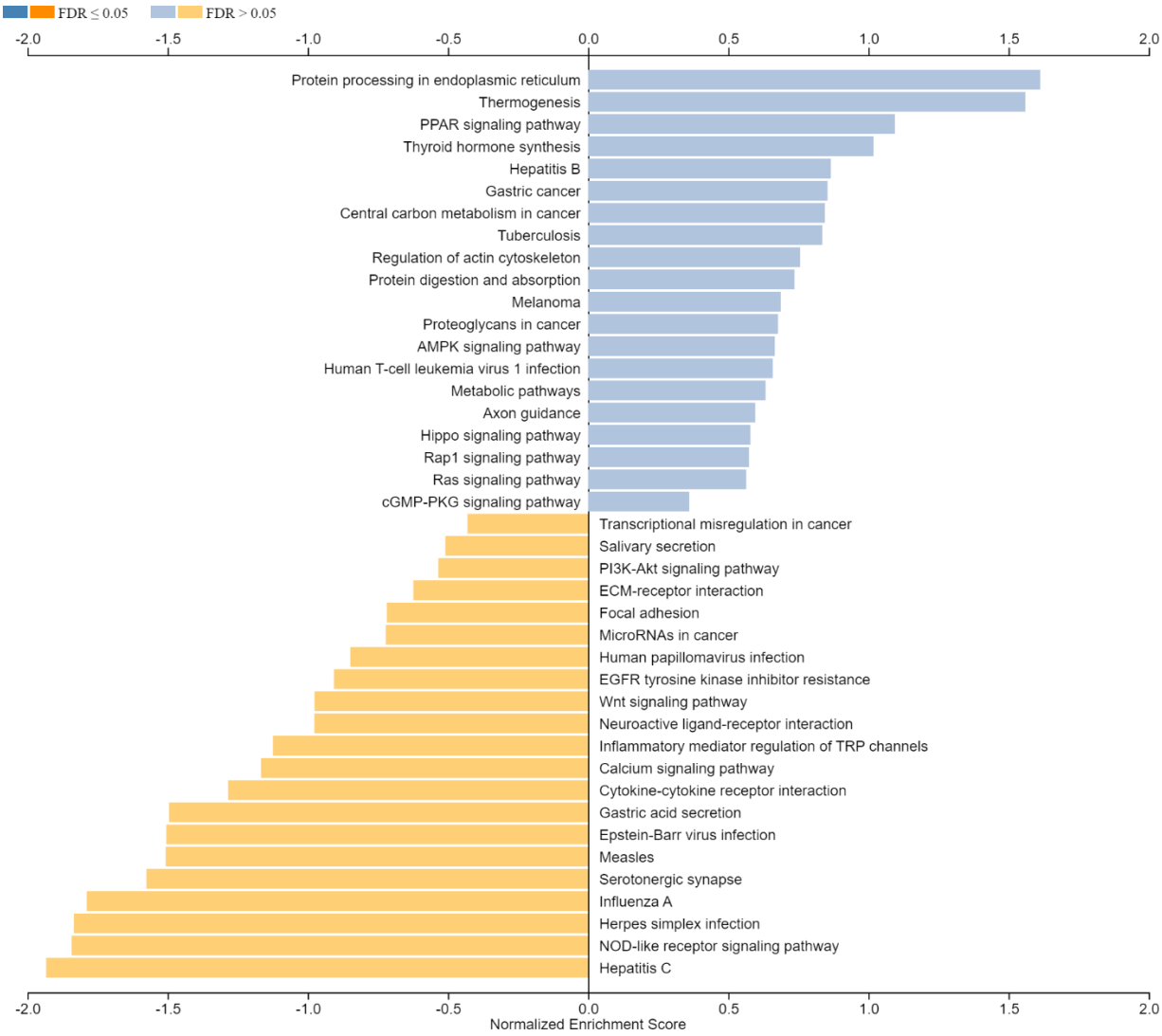

Supplementary figure 2.1.12: KEGG pathways analysis between RES and DOX+RES. Gene set enrichment analysis was done in webGestalt/geneontology/biological process noRedundant. Top-ranked categories based on FDR were ranked for each positive and negative related category. Additional information on other comparison groups is available on supplementary figures 2.1.6-8 on biological processes and supplementary table 2.1.1-2.1.4.

Supplementary Table 2.1.1

List of Up regulated and Down regulated GO-Biological function pathways among DEGs between DOX and CON

		DOX vs. CON		
GO-Biological Process	Symbol	Gene Name	Entrez Gene	Fold change
Positive regulation	*Slc6a4*	Slc 6 (neurotransmitter transporter, serotonin), 4	15567	6.5543
of cell cycle	*Tert*	telomerase reverse transcriptase	21752	6.086
	Rxfp3	relaxin family peptide receptor 3	239336	4.8627
	Cd28	CD28 antigen	12487	3.5311
	E2f8	E2F transcription factor 8	108961	3.0764
	Igf1	insulin-like growth factor 1	16000	2.9608
	Orc1	origin recognition complex, subunit 1	18392	2.7517
	Pidd1	p53 induced death domain protein 1	57913	2.6938
	Fap	fibroblast activation protein	14089	2.5865
	Ccn2	undefined	14219	2.5717
	Ccne1	cyclin E1	12447	2.4414
	Nusap1	nucleolar and spindle associated protein 1	108907	2.3887
	Cdc6	cell division cycle 6	23834	2.1942
	Kif23	kinesin family member 23	71819	2.1343
	Cenpe	centromere protein E	229841	2.0366
	Fam83d	family with sequence similarity 83, member D	71878	2.0033
	Apex1	apurinic/apyrimidinic endonuclease 1	11792	-2.0442
	Tfap4	transcription factor AP4	83383	-2.0667
	Wnt5a	wingless-type MMTV integration site family,5A	22418	-2.0749
	Eif4ebp1	eukaryotic translation initiation factor 4E-1	13685	-2.1416
	Rab11fip4	RAB11 family interacting protein 4 (class II)	268451	-2.1995
	Smoc2	SPARC related modular calcium binding 2	64074	-2.6398
	Gper1	G protein-coupled estrogen receptor 1	76854	-3.0107
	Calr	calreticulin	12317	-3.2058
	Fzd9	frizzled class receptor 9	14371	-3.5054
	Asns	asparagine synthetase	27053	-3.9442
Regulation of	*Oas1a*	2'-5' oligoadenylate synthetase 1A	246730	11.0879
multi-organism process	*Oas1g*	2'-5' oligoadenylate synthetase 1G	23960	119.4
	Oasl1	2'-5' oligoadenylate synthetase-like 1	231655	16.9074
	Rsad2	radical S-adenosyl methionine domain containing 2	58185	137.4194
Lymphocyte differentiation	*Nfam1*	Nfat activating molecule with ITAM motif 1	74039	20.9312
	Rsad2	radical S-adenosyl methionine domain containing 2	58185	137.4194
Regulation of G protein-	*Ccl5*	chemokine (C-C motif) ligand 5	20304	5.3491

Up regulated

coupled receptor	*Htr2b*	5-hydroxytryptamine (serotonin) receptor 2B	15559	10.0497
	Ptgdr2	prostaglandin D2 receptor 2	14764	4.1031
Cell growth	*Ostn*	osteocrin	239790	-239.9006
	Pi16	peptidase inhibitor 16	74116	-53.831
	Tfcp2l1	transcription factor CP2-like 1	81879	-34.9473
Positive regulation of	*Artn*	artemin	11876	-3.1208
response to external	*Calr*	calreticulin	12317	-3.2058
stimulus	*Cd74*	CD74 antigen (MHCII antigen-associated)	16149	-2.0832
	F7	coagulation factor VII	14068	-4.7061
	Fcer1g	Fc receptor, IgE, high affinity I, gamma polypeptide	14127	-2.8664
	Lbp	lipopolysaccharide binding protein	16803	-3.4387
	Ntrk3	neurotrophic tyrosine kinase, receptor, type 3	18213	-2.3487
	Pgf	placental growth factor	18654	-2.2545
	Smoc2	SPARC related modular calcium binding 2	64074	-2.6398
	Wnt5a	wingless-type MMTV integration site family, 5A	22418	-2.0749
Notch signaling pathway	*Chac1*	ChaC, cation transport regulator 1	69065	-4.1031
	Nrip2	nuclear receptor interacting protein 2	60345	-20.8248
	Timp4	tissue inhibitor of metalloproteinase 4	110595	-11.5684
Carbohydrate transport	*Klf15*	Kruppel-like factor 15	66277	-110.4957
	Ostn	osteocrin	239790	-239.9006
	Trib3	tribbles pseudokinase 3	228775	-18.125
Intrinsic apoptotic signaling pathway	*Chac1*	ChaC, cation transport regulator 1	69065	-4.1031
	Ddit3	DNA-damage inducible transcript 3	13198	-4.1909
	Trib3	tribbles pseudokinase 3	228775	-18.125

Down regulated

Supplementary Table 2.1.2

List of Up regulated and Down regulated GO-Biological function pathways among DEGs between DOX and RES

DOX vs. RES

GO-Biological Process	Symbol	Gene Name	Entrez Gene	Fold change
Regulation of nuclease activity	*Oas1a*	2'-5' oligoadenylate synthetase 1A	246730	7.4907
	Oas1b	2'-5' oligoadenylate synthetase 1B	23961	5.9884
	Oas1g	2'-5' oligoadenylate synthetase 1G	23960	119.6542
	Oas2	2'-5' oligoadenylate synthetase 2	246728	19.1058
	Oas3	2'-5' oligoadenylate synthetase 3	246727	5.4955
	Oasl1	2'-5' oligoadenylate synthetase-like 1	231655	6.2722
	Oasl2	2'-5' oligoadenylate synthetase-like 2	23962	5.888
Response to type I interferon	*Irf7*	interferon regulatory factor 7	54123	3.3175
	Isg15	ISG15 ubiquitin-like modifier	100038882	4.3793
	Mx2	MX dynamin-like GTPase 2	17858	5.219
	Nlrc5	NLR family, CARD domain containing 5	434341	3.0295
	Oas2	2'-5' oligoadenylate synthetase 2	246728	19.1058
	Zbp1	Z-DNA binding protein 1	58203	11.3983
Response to interferon-beta	*F830016B08Rik*	RIKEN cDNA F830016B08 gene	240328	10.3209
	Gbp3	guanylate binding protein 3	55932	6.154
	Gm4841	predicted gene 4841	225594	6.9036
	Gm4951	predicted gene 4951	240327	7.4305
	Ifi203	interferon activated gene 203	15950	3.214
	Ifi205	interferon activated gene 205	226695	10.8431
	Ifi207	interferon activated gene 207	226691	4.1076
	Ifi208	interferon activated gene 208	100033459	5.9562
	Ifit1	interferon-induced protein with tetratricopeptide 1	15957	6.2856
	Ifit1bl1	interferon induced protein with tetratricpeptide 1B-1	667373	4.7777
	Ifit3	interferon-induced protein with tetratricopeptid 3	15959	4.2243
	Ifit3b	interferon-induced protein with tetratricopeptide 3B	667370	6.5565
	Igtp	interferon gamma induced GTPase	16145	3.2046
	Iigp1	interferon inducible GTPase 1	60440	9.3116
	Tgtp2	T cell specific GTPase 2	100039796	3.3547
Regulation of multi-organism process	*Ccl5*	chemokine (C-C motif) ligand 5	20304	4.8721
	Mx2	MX dynamin-like GTPase 2	17858	5.219
	Oas1a	2'-5' oligoadenylate synthetase 1A	246730	7.4907

Up regulated

	Oas1b	2'-5' oligoadenylate synthetase 1B	23961	5.9884
	Oas1g	2'-5' oligoadenylate synthetase 1G	23960	119.6542
	Oas3	2'-5' oligoadenylate synthetase 3	246727	5.4955
	Oasl1	2'-5' oligoadenylate synthetase-like 1	231655	6.2722
	Oasl2	2'-5' oligoadenylate synthetase-like 2	23962	5.888
	Ptgdr2	prostaglandin D2 receptor 2	14764	5.221
	Rsad2	radical S-adenosyl methionine domain containing2	58185	15.493
Stem cell differentiation	*Htr2b*	5-hydroxytryptamine (serotonin) receptor 2B	15559	19.0196
Regulation of cell division	*Htr2b*	5-hydroxytryptamine (serotonin) receptor 2B	15559	19.0196
	Rxfp3	relaxin family peptide receptor 3	239336	8.2572
	Txnip	thioredoxin interacting protein	56338	10.7851
I-kappaB kinase/NF-kappaB	*Htr2b*	5-hydroxytryptamine (serotonin) receptor 2B	15559	19.0196
signaling	*Tnfsf10*	tumor necrosis factor (ligand) superfamily,10	22035	14.197
G protein-coupled receptor	*Htr2b*	5-hydroxytryptamine (serotonin) receptor 2B	15559	19.0196
signaling pathway	*Mc1r*	melanocortin 1 receptor	17199	5.0254
	Ptgdr2	prostaglandin D2 receptor 2	14764	5.221
	Ptger4	prostaglandin E receptor 4 (subtype EP4)	19219	4.5668
circulatory system process	*Bdkrb1*	bradykinin receptor, beta 1	12061	6.5761
	Cbs	cystathionine beta-synthase	12411	4.9996
	Htr2b	5-hydroxytryptamine (serotonin) receptor 2B	15559	19.0196
	Kcnj2	potassium inwardly-rectifying channel, subfamily J2	16518	3.4651
	Mrvi1	MRV integration site 1	17540	3.2394
	Mylk3	myosin light chain kinase 3	213435	3.823
	Sgcg	sarcoglycan, gamma (dystrophin-associated glycoprotei)	24053	3.9994
	Slc6a4	Slc 6 (neurotransmitter transporter, serotonin), 4	15567	13.0444

Up regulated

Down-regulated				
ossification	*Ostn*	osteocrin	239790	-133.2403
Negative regulation of	*Bst2*	bone marrow stromal cell antigen 2	69550	2.5825
immune system process	*Ccn3*	cellular communication network factor 3	18133	2.0095
	Cd300a	CD300A molecule	217303	-2.8193
	Cd74	CD74 antigen (MHC II antigen-associated)	16149	-2.0443
	Gper1	G protein-coupled estrogen receptor 1	76854	-3.6427
	Hspa9	heat shock protein 9	15526	-3.0741
	Igf1	insulin-like growth factor 1	16000	2.9654
	Il1rl1	interleukin 1 receptor-like 1	17082	2.5265
	Il33	interleukin 33	77125	2.6049

Down regulated

	Kitl	kit ligand	17311	2.2572
	Lag3	lymphocyte-activation gene 3	16768	-5.4915
	Nlrc3	NLR family, CARD domain containing 3	268857	2.6285
	Nlrc5	NLR family, CARD domain containing 5	434341	3.0295
	Parp14	poly (ADP-ribose) polymerase family, member 14	547253	2.2493
	Prdm16	PR domain containing 16	70673	-4.1439
	Ptk2b	PTK2 protein tyrosine kinase 2 beta	19229	2.2445
	Siglecg	sialic acid binding Ig-like lectin G	243958	3.0168
	Sox11	SRY (sex determining region Y)-box 11	20666	-2.4404
	Spn	sialophorin	20737	-2.8381
	Tnfrsf21	tumor necrosis factor receptor superfamily, 21	94185	2.9572
Notch signaling pathway	*Chac1*	ChaC, cation transport regulator 1	69065	-4.1197
	Nrip2	nuclear receptor interacting protein 2	60345	-19.7459
	Timp4	tissue inhibitor of metalloproteinase 4	110595	-12.4291
Carbohydrate transport	*Klf15*	Kruppel-like factor 15	66277	-182.5322
	Ostn	osteocrin	239790	-133.2403
	Trib3	tribbles pseudokinase 3	228775	-18.4655
Cell growth	*Ostn*	osteocrin	239790	-133.2403
	Pi16	peptidase inhibitor 16	74116	-53.9697
	Tfcp2l1	transcription factor CP2-like 1	81879	-31.43483172
Biomineral tissue development	*Ostn*	osteocrin	239790	-133.2403
	Klf15	Kruppel-like factor 15	66277	-182.5322

Down regulated

Supplementary Table 2.1.3

List of Up regulated and Down regulated GO-Biological function pathways among DEGs between RES and DOX+RES

RES vs. DOX+RES

GO-Biological Process	Symbol	Gene Name	Entrez Gene	Fold change
Epithelial cell development	*Pdzd7*	PDZ domain containing 7	100503041	4.1056
	Sox8	SRY (sex determining region Y)-box 8	20681	9.9209
	Tfcp2l1	transcription factor CP2-like 1	81879	17.1662
Regulation of leukocyte activation	*Cd28*	CD28 antigen	12487	-2.9792
	Cd74	CD74 antigen (MHC, class II antigen-associated)	16149	2.2331
	Egr3	early growth response 3	13655	2.5074
	Enpp3	ectonucleotide pyrophosphatase/phosphodiesterase 3	209558	-2.1755
	Gper1	G protein-coupled estrogen receptor 1	76854	2.3195
	Igf1	insulin-like growth factor 1	16000	-2.6712
	Il1rl1	interleukin 1 receptor-like 1	17082	-2.3312
	Il33	interleukin 33	77125	-2.7006
	Ptafr	platelet-activating factor receptor	19204	-2.4981
	Siglecg	sialic acid binding Ig-like lectin G	243958	-2.848
	Sox11	SRY (sex determining region Y)-box 11	20666	2.8309
	Spn	sialophorin	20737	3.742
	Tfrc	transferrin receptor	22042	2.5482
	Tnfrsf21	tumor necrosis factor receptor superfamily, 21	94185	-2.4346
Nervous system development	*Artn*	artemin	11876	2.8612
	Egr2	early growth response 2	13654	2.462
	Egr3	early growth response 3	13655	2.5074
	Lgi4	leucine-rich repeat LGI family, member 4	243914	2.918
	Ntrk3	neurotrophic tyrosine kinase, receptor, type 3	18213	2.392
	Sox8	SRY (sex determining region Y)-box 8	20681	9.9209
Drug transport	*Abcb1a*	ATP-binding cassette, sub-family B (MDR/TAP) 1A	18671	2.3263
	Aqp5	aquaporin 5	11830	-2.2065
	Ptger4	prostaglandin E receptor 4 (subtype EP4)	19219	-3.3248
	Slc17a8	Slc 17 (Na-dependent inorganic phosphate)8	216227	-3.8208
	Slc1a2	Slc 1(glial high affinity glutamate transporter)2	20511	-2.0219
	Slc6a9	Slc 6 (neurotransmitter transporter, glycine), member 9	14664	4.0705
	Slc7a11	Slc7 (cationic amino acid transporter), member 11	26570	3.2099
	Syt13	synaptotagmin XIII	80976	-2.0598
Regulation of cellular amide metabolic process	*Calr*	calreticulin	12317	3.5682
	Slc7a11	Slc 7 (cationic amino acid transporter, y+ system), member 11	26570	3.2099

Up regulated

Biomineralization	*Ostn*	osteocrin	239790	137.9429
Developmental growth	*Ostn*	osteocrin	239790	137.9429
involved in morphogenesis	*Pi16*	peptidase inhibitor 16	74116	16.2249
	Sema6d	sema domain and cytoplasmic domain (semaphorin) 6D	214968	9.6286
Regulation of hemopoiesis	*Cd28*	CD28 antigen	12487	-2.9792
	Cd74	CD74 antigen (MHC, class II antigen-associated)	16149	2.2331
	Cyp26b1	cytochrome P450, family 26, b-1	232174	-4.6705
	Egr3	early growth response 3	13655	2.5074
	Hspa9	heat shock protein 9	15526	2.6284
	Isg15	ISG15 ubiquitin-like modifier	100038882	-3.0493
	P4htm	prolyl 4-hydroxylase, transmembrane (ER)	74443	2.0315
	Prdm16	PR domain containing 16	70673	4.6821
	Ptk2b	PTK2 protein tyrosine kinase 2 beta	19229	-2.1781
	Siglec15	sialic acid binding Ig-like lectin 15	620235	-2.5765

Up regulated

Down-regulated				
G protein-coupled receptor	*Htr2b*	5-hydroxytryptamine (serotonin) receptor 2B	15559	-13.7491
signaling pathway	*Mc1r*	melanocortin 1 receptor	17199	-4.865
	Ptgdr2	prostaglandin D2 receptor 2	14764	-5.377
Response to wounding	*Duox2*	dual oxidase 2	214593	-5.4461
	Serpind1	serine (or cysteine) peptidase inhibitor, clade D-1	15160	-8.146
Negative regulation of	*Fmn2*	formin 2	54418	-10.2968
catabolic process	*Hp*	haptoglobin	15439	-6.4761
	Htr2b	5-hydroxytryptamine (serotonin) receptor 2B	15559	-13.7491
Cytokine-mediated	*Ccl8*	chemokine (C-C motif) ligand 8	20307	-6.3688
signaling pathway	*Csf2rb*	colony stimulating factor 2 receptor, beta,	12983	-11.236
	Duox2	dual oxidase 2	214593	-5.4461
	Iigp1	interferon inducible GTPase 1	60440	-6.4999
	Oas2	2'-5' oligoadenylate synthetase 2	246728	-13.7276
	Zbp1	Z-DNA binding protein 1	58203	-6.7576
Regulation of nuclease	*Oas1a*	2'-5' oligoadenylate synthetase 1A	246730	-5.5679
activity	*Oas1b*	2'-5' oligoadenylate synthetase 1B	23961	-5.993
	Oas2	2'-5' oligoadenylate synthetase 2	246728	-13.7276
	Oas3	2'-5' oligoadenylate synthetase 3	246727	-4.3902
	Oasl2	2'-5' oligoadenylate synthetase-like 2	23962	-3.7298

Down regulated

Response to interferon-gamma	*Ccl7*	chemokine (C-C motif) ligand 7	20306	-2.6396
	Ccl8	chemokine (C-C motif) ligand 8	20307	-6.3688
	Gbp10	guanylate-binding protein 10	626578	-3.5493
	Gbp2	guanylate binding protein 2	14469	-2.2683
	Gbp3	guanylate binding protein 3	55932	-3.7546
	Gbp4	guanylate binding protein 4	17472	-2.4354
	Gbp6	guanylate binding protein 6	100702	-2.5823
	Gbp7	guanylate binding protein 7	229900	-3.1409
	Gbp9	guanylate-binding protein 9	236573	-3.3542
	Nlrc5	NLR family, CARD domain containing 5	434341	-2.8844
	Tgtp2	T cell specific GTPase 2	100039796	-3.0692
Response to interferon-beta	*Gbp3*	guanylate binding protein 3	55932	-3.7546
	Gm4951	predicted gene 4951	240327	-5.4793
	Ifi205	interferon activated gene 205	226695	-6.7837
	Ifi207	interferon activated gene 207	226691	-3.4712
	Ifit1	interferon-induced protein with tetratricopeptide 1	15957	-3.972
	Ifit1bl1	interferon induced protein with tetratricpeptide 1B like 1	667373	-5.7014
	Ifit3	interferon-induced protein with tetratricopeptide 3	15959	-3.2073
	Ifit3b	interferon-induced protein with tetratricopeptide 3B	667370	-4.0199
	Iigp1	interferon inducible GTPase 1	60440	-6.4999
	Tgtp2	T cell specific GTPase 2	100039796	-3.0692
Regulation of cell division	*Htr2b*	5-hydroxytryptamine (serotonin) receptor 2B	15559	-13.7491
	Rxfp3	relaxin family peptide receptor 3	239336	-6.1584
	Txnip	thioredoxin interacting protein	56338	-9.0166

Down regulated

Supplementary Table 2.1.4

List of Up regulated and Down regulated GO-Biological function pathways among DEGs between DOX+RES and CON

DOX+RES vs. CON

GO-Biological Process	Symbol	Gene Name	Entrez Gene	Fold change
Negative regulation of cellular component movement	*Adgrg1*	adhesion G protein-coupled receptor G1	14766	2.237
	Angpt4	angiopoietin 4	11602	2.4881
	Bst2	bone marrow stromal cell antigen 2	69550	2.0663
	Cd300a	CD300A molecule	217303	-2.16
	Fas	Fas (TNF receptor superfamily member 6)	14102	2.1112
	Il33	interleukin 33	77125	2.4364
	Nrg1	neuregulin 1	211323	2.3408
	Pdgfb	platelet derived growth factor, B polypeptide	18591	-2.2093
	Ptger4	prostaglandin E receptor 4 (subtype EP4)	19219	2.514
	Sema3e	sema domain, immunoglobulin domain (semaphorin) 3E	20349	5.8409
	Sema7a	sema domain, immunoglobulin domain, GPI anchor7A	20361	-2.2517
	Slit1	slit guidance ligand 1	20562	4.5199
	Sp100	nuclear antigen Sp100	20684	2.366
	Tmeff2	transmembrane protein with EGF-like, follistatin-like 2	56363	-2.0494
Neural precursor cell proliferation	*Adgrg1*	adhesion G protein-coupled receptor G1	14766	2.237
	Aspm	abnormal spindle microtubule assembly	12316	2.3978
	Igf1	insulin-like growth factor 1	16000	2.6708
	Slc6a4	Slc 6 (neurotransmitter transporter, serotonin)4	15567	5.8574
	Wnt7b	wingless-type MMTV integration site family, 7B	22422	3.1231
Reproductive system development	*Brip1*	BRCA1 interacting protein C-terminal helicase 1	237911	2.6007
	E2f8	E2F transcription factor 8	108961	3.2515
	Esr2	estrogen receptor 2 (beta)	13983	2.9657
	Hoxb13	homeobox B13	15408	8.0126
	Igf1	insulin-like growth factor 1	16000	2.6708
	Nanog	Nanog homeobox	71950	2.5208
	Ptger4	prostaglandin E receptor 4 (subtype EP4)	19219	2.514
	Wnt7b	wingless-type MMTV integration site family, 7B	22422	3.1231
Negative regulation of locomotion	*Adgrg1*	adhesion G protein-coupled receptor G1	14766	2.237
	Angpt4	angiopoietin 4	11602	2.4881
	Bst2	bone marrow stromal cell antigen 2	69550	2.0663
	Cd300a	CD300A molecule	217303	-2.16
	Fas	Fas (TNF receptor superfamily member 6)	14102	2.1112
	Il33	interleukin 33	77125	2.4364
	Nrg1	neuregulin 1	211323	2.3408

Up regulated

	Pdgfb	platelet derived growth factor, B polypeptide	18591	-2.2093
	Ptger4	prostaglandin E receptor 4 (subtype EP4)	19219	2.514
	Sema3e	sema domain, immunoglobulin domain-3E	20349	5.8409
	Sema7a	sema domain, immunoglobulin domain,GPI -anchor-7A	20361	-2.2517
	Slit1	slit guidance ligand 1	20562	4.5199
	Sp100	nuclear antigen Sp100	20684	2.366
	Tmeff2	transmembrane protein with EGF-like, follistatin-like 2	56363	-2.0494
Cell activation involved	*Cd28*	CD28 antigen	12487	2.4043
in immune response	*Cdh17*	cadherin 17	12557	2.4588
	Dock10	dedicator of cytokinesis 10	210293	4.3578
	Exo1	exonuclease 1	26909	2.3737
	Il33	interleukin 33	77125	2.4364
	Ptafr	platelet-activating factor receptor	19204	2.1934
	Ptger4	prostaglandin E receptor 4 (subtype EP4)	19219	2.514
	Ptk2b	PTK2 protein tyrosine kinase 2 beta	19229	2.2743
	Rsad2	radical S-adenosyl methionine domain containing 2	58185	116.1724
Response to interferon-	*Ifit1*	interferon-induced protein with tetratricopeptide 1	15957	5.3466
alpha	*Ifit3*	interferon-induced protein with tetratricopeptide 3	15959	3.3849
	Ifit3b	interferon-induced protein with tetratricopeptide 3B	667370	4.3215
	Tgtp2	T cell specific GTPase 2	100039796	3.1538

Up regulated

Negative regulation of	*Ostn*	osteocrin	239790	-247.8283
cell development	*Pi16*	peptidase inhibitor 16	74116	-16.0331
Biomineralization	*Ostn*	osteocrin	239790	-247.8283
Positive regulation of	*Artn*	artemin	11876	-3.6392
response to external	*Calr*	calreticulin	12317	-3.4799
stimulus	*Cd74*	CD74 antigen (MHC class II antigen-associated)	16149	-2.272
	F7	coagulation factor VII	14068	-3.5419
	Ntrk3	neurotrophic tyrosine kinase, receptor, type 3	18213	-2.5496
	Pdgfb	platelet derived growth factor, B polypeptide	18591	-2.2093
	Pgf	placental growth factor	18654	-2.4948
	Smoc2	SPARC related modular calcium binding 2	64074	-2.3251
Response to steroid	*Calr*	calreticulin	12317	-3.4799
hormone	*Mgarp*	mitochondria localized glutamic acid rich protein	67749	-8.1858
	Ntrk3	neurotrophic tyrosine kinase, receptor, type 3	18213	-2.5496
	Pck2	phosphoenolpyruvate carboxykinase 2 (mitochondrial)	74551	-2.0832
	Ptpru	protein tyrosine phosphatase, receptor type, U	19273	-3.0245

Down regulated

	Spp1	secreted phosphoprotein 1	20750	-2.2454
	Sstr2	somatostatin receptor 2	20606	-2.0469
	Ugt1a1	UDP glucuronosyltransferase 1 family, polypeptide A1	394436	-2.2322
Homeostasis of number	*Hspa9*	heat shock protein 9	15526	-2.7413
of cells	*Slc7a11*	Slc 7 (cationic amino acid transporter), member 11	26570	-3.451
	Tnfrsf13c	tumor necrosis factor receptor superfamily, 13c	72049	-5.7573
Connective tissue	*Axin2*	axin 2	12006	2.2205
development	*Ccn1*	undefined	16007	2.2235
	Ccn2	undefined	14219	2.3712
	Col7a1	collagen, type VII, alpha 1	12836	2.3798
	Gdf6	growth differentiation factor 6	242316	4.2117
	Id4	inhibitor of DNA binding 4	15904	-3.1707
	Igf1	insulin-like growth factor 1	16000	2.6708
	Mmp13	matrix metallopeptidase 13	17386	-2.7608
	Pdgfb	platelet derived growth factor, B polypeptide	18591	-2.2093
	Vit	vitrin	74199	-3.2465
	Wnt7b	wingless-type MMTV integration site family, 7B	22422	3.1231
Response to	*Cth*	cystathionase (cystathionine gamma-lyase)	107869	-4.3039
leukemia inhibitory factor	*Egln3*	egl-9 family hypoxia-inducible factor 3	112407	-2.2984
	Fzd4	frizzled class receptor 4	14366	-2.1698
	Spp1	secreted phosphoprotein 1	20750	-2.2454
	Tfrc	transferrin receptor	22042	-2.5194
Gliogenesis	*Adgrg1*	adhesion G protein-coupled receptor G1	14766	2.237
	Aspa	aspartoacylase	11484	2.2839
	Atf5	activating transcription factor 5	107503	-2.0603
	Egr2	early growth response 2	13654	-2.7151
	Enpp2	ectonucleotide pyrophosphatase/phosphodiesterase 2	18606	2.2797
	Fas	Fas (TNF receptor superfamily member 6)	14102	2.1112
	Id4	inhibitor of DNA binding 4	15904	-3.1707
	Il33	interleukin 33	77125	2.4364
	Lgi4	leucine-rich repeat LGI family, member 4	243914	-2.2705
	Lif	leukemia inhibitory factor	16878	2.0862
	Nrg1	neuregulin 1	211323	2.3408
	Ntrk3	neurotrophic tyrosine kinase, receptor, type 3	18213	-2.5496
	Pdgfb	platelet derived growth factor, B polypeptide	18591	-2.2093
	Ptk2b	PTK2 protein tyrosine kinase 2 beta	19229	2.2743
	Sox11	SRY (sex determining region Y)-box 11	20666	-2.7869

Down regulated

Supplementary Table 2.1.5

List of Up regulated and Down regulated KEGG pathways among DEGs between DOX and CON

		DOX Vs CON		
Pathways	Symbol	Gene Name	Entrez Gene	Fold change
NOD-like receptor signaling pathway	*Gbp3*	guanylate binding protein 3	55932	7.4903
	Gbp7	guanylate binding protein 7	229900	8.733
	Oas1a	2'-5' oligoadenylate synthetase 1A	246730	11.0879
	Oas1g	2'-5' oligoadenylate synthetase 1G	23960	119.4
	Oas2	2'-5' oligoadenylate synthetase 2	246728	27.0276
	Txnip	thioredoxin interacting protein	56338	11.6354
Pathways in cancer	*Arnt2*	aryl hydrocarbon receptor nuclear translocator 2	11864	2.5523
	Axin2	axin 2	12006	2.1796
	Bdkrb1	bradykinin receptor, beta 1	12061	2.4826
	Ccne1	cyclin E1	12447	2.4414
	Fas	Fas (TNF receptor superfamily member 6)	14102	2.2723
	Fgfr4	fibroblast growth factor receptor 4	14186	5.3445
	Fzd9	frizzled class receptor 9	14371	-3.5054
	Gstm6	glutathione S-transferase, mu 6	14867	2.1205
	Hgf	hepatocyte growth factor	15234	2.6977
	Hsp90b1	heat shock protein 90, beta (Grp94), member 1	22027	-2.5271
	Igf1	insulin-like growth factor 1	16000	2.9608
	Lama1	laminin, alpha 1	16772	-3.9381
	Lama4	laminin, alpha 4	16775	-2.3008
	Met	met proto-oncogene	17295	2.0546
	Pgf	placental growth factor	18654	-2.2545
	Ptger4	prostaglandin E receptor 4 (subtype EP4)	19219	3.3996
	Stat1	signal transducer and activator of transcription 1	20846	2.0752
	Stat2	signal transducer and activator of transcription 2	20847	2.0344
	Tert	telomerase reverse transcriptase	21752	6.086
	Vegfd	vascular endothelial growth factor D	14205	2.8128
	Wnt5a	wingless-type MMTV integration site family, member 5A	22418	-2.0749
	Wnt6	wingless-type MMTV integration site family, member 6	22420	-2.4302
	Wnt7b	wingless-type MMTV integration site family, member 7B	22422	3.2736
Calcium signaling pathway	*Cacna1b*	calcium channel, voltage-dependent, N type, alpha 1B	12287	14.8545
	Htr2b	5-hydroxytryptamine (serotonin) receptor 2B	15559	10.0497
	Mylk3	myosin light chain kinase 3	213435	4.7163
	Plcd4	phospholipase C, delta 4	18802	5.3153
	Tbxa2r	thromboxane A2 receptor	21390	3.8614
Wnt signaling pathway	*Dkk2*	dickkopf WNT signaling pathway inhibitor 2	56811	4.8283

Up regulated

	Nkd2	naked cuticle 2	72293	12.4181
	Wif1	Wnt inhibitory factor 1	24117	4.4529
Rap1 signaling pathway	*Angpt4*	angiopoietin 4	11602	2.8141
	Efna3	ephrin A3	13638	2.5286
	Fgfr4	fibroblast growth factor receptor 4	14186	5.3445
	Hgf	hepatocyte growth factor	15234	2.6977
	Id1	inhibitor of DNA binding 1	15901	5.5032
	Igf1	insulin-like growth factor 1	16000	2.9608
	Vegfd	vascular endothelial growth factor D	14205	2.8128
MAPK signaling pathway	*Angpt4*	angiopoietin 4	11602	2.8141
	Cacna1b	calcium channel, voltage-dependent, N type, alpha 1B subunit	12287	14.8545
	Fgfr4	fibroblast growth factor receptor 4	14186	5.3445
	Hgf	hepatocyte growth factor	15234	2.6977
	Hspa1a	heat shock protein 1A	193740	6.0788
	Igf1	insulin-like growth factor 1	16000	2.9608
	Ptpn7	protein tyrosine phosphatase, non-receptor type 7	320139	3.4778
	Vegfd	vascular endothelial growth factor D	14205	2.8128
Pluripotency of stem cells	*Fgfr4*	fibroblast growth factor receptor 4	14186	5.3445
Regulating signaling pathways	*Id1*	inhibitor of DNA binding 1	15901	5.5032
	Igf1	insulin-like growth factor 1	16000	2.9608
	Inhbb	inhibin beta-B	16324	2.9496
	Wnt7b	wingless-type MMTV integration site family, member 7B	22422	3.2736
PI3K-Akt signaling pathway	*Angpt4*	angiopoietin 4	11602	2.8141
	Ccne1	cyclin E1	12447	2.4414
	Col6a4	collagen, type VI, alpha 4	68553	6.5803
	Efna3	ephrin A3	13638	2.5286
	Fgfr4	fibroblast growth factor receptor 4	14186	5.3445
	Hgf	hepatocyte growth factor	15234	2.6977
	Igf1	insulin-like growth factor 1	16000	2.9608
	Thbs2	thrombospondin 2	21826	2.5721
	Tnn	tenascin N	329278	6.9055
	Tnr	tenascin R	21960	2.7572
	Vegfd	vascular endothelial growth factor D	14205	2.8128
Focal adhesion	*Col6a4*	collagen, type VI, alpha 4	68553	6.5803
	Hgf	hepatocyte growth factor	15234	2.6977
	Igf1	insulin-like growth factor 1	16000	2.9608

Up regulated

	Mylk3	myosin light chain kinase 3	213435	4.7163
	Thbs2	thrombospondin 2	21826	2.5721
	Tnn	tenascin N	329278	6.9055
	Tnr	tenascin R	21960	2.7572
	Vegfd	vascular endothelial growth factor D	14205	2.8128
Chemokine signaling pathway	*Ccl2*	chemokine (C-C motif) ligand 2	20296	2.0784
	Ccl5	chemokine (C-C motif) ligand 5	20304	5.3491
	Ccl7	chemokine (C-C motif) ligand 7	20306	2.6521
	Ccl8	chemokine (C-C motif) ligand 8	20307	4.8889
	Ccl9	chemokine (C-C motif) ligand 9	20308	2.221
	Prex1	PI3-Rac exchange factor 1	277360	2.3342
	Ptk2b	PTK2 protein tyrosine kinase 2 beta	19229	2.3371
	Stat1	signal transducer and activator of transcription 1	20846	2.0752
	Stat2	signal transducer and activator of transcription 2	20847	2.0344
Cytokine-cytokine receptor interaction	*Ccl5*	chemokine (C-C motif) ligand 5	20304	5.3491
	Ccl7	chemokine (C-C motif) ligand 7	20306	2.6521
	Ccl8	chemokine (C-C motif) ligand 8	20307	4.8889
	Ccl9	chemokine (C-C motif) ligand 9	20308	2.221
	Fas	Fas (TNF receptor superfamily member 6)	14102	2.2723
	Gdf6	growth differentiation factor 6	242316	4.6515
	Il18rap	interleukin 18 receptor accessory protein	16174	2.442
	Il1rl1	interleukin 1 receptor-like 1	17082	2.1464
	Il33	interleukin 33	77125	2.3509
	Inhbb	inhibin beta-B	16324	2.9496
	Lepr	leptin receptor	16847	5.3501
	Lif	leukemia inhibitory factor	16878	2.1921
	Tnfrsf11b	tumor necrosis factor receptor superfamily, 11b	18383	2.2381
	Tnfrsf21	tumor necrosis factor receptor superfamily, m21	94185	2.5671
	Tnfrsf26	tumor necrosis factor receptor superfamily, m26	244237	3.257442753
p53 signaling	*Ccne1*	cyclin E1	12447	2.4414
	Fas	Fas (TNF receptor superfamily member 6)	14102	2.2723
	Gtse1	G two S phase expressed protein 1	29870	3.1694
	Igf1	insulin-like growth factor 1	16000	2.9608
	Pidd1	p53 induced death domain protein 1	57913	2.6938
Ras signaling pathway	*Angpt4*	angiopoietin 4	11602	2.8141
	Efna3	ephrin A3	13638	2.5286
	Hgf	hepatocyte growth factor	15234	2.6977

Up regulated

	Igf1	insulin-like growth factor 1	16000	2.9608
	Met	met proto-oncogene	17295	2.0546
	Ngfr	nerve growth factor receptor (TNFR superfamily, member 16)	18053	-2.8425
	Pgf	placental growth factor	18654	-2.2545
	Pla1a	phospholipase A1 member A	85031	2.0499
	Shc3	src homology 2 domain-containing transforming protein C3	20418	-5.761
	Vegfd	vascular endothelial growth factor D	14205	2.8128
	Zap70	zeta-chain (TCR) associated protein kinase	22637	2.1563
Proteoglycans in cancer	*Fas*	Fas (TNF receptor superfamily member 6)	14102	2.2723
	Fzd9	frizzled class receptor 9	14371	-3.5054
	Hgf	hepatocyte growth factor	15234	2.6977
	Igf1	insulin-like growth factor 1	16000	2.9608
	Met	met proto-oncogene	17295	2.0546
	Ppp1r12b	protein phosphatase 1, regulatory subunit 12B	329251	2.1314
	Tfap4	transcription factor AP4	83383	-2.0667
	Timp3	tissue inhibitor of metalloproteinase 3	21859	-2.0592
	Wnt5a	wingless-type MMTV integration site family, member 5A	22418	-2.0749
	Wnt6	wingless-type MMTV integration site family, member 6	22420	-2.4302
	Wnt7b	wingless-type MMTV integration site family, member 7B	22422	3.2736
Metabolic pathways	*Acot2*	acyl-CoA thioesterase 2	171210	-4.0284
	Acox2	acyl-Coenzyme A oxidase 2, branched chain	93732	-10.9061
	Akr1b7	aldo-keto reductase family 1, member B7	11997	-6.5519
	Asns	asparagine synthetase	27053	-3.9442
	Chac1	ChaC, cation transport regulator 1	69065	-4.1031
	Cndp1	carnosine dipeptidase 1 (metallopeptidase M20 family)	338403	-7.3818
	Cox6a2	cytochrome c oxidase subunit 6A2	12862	-33.8813
	Cth	cystathionase (cystathionine gamma-lyase)	107869	-3.7005
	Cyp2c23	cytochrome P450, family 2, subfamily c, polypeptide 23	226143	-3.4558
	Extl1	exostoses (multiple)-like 1	56219	-4.3771
	Hsd17b1	hydroxysteroid (17-beta) dehydrogenase 1	15485	-4.6329
	Mthfd2	methylenetetrahydrofolate dehydrogenase (NAD+ dependent)	17768	-3.0263
	Ndufa4l2	Ndufa4, mitochondrial complex associated like 2	407790	-3.0582
	Pck2	phosphoenolpyruvate carboxykinase 2 (mitochondrial)	74551	-3.2032
Hepatocellular carcinoma	*Axin2*	axin 2	12006	2.1796
	Fzd9	frizzled class receptor 9	14371	-3.5054
	Gstm6	glutathione S-transferase, mu 6	14867	2.1205
	Met	met proto-oncogene	17295	2.0546
	Shc3	src homology 2 domain-containing transforming protein C3	20418	-5.761
	Wnt5a	wingless-type MMTV integration site family, member 5A	22418	-2.0749

Down regulated

	Wnt6	wingless-type MMTV integration site family, member 6	22420	-2.4302
Gastric cancer	*Abcb1a*	ATP-binding cassette, sub-family B (MDR/TAP), member 1A	18671	-4.1209
	Fzd9	frizzled class receptor 9	14371	-3.5054
	Shc3	src homology 2 domain-containing transforming protein C3	20418	-5.761
Endochondral Ossification	*Mmp13*	matrix metallopeptidase 13	17386	-2.568
	Spp1	secreted phosphoprotein 1	20750	-2.2913
	Stat1	signal transducer and activator of transcription 1	20846	2.0752
	Timp3	tissue inhibitor of metalloproteinase 3	21859	-2.0592

Down regulated

Supplementary Table 2.1.6

List of Up regulated and Down regulated KEGG pathways among DEGs between DOX and RES

DOX Vs RES

Pathways	*Symbol*	Gene Name	Entrez Gene	Fold change
Calcium signaling pathway	*Bdkrb1*	bradykinin receptor, beta 1	12061	6.5761
	Htr2b	5-hydroxytryptamine (serotonin) receptor 2B	15559	19.0196
	Plcd4	phospholipase C, delta 4	18802	9.5451
Chemokine signaling pathway	*Ccl5*	chemokine (C-C motif) ligand 5	20304	4.8721
	Ccl8	chemokine (C-C motif) ligand 8	20307	9.3832
	Gm11787	predicted gene 11787	666513	22.4774
	Grk1	G protein-coupled receptor kinase 1	24013	5.6217
Wnt signaling pathway	*Dkk2*	dickkopf WNT signaling pathway inhibitor 2	56811	4.1881
	Nkd2	naked cuticle 2	72293	7.2079
	Wif1	Wnt inhibitory factor 1	24117	2.9715
NOD-like receptor signaling pathway	*Ccl5*	chemokine (C-C motif) ligand 5	20304	4.8721
	Gbp3	guanylate binding protein 3	55932	6.154
	Gbp7	guanylate binding protein 7	229900	5.2235
	Oas1a	2'-5' oligoadenylate synthetase 1A	246730	7.4907
	Oas1b	2'-5' oligoadenylate synthetase 1B	23961	5.9884
	Oas1g	2'-5' oligoadenylate synthetase 1G	23960	119.6542
	Oas2	2'-5' oligoadenylate synthetase 2	246728	19.1058
	Oas3	2'-5' oligoadenylate synthetase 3	246727	5.4955
	Txnip	thioredoxin interacting protein	56338	10.7851
TNF signaling pathway	*Ccl5*	chemokine (C-C motif) ligand 5	20304	4.8721
	Gm5431	predicted gene 5431	432555	7.2408
Oxytocin signaling pathway	*Cacnb4*	calcium channel, voltage-dependent, beta 4 subunit	12298	2.9803
	Egfr	epidermal growth factor receptor	13649	2.0753
	Kcnj2	potassium inwardly-rectifying channel, J2	16518	3.4651
	Mylk3	myosin light chain kinase 3	213435	3.823
	Ppp1r12b	protein phosphatase 1, regulatory subunit 12B	329251	2.0163
Parathyroid hormone synthesis, secretion	*Mmp15*	matrix metallopeptidase 15	17388	6.0075
MicroRNAs in cancer	*Ccne1*	cyclin E1	12447	2.0183

Up regulated

	Egfr	epidermal growth factor receptor	13649	2.0753
	Met	met proto-oncogene	17295	2.6408
	Slc7a1	solute carrier family 7, member 1	11987	-2.0263
	Timp3	tissue inhibitor of metalloproteinase 3	21859	-2.0102
	Tnn	tenascin N	329278	5.5402
	Tnr	tenascin R	21960	2.8979

EGFR tyrosine kinase	*Egfr*	epidermal growth factor receptor	13649	2.0753
inhibitor resistance	*Eif4ebp1*	eukaryotic translation initiation factor 4E 1	13685	-2.1513
	Gas6	growth arrest specific 6	14456	2.1235
	Igf1	insulin-like growth factor 1	16000	2.9654
	Met	met proto-oncogene	17295	2.6408
	Nrg1	neuregulin 1	211323	2.1486
	Shc3	src homology 2 domain-c C3	20418	-3.5212
Focal adhesion	*Col6a5*	collagen, type VI, alpha 5	665033	2.4932
	Egfr	epidermal growth factor receptor	13649	2.0753
	Igf1	insulin-like growth factor 1	16000	2.9654
	Itga8	integrin alpha 8	241226	2.0829
	Lama1	laminin, alpha 1	16772	-5.6292
	Lama4	laminin, alpha 4	16775	-2.2436
	Met	met proto-oncogene	17295	2.6408
	Mylk3	myosin light chain kinase 3	213435	3.823
	Pgf	placental growth factor	18654	-2.7924
	Ppp1r12b	protein phosphatase 1, regulatory subunit 12B	329251	2.0163
	Shc3	src homology 2 domain- C3	20418	-3.5212
	Thbs2	thrombospondin 2	21826	2.5325
	Tnn	tenascin N	329278	5.5402
	Tnr	tenascin R	21960	2.8979
	Vegfd	vascular endothelial growth factor D	14205	3.0601
HIF-1 signaling pathway	*Angpt4*	angiopoietin 4	11602	2.1121
	Egfr	epidermal growth factor receptor	13649	2.0753
	Egln3	egl-9 family hypoxia-inducible factor 3	112407	-2.3416
	Eif4ebp1	eukaryotic translation initiation factor 4E 1	13685	-2.1513
	Pgk1	phosphoglycerate kinase 1	18655	-2.0245
	Tfrc	transferrin receptor	22042	-2.6528
mTOR signaling pathway	*Eif4ebp1*	eukaryotic translation initiation factor 4E 1	13685	-2.1513
	Fzd9	frizzled class receptor 9	14371	-3.4603
	Slc3a2	solute carrier family 3 , member 2	17254	-2.2842
	Slc7a5	solute carrier family 7, member 5	20539	-2.6655
	Wnt6	wingless-type MMTV integration site family, 6	22420	-2.5944

Down regulated

	Wnt7b	wingless-type MMTV integration site family, 7B	22422	2.0256
RAP1 Signalling Pathways	*Angpt4*	angiopoietin 4	11602	2.1121
	Efna3	ephrin A3	13638	3.1148
	Egfr	epidermal growth factor receptor	13649	2.0753
	Fgfr4	fibroblast growth factor receptor 4	14186	2.6573
	Igf1	insulin-like growth factor 1	16000	2.9654
	Kitl	kit ligand	17311	2.2572
	Met	met proto-oncogene	17295	2.6408
	Ngfr	nerve growth factor receptor (TNFR-16)	18053	-2.5698
	Pgf	placental growth factor	18654	-2.7924
	Vegfd	vascular endothelial growth factor D	14205	3.0601
RAS Signalling Pathways	*Angpt4*	angiopoietin 4	11602	2.1121
	Efna3	ephrin A3	13638	3.1148
	Egfr	epidermal growth factor receptor	13649	2.0753
	Fgfr4	fibroblast growth factor receptor 4	14186	2.6573
	Igf1	insulin-like growth factor 1	16000	2.9654
	Kitl	kit ligand	17311	2.2572
	Met	met proto-oncogene	17295	2.6408
	Ngfr	nerve growth factor receptor (TNFR-16)	18053	-2.5698
	Pgf	placental growth factor	18654	-2.7924
	Pla1a	phospholipase A1 member A	85031	2.367
	Rgl1	ral guanine nucleotide dissociation stimulator,-like 1	19731	2.1137
	Shc3	src homology 2 domain-C3	20418	-3.5212
	Vegfd	vascular endothelial growth factor D	14205	3.0601
Pathways in Cancer	*Abcb1a*	ATP-binding cassette, sub-family B-1A	18671	-2.8293
	Ccne1	cyclin E1	12447	2.0183
	Cdh17	cadherin 17	12557	2.6735
	Egfr	epidermal growth factor receptor	13649	2.0753
	Fzd9	frizzled class receptor 9	14371	-3.4603
	Met	met proto-oncogene	14869	-2.2266
	Shc3	src homology 2 domain- C3	20418	-3.5212
	Wnt6	wingless-type MMTV integration site family, 6	22420	-2.5944
	Wnt7b	wingless-type MMTV integration site family, 7B	22422	2.0256
Metabolic pathways	*Acot2*	acyl-CoA thioesterase 2	171210	-3.7935
	Acox2	acyl-Coenzyme A oxidase 2, branched chain	93732	-12.6924
	Akr1b7	aldo-keto reductase family 1, member B7	11997	-11.7079
	Asns	asparagine synthetase	27053	-3.7846
	Chac1	ChaC, cation transport regulator 1	69065	-4.1197
	Cndp1	carnosine dipeptidase 1 (metallopeptidase M20)	338403	-7.2188
	Cox6a2	cytochrome c oxidase subunit 6A2	12862	-37.7737

Down regulated

	Cth	cystathionase (cystathionine gamma-lyase)	107869	-2.9978
	Cyp2c23	cytochrome P450, family 2, c, polypeptide 23	226143	-3.5612
	Extl1	exostoses (multiple)-like 1	56219	-3.7767
	Hsd17b1	hydroxysteroid (17-beta) dehydrogenase 1	15485	-3.8352
	Mthfd2	methylenetetrahydrofolate dehydrogenase (NAD+)	17768	-3.0812
	Ndufa4l2	Ndufa4, mitochondrial complex associated like 2	407790	-5.3354
	Pck2	phosphoenolpyruvate carboxykinase 2 (mitochondrial)	74551	-3.1675
	St3gal6	ST3 beta-galactoside alpha-2,3-sialyltransferase 6	54613	-3.1226
cGMP-PKG signaling pathway	*Adra1b*	adrenergic receptor, alpha 1b	11548	-2.7973
	Atp2a3	ATPase, Ca++ transporting, ubiquitous	53313	-9.2833
	Prkg2	protein kinase, cGMP-dependent, type II	19092	-2.559
ABC transporters	*Abca1*	ATP-binding cassette, sub-family A (ABC1), 1	11303	2.5732
	Abca4	ATP-binding cassette, sub-family A (ABC1), 4	11304	-2.2824
	Abca6	ATP-binding cassette, sub-family A (ABC1), 6	76184	2.6897
	Abca8a	ATP-binding cassette, sub-family A (ABC1), 8a	217258	2.2143
	Abcb1a	ATP-binding cassette, sub-family B (MDR/TAP), 1A	18671	-2.8293
MAPK signaling pathway	*Ddit3*	DNA-damage inducible transcript 3	13198	-4.164
	Hspa5	heat shock protein 5	14828	-3.7454

Down regulated

Supplementary Table 2.1.7

List of Up regulated and Down regulated KEGG pathways among DEGs between RES and DOX+RES

RES vs. DOX+ RES

Pathways	Symbol	Gene Name	Entrez Gene	Fold change
Upregulated				
PPAR signaling pathway	*Cpt1b*	carnitine palmitoyltransferase 1b, muscle	12895	9.0804
	Slc27a6	solute carrier family 27 (fatty acid transporter),6	225579	4.172
Ras signaling pathway	*Efna3*	ephrin A3	13638	-3.0696
	Egfr	epidermal growth factor receptor	13649	-2.1789
	Igf1	insulin-like growth factor 1	16000	-2.6712
	Met	met proto-oncogene	17295	-2.3668
	Ngfr	nerve growth factor receptor (TNFR-16)	18053	2.1138
	Pdgfb	platelet derived growth factor, B polypeptide	18591	2.0132
	Pgf	placental growth factor	18654	3.08
	Pla1a	phospholipase A1 member A	85031	-2.0054
	Pla2g4c	phospholipase A2, IVC (cytosolic, calcium-independent)	232889	2.1804
	Vegfd	vascular endothelial growth factor D	14205	-2.9929
Rap1 signaling pathway	*Cdh1*	cadherin 1	12550	2.9428
	Efna3	ephrin A3	13638	-3.0696
	Egfr	epidermal growth factor receptor	13649	-2.1789
	Igf1	insulin-like growth factor 1	16000	-2.6712
	Met	met proto-oncogene	17295	-2.3668
	Ngfr	nerve growth factor receptor (TNFR -16)	18053	2.1138
	Pdgfb	platelet derived growth factor, B polypeptide	18591	2.0132
	Pgf	placental growth factor	18654	3.08
	Vegfd	vascular endothelial growth factor D	14205	-2.9929
cGMP-PKG signaling	*Adra1b*	adrenergic receptor, alpha 1b	11548	2.7512
pathway	*Adrb2*	adrenergic receptor, beta 2	11555	-2.7443
	Atp2a3	ATPase, Ca++ transporting, ubiquitous	53313	6.3766
	Atp2b3	ATPase, Ca++ transporting, plasma membrane 3	320707	-3.9159
	Kcnma1	potassium conductance calcium-activated channel, Ma 1	16531	2.0987
	Mrvi1	MRV integration site 1	17540	-2.6227
	Mylk3	myosin light chain kinase 3	213435	-3.2195
	Prkg2	protein kinase, cGMP-dependent, type II	19092	2.3997
	Slc8a1	solute carrier family 8 (sodium/calcium exchanger),1	20541	-2.0864
AMPK signaling pathway	*Cpt1b*	carnitine palmitoyltransferase 1b, muscle	12895	9.0804
Metabolic pathways	*Acot2*	acyl-CoA thioesterase 2	171210	3.3874
	Akr1b7	aldo-keto reductase family 1, member B7	11997	4.8061

Up regulated

Up regulated

	Cndp1	carnosine dipeptidase 1 (metallopeptidase M20 family)	338403	18.8217
	Cox6a2	cytochrome c oxidase subunit 6A2	12862	10.5055
	Cth	cystathionase (cystathionine gamma-lyase)	107869	3.4868
	Cyp2c23	cytochrome P450, family 2, subfamily c, polypeptide 23	226143	3.8591
	Ndufa4l2	Ndufa4, mitochondrial complex associated like 2	407790	4.2406
	Rimklb	ribosomal modification protein rimK-like family member B	108653	3.2351
Protein digestion/absorption	*Eln*	elastin	13717	11.633
Hippo signaling pathway	*Cdh1*	cadherin 1	12550	2.9428
	Fzd9	frizzled class receptor 9	14371	2.915
	Tead4	TEA domain family member 4	21679	2.3378
Pathways in cancer	*Egfr*	epidermal growth factor receptor	13649	-2.1789
	Fzd9	frizzled class receptor 9	14371	2.915
	Igf1	insulin-like growth factor 1	16000	-2.6712
	Lum	lumican	17022	-2.0493
	Met	met proto-oncogene	17295	-2.3668
	Cdh1	cadherin 1	12550	2.9428
	Pdgfb	platelet derived growth factor, B polypeptide	18591	2.0132
	Abcb1a	ATP-binding cassette, sub-family B (MDR/TAP), 1A	18671	2.3263
	Ccne1	cyclin E1	12447	-2.2133
	Cdh1	cadherin 1	12550	2.9428
	Cdh17	cadherin 17	12557	-2.4214

Down regulated

EGFR tyrosine kinase inhibitor resistance	*Egfr*	epidermal growth factor receptor	13649	-2.1789
	Igf1	insulin-like growth factor 1	16000	-2.6712
	Met	met proto-oncogene	17295	-2.3668
	Nrg1	neuregulin 1	211323	-2.0881
	Pdgfb	platelet derived growth factor, B polypeptide	18591	2.0132
Calcium signaling pathway	*Atp2b3*	ATPase, Ca++ transporting, plasma membrane 3	320707	-3.9159
	Bdkrb1	bradykinin receptor, beta 1	12061	-5.1498
	Htr2b	5-hydroxytryptamine (serotonin) receptor 2B	15559	-13.7491
	Plcd4	phospholipase C, delta 4	18802	-10.3572
Cytokine-cytokine receptor interaction	*Ccl7*	chemokine (C-C motif) ligand 7	20306	-2.6396
	Ccl8	chemokine (C-C motif) ligand 8	20307	-6.3688
	Csf2rb	colony stimulating factor 2 receptor, beta,	12983	-11.236
	Gdf6	growth differentiation factor 6	242316	-3.5634
	Il18rap	interleukin 18 receptor accessory protein	16174	-3.0675
	Il1r2	interleukin 1 receptor, type II	16178	-3.895

	Il1rl1	interleukin 1 receptor-like 1	17082	-2.3312
	Il33	interleukin 33	77125	-2.7006
	Lepr	leptin receptor	16847	-2.276
	Tnfrsf21	tumor necrosis factor receptor superfamily, 21	94185	-2.4346
PI3K-Akt signaling pathway	*Ccne1*	cyclin E1	12447	-2.2133
	Col6a4	collagen, type VI, alpha 4	68553	-4.7274
	Col6a5	collagen, type VI, alpha 5	665033	-2.3501
	Efna3	ephrin A3	13638	-3.0696
	Egfr	epidermal growth factor receptor	13649	-2.1789
	Igf1	insulin-like growth factor 1	16000	-2.6712
	Lama4	laminin, alpha 4	16775	2.0526
	Met	met proto-oncogene	17295	-2.3668
	Ngfr	nerve growth factor receptor (TNFR- 16)	18053	2.1138
	Pck2	phosphoenolpyruvate carboxykinase 2 (mitochondrial)	74551	2.0635
	Pdgfb	platelet derived growth factor, B polypeptide	18591	2.0132
	Thbs2	thrombospondin 2	21826	-2.463
	Tnn	tenascin N	329278	-4.7566
	Tnr	tenascin R	21960	-2.3455
	Vegfd	vascular endothelial growth factor D	14205	-2.9929
Wnt signaling pathway	*Dkk2*	dickkopf WNT signaling pathway inhibitor 2	56811	-3.6624
	Nkd2	naked cuticle 2	72293	-6.6996
	Wif1	Wnt inhibitory factor 1	24117	-2.9365
Focal adhesion	*Col6a4*	collagen, type VI, alpha 4	68553	-4.7274
	Col6a5	collagen, type VI, alpha 5	665033	-2.3501
	Igf1	insulin-like growth factor 1	16000	-2.6712
	Met	met proto-oncogene	17295	-2.3668
	Mylk3	myosin light chain kinase 3	213435	-3.2195
	Thbs2	thrombospondin 2	21826	-2.463
	Tnn	tenascin N	329278	-4.7566
	Tnr	tenascin R	21960	-2.3455
	Vegfd	vascular endothelial growth factor D	14205	-2.9929
NOD-like receptor signaling pathway	*Gbp3*	guanylate binding protein 3	55932	-3.7546
	Gbp7	guanylate binding protein 7	229900	-3.1409
	Ifi207	interferon activated gene 207	226691	-3.4712
	Oas1a	2'-5' oligoadenylate synthetase 1A	246730	-5.5679
	Oas1b	2'-5' oligoadenylate synthetase 1B	23961	-5.993
	Oas2	2'-5' oligoadenylate synthetase 2	246728	-13.7276
	Oas3	2'-5' oligoadenylate synthetase 3	246727	-4.3902
	Txnip	thioredoxin interacting protein	56338	-9.0166

Down regulated

Inflammatory mediator regulation of TRP channels	*Bdkrb1*	bradykinin receptor, beta 1	12061	-5.1498
	Cyp2j9	cytochrome P450, family 2, subfamily j, polypeptide 9	74519	-2.565
	Htr2b	5-hydroxytryptamine (serotonin) receptor 2B	15559	-13.7491
	Igf1	insulin-like growth factor 1	16000	-2.6712
	Ptger4	prostaglandin E receptor 4 (subtype EP4)	19219	-3.3248
MicroRNAs in cancer	*Abcb1a*	ATP-binding cassette, sub-family B (MDR/TAP), 1A	18671	2.3263
	Ccne1	cyclin E1	12447	-2.2133
	Egfr	epidermal growth factor receptor	13649	-2.1789
	Met	met proto-oncogene	17295	-2.3668
	Pdgfb	platelet derived growth factor, B polypeptide	18591	2.0132
	Tnn	tenascin N	329278	-4.7566
	Tnr	tenascin R	21960	-2.3455
Transcriptional misregulation in cancer	*Igf1*	insulin-like growth factor 1	16000	-2.6712
	Il1r2	interleukin 1 receptor, type II	16178	-3.895
	Met	met proto-oncogene	17295	-2.3668
ECM-receptor interaction	*Col6a4*	collagen, type VI, alpha 4	68553	-4.7274
	Tnn	tenascin N	329278	-4.7566

Down regulated

Supplementary Table 2.1.8

List of Up regulated and Down regulated KEGG pathways among DEGs between DOX+RES vs. CON

DOX+ RES vs. CON

Pathways	Symbol	Gene Name	Entrez Gene	Fold change
Cell cycle	*Ccnb2*	cyclin B2	12442	2.1469
	Ccne1	cyclin E1	12447	2.6842
	Cdc25c	cell division cycle 25C	12532	2.0645
	Cdc6	cell division cycle 6	23834	2.3495
	Espl1	extra spindle pole bodies 1, separase	105988	2.01
	Mcm5	minichromosome maintenance complex component 5	17218	2.0094
	Orc1	origin recognition complex, subunit 1	18392	2.7028
	Plk1	polo like kinase 1	18817	2.9501
	Ttk	Ttk protein kinase	22137	2.6223
Chemokine signaling pathway	*Ccl5*	chemokine (C-C motif) ligand 5	20304	3.6658
	Ccl8	chemokine (C-C motif) ligand 8	20307	3.3397
	Hck	hemopoietic cell kinase	15162	7.5895
Calcium signaling pathway	*Atp2b3*	ATPase, Ca++ transporting, plasma membrane 3	320707	4.127
	Cacna1b	calcium channel, voltage-dependent, N 1B subunit	12287	11.4659
	Htr2b	5-hydroxytryptamine (serotonin) receptor 2B	15559	7.5805
	Mylk3	myosin light chain kinase 3	213435	3.981
	Plcd4	phospholipase C, delta 4	18802	5.7746
Rap1 signaling pathway	*Angpt4*	angiopoietin 4	11602	2.4881
	Efna3	ephrin A3	13638	2.5064
	Fgfr4	fibroblast growth factor receptor 4	14186	3.9079
	Igf1	insulin-like growth factor 1	16000	2.6708
	Vegfd	vascular endothelial growth factor D	14205	2.7551
MAPK signaling pathway	*Angpt4*	angiopoietin 4	11602	2.4881
	Cacna1b	calcium channel, voltage-dependent, N-alpha 1B subunit	12287	11.4659
	Efna3	ephrin A3	13638	2.5064
	Fgfr4	fibroblast growth factor receptor 4	14186	3.9079
	Hspa1a	heat shock protein 1A	193740	5.0107
	Igf1	insulin-like growth factor 1	16000	2.6708
	Ptpn7	protein tyrosine phosphatase, non-receptor type 7	320139	3.275
	Vegfd	vascular endothelial growth factor D	14205	2.7551
TNF signaling pathway	*Ccl5*	chemokine (C-C motif) ligand 5	20304	3.6658
	Fas	Fas (TNF receptor superfamily member 6)	14102	2.1112

Up regulated

	Ifi47	interferon gamma inducible protein 47	15953	2.0098
	Lif	leukemia inhibitory factor	16878	2.0862
	Nod2	nucleotide-binding oligomerization domain containing 2	257632	2.1774
NOD-like receptor signaling pathway	*Gbp3*	guanylate binding protein 3	55932	4.7217
	Gbp7	guanylate binding protein 7	229900	5.271
	Oas1a	2'-5' oligoadenylate synthetase 1A	246730	8.0724
	Oas1b	2'-5' oligoadenylate synthetase 1B	23961	5.7284
	Oas2	2'-5' oligoadenylate synthetase 2	246728	19.4522
	Txnip	thioredoxin interacting protein	56338	9.7675
Hippo signaling pathway	*Axin2*	axin 2	12006	2.2205
	Ccn2	undefined	14219	2.3712
	Fzd4	frizzled class receptor 4	14366	-2.1698
	Fzd9	frizzled class receptor 9	14371	-2.9104
	Gdf6	growth differentiation factor 6	242316	4.2117
	Tead4	TEA domain family member 4	21679	-2.5145
	Wnt7b	wingless-type MMTV integration site family, member 7B	22422	3.1231
Wnt signaling pathway	*Dkk2*	dickkopf WNT signaling pathway inhibitor 2	56811	4.2488
	Nkd2	naked cuticle 2	72293	11.5122
	Notum	notum palmitoleoyl-protein carboxylesterase	77583	2.6571
	Wif1	Wnt inhibitory factor 1	24117	4.3979
	Wnt7b	wingless-type MMTV integration site family, member 7B	22422	3.1231
p53 signaling pathway	*Ccnb2*	cyclin B2	12442	2.1469
	Ccne1	cyclin E1	12447	2.6842
	Fas	Fas (TNF receptor superfamily member 6)	14102	2.1112
	Gtse1	G two S phase expressed protein 1	29870	3.0763
	Igf1	insulin-like growth factor 1	16000	2.6708
	Pidd1	p53 induced death domain protein 1	57913	2.4126
ECM-receptor interaction	*Col6a4*	collagen, type VI, alpha 4	68553	8.4312
	Tnn	tenascin N	329278	5.9377
Ras signaling pathway	*Angpt4*	angiopoietin 4	11602	2.4881
	Efna3	ephrin A3	13638	2.5064
	Fgfr4	fibroblast growth factor receptor 4	14186	3.9079
	Igf1	insulin-like growth factor 1	16000	2.6708
	Ngfr	nerve growth factor receptor (TNFR-16)	18053	-2.3364
	Pdgfb	platelet derived growth factor, B polypeptide	18591	-2.2093
	Pgf	placental growth factor	18654	-2.4948

Up regulated

	Pla2g4c	phospholipase A2, IVC (cytosolic, calcium-independent)	232889	-2.3632
	Shc3	src homology 2 domain-C3	20418	-2.9734
	Vegfd	vascular endothelial growth factor D	14205	2.7551
	Zap70	zeta-chain (TCR) associated protein kinase	22637	2.0193
mTOR signaling pathway	*Fzd4*	frizzled class receptor 4	14366	-2.1698
	Fzd9	frizzled class receptor 9	14371	-2.9104
	Slc3a2	Slc3(activators of dibasic,neutral amino acid transport)2	17254	-2.0834
	Slc7a5	solute carrier family 7(cationic amino acid transporter) 5	20539	-2.153
Proteoglycans in cancer	*Fas*	Fas (TNF receptor superfamily member 6)	14102	2.1112
	Fzd4	frizzled class receptor 4	14366	-2.1698
	Fzd9	frizzled class receptor 9	14371	-2.9104
	Igf1	insulin-like growth factor 1	16000	2.6708
	Nanog	Nanog homeobox	71950	2.5208
	Ppp1r12b	protein phosphatase 1, regulatory subunit 12B	329251	2.0098
	Timp3	tissue inhibitor of metalloproteinase 3	21859	-2.0027
	Wnt7b	wingless-type MMTV integration site family, 7B	22422	3.1231
Breast cancer	*Axin2*	axin 2	12006	2.2205
	Esr2	estrogen receptor 2 (beta)	13983	2.9657
	Fzd4	frizzled class receptor 4	14366	-2.1698
	Fzd9	frizzled class receptor 9	14371	-2.9104
	Igf1	insulin-like growth factor 1	16000	2.6708
	Shc3	src homology 2 domain-C3	20418	-2.9734
	Wnt7b	wingless-type MMTV integration site family, 7B	22422	3.1231
Viral carcinogenesis	*Ccne1*	cyclin E1	12447	2.6842
	Egr2	early growth response 2	13654	-2.7151
	Egr3	early growth response 3	13655	-2.6222
	Irf7	interferon regulatory factor 7	54123	2.3676
	Sp100	nuclear antigen Sp100	20684	2.366
cGMP-PKG signaling pathway	*Adra1b*	adrenergic receptor, alpha 1b	11548	-2.7342
	Atp2a3	ATPase, Ca++ transporting, ubiquitous	53313	-5.5554
	Prkg2	protein kinase, cGMP-dependent, type II	19092	-2.9106
PPAR signaling pathway	*Cpt1b*	carnitine palmitoyltransferase 1b, muscle	12895	-11.596
	Slc27a6	solute carrier family 27 (fatty acid transporter), 6	225579	-4.6288
Metabolic pathways	*Acot2*	acyl-CoA thioesterase 2	171210	-3.5914
	Asns	asparagine synthetase	27053	-2.3066
	Chac1	ChaC, cation transport regulator 1	69065	-2.7274

Down regulated

Cndp1	carnosine dipeptidase 1 (metallopeptidase M20 family)	338403	-19.2842
Cox6a2	cytochrome c oxidase subunit 6A2	12862	-9.2612
Cth	cystathionase (cystathionine gamma-lyase)	107869	-4.3039
Cyp2c23	cytochrome P450, family 2, subfamily c, 23	226143	-3.7258
Elovl6	ELOVL family member 6,	170439	-2.0868
Extl1	exostoses (multiple)-like 1	56219	-2.6263
Gpat3	glycerol-3-phosphate acyltransferase 3	231510	-2.4703
Hsd17b1	hydroxysteroid (17-beta) dehydrogenase 1	15485	-2.8952
Mthfd2	methylenetetrahydrofolate dehydrogenase (NAD+)	17768	-2.0623
Ndufa4l2	Ndufa4, mitochondrial complex associated like 2	407790	-2.4418
Pck2	phosphoenolpyruvate carboxykinase 2 (mitochondrial)	74551	-2.0832
Pla2g4c	phospholipase A2, IVC (cytosolic, calcium-independent)	232889	-2.3632
Psph	phosphoserine phosphatase	100678	-2.0553
Rimklb	ribosomal modification protein rimK-like family B	108653	-2.1576
Ugt1a1	UDP glucuronosyltransferase 1 family, A1	394436	-2.2322
Ugt1a6a	UDP glucuronosyltransferase 1 family, A6A	94284	-2.6279

Down regulated

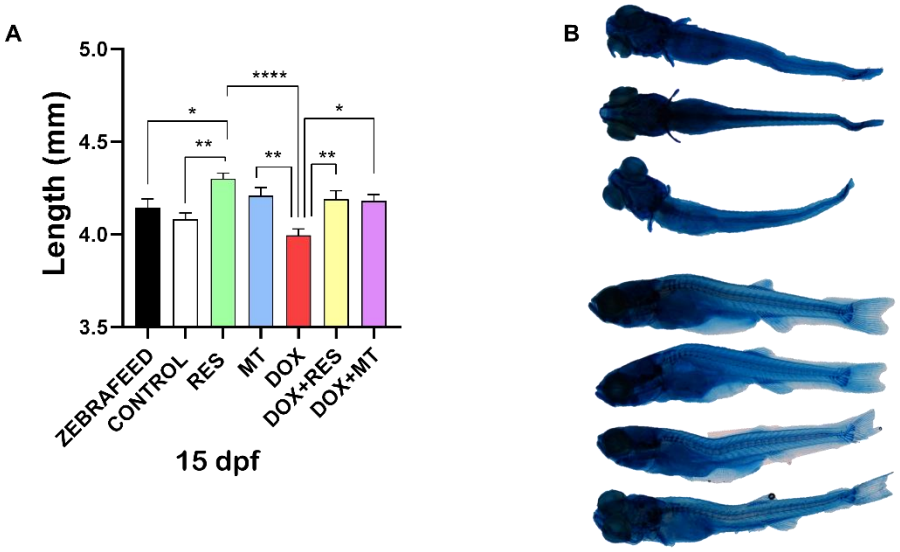

Supplementary figure 3.1: Comparison of the microdiets prepared with commercially available zebrafish fed (ZEBRAFEED) (A), Some of the skeletal deformities observed during the trial (B) . One-way ANOVA, Tukey's multiple comparisons test, ns- P>0.05, *- P≤0.05, **-P≤0.01, ***-P≤0.001, ****-P≤0.0001

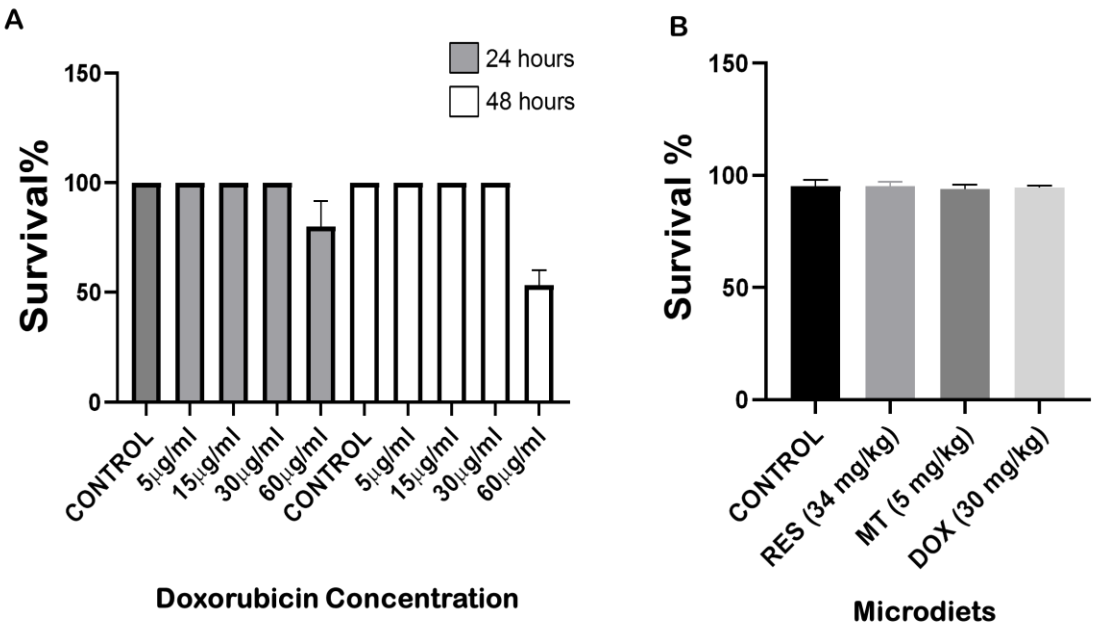

Supplementary figure 4.1: Survival of gilthead seabream larvae. Survival of seabream on waterborne exposure on different concentration of DOX for 48 hours (A), survival of the larvae up to 24 hours with microdiets prepared (B). Graph prepared in Graphpad prism 8 ±SEM. Acronyms: Resveratrol (RES), Doxorubicin (DOX) and MitoTEMPO (MT).

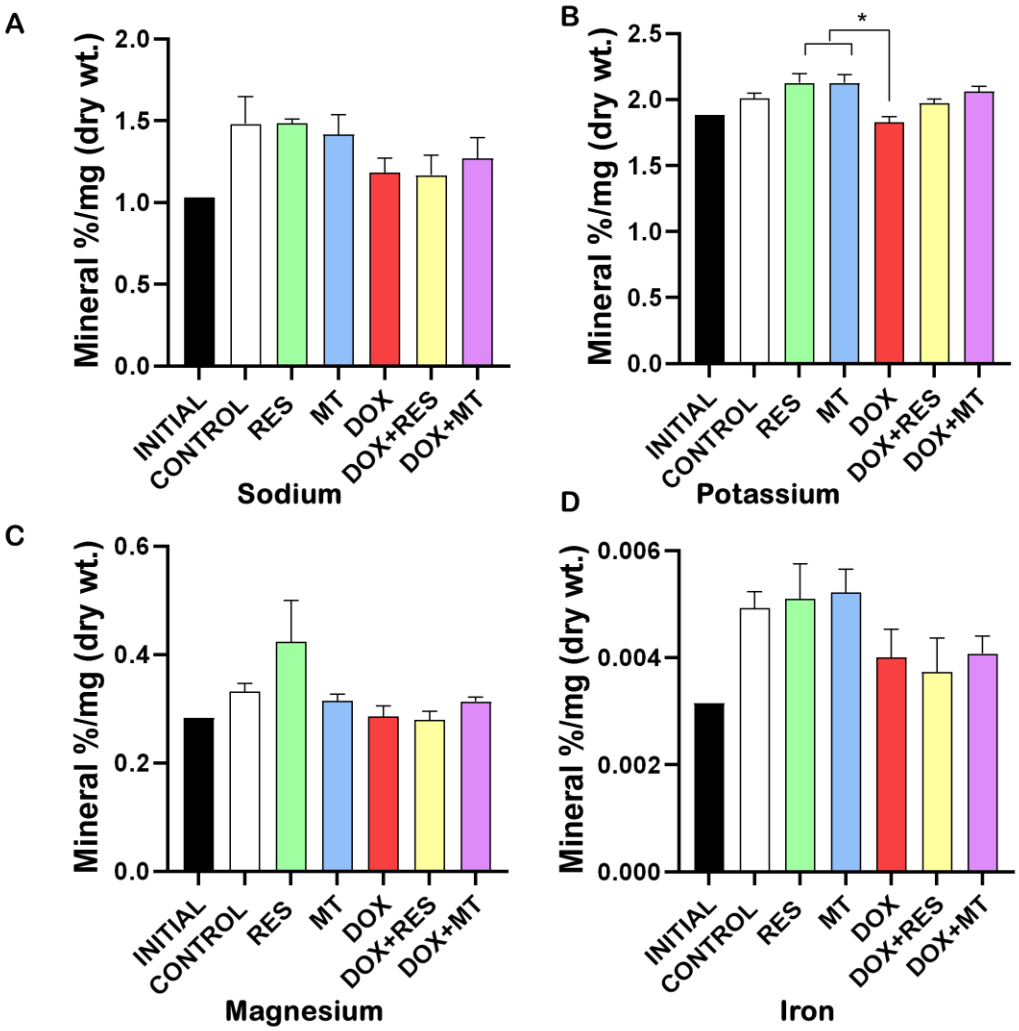

Supplementary figure 4.2: Mineral analysis of gilthead seabream fed with antioxidants and pro-oxidant supplemented microdiets. Sodium (A), potassium (B), magnesium (C) and iron (D). One-way ANOVA, Tukey's multiple comparisons test, ns- P>0.05, *- P≤0.05, **-P≤0.01, ***-P≤0.001, ****-P≤0.0001. Acronyms: Resveratrol (RES), Doxorubicin (DOX), MitoTEMPO (MT), Doxorubicin+Resveratrol (DOX+RES) and Doxorubicin+MitoTEMPO (DOX+MT).

Supplementary Table 4.1: Temperature, oxygen, and oxygen saturation during the seabream rearing trial

Temperature (°C)	CONTROL	RES	MT	DOX	DOX+ RES	DOX+MT
Mean	20.18	20.16	20.08	20.06	20.06	20.07
Std. Deviation	0.253	0.2606	0.2025	0.1819	0.2288	0.2739
Std. Error of Mean	0.08001	0.08241	0.06403	0.05753	0.07236	0.08661
Oxygen (mg/l)						
Mean	6.557	6.31	6.387	6.55	6.533	6.53
Std. Deviation	0.1325	0.2644	0.1679	0.123	0.1324	0.1401
Std. Error of Mean	0.04188	0.0836	0.0531	0.03889	0.04187	0.04429
Saturation (%)						
Mean	89.5	84.93	86.57	89.07	88.87	88.57
Std. Deviation	1.408	4.277	2.577	1.858	1.906	2.031
Std. Error of Mean	0.4451	1.352	0.8151	0.5875	0.6029	0.6422

Acronyms: Resveratrol (RES), Doxorubicin (DOX), MitoTEMPO (MT), Doxorubicin+Resveratrol (DOX+RES) and Doxorubicin+MitoTEMPO (DOX+MT).

REFERENCES

1. Zaidi M. Skeletal remodeling in health and disease. Nat Med. 2007 Jul;13(7):791–801.
2. Karner CM, Long F. Wnt signaling and cellular metabolism in osteoblasts. Cell Mol Life Sci. 2017 May;74(9):1649–57.
3. Pietschmann P, Mechtcheriakova D, Meshcheryakova A, Föger-Samwald U, Ellinger I. Immunology of Osteoporosis: A Mini-Review. Gerontology. 2016;62(2):128–37.
4. Rodan GA. Bone homeostasis. Proc Natl Acad Sci U S A. 1998 Nov;95(23):13361–2.
5. Pfeilschifter J, Mundy GR. Modulation of type beta transforming growth factor activity in bone cultures by osteotropic hormones. Proc Natl Acad Sci U S A. 1987 Apr;84(7):2024–8.
6. Hauschka P V, Mavrakos AE, Iafrati MD, Doleman SE, Klagsbrun M. Growth factors in bone matrix. Isolation of multiple types by affinity chromatography on heparin-Sepharose. J Biol Chem. 1986 Sep;261(27):12665–74.
7. Bhansali A. Metabolic bone disease: Newer perspectives. Indian J Endocrinol Metab. 2012;16(Suppl 2):S140-1.
8. Han Y, You X, Xing W, Zhang Z, Zou W. Paracrine and endocrine actions of bone-the functions of secretory proteins from osteoblasts, osteocytes, and osteoclasts. Bone Res. 2018;6:16.
9. Cohen MM. The new bone biology: pathologic, molecular, and clinical correlates. Am J Med Genet A. 2006 Dec;140(23):2646–706.
10. Sims NA, Gooi JH. Bone remodeling: Multiple cellular interactions required for coupling of bone formation and resorption. Semin Cell Dev Biol. 2008 Oct;19(5):444–51.
11. Matsuo K, Irie N. Osteoclast-osteoblast communication. Arch Biochem Biophys. 2008 May;473(2):201–9.
12. Florencio-Silva R, Sasso GR da S, Sasso-Cerri E, Simões MJ, Cerri PS. Biology of Bone Tissue: Structure, Function, and Factors That Influence Bone Cells. Biomed Res Int. 2015;2015:421746.
13. Capulli M, Paone R, Rucci N. Osteoblast and osteocyte: games without frontiers. Arch Biochem Biophys. 2014 Nov;561:3–12.
14. Grigoriadis AE, Heersche JN, Aubin JE. Differentiation of muscle, fat, cartilage, and bone from progenitor cells present in a bone-derived clonal cell population: effect of dexamethasone. J Cell Biol. 1988 Jun;106(6):2139–51.
15. Gavaia PJ, Simes DC, Ortiz-Delgado JB, Viegas CSB, Pinto JP, Kelsh RN, et al. Osteocalcin and matrix Gla protein in zebrafish (Danio rerio) and Senegal sole (Solea senegalensis): Comparative gene and protein expression during larval development through adulthood. Gene Expr Patterns. 2006 Aug;6(6):637–52.
16. Franz-Odendaal TA, Hall BK, Witten PE. Buried alive: how osteoblasts become osteocytes. Dev Dyn. 2006 Jan;235(1):176–90.
17. Schaffler MB, Cheung WY, Majeska R, Kennedy O. Osteocytes: master orchestrators of bone. Calcif Tissue Int. 2014 Jan;94(1):5–24.

18. Komori T, Yagi H, Nomura S, Yamaguchi A, Sasaki K, Deguchi K, et al. Targeted disruption of Cbfa1 results in a complete lack of bone formation owing to maturational arrest of osteoblasts. Cell. 1997 May;89(5):755–64.
19. Li Y, Ge C, Long JP, Begun DL, Rodriguez JA, Goldstein SA, et al. Biomechanical stimulation of osteoblast gene expression requires phosphorylation of the RUNX2 transcription factor. J Bone Miner Res. 2012 Jun;27(6):1263–74.
20. Johnson ML, Rajamannan N. Diseases of Wnt signaling. Rev Endocr Metab Disord. 2006 Jun;7(1–2):41–9.
21. Canalis E. Notch signaling in osteoblasts. Sci Signal. 2008 Apr;1(17):pe17.
22. Jensen ED, Gopalakrishnan R, Westendorf JJ. Regulation of gene expression in osteoblasts. Biofactors. 2010;36(1):25–32.
23. Nakashima K, Zhou X, Kunkel G, Zhang Z, Deng JM, Behringer RR, et al. The novel zinc finger-containing transcription factor osterix is required for osteoblast differentiation and bone formation. Cell. 2002 Jan;108(1):17–29.
24. Long F. Building strong bones: molecular regulation of the osteoblast lineage. Nat Rev Mol Cell Biol. 2011 Dec;13(1):27–38.
25. Rosen V. BMP2 signaling in bone development and repair. Cytokine Growth Factor Rev. 2009 Oct;20(5–6):475–80.
26. Salazar VS, Gamer LW, Rosen V. BMP signalling in skeletal development, disease and repair. Nat Rev Endocrinol. 2016 Apr;12(4):203–21.
27. Chen D, Harris MA, Rossini G, Dunstan CR, Dallas SL, Feng JQ, et al. Bone morphogenetic protein 2 (BMP-2) enhances BMP-3, BMP-4, and bone cell differentiation marker gene expression during the induction of mineralized bone matrix formation in cultures of fetal rat calvarial osteoblasts. Calcif Tissue Int. 1997 Mar;60(3):283–90.
28. Papachroni KK, Karatzas DN, Papavassiliou KA, Basdra EK, Papavassiliou AG. Mechanotransduction in osteoblast regulation and bone disease. Trends Mol Med. 2009 May;15(5):208–16.
29. Kreke MR, Sharp LA, Lee YW, Goldstein AS. Effect of intermittent shear stress on mechanotransductive signaling and osteoblastic differentiation of bone marrow stromal cells. Tissue Eng Part A. 2008 Apr;14(4):529–37.
30. Montecino M, Lian J, Stein G, Stein J. Changes in chromatin structure support constitutive and developmentally regulated transcription of the bone-specific osteocalcin gene in osteoblastic cells. Biochemistry. 1996 Apr;35(15):5093–102.
31. Laplante M, Sabatini DM. mTOR signaling in growth control and disease. Cell. 2012 Apr;149(2):274–93.
32. Karner CM, Lee SY, Long F. Bmp Induces Osteoblast Differentiation through both Smad4 and mTORC1 Signaling. Mol Cell Biol. 2017 Feb;37(4):e00253-16.
33. Chen J, Long F. mTORC1 Signaling Promotes Osteoblast Differentiation from Preosteoblasts. Shi XM, editor. PLoS One. 2015 Jun;10(6):e0130627.
34. Esen E, Lee SY, Wice BM, Long F. PTH Promotes Bone Anabolism by Stimulating Aerobic Glycolysis via IGF Signaling. J Bone Miner Res. 2015 Nov;30(11):1959–68.

35. Chen Q, Shou P, Zheng C, Jiang M, Cao G, Yang Q, et al. Fate decision of mesenchymal stem cells: adipocytes or osteoblasts? Cell Death Differ. 2016 Jul;23(7):1128–39.
36. Kim JH, Kim N. Signaling Pathways in Osteoclast Differentiation. Chonnam Med J. 2016;52(1):12.
37. Feng X, Teitelbaum SL. Osteoclasts: New Insights. Vol. 1, Bone Research. Sichuan University; 2013. p. 11–26.
38. Feng X, Teitelbaum SL. Osteoclasts: New Insights. Vol. 1, Bone Research. Sichuan University; 2013. p. 11–26.
39. Bourette RP, Rohrschneider LR. Early events in M-CSF receptor signaling. Vol. 17, Growth Factors. Harwood Academic Publishers GmbH; 2000. p. 155–66.
40. Wong BR, Josien R, Lee SY, Vologodskaia M, Steinman RM, Choi Y. The TRAF family of signal transducers mediates NF-κB activation by the TRANCE receptor. J Biol Chem. 1998 Oct;273(43):28355–9.
41. Boyce BF, Xing L. The RANKL/RANK/OPG pathway. Vol. 5, Current Osteoporosis Reports. Current Medicine Group LLC 1; 2007. p. 98–104.
42. Domazetovic V. Oxidative stress in bone remodeling: role of antioxidants. Clin Cases Miner Bone Metab. 2017;14(2):209.
43. Hussain T, Tan B, Yin Y, Blachier F, Tossou MCB, Rahu N. Oxidative Stress and Inflammation: What Polyphenols Can Do for Us? Oxid Med Cell Longev. 2016;2016.
44. Baek KH, Oh KW, Lee WY, Lee SS, Kim MK, Kwon HS, et al. Association of oxidative stress with postmenopausal osteoporosis and the effects of hydrogen peroxide on osteoclast formation in human bone marrow cell cultures. Calcif Tissue Int. 2010;87(3):226–35.
45. Maggio D, Barabani M, Pierandrei M, Polidori MC, Catani M, Mecocci P, et al. Marked decrease in plasma antioxidants in aged osteoporotic women: Results of a cross-sectional study. J Clin Endocrinol Metab. 2003 Apr;88(4):1523–7.
46. Yousefzadeh G, Larijani B, Mohammadirad A, Heshmat R, Dehghan G, Rahimi R, et al. Determination of oxidative stress status and concentration of TGF-β1 in the blood and saliva of osteoporotic subjects. In: Annals of the New York Academy of Sciences. Blackwell Publishing Inc.; 2006. p. 142–50.
47. Östman B, Michaëlsson K, Helmersson J, Byberg L, Gedeborg R, Melhus H, et al. Oxidative stress and bone mineral density in elderly men: Antioxidant activity of alpha-tocopherol. Vol. 47, Free Radical Biology and Medicine. Free Radic Biol Med; 2009. p. 668–73.
48. Romagnoli C, Marcucci G, Favilli F, Zonefrati R, Mavilia C, Galli G, et al. Role of GSH/GSSG redox couple in osteogenic activity and osteoclastogenic markers of human osteoblast-like SaOS-2 cells. FEBS J. 2013 Feb;280(3):867–79.
49. Lean JM, Jagger CJ, Kirstein B, Fuller K, Chambers TJ. Hydrogen peroxide is essential for estrogen-deficiency bone loss and osteoclast formation. Endocrinology. 2005 Feb;146(2):728–35.

50. Sheweita SA, Khoshhal KI, Baghdadi HH. Osteoporosis and oxidative stress - Role of antioxidants. In: Systems Biology of Free Radicals and Antioxidants. 2012.
51. Fontani F, Marcucci G, Iantomasi T, Brandi ML, Vincenzini MT. Glutathione, N-acetylcysteine and Lipoic Acid Down-Regulate Starvation-Induced Apoptosis, RANKL/OPG Ratio and Sclerostin in Osteocytes: Involvement of JNK and ERK1/2 Signalling. Calcif Tissue Int. 2015 Mar;96(4):335–46.
52. Plotkin LI, Aguirre JI, Kousteni S, Manolagas SC, Bellido T. Bisphosphonates and estrogens inhibit osteocyte apoptosis via distinct molecular mechanisms downstream of extracellular signal-regulated kinase activation. J Biol Chem. 2005 Feb;280(8):7317–25.
53. Marathe N, Rangaswami H, Zhuang S, Boss GR, Pilz RB. Pro-survival effects of 17β-estradiol on osteocytes are mediated by nitric oxide/cGMP via differential actions of cGMP-dependent protein kinases I and II. J Biol Chem. 2012 Jan;287(2):978–88.
54. Lee DH, Lim BS, Lee YK, Yang HC. Effects of hydrogen peroxide (H2O2) on alkaline phosphatase activity and matrix mineralization of odontoblast and osteoblast cell lines. Cell Biol Toxicol. 2006 Jan;22(1):39–46.
55. Bai XC, Lu D, Bai J, Zheng H, Ke ZY, Li XM, et al. Oxidative stress inhibits osteoblastic differentiation of bone cells by ERK and NF-κB. Biochem Biophys Res Commun. 2004 Jan;314(1):197–207.
56. Banfi G, Iorio EL, Corsi MM. Oxidative stress, free radicals and bone remodeling. Clinical Chemistry and Laboratory Medicine. 2008.
57. Hall SL, Greendale GA. The relation of dietary vitamin C intake to bone mineral density: Results from the PEPI study. Calcif Tissue Int. 1998 Sep;63(3):183–9.
58. Shuid AN, Mohamad S, Muhammad N, Fadzilah FM, Mokhtar SA, Mohamed N, et al. Effects of α-tocopherol on the early phase of osteoporotic fracture healing. J Orthop Res. 2011 Nov;29(11):1732–8.
59. Agidigbi TS, Kim C. Reactive Oxygen Species in Osteoclast Differentiation and Possible Pharmaceutical Targets of ROS-Mediated Osteoclast Diseases. Int J Mol Sci. 2019 Jul;20(14):3576.
60. Dickinson BC, Chang CJ. Chemistry and biology of reactive oxygen species in signaling or stress responses. Vol. 7, Nature Chemical Biology. Nature Publishing Group; 2011. p. 504–11.
61. Moloney JN, Cotter TG. ROS signalling in the biology of cancer. Vol. 80, Seminars in Cell and Developmental Biology. Elsevier Ltd; 2018. p. 50–64.
62. Wauquier F, Leotoing L, Coxam V, Guicheux J, Wittrant Y. Oxidative stress in bone remodelling and disease. Trends Mol Med. 2009;15(10):468–77.
63. Reczek CR, Chandel NS. ROS-dependent signal transduction. Vol. 33, Current Opinion in Cell Biology. Elsevier Ltd; 2015. p. 8–13.
64. Phaniendra A, Jestadi DB, Periyasamy L. Free Radicals: Properties, Sources, Targets, and Their Implication in Various Diseases. Vol. 30, Indian Journal of Clinical Biochemistry. Springer India; 2015. p. 11–26.
65. Kröller-Schön S, Steven S, Kossmann S, Scholz A, Daub S, Oelze M, et al.

Molecular mechanisms of the crosstalk between mitochondria and NADPH oxidase through reactive oxygen species - Studies in white blood cells and in animal models. Antioxidants Redox Signal. 2014 Jan;20(2):247–66.
66. Jeoung NH. Pyruvate Dehydrogenase Kinases: Therapeutic Targets for Diabetes and Cancers. Diabetes Metab J. 2015 Jun;39(3):188–97.
67. Jeoung NH, Harris CR, Harris RA. Regulation of pyruvate metabolism in metabolic-related diseases. Rev Endocr Metab Disord. 2014 Mar;15(1):99–110.
68. Holmström KM, Finkel T. Cellular mechanisms and physiological consequences of redox-dependent signalling. Vol. 15, Nature Reviews Molecular Cell Biology. Nature Publishing Group; 2014. p. 411–21.
69. Panieri E, Santoro MM. Ros homeostasis and metabolism: A dangerous liason in cancer cells. Vol. 7, Cell Death and Disease. Nature Publishing Group; 2016. p. e2253–e2253.
70. Houschyar KS, Tapking C, Borrelli MR, Popp D, Duscher D, Maan ZN, et al. Wnt Pathway in Bone Repair and Regeneration – What Do We Know So Far. Front Cell Dev Biol. 2019 Jan;6:170.
71. Essers MAG, De Vries-Smits LMM, Barker N, Polderman PE, Burgering BMT, Korswagen HC. Functional interaction between β-catenin and FOXO in oxidative stress signaling. Science (80-). 2005 May;308(5725):1181–4.
72. Glass DA, Bialek P, Ahn JD, Starbuck M, Patel MS, Clevers H, et al. Canonical Wnt signaling in differentiated osteoblasts controls osteoclast differentiation. Dev Cell. 2005 May;8(5):751–64.
73. Manolagas SC, Almeida M. Gone with the Wnts: β-Catenin, T-Cell Factor, Forkhead Box O, and Oxidative Stress in Age-Dependent Diseases of Bone, Lipid, and Glucose Metabolism. Mol Endocrinol. 2007 Nov;21(11):2605–14.
74. Armoni M, Harel C, Karni S, Chen H, Bar-Yoseph F, Ver MR, et al. FOXO1 represses peroxisome proliferator-activated receptor-γ1 and -γ2 gene promoters in primary adipocytes: A novel paradigm to increase insulin sensitivity. J Biol Chem. 2006 Jul;281(29):19881–91.
75. Franceschi RT, Ge C. Control of the Osteoblast Lineage by Mitogen-Activated Protein Kinase Signaling. Curr Mol Biol Reports. 2017 Jun;3(2):122–32.
76. Greenblatt MB, Shim JH, Glimcher LH. Mitogen-Activated Protein Kinase Pathways in Osteoblasts. Annu Rev Cell Dev Biol. 2013 Oct;29(1):63–79.
77. Greenblatt MB, Shim JH, Zou W, Sitara D, Schweitzer M, Hu D, et al. The p38 MAPK pathway is essential for skeletogenesis and bone homeostasis in mice. J Clin Invest. 2010 Jul;120(7):2457–73.
78. Ge C, Xiao G, Jiang D, Franceschi RT. Critical role of the extracellular signal-regulated kinase-MAPK pathway in osteoblast differentiation and skeletal development. J Cell Biol. 2007 Feb;176(5):709–18.
79. Zou W, Greenblatt MB, Shim JH, Kant S, Zhai B, Lotinun S, et al. MLK3 regulates bone development downstream of the faciogenital dysplasia protein FGD1 in mice. J Clin Invest. 2011 Nov;121(11):4383–92.
80. Matsushita T, Chan YY, Kawanami A, Balmes G, Landreth GE, Murakami

S. Extracellular Signal-Regulated Kinase 1 (ERK1) and ERK2 Play Essential Roles in Osteoblast Differentiation and in Supporting Osteoclastogenesis. Mol Cell Biol. 2009 Nov;29(21):5843–57.
81. Kim JM, Yang YS, Park KH, Oh H, Greenblatt MB, Shim JH. The ERK MAPK pathway is essential for skeletal development and homeostasis. Int J Mol Sci. 2019 Apr;20(8).
82. Li Y, Ge C, Franceschi RT. Differentiation-dependent association of phosphorylated extracellular signal-regulated kinase with the chromatin of osteoblast-related genes. J Bone Miner Res. 2010 Jan;25(1):154–63.
83. Yamashita M, Ying SX, Zhang GM, Li C, Cheng SY, Deng CX, et al. Ubiquitin ligase Smurf1 controls osteoblast activity and bone homeostasis by targeting MEKK2 for degradation. Cell. 2005 Apr;121(1):101–13.
84. Liu H, Liu Y, Viggeswarapu M, Zheng Z, Titus L, Boden SD. Activation of c-Jun NH2-terminal kinase 1 increases cellular responsiveness to BMP-2 and decreases binding of inhibitory Smad6 to the type 1 BMP receptor. J Bone Miner Res. 2011 May;26(5):1122–32.
85. Lee NK, Choi YG, Baik JY, Han SY, Jeong DW, Bae YS, et al. A crucial role for reactive oxygen species in RANKL-induced osteoclast differentiation. Blood. 2005 Aug;106(3):852–9.
86. Bai XC, Lu D, Liu AL, Zhang ZM, Li XM, Zou ZP, et al. Reactive oxygen species stimulates receptor activator of NF-κB ligand expression in osteoblast. J Biol Chem. 2005 Apr;280(17):17497–506.
87. Liu T, Zhang L, Joo D, Sun SC. NF-κB signaling in inflammation. Vol. 2, Signal Transduction and Targeted Therapy. Springer Nature; 2017. p. 1–9.
88. Abu-Amer Y. NF-κB signaling and bone resorption. Vol. 24, Osteoporosis International. NIH Public Access; 2013. p. 2377–86.
89. Boyce BF, Yao Z, Xing L. Functions of nuclear factor κb in bone. In: Annals of the New York Academy of Sciences. Blackwell Publishing Inc.; 2010. p. 367–75.
90. Yamashita T, Yao Z, Li F, Zhang Q, Badell IR, Schwarz EM, et al. NF-κB p50 and p52 regulate receptor activator of NF-κB ligand (RANKL) and tumor necrosis factor-induced osteoclast precursor differentiation by activating c-Fos and NFATc1. J Biol Chem. 2007 Jun;282(25):18245–53.
91. Ha H, Bok Kwak H, Woong Lee S, Mi Jin H, Kim HM, Kim HH, et al. Reactive oxygen species mediate RANK signaling in osteoclasts. Exp Cell Res. 2004 Dec;301(2):119–27.
92. Chang J, Wang Z, Tang E, Fan Z, McCauley L, Franceschi R, et al. Inhibition of osteoblastic bone formation by nuclear factor-B. Nat Med. 2009 Jun;15(6):682–9.
93. Yao Z, Li Y, Yin X, Dong Y, Xing L, Boyce BF. NF-κB RelB negatively regulates osteoblast differentiation and bone formation. J Bone Miner Res. 2014;29(4):866–77.
94. Callaway DA, Jiang JX. Reactive oxygen species and oxidative stress in osteoclastogenesis, skeletal aging and bone diseases. Vol. 33, Journal of Bone and Mineral Metabolism. Springer Tokyo; 2015. p. 359–70.
95. Garrett IR, Boyce BF, Oreffo ROC, Bonewald L, Poser J, Mundy GR.

Oxygen-derived free radicals stimulate osteoclastic bone resorption in rodent bone in vitro and in vivo. J Clin Invest. 1990;85(3):632–9.
96. Kim MS, Yang YM, Son A, Tian YS, Lee SI, Kang SW, et al. RANKL-mediated reactive oxygen species pathway that induces long lasting Ca2+ oscillations essential for osteoclastogenesis. J Biol Chem. 2010 Mar;285(10):6913–21.
97. Steinbeck MJ, Kim JK, Trudeau MJ, Hauschka P V., Karnovsky MJ. Involvement of Hydrogen Peroxide in the Differentiation of Clonal HD-11EM Cells Into Osteoclast-Like Cells. J Cell Physiol. 1998;176(3):574.
98. Moon HJ, Kim SE, Yun YP, Hwang YS, Bang JB, Park JH, et al. Simvastatin inhibits osteoclast differentiation by scavenging reactive oxygen species. Exp Mol Med. 2011;43(11):605–12.
99. Wang X, Chen B, Sun J, Jiang Y, Zhang H, Zhang P, et al. Iron-induced oxidative stress stimulates osteoclast differentiation via NF-κB signaling pathway in mouse model. Metabolism. 2018 Jun;83:167–76.
100. Akina O, Yoshimura Y, Deyama Y, Suzuki K. Rosmarinic acid and arbutin suppress osteoclast differentiation by inhibiting superoxide and NFATc1 downregulation in RAW 264.7 cells. Biomed Reports. 2015 Jul;3(4):483–90.
101. Kharkwal G, Chandra V, Fatima I, Dwivedi A. Ormeloxifene inhibits osteoclast differentiation in parallel to downregulating RANKL-induced ros generation and suppressing the activation of ERK and JNK in murine RAW264.7 cells. J Mol Endocrinol. 2012 Jun;48(3):261–70.
102. Wittrant Y, Gorin Y, Woodruff K, Horn D, Abboud HE, Mohan S, et al. High d(+)glucose concentration inhibits RANKL-induced osteoclastogenesis. Bone. 2008 Jun;42(6):1122–30.
103. Liu AL, Zhang Z, Zhu B, Liao Z, Liu Z. Metallothionein protects bone marrow stromal cells against hydrogen peroxide-induced inhibition of osteoblastic differentiation. Cell Biol Int. 2004 Dec;28(12):905–11.
104. Zhu FB, Wang JY, Zhang YL, Hu YG, Yue ZS, Zeng LR, et al. Mechanisms underlying the antiapoptotic and anti-inflammatory effects of monotropein in hydrogen peroxide-treated osteoblasts. Mol Med Rep. 2016 Dec;14(6):5377–84.
105. Li M, Zhao L, Liu J, Liu AL, Zeng WS, Luo SQ, et al. Hydrogen Peroxide Induces G $_2$ Cell Cycle Arrest and Inhibits Cell Proliferation in Osteoblasts. Anat Rec Adv Integr Anat Evol Biol. 2009 Aug;292(8):1107–13.
106. Arai M, Shibata Y, Pugdee K, Abiko Y, Ogata Y. Effects of reactive oxygen species (ROS) on antioxidant system and osteoblastic differentiation in MC3T3-E1 cells. IUBMB Life. 2007;59(1):27–33.
107. Pérez-Sayáns M, Somoza-Martín JM, Barros-Angueira F, Rey JMG, García-García A. RANK/RANKL/OPG role in distraction osteogenesis. Vol. 109, Oral Surgery, Oral Medicine, Oral Pathology, Oral Radiology and Endodontology. Elsevier; 2010. p. 679–86.
108. Boyce BF, Xing L. Biology of RANK, RANKL, and osteoprotegerin. Vol. 9, Arthritis Research and Therapy. BioMed Central; 2007. p. S1.
109. US Department of Health and Human Services. Bone health and

osteoporosis: a report of the Surgeon General. US Heal Hum Serv. 2004;437.
110. EL Demellawy D, Davila J, Shaw A, Nasr Y. Brief Review on Metabolic Bone Disease. Vol. 8, Academic Forensic Pathology. SAGE Publications Inc.; 2018. p. 611–40.
111. Khosla S, Monroe DG. Regulation of bone metabolism by sex steroids. Vol. 8, Cold Spring Harbor Perspectives in Medicine. Cold Spring Harbor Laboratory Press; 2018.
112. Zhou Q, Zhu L, Zhang D, Li N, Li Q, Dai P, et al. Oxidative Stress-Related Biomarkers in Postmenopausal Osteoporosis: A Systematic Review and Meta-Analyses. Dis Markers. 2016;2016.
113. Manolagas SC. From estrogen-centric to aging and oxidative stress: A revised perspective of the pathogenesis of osteoporosis. Vol. 31, Endocrine Reviews. Oxford Academic; 2010. p. 266–300.
114. Sendur OF, Turan Y, Tastaban E, Serter M. Antioxidant status in patients with osteoporosis: A controlled study. Jt Bone Spine. 2009 Oct;76(5):514–8.
115. Bellanti F, Matteo M, Rollo T, De Rosario F, Greco P, Vendemiale G, et al. Sex hormones modulate circulating antioxidant enzymes: Impact of estrogen therapy. Redox Biol. 2013;1(1):340–6.
116. Portal-Núñez S, de la Fuente M, Díez A, Esbrit P. El estrés oxidativo como posible diana terapéutica en la osteoporosis asociada al envejecimiento. Rev Osteoporos y Metab Miner. 2016;
117. Mirza F, Canalis E. Secondary osteoporosis: Pathophysiology and management. Vol. 173, European Journal of Endocrinology. BioScientifica Ltd.; 2015. p. R131–51.
118. Olarte OR, Andrade MA. Underlying mechanisms between diabetes mellitus and osteoporosis. US Endocrinol. 2018 Dec;14(2):65–6.
119. Notsu M, Yamaguchi T. [Secondary osteoporosis or secondary contributors to bone loss in fracture. Effects of oxidative stress on bone metabolism]. Clin Calcium. 2013 Sep;23(9):1285–92.
120. Reni C, Mangialardi G, Meloni M, Madeddu P. Diabetes Stimulates Osteoclastogenesis by Acidosis-Induced Activation of Transient Receptor Potential Cation Channels. Sci Rep. 2016 Jul;6.
121. Hamada Y, Kitazawa S, Kitazawa R, Fujii H, Kasuga M, Fukagawa M. Histomorphometric analysis of diabetic osteopenia in streptozotocin-induced diabetic mice: A possible role of oxidative stress. Bone. 2007 May;40(5):1408–14.
122. Notsu M, Yamaguchi T, Okazaki K, Tanaka KI, Ogawa N, Kanazawa I, et al. Advanced glycation end product 3 (AGE3) suppresses the mineralization of mouse stromal ST2 cells and human mesenchymal stem cells by increasing TGF-β expression and secretion. Endocrinology. 2014;155(7):2402–10.
123. Marycz K, Tomaszewski KA, Kornicka K, Henry BM, Wroński S, Tarasiuk J, et al. Metformin Decreases Reactive Oxygen Species, Enhances Osteogenic Properties of Adipose-Derived Multipotent Mesenchymal Stem

Cells In Vitro, and Increases Bone Density In Vivo. Oxid Med Cell Longev. 2016;2016.
124. L J, J B, Z Y. Role of Metformin on Osteoblast Differentiation in Type 2 Diabetes. Biomed Res Int. 2019;2019.
125. LJS da F, V NS, MOF G, LA R. Oxidative Stress in Rheumatoid Arthritis: What the Future Might Hold Regarding Novel Biomarkers and Add-On Therapies. Oxid Med Cell Longev. 2019;2019.
126. Mateen S, Moin S, Khan AQ, Zafar A, Fatima N. Increased Reactive Oxygen Species Formation and Oxidative Stress in Rheumatoid Arthritis. Sheweita SA, editor. PLoS One. 2016 Apr;11(4):e0152925.
127. Lepetsos P, Papavassiliou AG. ROS/oxidative stress signaling in osteoarthritis. Vol. 1862, Biochimica et Biophysica Acta - Molecular Basis of Disease. Elsevier B.V.; 2016. p. 576–91.
128. Altindag O, Erel O, Aksoy N, Selek S, Celik H, Karaoglanoglu M. Increased oxidative stress and its relation with collagen metabolism in knee osteoarthritis. Rheumatol Int. 2007 Feb;27(4):339–44.
129. Altay MA, Ertürk C, Bilge A, Yaptı M, Levent A, Aksoy N. Evaluation of prolidase activity and oxidative status in patients with knee osteoarthritis: relationships with radiographic severity and clinical parameters. Rheumatol Int. 2015 Oct;35(10):1725–31.
130. Fay J, Varoga D, Wruck CJ, Kurz B, Goldring MB, Pufe T. Reactive oxygen species induce expression of vascular endothelial growth factor in chondrocytes and human articular cartilage explants. Arthritis Res Ther. 2006;8(6).
131. van Lent PLEM, Nabbe KCAM, Blom AB, Sloetjes A, Holthuysen AEM, Kolls J, et al. NADPH-oxidase-driven oxygen radical production determines chondrocyte death and partly regulates metalloproteinase-mediated cartilage matrix degradation during interferon-gamma-stimulated immune complex arthritis. Arthritis Res Ther. 2005 May;7(4):R885.
132. Yin W, Park JI, Loeser RF. Oxidative stress inhibits insulin-like growth factor-I induction of chondrocyte proteoglycan synthesis through differential regulation of phosphatidylinositol 3-kinase-Akt and MEK-ERK MAPK signaling pathways. J Biol Chem. 2009 Nov;284(46):31972–81.
133. Lo YYC, Conquer JA, Grinstein S, Cruz TF. Interleukin-1β induction of c-fos and collagenase expression in articular chondrocytes: Involvement of reactive oxygen species. J Cell Biochem. 1998 Apr;69(1):19–29.
134. He L, He T, Farrar S, Ji L, Liu T, Ma X. Antioxidants Maintain Cellular Redox Homeostasis by Elimination of Reactive Oxygen Species. Vol. 44, Cellular Physiology and Biochemistry. S. Karger AG; 2017. p. 532–53.
135. Birben E, Sahiner UM, Sackesen C, Erzurum S, Kalayci O. Oxidative stress and antioxidant defense. Vol. 5, World Allergy Organization Journal. BioMed Central Ltd.; 2012. p. 9–19.
136. D'Aniello C, Cermola F, Patriarca EJ, Minchiotti G. Vitamin C in Stem Cell Biology: Impact on Extracellular Matrix Homeostasis and Epigenetics. Stem Cells Int. 2017;2017.
137. Carcamo JM, Pedraza A, Borquez-Ojeda O, Zhang B, Sanchez R, Golde

DW. Vitamin C Is a Kinase Inhibitor: Dehydroascorbic Acid Inhibits I B Kinase . Mol Cell Biol. 2004 Aug;24(15):6645–52.
138. Franceschi RT, Iyer BS, Cui Y. Effects of ascorbic acid on collagen matrix formation and osteoblast differentiation in murine MC3T3-E1 cells. J Bone Miner Res. 1994;9(6):843–54.
139. Franceschi RT, Iyer BS. Relationship between collagen synthesis and expression of the osteoblast phenotype in MC3T3-E1 cells. J Bone Miner Res. 1992;7(2):235–46.
140. Xiao G, Cui Y, Ducy P, Karsenty G, Franceschi RT. Ascorbic acid-dependent activation of the osteocalcin promoter in MC3T3- E1 preosteoblasts: Requirement for collagen matrix synthesis and the presence of an intact OSE2 sequence. Mol Endocrinol. 1997;11(8):1103–13.
141. Hadzir SN, Ibrahim SN, Abdul Wahab RM, Zainol Abidin IZ, Senafi S, Ariffin ZZ, et al. Ascorbic acid induces osteoblast differentiation of human suspension mononuclear cells. Cytotherapy. 2014;16(5):674–82.
142. Otsuka E, Yamaguchi A, Hirose S, Hagiwara H. Characterization of osteoblastic differentiation of stromal cell line ST2 that is induced by ascorbic acid. Am J Physiol - Cell Physiol. 1999;277(1 46-1).
143. Buttery LDK, Bourne S, Xynos JD, Wood H, Hughes FJ, Hughes SPF, et al. Differentiation of osteoblasts and in Vitro bone formation from murine embryonic stem cells. Tissue Eng. 2001;7(1):89–99.
144. Xiao XH, Liao EY, Zhou HD, Dai RC, Yuan LQ, Wu XP. Ascorbic acid inhibits osteoclastogenesis of RAW264.7 cells induced by receptor activated nuclear factor kappaB ligand (RANKL) in vitro. J Endocrinol Invest. 2005;28(5):253–60.
145. Tsuneto M, Yamazaki H, Yoshino M, Yamada T, Hayashi SI. Ascorbic acid promotes osteoclastogenesis from embryonic stem cells. Biochem Biophys Res Commun. 2005 Oct;335(4):1239–46.
146. Otsuka E, Kato Y, Hirose S, Hagiwara H. Role of Ascorbic Acid in the Osteoclast Formation: Induction of Osteoclast Differentiation Factor with Formation of the Extracellular Collagen Matrix*. Endocrinology. 2000 Aug;141(8):3006–11.
147. Zhu LL, Cao J, Sun M, Yuen T, Zhou R, Li J, et al. Vitamin C Prevents Hypogonadal Bone Loss. PLoS One. 2012 Oct;7(10).
148. Wong SK, Mohamad NV, Ibrahim N 'Izzah, Chin KY, Shuid AN, Ima-Nirwana S. The molecular mechanism of Vitamin E as a bone-protecting agent: A review on current evidence. Vol. 20, International Journal of Molecular Sciences. MDPI AG; 2019.
149. Lee PL, Lukman HI, Nazrun AS, Ima-Nirwana S, Norazlina M. Effects of vitamin E supplementation on bone metabolism in nicotine-treated rats. Singapore Med J. 2007;48(3):195–9.
150. Soeta S, Higuchi M, Yoshimura I, Itoh R, Kimura N, Aamsaki H. Effects of vitamin E on the osteoblast differentiation. J Vet Med Sci. 2010 Jul;72(7):951–7.
151. Ahn KH, Jung HK, Jung SE, Yi KW, Park HT, Shin JH, et al. Microarray

Analysis of Gene Expression During Differentiation of Human Mesenchymal Stem Cells Treated with Vitamin E in vitro into Osteoblasts. Korean J Bone Metab. 2011;18(1):23–32.
152. Kim HN, Lee JH, Jin WJ, Lee ZH. α-Tocopheryl Succinate Inhibits Osteoclast Formation by Suppressing Receptor Activator of Nuclear Factor-kappaB Ligand (RANKL) Expression and Bone Resorption. J Bone Metab. 2012;19(2):111.
153. Lionikaite V, Gustafsson KL, Westerlund A, Windahl SH, Koskela A, Tuukkanen J, et al. Clinically relevant doses of Vitamin A decrease cortical bone mass in mice. J Endocrinol. 2018 Dec;239(3):389–402.
154. Henning P, Conaway HH, Lerner UH. Retinoid receptors in bone and their role in bone remodeling. Vol. 6, Frontiers in Endocrinology. Frontiers Media S.A.; 2015.
155. Dao DQ, Ngo TC, Thong NM, Nam PC. Is Vitamin A an Antioxidant or a Pro-oxidant? J Phys Chem B. 2017 Oct;121(40):9348–57.
156. Ohishi K, Nishikawa S, Nagata T, Yamauchi N, Shinohara H, Kido JI, et al. Physiological concentrations of retinoic acid suppress the osteoblastic differentiation of fetal rat calvaria cells in vitro. Eur J Endocrinol. 1995;133(3):335–41.
157. Iba K, Chiba H, Yamashita T, Ishii S, Sawada N. Phase-independent inhibition by retinoic acid of mineralization correlated with loss of tetranectin expression in a human osteoblastic cell line. Cell Struct Funct. 2001;26(4):227–33.
158. Nuka S, Sawada N, Iba K, Chiba H, Ishii S, Mori M. All-trans retinoic acid inhibits dexamethasone-induced ALP activity and mineralization in human osteoblastic cell line SV HFO. Cell Struct Funct. 1997;22(1):27–32.
159. Conaway HH, Pirhayati A, Persson E, Pettersson U, Svensson O, Lindholm C, et al. Retinoids stimulate periosteal bone resorption by enhancing the protein RANKL, a response inhibited by monomeric glucocorticoid receptor. J Biol Chem. 2011 Sep;286(36):31425–36.
160. Lind T, Sundqvist A, Hu L, Pejler G, Andersson G, Jacobson A, et al. Vitamin A is a negative regulator of osteoblast mineralization. PLoS One. 2013 Dec;8(12).
161. Pepa G Della, Brandi ML. Microelements for bone boost: the last but not the least. Clin Cases Miner Bone Metab. 2016;13(3):181.
162. Prasad AS. Zinc is an Antioxidant and Anti-Inflammatory Agent: Its Role in Human Health. Vol. 1, Frontiers in Nutrition. Frontiers Media S.A.; 2014.
163. Yamaguchi M, Yamaguchi R. Action of zinc on bone metabolism in rats. Increases in alkaline phosphatase activity and DNA content. Biochem Pharmacol. 1986 Mar;35(5):773–7.
164. Hall SL, Dimai HP, Farley JR. Effects of zinc on human skeletal alkaline phosphatase activity in vitro. Calcif Tissue Int. 1999;64(2):163–72.
165. Saltman PD, Strause LG. The role of trace minerals in osteoporosis. J Am Coll Nutr. 1993 Aug;12(4):384–9.
166. Yamaguchi M, Oishi H, Suketa Y. Stimulatory effect of zinc on bone formation in tissue culture. Biochem Pharmacol. 1987 Nov;36(22):4007–

12.
167. Seo HJ, Cho YE, Kim T, Shin HI, Kwun IS. Zinc may increase bone formation through stimulating cell proliferation, alkaline phosphatase activity and collagen synthesis in osteoblastic MC3T3-E1 cells. Nutr Res Pract. 2010;4(5):356.
168. Suzuki T, Katsumata SI, Matsuzaki H, Suzuki K. Dietary zinc deficiency induces oxidative stress and promotes tumor necrosis factor-α- and interleukin-1β-induced RANKL expression in rat bone. J Clin Biochem Nutr. 2016 Mar;58(2):122–9.
169. Qu X, He Z, Qiao H, Zhai Z, Mao Z, Yu Z, et al. Serum copper levels are associated with bone mineral density and total fracture. J Orthop Transl. 2018 Jul;14:34–44.
170. Cao JJ, Gregoire BR, Zeng H. Selenium Deficiency Decreases Antioxidative Capacity and Is Detrimental to Bone Microarchitecture in Mice. J Nutr. 2012 Aug;142(8):1526–31.
171. Rayman MP. Selenoproteins and human health: Insights from epidemiological data. Vol. 1790, Biochimica et Biophysica Acta - General Subjects. Biochim Biophys Acta; 2009. p. 1533–40.
172. Moreno-Reyes R, Egrise D, Nève J, Pasteels JL, Schoutens A. Selenium deficiency-induced growth retardation is associated with an impaired bone metabolism and osteopenia. J Bone Miner Res. 2001;16(8):1556–63.
173. Hoeg A, Gogakos A, Murphy E, Mueller S, Köhrle J, Reid DM, et al. Bone Turnover and Bone Mineral Density Are Independently Related to Selenium Status in Healthy Euthyroid Postmenopausal Women. J Clin Endocrinol Metab. 2012 Nov;97(11):4061–70.
174. Tou JC. Resveratrol supplementation affects bone acquisition and osteoporosis: Pre-clinical evidence toward translational diet therapy. Vol. 1852, Biochimica et Biophysica Acta - Molecular Basis of Disease. Elsevier B.V.; 2014. p. 1186–94.
175. Cottart CH, Nivet-Antoine V, Beaudeux JL. Review of recent data on the metabolism, biological effects, and toxicity of resveratrol in humans. Mol Nutr Food Res. 2014 Jan;58(1):7–21.
176. Mobasheri A, Shakibaei M. Osteogenic effects of resveratrol *in vitro*: potential for the prevention and treatment of osteoporosis. Ann N Y Acad Sci. 2013 Jul;1290(1):59–66.
177. Mizutani K, Ikeda K, Kawai Y, Yamori Y. Resveratrol stimulates the proliferation and differentiation of osteoblastic MC3T3-E1 cells. Biochem Biophys Res Commun. 1998 Dec;253(3):859–63.
178. Chachay VS, Kirkpatrick CMJ, Hickman IJ, Ferguson M, Prins JB, Martin JH. Resveratrol - pills to replace a healthy diet? Br J Clin Pharmacol. 2011 Jul;72(1):27–38.
179. Petrovski G, Gurusamy N, Das DK. Resveratrol in cardiovascular health and disease. Ann N Y Acad Sci. 2011 Jan;1215(1):22–33.
180. Dai Z, Li Y, Quarles LD, Song T, Pan W, Zhou H, et al. Resveratrol enhances proliferation and osteoblastic differentiation in human mesenchymal stem cells via ER-dependent ERK1/2 activation.

Phytomedicine. 2007 Dec;14(12):806–14.
181. Lee YS, Kim YS, Lee SY, Kim GH, Kim BJ, Lee SH, et al. AMP kinase acts as a negative regulator of RANKL in the differentiation of osteoclasts. Bone. 2010 Nov;47(5):926–37.
182. Zhou H, Shang L, Li X, Zhang X, Gao G, Guo C, et al. Resveratrol augments the canonical Wnt signaling pathway in promoting osteoblastic differentiation of multipotent mesenchymal cells. Exp Cell Res. 2009 Oct;315(17):2953–62.
183. Shakibaei M, Shayan P, Busch F, Aldinger C, Buhrmann C, Lueders C, et al. Resveratrol mediated modulation of sirt-1/Runx2 promotes osteogenic differentiation of mesenchymal stem cells: Potential role of Runx2 deacetylation. PLoS One. 2012 Apr;7(4).
184. Titorencu I, Pruna V, Jinga V V., Simionescu M. Osteoblast ontogeny and implications for bone pathology: An overview. Vol. 355, Cell and Tissue Research. 2014. p. 23–33.
185. Shakibaei M, Buhrmann C, Mobasheri A. Resveratrol-mediated SIRT-1 interactions with p300 modulate receptor activator of NF-κB ligand (RANKL) activation of NF-κB Signaling and inhibit osteoclastogenesis in bone-derived cells. J Biol Chem. 2011 Apr;286(13):11492–505.
186. Nakagawa H, Murata M, Tachibana K, Shiba T. Screening of epiphytic dinoflagellates for radical scavenging and cytotoxic activities. Phycol Res. 1998 Dec;46(s2):9–12.
187. Miyashita K. Marine antioxidants. In: Antioxidants and Functional Components in Aquatic Foods. Chichester, UK: John Wiley & Sons, Ltd; 2014. p. 219–35.
188. Yamamoto Y, Fujisawa A, Hara A, Dunlap WC. An unusual vitamin E constituent (α-tocomonoenol) provides enhanced antioxidant protection in marine organisms adapted to cold-water environments. Proc Natl Acad Sci U S A. 2001 Nov;98(23):13144–8.
189. Fujimoto K, Kaneda T. Separation of antioxygenic (antioxidant) compounds from marine algae. In: Eleventh International Seaweed Symposium. Springer Netherlands; 1984. p. 111–3.
190. Fidelis GP, Silva CHF, Nobre LTDB, Medeiros VP, Rocha HAO, Costa LS. Antioxidant Fucoidans Obtained from Tropical Seaweed Protect Pre-Osteoblastic Cells from Hydrogen Peroxide-Induced Damage. Mar Drugs. 2019 Aug;17(9):506.
191. Igondjo Tchen Changotade S, Korb G, Bassil J, Barroukh B, Willig C, Colliec-Jouault S, et al. Potential effects of a low-molecular-weight fucoidan extracted from brown algae on bone biomaterial osteoconductive properties. J Biomed Mater Res - Part A. 2008 Dec;87(3):666–75.
192. Hwang PA, Hung YL, Phan NN, Hieu BTN, Chang PM, Li KL, et al. The in vitro and in vivo effects of the low molecular weight fucoidan on the bone osteogenic differentiation properties. Cytotechnology. 2016 Aug;68(4):1349–59.
193. Kim BS, Kang HJ, Park JY, Lee J. Fucoidan promotes osteoblast differentiation via JNK- and ERK-dependent BMP2-Smad 1/5/8 signaling in

human mesenchymal stem cells. Exp Mol Med. 2015 Jan;47(1):e128–e128.
194. AlQranei MS, Aljohani H, Majumdar S, Senbanjo LT, Chellaiah MA. C-phycocyanin attenuates RANKL-induced osteoclastogenesis and bone resorption in vitro through inhibiting ROS levels, NFATc1 and NF-κB activation. Sci Rep. 2020 Dec;10(1):1–13.
195. Fernando IPS, Kim M, Son KT, Jeong Y, Jeon YJ. Antioxidant Activity of Marine Algal Polyphenolic Compounds: A Mechanistic Approach. J Med Food. 2016 Jul;19(7):615–28.
196. Carson MA, Clarke SA. Bioactive compounds from marine organisms: Potential for bone growth and healing. Vol. 16, Marine Drugs. MDPI AG; 2018.
197. Miura S, Saitoh SI, Kokubun T, Owada T, Yamauchi H, Machii H, et al. Mitochondrial-targeted antioxidant maintains blood flow, mitochondrial function, and redox balance in old mice following prolonged limb ischemia. Int J Mol Sci. 2017 Sep;18(9).
198. Ni R, Cao T, Xiong S, Ma J, Fan GC, Lacefield JC, et al. Therapeutic inhibition of mitochondrial reactive oxygen species with mito-TEMPO reduces diabetic cardiomyopathy. Free Radic Biol Med. 2016 Jan;90:12–23.
199. Dai P, Mao Y, Sun X, Li X, Muhammad I, Gu W, et al. Attenuation of Oxidative Stress-Induced Osteoblast Apoptosis by Curcumin is Associated with Preservation of Mitochondrial Functions and Increased Akt-GSK3β Signaling. Cell Physiol Biochem. 2017;41(2):661–77.
200. Knowles H. Hypoxic regulation of osteoclast differentiation and bone resorption activity. Hypoxia. 2015 Nov;73.
201. Srinivasan S, Koenigstein A, Joseph J, Sun L, Kalyanaraman B, Zaidi M, et al. Role of mitochondrial reactive oxygen species in osteoclast differentiation. In: Annals of the New York Academy of Sciences. Blackwell Publishing Inc.; 2010. p. 245–52.
202. Biewenga GP, Haenen GRMM, Bast A. The pharmacology of the antioxidant: Lipoic acid. Vol. 29, General Pharmacology. Gen Pharmacol; 1997. p. 315–31.
203. Roy S, Packer L. Redox regulation of cell functions by α-lipoate: biochemical and molecular aspects. BioFactors. 1998 Jan;7(3):263–7.
204. Han D, Handelman G, Marcocci L, Sen CK, Roy S, Kobuchi H, et al. Lipoic acid increases de novo synthesis of cellular glutathione by improving cystine utilization. BioFactors. 1997;6(3):321–38.
205. Von Wilmowsky C, Schlegel KA, Baran C, Nkenke E, Neukam FW, Moest T. Peri-implant defect regeneration in the diabetic pig: A preclinical study. J Cranio-Maxillofacial Surg. 2016 Jul;44(7):827–34.
206. Aydin A, Halici Z, Akoz A, Karaman A, Ferah I, Bayir Y, et al. Treatment with α-lipoic acid enhances the bone healing after femoral fracture model of rats. Naunyn Schmiedebergs Arch Pharmacol. 2014 Jul;387(11):1025–36.
207. Ha H, Lee JH, Kim HN, Kim HM, Kwak HB, Lee S, et al. α-Lipoic Acid Inhibits Inflammatory Bone Resorption by Suppressing Prostaglandin E 2

Synthesis . J Immunol. 2006 Jan;176(1):111–7.
208. Kim HJ, Chang EJ, Kim HM, Lee SB, Kim HD, Su Kim G, et al. Antioxidant α-lipoic acid inhibits osteoclast differentiation by reducing nuclear factor-κB DNA binding and prevents in vivo bone resorption induced by receptor activator of nuclear factor-κB ligand and tumor necrosis factor-α. Free Radic Biol Med. 2006 May;40(9):1483–93.
209. Turrens JF. Mitochondrial formation of reactive oxygen species. Vol. 552, Journal of Physiology. 2003. p. 335–44.
210. Marinho HS, Real C, Cyrne L, Soares H, Antunes F. Hydrogen peroxide sensing, signaling and regulation of transcription factors. Vol. 2, Redox Biology. Elsevier B.V.; 2014. p. 535–62.
211. Abdollahi M, Larijani B, Rahimi R, Salari P. Role of oxidative stress in osteoporosis. Therapy. 2005;2(5):787–96.
212. Cappetta D, De Angelis A, Sapio L, Prezioso L, Illiano M, Quaini F, et al. Oxidative stress and cellular response to doxorubicin: A common factor in the complex milieu of anthracycline cardiotoxicity. Vol. 2017, Oxidative Medicine and Cellular Longevity. Hindawi Limited; 2017.
213. Rana T, Chakrabarti A, Freeman M, Biswas S. Doxorubicin-mediated bone loss in breast cancer bone metastases is driven by an interplay between oxidative stress and induction of TGFβ. PLoS One. 2013;8(10).
214. Shusterman S, Meadows AT. Long term survivors of childhood leukemia. Vol. 7, Current Opinion in Hematology. 2000. p. 217–22.
215. Hadji P, Ziller M, Maskow C, Albert U, Kalder M. The influence of chemotherapy on bone mineral density, quantitative ultrasonometry and bone turnover in pre-menopausal women with breast cancer. Eur J Cancer. 2009 Dec;45(18):3205–12.
216. Van Leeuwen BL, Kamps WA, Hartel RM, Veth RPH, Sluiter WJ, Hoekstra HJ. Effect of single chemotherapeutic agents on the growing skeleton of the rat. Ann Oncol. 2000;11(9):1121–6.
217. Friedlaender GE, Tross RB, Doganis AC, Kirkwood JM, Baron R. Effects of chemotherapeutic agents on bone. I. Short-term methotrexate and doxorubicin (adriamycin) treatment in a rat model. J Bone Jt Surg - Ser A. 1984;66(4):602–7.
218. Young DM, Fioravanti JL, Olson HM, Prieur DJ. Chemical and morphologic alterations of rabbit bone induced by adriamycin. Calcif Tissue Res. 1975 Dec;18(1):47–63.
219. Glackin CA, Murray EJ, Murray SS. Doxorubicin inhibits differentiation and enhances expression of the helix-loop-helix genes Id and mTwi in mouse osteoblastic cells. Biochem Int. 1992 Oct;28(1):67–75.
220. Asensio-López MC, Soler F, Pascual-Figal D, Fernández-Belda F, Lax A. Doxorubicin-induced oxidative stress: The protective effect of nicorandil on HL-1 cardiomyocytes. Bachschmid MM, editor. PLoS One. 2017 Feb;12(2):e0172803.
221. Murgia D, Mauceri R, Campisi G, De Caro V. Advance on resveratrol application in bone regeneration: Progress and perspectives for use in oral and maxillofacial surgery. Biomolecules. 2019;9(3).

222. Zainabadi K. Drugs targeting SIRT1, a new generation of therapeutics for osteoporosis and other bone related disorders? Vol. 143, Pharmacological Research. Academic Press; 2019. p. 97–105.
223. Heo JR, Kim SM, Hwang KA, Kang JH, Choi KC. Resveratrol induced reactive oxygen species and endoplasmic reticulum stress-mediated apoptosis, and cell cycle arrest in the A375SM malignant melanoma cell line. Int J Mol Med. 2018 Sep;42(3):1427–35.
224. Song J, Huang Y, Zheng W, Yan J, Cheng M, Zhao R, et al. Resveratrol reduces intracellular reactive oxygen species levels by inducing autophagy through the AMPK-mTOR pathway. Front Med. 2018 Dec;12(6):697–706.
225. Luo Q, Liu S, Xie L, Yu Y, Zhou L, Feng Y, et al. Resveratrol Ameliorates Glucocorticoid-Induced Bone Damage in a Zebrafish Model. Front Pharmacol. 2019;10:195.
226. Zhao L, Wang Y, Wang Z, Xu Z, Zhang Q, Yin M. Effects of dietary resveratrol on excess-iron-induced bone loss via antioxidative character. J Nutr Biochem. 2015 Nov;26(11):1174–82.
227. Bo S, Gambino R, Ponzo V, Cioffi I, Goitre I, Evangelista A, et al. Effects of resveratrol on bone health in type 2 diabetic patients. A double-blind randomized-controlled trial. Nutr Diabetes. 2018 Dec;8(1):51.
228. Mohamadin AM, Elberry AA, Abdel Gawad HS, Morsy GM, Al-Abbasi FA. Protective Effects of Simvastatin, a Lipid Lowering Agent, against Oxidative Damage in Experimental Diabetic Rats [Internet]. Vol. 2011, Journal of Lipids. 2011. p. 1–13.
229. Yu SM, Kim SJ. The thymoquinone-induced production of reactive oxygen species promotes dedifferentiation through the ERK pathway and inflammation through the p38 and PI3K pathways in rabbit articular chondrocytes. Int J Mol Med. 2015 Feb;35(2):325–32.
230. Zhang ZZ, Song L, Zhang ZY, Lv MM. Control-released Alpha-lipoic acid-loaded PLGA microspheres enhance bone formation in type 2 diabetic rat model. Int J Clin Exp Pathol. 2017;10(9):10019–31.
231. Markiewicz-Górka I, Pawlas K, Jaremków A, Januszewska L, Pawłowski P, Pawlas N. Alleviating effect of α-lipoic acid and magnesium on cadmium-induced inflammatory processes, oxidative stress and bone metabolism disorders in wistar rats. Int J Environ Res Public Health. 2019 Nov;16(22).
232. Lu SY, Wang CY, Jin Y, Meng Q, Liu Q, Liu ZH, et al. The osteogenesis-promoting effects of alpha-lipoic acid against glucocorticoid-induced osteoporosis through the NOX4, NF-kappaB, JNK and PI3K/AKT pathways. Sci Rep. 2017 Dec;7(1):1–16.
233. Kim B, Lee SH, Song SJ, Kim WH, Song ES, Lee JC, et al. Protective Effects of Melon Extracts on Bone Strength, Mineralization, and Metabolism in Rats with Ovariectomy-Induced Osteoporosis. Antioxidants. 2019 Aug;8(8):306.
234. Ebert R, Ulmer M, Zeck S, Meissner-Weigl J, Schneider D, Stopper H, et al. Selenium Supplementation Restores the Antioxidative Capacity and Prevents Cell Damage in Bone Marrow Stromal Cells In Vitro. Stem Cells. 2006 May;24(5):1226–35.

235. Liu H, Bian W, Liu S, Huang K. Selenium protects bone marrow stromal cells against hydrogen peroxide-induced inhibition of osteoblastic differentiation by suppressing oxidative stress and ERK signaling pathway. Biol Trace Elem Res. 2012 Dec;150(1–3):441–50.
236. Chavan SN, More U, Mulgund S, Saxena V, Sontakke AN. Effect of supplementation of vitamin C and E on oxidative stress in osteoporosis. Indian J Clin Biochem. 2007;22(2):101–5.
237. Arslan A, Orkun S, Aydin G, Keles I, Tosun A, Arslan M, et al. Effects of ovariectomy and ascorbic acid supplement on oxidative stress parameters and bone mineral density in rats. Libyan J Med. 2011;6(1):1–9.
238. Lleras-Forero L, Winkler C, Schulte-Merker S. Zebrafish and medaka as models for biomedical research of bone diseases. Dev Biol. 2019 Jul;
239. Laizé V, Gavaia PJ, Cancela ML. Fish: A suitable system to model human bone disorders and discover drugs with osteogenic or osteotoxic activities. Drug Discov Today Dis Model. 2014;13(xx):29–37.
240. Witten PE, Harris MP, Huysseune A, Winkler C. Small teleost fish provide new insights into human skeletal diseases. Methods Cell Biol. 2017 Jan;138:321–46.
241. Boswell CW, Ciruna B. Understanding Idiopathic Scoliosis: A New Zebrafish School of Thought. Vol. 33, Trends in Genetics. Elsevier Ltd; 2017. p. 183–96.
242. Howe K, Clark MD, Torroja CF, Torrance J, Berthelot C, Muffato M, et al. The zebrafish reference genome sequence and its relationship to the human genome. Nature. 2013 Apr;496(7446):498–503.
243. Kasahara M, Naruse K, Sasaki S, Nakatani Y, Qu W, Ahsan B, et al. The medaka draft genome and insights into vertebrate genome evolution. Nature. 2007 Jun;447(7145):714–9.
244. Tavares B, Santos Lopes S. The importance of Zebrafish in biomedical research. Acta Med Port. 2013;26(5):583–92.
245. Lopez-Baez JC, Simpson DJ, Forero LLl, Zeng Z, Brunsdon H, Salzano A, et al. Wilms tumor 1b defines a wound-specific sheath cell subpopulation associated with notochord repair. Elife. 2018 Feb;7.
246. Geurtzen K, Knopf F, Wehner D, Huitema LFA, Schulte-Merker S, Weidinger G. Mature osteoblasts dedifferentiate in response to traumatic bone injury in the zebrafish fin and skull. Dev. 2014 Jun;141(11):2225–34.
247. Dasyani M, Tan WH, Sundaram S, Imangali N, Centanin L, Wittbrodt J, et al. Lineage tracing of col10a1 cells identifies distinct progenitor populations for osteoblasts and joint cells in the regenerating fin of medaka (Oryzias latipes). Dev Biol. 2019 Nov;455(1):85–99.
248. Knopf F, Hammond C, Chekuru A, Kurth T, Hans S, Weber CW, et al. Bone regenerates via dedifferentiation of osteoblasts in the zebrafish fin. Dev Cell. 2011 May;20(5):713–24.
249. Vijayakumar P, Laizé V, Cardeira J, Trindade M, Cancela ML. Development of an *In Vitro* Cell System from Zebrafish Suitable to Study Bone Cell Differentiation and Extracellular Matrix Mineralization. Zebrafish. 2013;

250. Marques CL, Rafael MS, Cancela ML, Laizé V. Establishment of primary cell cultures from fish calcified tissues. Cytotechnology. 2007;55(1):9–13.
251. Tiago DM, Laizé V, Cancela ML, Aureliano M. Impairment of mineralization by metavanadate and decavanadate solutions in a fish bone-derived cell line. Cell Biol Toxicol. 2008 Jun;24(3):253–63.
252. Pasqualetti S, Banfi G, Mariotti M. Osteoblast and osteoclast behavior in zebrafish cultured scales. Cell Tissue Res. 2012 Oct;350(1):69–75.
253. Suzuki N, Hattori A. Bisphenol a suppresses osteoclastic and osteoblastic activities in the cultured scales of goldfish. Life Sci. 2003 Sep;73(17):2237–47.
254. Suzuki N, Suzuki T, Kurokawa T. Suppression of osteoclastic activities by calcitonin in the scales of goldfish (freshwater teleost) and nibbler fish (seawater teleost). Peptides. 2000 Jan;21(1):115–24.
255. Carson MA, Nelson J, Cancela ML, Laizé V, Gavaia PJ, Rae M, et al. Screening for osteogenic activity in extracts from Irish marine organisms: The potential of Ceramium pallidum. PLoS One. 2018 Nov;13(11).
256. Tarasco M, Laizé V, Cardeira J, Cancela ML, Gavaia PJ. The zebrafish operculum: A powerful system to assess osteogenic bioactivities of molecules with pharmacological and toxicological relevance. Comp Biochem Physiol Part - C Toxicol Pharmacol. 2017 Jul;197:45–52.
257. Fernández I, Gavaia PJ, Laizé V, Cancela ML. Fish as a model to assess chemical toxicity in bone [Internet]. Vol. 194, Aquatic Toxicology. Elsevier B.V.; 2018. 208–226 p.
258. Luo S, Yang Y, Chen J, Zhong Z, Huang H, Zhang J, et al. Tanshinol stimulates bone formation and attenuates dexamethasone-induced inhibition of osteogenesis in larval zebrafish. J Orthop Transl. 2016 Jan;4:35–45.
259. Zhao Y, Wang HL, Li TT, Yang F, Tzeng CM. Baicalin Ameliorates Dexamethasone-Induced Osteoporosis by Regulation of the RANK/RANKL/OPG Signaling Pathway . Drug Des Devel Ther. 2020 Jan;Volume 14:195–206.
260. Luo SY, Chen JF, Zhong ZG, Lv XH, Yang YJ, Zhang JJ, et al. Salvianolic acid B stimulates osteogenesis in dexamethasone-treated zebrafish larvae. Acta Pharmacol Sin. 2016 Sep;37(10):1370–80.
261. Anampa J, Makower D, Sparano JA. Progress in adjuvant chemotherapy for breast cancer: an overview. BMC Med. 2015 Aug;13:195.
262. Kanter PM, Schwartz HS. Adriamycin-induced DNA damage in human leukemia cells. Leuk Res. 1979;3(5):277–83.
263. Yi X, Bekeredjian R, DeFilippis NJ, Siddiquee Z, Fernandez E, Shohet R V. Transcriptional analysis of doxorubicin-induced cardiotoxicity. Am J Physiol Heart Circ Physiol. 2006 Mar;290(3):H1098-102.
264. Powis G. Free radical formation by antitumor quinones. Free Radic Biol Med. 1989;6(1):63–101.
265. Doroshow JH. Effect of anthracycline antibiotics on oxygen radical formation in rat heart. Cancer Res. 1983 Feb;43(2):460–72.
266. Yin J, Guo J, Zhang Q, Cui L, Zhang L, Zhang T, et al. Doxorubicin-

induced mitophagy and mitochondrial damage is associated with dysregulation of the PINK1/parkin pathway. Toxicol In Vitro. 2018 Sep;51:1–10.
267. Gutteridge JMC, Quinlan GJ. Free radical damage to deoxyribose by anthracycline, aureolic acid and aminoquinone antitumour antibiotics: An essential requirement for iron, semiquinones and hydrogen peroxide. Biochem Pharmacol. 1985 Dec;34(23):4099–103.
268. Feinstein E, Canaani E, Weiner LM. Dependence of nucleic acid degradation on in situ free-radical production by Adriamycin. Biochemistry. 2002;32(48):13156–61.
269. Huertas JR, Battino M, Lenaz G, Mataix FJ. Changes in mitochondrial and microsomal rat liver coenzyme Q9, and Q10 content induced by dietary fat and endogenous lipid peroxidation. FEBS Lett. 1991 Aug;287(1–2):89–92.
270. Huertas JR, Battino M, Mataix FJ, Lenaz G. Cytochrome oxidase induction after oxidative stress induced by adriamycin in liver of rats fed with dietary olive oil. Biochem Biophys Res Commun. 1991 Nov;181(1):375–82.
271. Huertas JR, Battino M, Barzanti V, Maranesi M, Parenti-Castelli G, Littarru GP, et al. Mitochondrial and microsomal cholesterol mobilization after oxidative stress induced by adriamycin in rats fed with dietary olive and corn oil. Life Sci. 1992 Jan;50(26):2111–8.
272. Mataix J, Mañas M, Quiles J, Battino M, Cassinello M, Lopez-Frias M, et al. Coenzyme Q content depends upon oxidative stress and dietary fat unsaturation. Mol Aspects Med. 1997 Jan;18(SUPPL.):129–35.
273. Quiles JL, Ramirez-Tortosa MC, Huertas JR, Ibañez S, Gomez JA, Battino M, et al. Olive oil supplemented with vitamin E affects mitochondrial coenzyme Q levels in liver of rats after an oxidative stress induced by adriamycin. BioFactors. 1999 Jan;9(2–4):331–6.
274. Quiles JL, Ramírez-Tortosa MC, Ibéñez S, Gonzélez JA, Duthie GG, Fiuertas JR, et al. Vitamin E Supplementation Increases the Stability and the In Vivo Antioxidant Capacity of Refined Olive Oil. Free Radic Res. 1999;31(SUPPL.):129–35.
275. Mathis KM, Sturgeon KM, Winkels RM, Wiskemann J, De Souza MJ, Schmitz KH. Bone resorption and bone metastasis risk. Med Hypotheses. 2018 Sep;118:36–41.
276. Giordo R, Nasrallah GK, Al-Jamal O, Paliogiannis P, Pintus G. Resveratrol Inhibits Oxidative Stress and Prevents Mitochondrial Damage Induced by Zinc Oxide Nanoparticles in Zebrafish (Danio rerio). Int J Mol Sci. 2020 May;21(11):3838.
277. Feng J, Liu S, Ma S, Zhao J, Zhang W, Qi W, et al. Protective effects of resveratrol on postmenopausal osteoporosis: regulation of SIRT1-NF-κB signaling pathway. Acta Biochim Biophys Sin (Shanghai). 2014 Dec;46(12):1024–33.
278. Quarles LD, Wenstrup RJ, Castillo SA, Drezner MK. Aluminum-induced mitogenesis in MC3T3-E1 osteoblasts: potential mechanism underlying neoosteogenesis. Endocrinology. 1991 Jun;128(6):3144–51.
279. Quarles LD, Yohay DA, Lever LW, Caton R, Wenstrup RJ. Distinct

proliferative and differentiated stages of murine MC3T3-E1 cells in culture: an in vitro model of osteoblast development. J bone Miner Res Off J Am Soc Bone Miner Res. 1992 Jun;7(6):683–92.
280. Wang D, Christensen K, Chawla K, Xiao G, Krebsbach PH, Franceschi RT. Isolation and characterization of MC3T3-E1 preosteoblast subclones with distinct in vitro and in vivo differentiation/mineralization potential. J bone Miner Res Off J Am Soc Bone Miner Res. 1999 Jun;14(6):893–903.
281. Pombinho AR, Laizé V, Molha DM, Marques SMP, Cancela ML. Development of two bone-derived cell lines from the marine teleost Sparus aurata; evidence for extracellular matrix mineralization and cell-type-specific expression of matrix Gla protein and osteocalcin. Cell Tissue Res. 2004;315(3):393–406.
282. Chomczynski P, Sacchi N. Single-step method of RNA isolation by acid guanidinium thiocyanate-phenol-chloroform extraction. Anal Biochem. 1987 Apr;162(1):156–9.
283. QIAGEN CLC Genomics Workbench | QIAGEN Digital Insights [Internet].
284. Mortazavi A, Williams BA, McCue K, Schaeffer L, Wold B. Mapping and quantifying mammalian transcriptomes by RNA-Seq. Nat Methods. 2008;5(7):621–8.
285. Robinson MD, McCarthy DJ, Smyth GK. edgeR: a Bioconductor package for differential expression analysis of digital gene expression data. Bioinformatics. 2009/11/11. 2010 Jan;26(1):139–40.
286. Raza K, Mishra A. A Novel Anticlustering Filtering Algorithm for the Prediction of Genes as a Drug Target. Am J Biomed Eng. 2012 Dec;2(5):206–11.
287. Ge SX, Son EW, Yao R. iDEP: an integrated web application for differential expression and pathway analysis of RNA-Seq data. BMC Bioinformatics. 2018;19(1):534.
288. Liao Y, Wang J, Jaehnig EJ, Shi Z, Zhang B. WebGestalt 2019: gene set analysis toolkit with revamped UIs and APIs. Nucleic Acids Res. 2019 Jul;47(W1):W199–205.
289. Yang F, Chen H, Liu Y, Yin K, Wang Y, Li X, et al. Doxorubicin caused apoptosis of mesenchymal stem cells via p38, JNK and p53 Pathway. Cell Physiol Biochem. 2013;32(4):1072–82.
290. Bardou P, Mariette J, Escudié F, Djemiel C, Klopp C. jvenn: an interactive Venn diagram viewer. BMC Bioinformatics. 2014;15(1):293.
291. Jang J, Jung Y, Chae S, Chung SI, Kim SM, Yoon Y. WNT/β-catenin pathway modulates the TNF-α-induced inflammatory response in bronchial epithelial cells. Biochem Biophys Res Commun. 2017 Mar;484(2):442–9.
292. Aubrey BJ, Kelly GL, Janic A, Herold MJ, Strasser A. How does p53 induce apoptosis and how does this relate to p53-mediated tumour suppression? Cell Death Differ. 2018;25(1):104–13.
293. Painter SE, Kleerekoper M, Camacho PM. Secondary osteoporosis: a review of the recent evidence. Endocr Pract Off J Am Coll Endocrinol Am Assoc Clin Endocrinol. 2006;12(4):436–45.
294. Harper KD, Weber TJ. Secondary osteoporosis. Diagnostic considerations.

Endocrinol Metab Clin North Am. 1998 Jun;27(2):325–48.
295. Pfeilschifter J, Diel IJ. Osteoporosis Due to Cancer Treatment: Pathogenesis and Management. J Clin Oncol. 2000 Apr;18(7):1570–93.
296. McSweeney KM, Bozza WP, Alterovitz WL, Zhang B. Transcriptomic profiling reveals p53 as a key regulator of doxorubicin-induced cardiotoxicity. Cell death Discov. 2019 Jun;5:102.
297. Williams AB, Schumacher B. p53 in the DNA-Damage-Repair Process. Cold Spring Harb Perspect Med. 2016 May;6(5).
298. Kumar R, Herbert PE, Warrens AN. An introduction to death receptors in apoptosis. Int J Surg. 2005;3(4):268–77.
299. Ferrajoli A, Keating MJ, Manshouri T, Giles FJ, Dey A, Estrov Z, et al. The clinical significance of tumor necrosis factor-alpha plasma level in patients having chronic lymphocytic leukemia. Blood. 2002 Aug;100(4):1215–9.
300. Pietsch EC, Sykes SM, McMahon SB, Murphy ME. The p53 family and programmed cell death. Oncogene. 2008 Oct;27(50):6507–21.
301. Gottlieb E, Vousden KH. p53 regulation of metabolic pathways. Cold Spring Harb Perspect Biol. 2009/12/02. 2010 Apr;2(4):a001040–a001040.
302. Yu T, Wang Z, You X, Zhou H, He W, Li B, et al. Resveratrol promotes osteogenesis and alleviates osteoporosis by inhibiting p53. Aging (Albany NY). 2020/05/27. 2020 May;12(11):10359–69.
303. Monteith GR, Prevarskaya N, Roberts-Thomson SJ. The calcium–cancer signalling nexus. Nat Rev Cancer. 2017;17(6):373–80.
304. Wallace KB. Adriamycin-induced interference with cardiac mitochondrial calcium homeostasis. Cardiovasc Toxicol. 2007;7(2):101–7.
305. Bong AHL, Bassett JJ, Roberts-Thomson SJ, Monteith GR. Assessment of doxorubicin-induced remodeling of Ca(2+) signaling and associated Ca(2+) regulating proteins in MDA-MB-231 breast cancer cells. Biochem Biophys Res Commun. 2020 Feb;522(2):532–8.
306. Kanai Y, Yasoda A, Mori KP, Watanabe-Takano H, Nagai-Okatani C, Yamashita Y, et al. Circulating osteocrin stimulates bone growth by limiting C-type natriuretic peptide clearance. J Clin Invest. 2017/10/09. 2017 Nov;127(11):4136–47.
307. Moffatt P, Thomas GP. Osteocrin – Beyond just another bone protein? Cell Mol Life Sci. 2009;66(7):1135–9.
308. Thomas G, Moffatt P, Salois P, Gaumond MH, Gingras R, Godin E, et al. Osteocrin, a novel bone-specific secreted protein that modulates the osteoblast phenotype. J Biol Chem. 2003 Dec;278(50):50563–71.
309. Bord S, Ireland DC, Moffatt P, Thomas GP, Compston JE. Characterization of osteocrin expression in human bone. J Histochem Cytochem. 2005;53(10):1181–7.
310. Moffatt P, Thomas G, Sellin K, Bessette MC, Lafrenière F, Akhouayri O, et al. Osteocrin is a specific ligand of the natriuretic Peptide clearance receptor that modulates bone growth. J Biol Chem. 2007 Dec;282(50):36454–62.
311. Chiba A, Watanabe-Takano H, Terai K, Fukui H, Miyazaki T, Uemura M, et al. Osteocrin, a peptide secreted from the heart and other tissues,

contributes to cranial osteogenesis and chondrogenesis in zebrafish. Development. 2017 Jan;144(2):334–44.
312. El-Mowafy AM, Alkhalaf M, Jaffal SM. Nongenomic activation of the GC-A enzyme by resveratrol and estradiol downstream from membrane estrogen receptors in human coronary arterial cells. Nutr Metab Cardiovasc Dis. 2007 Sep;17(7):508–16.
313. Ataman B, Boulting GL, Harmin DA, Yang MG, Baker-Salisbury M, Yap EL, et al. Evolution of Osteocrin as an activity-regulated factor in the primate brain. Nature. 2016;539(7628):242–7.
314. Saha S, Li Y, Lappas G, Anand-Srivastava MB. Activation of natriuretic peptide receptor-C attenuates the enhanced oxidative stress in vascular smooth muscle cells from spontaneously hypertensive rats: implication of Gialpha protein. J Mol Cell Cardiol. 2008 Feb;44(2):336–44.
315. Yasui A, Nishizawa H, Okuno Y, Morita K, Kobayashi H, Kawai K, et al. Foxo1 represses expression of musclin, a skeletal muscle-derived secretory factor. Biochem Biophys Res Commun. 2007 Dec;364(2):358–65.
316. Hu C, Zhang X, Zhang N, Wei WY, Li LL, Ma ZG, et al. Osteocrin attenuates inflammation, oxidative stress, apoptosis, and cardiac dysfunction in doxorubicin-induced cardiotoxicity. Clin Transl Med. 2020/07/03. 2020 Jul;10(3):e124–e124.
317. Thannickal VJ, Fanburg BL. Reactive oxygen species in cell signaling. Am J Physiol Lung Cell Mol Physiol. 2000 Dec;279(6):L1005-28.
318. Dröge W. Free radicals in the physiological control of cell function. Physiol Rev. 2002 Jan;82(1):47–95.
319. Lee NK, Choi YG, Baik JY, Han SY, Jeong DW, Bae YS, et al. A crucial role for reactive oxygen species in RANKL-induced osteoclast differentiation. Blood. 2005 Aug;106(3):852–9.
320. H H, Ha H, Bok Kwak H, Woong Lee S, Mi Jin H, Kim HM, et al. Reactive oxygen species mediate RANK signaling in osteoclasts. Exp Cell Res. 2004 Dec;301(2):119–27.
321. Jiang F, Zhang Y, Dusting GJ. NADPH oxidase-mediated redox signaling: roles in cellular stress response, stress tolerance, and tissue repair. Pharmacol Rev. 2011 Mar;63(1):218–42.
322. Hirotani H, Tuohy NA, Woo JT, Stern PH, Clipstone NA. The calcineurin/nuclear factor of activated T cells signaling pathway regulates osteoclastogenesis in RAW264.7 cells. J Biol Chem. 2004 Apr;279(14):13984–92.
323. Yang S, Zhang Y, Ries W, Key L. Expression of Nox4 in osteoclasts. J Cell Biochem. 2004 May;92(2):238–48.
324. Sasaki H, Yamamoto H, Tominaga K, Masuda K, Kawai T, Teshima-Kondo S, et al. NADPH oxidase-derived reactive oxygen species are essential for differentiation of a mouse macrophage cell line (RAW264.7) into osteoclasts. J Med Invest. 2009 Feb;56(1–2):33–41.
325. Kim K, Kim JH, Lee J, Jin HM, Lee SH, Fisher DE, et al. Nuclear factor of activated T cells c1 induces osteoclast-associated receptor gene

expression during tumor necrosis factor-related activation-induced cytokine-mediated osteoclastogenesis. J Biol Chem. 2005 Oct;280(42):35209–16.
326. Park HJ, Carr JR, Wang Z, Nogueira V, Hay N, Tyner AL, et al. FoxM1, a critical regulator of oxidative stress during oncogenesis. EMBO J. 2009 Oct;28(19):2908–18.
327. Laoukili J, Kooistra MRH, Brás A, Kauw J, Kerkhoven RM, Morrison A, et al. FoxM1 is required for execution of the mitotic programme and chromosome stability. Nat Cell Biol. 2005 Feb;7(2):126–36.
328. Wang IC, Chen YJ, Hughes D, Petrovic V, Major ML, Park HJ, et al. Forkhead box M1 regulates the transcriptional network of genes essential for mitotic progression and genes encoding the SCF (Skp2-Cks1) ubiquitin ligase. Mol Cell Biol. 2005 Dec;25(24):10875–94.
329. Yao S, Fan LYN, Lam EWF. The FOXO3-FOXM1 axis: A key cancer drug target and a modulator of cancer drug resistance. Semin Cancer Biol. 2018 Jun;50:77–89.
330. de Olano N, Koo CY, Monteiro LJ, Pinto PH, Gomes AR, Aligue R, et al. The p38 MAPK-MK2 axis regulates E2F1 and FOXM1 expression after epirubicin treatment. Mol Cancer Res. 2012 Sep;10(9):1189–202.
331. Behren A, Mühlen S, Acuna Sanhueza GA, Schwager C, Plinkert PK, Huber PE, et al. Phenotype-assisted transcriptome analysis identifies FOXM1 downstream from Ras-MKK3-p38 to regulate in vitro cellular invasion. Oncogene. 2010 Mar;29(10):1519–30.
332. Kim HN, Han L, Iyer S, de Cabo R, Zhao H, O'Brien CA, et al. Sirtuin1 Suppresses Osteoclastogenesis by Deacetylating FoxOs. Mol Endocrinol. 2015 Oct;29(10):1498–509.
333. Artsi H, Cohen-Kfir E, Gurt I, Shahar R, Bajayo A, Kalish N, et al. The Sirtuin1 activator SRT3025 down-regulates sclerostin and rescues ovariectomy-induced bone loss and biomechanical deterioration in female mice. Endocrinology. 2014 Sep;155(9):3508–15.
334. Su JL, Yang CY, Zhao M, Kuo ML, Yen ML. Forkhead proteins are critical for bone morphogenetic protein-2 regulation and anti-tumor activity of resveratrol. J Biol Chem. 2007 Jul;282(27):19385–98.
335. Momken I, Stevens L, Bergouignan A, Desplanches D, Rudwill F, Chery I, et al. Resveratrol prevents the wasting disorders of mechanical unloading by acting as a physical exercise mimetic in the rat. FASEB J Off Publ Fed Am Soc Exp Biol. 2011 Oct;25(10):3646–60.
336. Mercken EM, Mitchell SJ, Martin-Montalvo A, Minor RK, Almeida M, Gomes AP, et al. SRT2104 extends survival of male mice on a standard diet and preserves bone and muscle mass. Aging Cell. 2014 Oct;13(5):787–96.
337. Pearson KJ, Baur JA, Lewis KN, Peshkin L, Price NL, Labinskyy N, et al. Resveratrol delays age-related deterioration and mimics transcriptional aspects of dietary restriction without extending life span. Cell Metab. 2008 Aug;8(2):157–68.
338. Boissy P, Andersen TL, Abdallah BM, Kassem M, Plesner T, Delaissé JM.

Resveratrol inhibits myeloma cell growth, prevents osteoclast formation, and promotes osteoblast differentiation. Cancer Res. 2005 Nov;65(21):9943–52.
339. He X, Andersson G, Lindgren U, Li Y. Resveratrol prevents RANKL-induced osteoclast differentiation of murine osteoclast progenitor RAW 264.7 cells through inhibition of ROS production. Biochem Biophys Res Commun. 2010 Oct;401(3):356–62.
340. Shakibaei M, Buhrmann C, Mobasheri A. Resveratrol-mediated SIRT-1 interactions with p300 modulate receptor activator of NF-kappaB ligand (RANKL) activation of NF-kappaB signaling and inhibit osteoclastogenesis in bone-derived cells. J Biol Chem. 2011 Apr;286(13):11492–505.
341. Rubiolo JA, Mithieux G, Vega FV. Resveratrol protects primary rat hepatocytes against oxidative stress damage: activation of the Nrf2 transcription factor and augmented activities of antioxidant enzymes. Eur J Pharmacol. 2008 Sep;591(1–3):66–72.
342. Shin SM, Cho IJ, Kim SG. Resveratrol protects mitochondria against oxidative stress through AMP-activated protein kinase-mediated glycogen synthase kinase-3beta inhibition downstream of poly(ADP-ribose)polymerase-LKB1 pathway. Mol Pharmacol. 2009 Oct;76(4):884–95.
343. Kang IS, Kim C. NADPH oxidase gp91(phox) contributes to RANKL-induced osteoclast differentiation by upregulating NFATc1. Sci Rep. 2016 Nov;6:38014.
344. Agidigbi TS, Kim C. Reactive Oxygen Species in Osteoclast Differentiation and Possible Pharmaceutical Targets of ROS-Mediated Osteoclast Diseases. Int J Mol Sci. 2019 Jul;20(14).
345. Jeoung NH. Pyruvate Dehydrogenase Kinases: Therapeutic Targets for Diabetes and Cancers. Diabetes Metab J. 2015;39(3):188.
346. He Q, Harris N, Ren J, Han X. Mitochondria-targeted antioxidant prevents cardiac dysfunction induced by tafazzin gene knockdown in cardiac myocytes. Oxid Med Cell Longev. 2014;2014.
347. Zhou L, Kuai F, Shi Q, Yang H. Doxorubicin restrains osteogenesis and promotes osteoclastogenesis in vitro. Am J Transl Res. 2020 Sep;12(9):5640–54.
348. Li Q, Zhang J, Liu D, Liu Y, Zhou Y. Force-induced decline of FOXM1 in human periodontal ligament cells contributes to osteoclast differentiation. Angle Orthod. 2019/03/28. 2019 Sep;89(5):804–11.
349. Caetano-Lopes J, Henke K, Urso K, Duryea J, Charles JF, Warman ML, et al. Unique and non-redundant function of csf1r paralogues in regulation and evolution of post-embryonic development of the zebrafish. Development. 2020 Jan;147(2):dev181834.
350. Burstone MS. Histochemical demonstration of acid phosphatase activity in osteoclasts. J Histochem Cytochem. 1959 Jan;7(1):39–41.
351. Viegas MN, Dias J, Cancela ML, Laizé V. Polyunsaturated fatty acids regulate cell proliferation, extracellular matrix mineralization and gene expression in a gilthead seabream skeletal cell line. J Appl Ichthyol. 2012

Jun;28(3):427–32.
352. Halasi M, Pandit B, Wang M, Nogueira V, Hay N, Gartel AL. Combination of oxidative stress and FOXM1 inhibitors induces apoptosis in cancer cells and inhibits xenograft tumor growth. Am J Pathol. 2013 Jul;183(1):257–65.
353. Buchner M, Park E, Geng H, Klemm L, Flach J, Passegué E, et al. Identification of FOXM1 as a therapeutic target in B-cell lineage acute lymphoblastic leukaemia. Nat Commun. 2015 Mar;6:6471.
354. Ge H, Tollner TL, Hu Z, Dai M, Li X, Guan H, et al. The importance of mitochondrial metabolic activity and mitochondrial DNA replication during oocyte maturation in vitro on oocyte quality and subsequent embryo developmental competence. Mol Reprod Dev. 2012 Jun;79(6):392–401.
355. Le Gal K, Wiel C, Ibrahim MX, Henricsson M, Sayin VI, Bergo MO. Mitochondria-Targeted Antioxidants MitoQ and MitoTEMPO Do Not Influence BRAF-Driven Malignant Melanoma and KRAS-Driven Lung Cancer Progression in Mice. Antioxidants (Basel, Switzerland). 2021 Jan;10(2).
356. Yagi M, Miyamoto T, Sawatani Y, Iwamoto K, Hosogane N, Fujita N, et al. DC-STAMP is essential for cell-cell fusion in osteoclasts and foreign body giant cells. J Exp Med. 2005 Aug;202(3):345–51.
357. Pirola L, Fröjdö S. Resveratrol: one molecule, many targets. IUBMB Life. 2008 May;60(5):323–32.
358. Howitz KT, Bitterman KJ, Cohen HY, Lamming DW, Lavu S, Wood JG, et al. Small molecule activators of sirtuins extend Saccharomyces cerevisiae lifespan. Nature. 2003;425(6954):191–6.
359. Li Y, Bäckesjö CM, Haldosén LA, Lindgren U. Resveratrol inhibits proliferation and promotes apoptosis of osteosarcoma cells. Eur J Pharmacol. 2009 May;609(1–3):13–8.
360. Bäckesjö CM, Li Y, Lindgren U, Haldosén LA. Activation of Sirt1 decreases adipocyte formation during osteoblast differentiation of mesenchymal stem cells. J bone Miner Res Off J Am Soc Bone Miner Res. 2006 Jul;21(7):993–1002.
361. Gehm BD, McAndrews JM, Chien PY, Jameson JL. Resveratrol, a polyphenolic compound found in grapes and wine, is an agonist for the estrogen receptor. Proc Natl Acad Sci U S A. 1997 Dec;94(25):14138–43.
362. Shevde NK, Bendixen AC, Dienger KM, Pike JW. Estrogens suppress RANK ligand-induced osteoclast differentiation via a stromal cell independent mechanism involving c-Jun repression. Proc Natl Acad Sci U S A. 2000 Jul;97(14):7829–34.
363. Savinova O V, Hoffmann A, Ghosh G. The Nfkb1 and Nfkb2 proteins p105 and p100 function as the core of high-molecular-weight heterogeneous complexes. Mol Cell. 2009 Jun;34(5):591–602.
364. Yeung F, Hoberg JE, Ramsey CS, Keller MD, Jones DR, Frye RA, et al. Modulation of NF-kappaB-dependent transcription and cell survival by the SIRT1 deacetylase. EMBO J. 2004 Jun;23(12):2369–80.
365. Mills PJ, Parker B, Dimsdale JE, Sadler GR, Ancoli-Israel S. The relationship between fatigue and quality of life and inflammation during

anthracycline-based chemotherapy in breast cancer. Biol Psychol. 2005 Apr;69(1):85–96.
366. Kodama J, Kaito T. Osteoclast Multinucleation: Review of Current Literature. Int J Mol Sci. 2020 Aug;21(16):5685.
367. Dai R, Wu Z, Chu HY, Lu J, Lyu A, Liu J, et al. Cathepsin K: The Action in and Beyond Bone. Front cell Dev Biol. 2020;8:433.
368. Medina C, Radomski MW. Role of matrix metalloproteinases in intestinal inflammation. J Pharmacol Exp Ther. 2006 Sep;318(3):933–8.
369. Menzel K, Hausmann M, Obermeier F, Schreiter K, Dunger N, Bataille F, et al. Cathepsins B, L and D in inflammatory bowel disease macrophages and potential therapeutic effects of cathepsin inhibition in vivo. Clin Exp Immunol. 2006 Oct;146(1):169–80.
370. Kaczmarek A, Brinkman BM, Heyndrickx L, Vandenabeele P, Krysko D V. Severity of doxorubicin-induced small intestinal mucositis is regulated by the TLR-2 and TLR-9 pathways. J Pathol. 2012 Mar;226(4):598–608.
371. Savard J, Liu L, Natarajan L, Rissling MB, Neikrug AB, He F, et al. Breast cancer patients have progressively impaired sleep-wake activity rhythms during chemotherapy. Sleep. 2009 Sep;32(9):1155–60.
372. Lira FS, Esteves AM, Pimentel GD, Rosa JC, Frank MK, Mariano MO, et al. Sleep pattern and locomotor activity are impaired by doxorubicin in non-tumor-bearing rats. Sleep Sci (Sao Paulo, Brazil). 2016;9(3):232–5.
373. Sanford SD, Wagner LI, Beaumont JL, Butt Z, Sweet JJ, Cella D. Longitudinal prospective assessment of sleep quality: before, during, and after adjuvant chemotherapy for breast cancer. Support care cancer Off J Multinatl Assoc Support Care Cancer. 2013 Apr;21(4):959–67.
374. Olson RD, Mushlin PS. Doxorubicin cardiotoxicity: analysis of prevailing hypotheses. FASEB J. 1990 Oct;4(13):3076–86.
375. De Beer EL, Bottone AE, Voest EE. Doxorubicin and mechanical performance of cardiac trabeculae after acute and chronic treatment: a review. Eur J Pharmacol. 2001 Mar;415(1):1–11.
376. Singal P, Li T, Kumar D, Danelisen I, Iliskovic N. Adriamycin-induced heart failure: mechanisms and modulation. Mol Cell Biochem 2000 2071. 2000;207(1):77–86.
377. Gianni L, Zweier JL, Levy A, Myers CE. Characterization of the cycle of iron-mediated electron transfer from Adriamycin to molecular oxygen. J Biol Chem. 1985 Jun;260(11):6820–6.
378. Sinha BK, Politi PM. Anthracyclines. Cancer Chemother Biol Response Modif. 1990 Jan;11:45–57.
379. Izquierdo MS, Scolamacchia M, Betancor M, Roo J, Caballero MJ, Terova G, et al. Effects of dietary DHA and α-tocopherol on bone development, early mineralisation and oxidative stress in Sparus aurata (Linnaeus, 1758) larvae. Br J Nutr. 2013 May;109(10):1796–805.
380. Saleh R, Betancor MB, Roo J, Benítez-Santana T, Zamorano MJ, Izquierdo M. Biomarkers of bone development and oxidative stress in gilthead sea bream larvae fed microdiets with several levels of polar lipids and α-tocopherol. Aquac Nutr. 2015 Jun;21(3):341–54.

381. Winston GW, Di Giulio RT. Prooxidant and antioxidant mechanisms in aquatic organisms. Aquat Toxicol. 1991 Apr;19(2):137–61.
382. Ran G, Ying L, Li L, Yan Q, Yi W, Ying C, et al. Resveratrol ameliorates diet-induced dysregulation of lipid metabolism in zebrafish (Danio rerio). PLoS One. 2017 Jul;12(7):e0180865.
383. Poudel S, Izquierdo M, Cancela ML, Gavaia PJ. Reversal of Doxorubicin-Induced Bone Loss and Mineralization by Supplementation of Resveratrol and MitoTEMPO in the Early Development of Sparus aurata. Nutr 2022, Vol 14, Page 1154. 2022 Mar;14(6):1154.
384. Diogo P, Martins G, Quinzico I, Nogueira R, Gavaia PJ, Cabrita E. Electric ultrafreezer (− 150 °C) as an alternative for zebrafish sperm cryopreservation and storage. Fish Physiol Biochem. 2018;44(6):1443–55.
385. Martins G, Diogo P, Pinto W, Gavaia PJ. Early Transition to Microdiets Improves Growth, Reproductive Performance and Reduces Skeletal Anomalies in Zebrafish (Danio rerio). Zebrafish. 2019 Jun;16(3):300–7.
386. Poudel S, Izquierdo M, Cancela ML, Gavaia PJ. Reversal of Doxorubicin-induced bone loss by antioxidant supplement. Bone Reports. 2021;14:100984.
387. Peterman EM, Sullivan C, Goody MF, Rodriguez-Nunez I, Yoder JA, Kim CH. Neutralization of mitochondrial superoxide by superoxide dismutase 2 promotes bacterial clearance and regulates phagocyte numbers in zebrafish. Infect Immun. 2015;83(1):430–40.
388. Diogo P, Martins G, Gavaia P, Pinto W, Dias J, Cancela L, et al. Assessment of nutritional supplementation in phospholipids on the reproductive performance of zebrafish, Danio rerio (Hamilton, 1822). J Appl Ichthyol. 2015 Jun;31(S1):3–9.
389. Westerfield M. The Zebrafish Book: A Guide for the Laboratory Use of Zebrafish Danio (“ Brachydanio Rerio”). University of Oregon; 2007.
390. Martins S, Monteiro JF, Vito M, Weintraub D, Almeida J, Certal AC. Toward an Integrated Zebrafish Health Management Program Supporting Cancer and Neuroscience Research. Zebrafish. 2016 Jul;13 Suppl 1:S47-55.
391. Gavaia PJ, Sarasquete C, Cancela ML. Detection of mineralized structures in early stages of development of marine Teleostei using a modified alcian blue-alizarin red double staining technique for bone and cartilage. Biotech Histochem. 2000;75(2):79–84.
392. Walker MB, Kimmel CB. A two-color acid-free cartilage and bone stain for zebrafish larvae. Biotech Histochem. 2007 Feb;82(1):23–8.
393. Bird NC, Mabee PM. Developmental morphology of the axial skeleton of the zebrafish, Danio rerio (Ostariophysi: Cyprinidae). Dev Dyn. 2003 Nov;228(3):337–57.
394. Dominguez D, Sehnine Z, Castro P, Zamorano MJ, Robaina L, Fontanillas R, et al. Dietary manganese levels for gilthead sea bream (Sparus aurata) fingerlings fed diets high in plant ingredients. Aquaculture. 2020 Dec;529:735614.
395. Xu H, Li C, Zeng Q, Agrawal I, Zhu X, Gong Z. Genome-wide identification of suitable zebrafish Danio rerio reference genes for normalization of gene

expression data by RT-qPCR. J Fish Biol. 2016 Jun;88(6):2095–110.
396. Cardiff RD, Miller CH, Munn RJ. Manual Hematoxylin and Eosin Staining of Mouse Tissue Sections. Cold Spring Harb Protoc. 2014 Jun;2014(6):pdb.prot073411.
397. Fischer AH, Jacobson KA, Rose J, Zeller R. Hematoxylin and Eosin Staining of Tissue and Cell Sections. Cold Spring Harb Protoc. 2008 May;2008(5):pdb.prot4986.
398. Baeverfjord G, Krogdahl A. Development and regression of soybean meal induced enteritis in Atlantic salmon, Salmo salar L., distal intestine: a comparison with the intestines of fasted fish. J Fish Dis. 1996 Sep;19(5):375–87.
399. Magalhães R, Guerreiro I, Santos RA, Coutinho F, Couto A, Serra CR, et al. Oxidative status and intestinal health of gilthead sea bream (Sparus aurata) juveniles fed diets with different ARA/EPA/DHA ratios. Sci Reports 2020 101. 2020 Aug;10(1):1–13.
400. Pang Z, Chong J, Li S, Xia J. MetaboAnalystR 3.0: Toward an Optimized Workflow for Global Metabolomics. Metab 2020, Vol 10, Page 186. 2020 May;10(5):186.
401. Pang Z, Chong J, Zhou G, De Lima Morais DA, Chang L, Barrette M, et al. MetaboAnalyst 5.0: narrowing the gap between raw spectra and functional insights. Nucleic Acids Res. 2021 Jul;49(W1):W388–96.
402. Bijlsma S, Bobeldijk I, Verheij ER, Ramaker R, Kochhar S, Macdonald IA, et al. Large-scale human metabolomics studies: a strategy for data (pre-) processing and validation. Anal Chem. 2006 Jan;78(2):567–74.
403. Yarmohammadi F, Rezaee R, Karimi G. Natural compounds against doxorubicin-induced cardiotoxicity: A review on the involvement of Nrf2/ARE signaling pathway. Phyther Res. 2021 Mar;35(3):1163–75.
404. Pfeiffer T, Krause U, Thome U, Rajewski A, Skorzek M, Scheulen ME. Tissue toxicity of doxorubicin in first and second hyperthermic isolated limb perfusion—an experimental study in dogs. Eur J Surg Oncol. 1997 Oct;23(5):439–44.
405. Ibrahim MA, Ashour OM, Ibrahim YF, EL-Bitar HI, Gomaa W, Abdel-Rahim SR. Angiotensin-converting enzyme inhibition and angiotensin AT1-receptor antagonism equally improve doxorubicin-induced cardiotoxicity and nephrotoxicity. Pharmacol Res. 2009 Nov;60(5):373–81.
406. Zakaria ZZ, Benslimane FM, Nasrallah GK, Shurbaji S, Younes NN, Mraiche F, et al. Using Zebrafish for Investigating the Molecular Mechanisms of Drug-Induced Cardiotoxicity. 2018;
407. Calienni MN, Cagel M, Montanari J, Moretton MA, Prieto MJ, Chiappetta DA, et al. Zebrafish (Danio rerio) model as an early stage screening tool to study the biodistribution and toxicity profile of doxorubicin-loaded mixed micelles. Toxicol Appl Pharmacol. 2018;357(July):106–14.
408. Chang C, Wu SL, Zhao XD, Zhao CT, Li YH. Developmental toxicity of doxorubicin hydrochloride in embryo-larval stages of zebrafish. In: Bio-Medical Materials and Engineering. IOS Press; 2014. p. 909–16.
409. Torno C, Staats S, de Pascual-Teresa S, Rimbach G, Schulz C. Effects of

resveratrol and genistein on growth, nutrient utilization and fatty acid composition of rainbow trout. Animal. 2019 May;13(5):933–40.
410. Wilson WN, Baumgarner BL, Watanabe WO, Alam MS, Kinsey ST. Effects of resveratrol on growth and skeletal muscle physiology of juvenile southern flounder. Comp Biochem Physiol Part A Mol Integr Physiol. 2015;183:27–35.
411. Yang SG, Park HJ, Kim JW, Jung JM, Kim MJ, Jegal HG, et al. Mito-TEMPO improves development competence by reducing superoxide in preimplantation porcine embryos. Sci Reports 2018 81. 2018 Jul;8(1):1–10.
412. Valenzuela CA, Escobar-Aguirre S, Zuloaga R, Vera-Tobar T, Mercado L, Björnsson BT, et al. Stocking density induces differential expression of immune-related genes in skeletal muscle and head kidney of fine flounder (Paralichthys adspersus). Vet Immunol Immunopathol. 2019 Apr;210:23–7.
413. Rigby RJ, Carr J, Orgel K, King SL, Lund PK, Dekaney CM. Intestinal bacteria are necessary for doxorubicin-induced intestinal damage but not for doxorubicin-induced apoptosis. https://doi.org/101080/1949097620161215806. 2016 Sep;7(5):414–23.
414. Kaczmarek A, Brinkman BM, Heyndrickx L, Vandenabeele P, Krysko D V. Severity of doxorubicin-induced small intestinal mucositis is regulated by the TLR-2 and TLR-9 pathways. J Pathol. 2012 Mar;226(4):598–608.
415. Zhu LH, Zhao KL, Chen XL, Xu JX. Impact of weaning and an antioxidant blend on intestinal barrier function and antioxidant status in pigs. J Anim Sci. 2012 Aug;90(8):2581–9.
416. Ahmad N, Ahmad R, Alam MA, Ahmad FJ. Enhancement of oral bioavailability of doxorubicin through surface modified biodegradable polymeric nanoparticles. Chem Cent J. 2018 May;12(1):65.
417. Alhadi Ighwela K, Bin Ahmad A, Abol-Munafi A, Terengganu M. Water Stability and Nutrient Leaching of Different Levels of Maltose Formulated Fish Pellets. 2014 Sep;
418. Watts SA, Powell M, D'Abramo LR. Fundamental approaches to the study of zebrafish nutrition. ILAR J. 2012;53(2):144–60.
419. Prestinicola L, Boglione C, Makridis P, Spanò A, Rimatori V, Palamara E, et al. Environmental Conditioning of Skeletal Anomalies Typology and Frequency in Gilthead Seabream (Sparus aurata L., 1758) Juveniles. Monsonego-Ornan E, editor. PLoS One. 2013 Feb;8(2):e55736.
420. Koumoundouros G, Gagliardi F, Divanach P, Boglione C, Cataudella S, Kentouri M. Normal and abnormal osteological development of caudal fin in Sparus aurata L. fry. Aquaculture. 1997;149(3):215–26.
421. Koumoundouros G, Gagliardi F, Divanach P, Stefanakis S, Kentouri M. Osteological study of the origin and development of the abnormal caudal fin in gilthead sea bream (Sparus aurata) fry. In: Quality in Aquaculture Aquaculture Europe '95 Int Conference,. Trondheim, Norway; 1995. p. 413.
422. Fazenda C, Martins G, Gavaia PJ, Cancela ML, Conceição N. Generation of zebrafish Danio rerio (Hamilton, 1822) transgenic lines overexpressing a heat-shock mediated Gla-rich protein. J Appl Ichthyol. 2018 Apr;34(2):472–80.

423. Fernández I, Hontoria F, Ortiz-Delgado JB, Kotzamanis Y, Estévez A, Zambonino-Infante JL, et al. Larval performance and skeletal deformities in farmed gilthead sea bream (Sparus aurata) fed with graded levels of Vitamin A enriched rotifers (Brachionus plicatilis). Aquaculture. 2008;283(1):102–15.
424. Boglione C, Pulcini D, Scardi M, Palamara E, Russo T, Cataudella S. Skeletal Anomaly Monitoring in Rainbow Trout (Oncorhynchus mykiss, Walbaum 1792) Reared under Different Conditions. PLoS One. 2014 May;9(5):e96983.
425. Divanach P, Boglione C, Menu B, Koumoundouros G, Kentouri M, Cataudella S. Abnormalities in finfish mariculture: An overview of the problem, causes and solutions. In 1996.
426. Klein-Nulend J, Bakker AD, Bacabac RG, Vatsa A, Weinbaum S. Mechanosensation and transduction in osteocytes. Bone. 2013 Jun;54(2):182–90.
427. Bensimon-Brito A, Cardeira J, Cancela ML, Huysseune A, Witten PE. Distinct patterns of notochord mineralization in zebrafish coincide with the localization of Osteocalcin isoform 1 during early vertebral centra formation. BMC Dev Biol. 2012;12(1):28.
428. Lall SP, Kaushik SJ. Nutrition and Metabolism of Minerals in Fish. Anim an open access J from MDPI. 2021 Sep;11(9):2711.
429. Berillis P, Panagiotopoulos N, Boursiaki V, Karapanagiotidis IT, Mente E. Vertebrae length and ultra-structure measurements of collagen fibrils and mineral content in the vertebrae of lordotic gilthead seabreams (Sparus aurata). Micron. 2015 Aug;75:27–33.
430. Lall SP. The Minerals. Fish Nutr. 2003 Jan;259–308.
431. Lall SP, Lewis-McCrea LM. Role of nutrients in skeletal metabolism and pathology in fish — An overview. Aquaculture. 2007 Jul;267(1–4):3–19.
432. Sun M, Wu X, Yu Y, Wang L, Xie D, Zhang Z, et al. Disorders of Calcium and Phosphorus Metabolism and the Proteomics/Metabolomics-Based Research [Internet]. Vol. 8, Frontiers in Cell and Developmental Biology . 2020. p. 928.
433. Carvalho FS, Burgeiro A, Garcia R, Moreno AJ, Carvalho RA, Oliveira PJ. Doxorubicin-Induced Cardiotoxicity: From Bioenergetic Failure and Cell Death to Cardiomyopathy. Med Res Rev. 2014 Jan;34(1):106–35.
434. Filho DW, Giulivi C, Boveris A. Antioxidant defences in marine fish—I. Teleosts. Comp Biochem Physiol Part C Pharmacol Toxicol Endocrinol. 1993 Oct;106(2):409–13.
435. Betancor MB, Nordrum S, Atalah E, Caballero MJ, Benítez-Santana T, Roo J, et al. Potential of three new krill products for seabream larval production. Aquac Res. 2012 Feb;43(3):395–406.
436. Saleh R, Betancor MB, Roo J, Montero D, Zamorano MJ, Izquierdo M. Selenium levels in early weaning diets for gilthead seabream larvae. Aquaculture. 2014;426–427:256–63.
437. Carvalho FR, Fernandes AR, Cancela ML, Gavaia PJ. Improved regeneration and de novo bone formation in a diabetic zebrafish model

treated with paricalcitol and cinacalcet. Wound Repair Regen. 2017 May;25(3):432–42.
438. Li N, Felber K, Elks P, Croucher P, Roehl HH. Tracking gene expression during zebrafish osteoblast differentiation. Dev Dyn. 2009 Feb;238(2):459–66.
439. Boskey AL, Gadaleta S, Gundberg C, Doty SB, Ducy P, Karsenty G. Fourier transform infrared microspectroscopic analysis of bones of osteocalcin-deficient mice provides insight into the function of osteocalcin. Bone. 1998 Sep;23(3):187–96.
440. Balaban RS, Nemoto S, Finkel T. Mitochondria, oxidants, and aging. Cell. 2005 Feb;120(4):483–95.
441. Tian Y, Ma X, Yang C, Su P, Yin C, Qian AR. The impact of oxidative stress on the bone system in response to the space special environment. International Journal of Molecular Sciences. 2017.
442. Boglione C, Gavaia P, Koumoundouros G, Gisbert E, Moren M, Fontagné S, et al. Skeletal anomalies in reared European fish larvae and juveniles. Part 1: normal and anomalous skeletogenic processes. Rev Aquac. 2013 May;5(SUPPL.1):S99–120.
443. Boglione C, Gisbert E, Gavaia P, E. Witten P, Moren M, Fontagné S, et al. Skeletal anomalies in reared European fish larvae and juveniles. Part 2: main typologies, occurrences and causative factors. Rev Aquac. 2013 May;5(SUPPL.1):S121–67.
444. Hamre K, Yúfera M, Rønnestad I, Boglione C, Conceição LEC, Izquierdo M. Fish larval nutrition and feed formulation: knowledge gaps and bottlenecks for advances in larval rearing. Rev Aquac. 2013 May;5(SUPPL.1):S26–58.
445. Faustino M, Power DM. Development of the pectoral, pelvic, dorsal and anal fins in cultured sea bream. J Fish Biol. 1999 May;54(5):1094–110.
446. Faustino M, Power DM. Development of osteological structures in the sea bream: vertebral column and caudal fin complex. J Fish Biol. 1998 Jan;52(1):11–22.
447. Matsuoka M. Comparison of Meristic Variations and Bone Abnormalities between Wild and Laboratory-Reared Red Sea Bream. Japan Agric Res Q JARQ. 2003 Jan;37(1):21–30.
448. Vijayakumar P, Laizé V, Cardeira J, Trindade M, Cancela ML. Development of an in vitro cell system from zebrafish suitable to study bone cell differentiation and extracellular matrix mineralization. Zebrafish. 2013;10(4):500–9.
449. Peterman EM, Sullivan C, Goody MF, Rodriguez-Nunez I, Yoder JA, Kim CH. Neutralization of mitochondrial superoxide by superoxide dismutase 2 promotes bacterial clearance and regulates phagocyte numbers in zebrafish. Infect Immun. 2015;83(1):430–40.
450. Eryalçın KM, Domínguez D, Roo J, Hernandez-Cruz CM, Zamorano MJ, Castro P, et al. Effect of dietary microminerals in early weaning diets on growth, survival, mineral contents and gene expression in gilthead sea bream (Sparus aurata, L) larvae. Aquac Nutr. 2020;26(5):1760–70.

451. Puchtler H, Meloan SN, Terry MS. On the history and mechanism of alizarin and alizarin red S stains for calcium. J Histochem Cytochem. 1969 Feb;17(2):110–24.
452. Kiela PR, Ghishan FK. Physiology of Intestinal Absorption and Secretion. Best Pract Res Clin Gastroenterol. 2016/02/10. 2016 Apr;30(2):145–59.
453. Kiskova T, Kubatka P, Büsselberg D, Kassayova M. The Plant-Derived Compound Resveratrol in Brain Cancer: A Review. Vol. 10, Biomolecules . 2020.
454. Weisbrode SE. Bone and joints. Tomson's special veterinary pathology [Internet]. Tomson's special veterinary pathology. Mosby; 2001. 499–536 p.
455. Moro L, Romanello M, Favia A, Lamanna MP, Lozupone E. Posttranslational Modifications of Bone Collagen Type I are Related to the Function of Rat Femoral Regions. Calcif Tissue Int 2000 662. 2000;66(2):151–6.
456. Lim C, Lovell RT. Pathology of the Vitamin C Deficiency Syndrome in Channel Catfish (Ictalurus punctatus). J Nutr. 1978 Jul;108(7):1137–46.
457. Santamaría JA, Andrades JA, Herráez P, Fernández-Llebrez P, Becerra J. Perinotochordal connective sheet of gilthead sea bream larvae (Sparus aurata, L.) affected by axial malformations: An histochemical and immunocytochemical study. Anat Rec. 1994 Oct;240(2):248–54.
458. Hall BK. Bones and Cartilage: Developmental and Evolutionary Skeletal Biology. 2005.
459. Fragkoulis S, Printzi A, Geladakis G, Katribouzas N, Koumoundouros G. Recovery of haemal lordosis in Gilthead seabream (Sparus aurata L.). Sci Rep. 2019;9(1):9832.
460. Kranenbarg S, Waarsing JH, Muller M, Weinans H, van Leeuwen JL. Lordotic vertebrae in sea bass (Dicentrarchus labrax L.) are adapted to increased loads. J Biomech. 2005;38(6):1239–46.
461. Witten PE, Gil-Martens L, Hall BK, Huysseune A, Obach A. Compressed vertebrae in Atlantic salmon Salmo salar: evidence for metaplastic chondrogenesis as a skeletogenic response late in ontogeny. Dis Aquat Organ. 2005 May;64(3):237–46.
462. Holm E, Gleberzon JS, Liao Y, Sørensen ES, Beier F, Hunter GK, et al. Osteopontin mediates mineralization and not osteogenic cell development in vitro. Biochem J. 2014 Dec;464(3):355–64.
463. Chen J, McKee MD, Nanci A, Sodek J. Bone sialoprotein mRNA expression and ultrastructural localization in fetal porcine calvarial bone: comparisons with osteopontin. Histochem J. 1994;26(1):67–78.
464. Sodek J, Chen J, Nagata T, Kasugai S, Todescan RJ, Li IW, et al. Regulation of osteopontin expression in osteoblasts. Ann N Y Acad Sci. 1995 Apr;760:223–41.
465. Shen C, Yang C, Xu S, Zhao H. Comparison of osteogenic differentiation capacity in mesenchymal stem cells derived from human amniotic membrane (AM), umbilical cord (UC), chorionic membrane (CM), and decidua (DC). Cell Biosci. 2019;9(1):17.

466. Morinobu M, Ishijima M, Rittling SR, Tsuji K, Yamamoto H, Nifuji A, et al. Osteopontin Expression in Osteoblasts and Osteocytes During Bone Formation Under Mechanical Stress in the Calvarial Suture In Vivo. J Bone Miner Res. 2003 Sep;18(9):1706–15.
467. Russo T, Prestinicola L, Scardi M, Palamara E, Cataudella S, Boglione C. Progress in modeling quality in aquaculture: an application of the Self-Organizing Map to the study of skeletal anomalies and meristic counts in gilthead seabream (Sparus aurata, L. 1758). J Appl Ichthyol. 2010 Apr;26(2):360–5.
468. Kong D, Yan Y, He XY, Yang H, Liang B, Wang J, et al. Effects of Resveratrol on the Mechanisms of Antioxidants and Estrogen in Alzheimer's Disease. Aliev G, editor. Biomed Res Int. 2019;2019:8983752.
469. Wang S, Yang J, Lin T, Huang S, Ma J, Xu X. Excessive production of mitochondrion‐derived reactive oxygen species induced by titanium ions leads to autophagic cell death of osteoblasts via the SIRT3/SOD2 pathway. Mol Med Rep. 2020 Jul;22(1):257–64.
470. Oliveira PJ, Bjork JA, Santos MS, Leino RL, Froberg MK, Moreno AJ, et al. Carvedilol-mediated antioxidant protection against doxorubicin-induced cardiac mitochondrial toxicity. Toxicol Appl Pharmacol. 2004;200(2):159–68.
471. Ascensão A, Lumini-Oliveira J, Machado NG, Ferreira RM, Gonçalves IO, Moreira AC, et al. Acute exercise protects against calcium-induced cardiac mitochondrial permeability transition pore opening in doxorubicin-treated rats. Clin Sci. 2010 Sep;120(1):37–49.
472. Santos D, Moreno A, Leino R, Froberg M, Wallace K. Carvedilol protects against doxorubicin-induced mitochondrial cardiomyopathy. Toxicol Appl Pharmacol. 2002;185(3):218–27.
473. Clementi ME, Giardina B, Di Stasio E, Mordente A, Misiti F. Doxorubicin-derived metabolites induce release of cytochrome C and inhibition of respiration on cardiac isolated mitochondria. Anticancer Res. 2003 May;23(3B):2445–50.
474. Zhou Shaoyu, Starkov A, Kent FM, And LLR, Kendall WB. Cumulative and Irreversible Cardiac Mitochondrial Dysfunction Induced by Doxorubicin | Cancer Research. cancer rese. 2001;
475. Bushinsky DA, Riordon DR, Chan JS, Krieger NS. Decreased potassium stimulates bone resorption. Am J Physiol. 1997 Jun;272(6 Pt 2):F774-80.
476. Betancor MB, Caballero MJ, Terova G, Corà S, Saleh R, Benítez-Santana T, et al. Vitamin C Enhances Vitamin E Status and Reduces Oxidative Stress Indicators in Sea Bass Larvae Fed High DHA Microdiets. Lipids. 2012 Dec;47(12):1193–207.
477. Meng Q, Guo T, Li G, Sun S, He S, Cheng B, et al. Dietary resveratrol improves antioxidant status of sows and piglets and regulates antioxidant gene expression in placenta by Keap1-Nrf2 pathway and Sirt1. J Anim Sci Biotechnol 2018 91. 2018 Apr;9(1):1–13.
478. Lian K, Wang Q, Zhao S, Yang M, Chen G, Chen Y, et al. Pretreatment of Diabetic Adipose-derived Stem Cells with mitoTEMPO Reverses their

Defective Proangiogenic Function in Diabetic Mice with Critical Limb Ischemia. Cell Transplant. 2019/11/05. 2019 Dec;28(12):1652–63.
479. Liang Y, Liu J, Feng Z. The regulation of cellular metabolism by tumor suppressor p53. Cell Biosci. 2013;3(1):9.
480. Watanabe-Takano H, Ochi H, Chiba A, Matsuo A, Kanai Y, Fukuhara S, et al. Mechanical load regulates bone growth via periosteal Osteocrin. Cell Rep. 2021;36(2):109380.
481. Subbotina E, Sierra A, Zhu Z, Gao Z, Koganti SRK, Reyes S, et al. Musclin is an activity-stimulated myokine that enhances physical endurance. Proc Natl Acad Sci U S A. 2015/12/14. 2015 Dec;112(52):16042–7.
482. Re Cecconi AD, Forti M, Chiappa M, Zhu Z, Zingman L V, Cervo L, et al. Musclin, A Myokine Induced by Aerobic Exercise, Retards Muscle Atrophy During Cancer Cachexia in Mice. Cancers (Basel). 2019 Oct;11(10).
483. Songbo M, Lang H, Xinyong C, Bin X, Ping Z, Liang S. Oxidative stress injury in doxorubicin-induced cardiotoxicity. Toxicol Lett. 2019;307:41–8.
484. Walker D, Bichet D, Campbell KP, De Waard M. A beta 4 isoform-specific interaction site in the carboxyl-terminal region of the voltage-dependent Ca2+ channel alpha 1A subunit. J Biol Chem. 1998 Jan;273(4):2361–7.
485. Walker D, Bichet D, Geib S, Mori E, Cornet V, Snutch TP, et al. A new beta subtype-specific interaction in alpha1A subunit controls P/Q-type Ca2+ channel activation. J Biol Chem. 1999 Apr;274(18):12383–90.